# CYTOSOLIC SIGNALLING AND BEHAVIOUR OF ORAL NEUTROPHILS

## *"SEARCH FOR BIOCHEMICAL MEMORY"*

---

**by**

**Geetha Lakshmi Elumalai**

**Neutrophil Signaling Group**

**Cardiff University School of Medicine**

**Cardiff**

**September 2012**

**Thesis submitted to Cardiff University for the degree of Doctor of Philosophy**

# Dedicated

*To my Guru Shri Sai Baba*

# Acknowledgement

This thesis would not have been possible without the guidance and the help of several individuals who extended their valuable assistance and guidance in the preparation and completion of this study. First and foremost, my sincerest gratitude to my supervisor Professor Maurice Hallett, who has supported me throughout my thesis with his patience and knowledge whilst allowing me the room to work in my own way. I attribute the level of my research knowledge to his encouragement and effort and without him this thesis would not have been completed or written. One simply could not wish for a better and friendly supervisor.

Furthermore, I am very grateful to my co-supervisor Dr. Sharon Dewitt Parr for insightful comments both in my work and in this thesis and also supporting me through the phagocytosis experiments, helping me to get osteoarthritis samples and also for many motivating advice and great technical tips and suggestions. I would also like to thank Dr. Chris Parr and Martin Langley for guiding me through Western blotting, Iraj Laffafian for helping me to setup transmigration assay, finally Dr.Kimbley Lewis for helping me to purify ezrin plasmid and for many helpful discussions and for friendly advice and support over the last four years.

I would also like to thank the following people who have allowed me to work in their laboratories and helped me through the course of this reasarch: Professor Rachel Waddington and Professor Jeremey Rees for allowing me to collect gingival fluid from dental patients. Dr. Ian A Brewis and Mrs. Swee Nixon for guiding me through the world of proteomics.

I wish to thank my entire extended family for providing a loving environment for me and were particularly supportive. I have to thank my parents Dr. Elumalai and Dr. Chitra Elumalai for their endless support and love. Lastly and most importantly, I wish to thank my husband Mr. Bhaskar Sivanesan and my brother, they were always there for cheering me up and stood by me through the good and bad times and being there to listen at the end of the day. To them I dedicate this thesis.

# Summary

All inflammatory events are mark by infiltration by leukocytes including neutrophils, which cross the endothelium before following migratory cues to the site of infection, and phagocytosing the infectious microorganisms. Before crossing the endothelial wall, the neutrophils spread on the endothelium. It has been proposed that the necessary additional membrane for cell spreading results from unfolding of wrinkled cell membrane held in place by molecule like membrane linker protein (such as talin or ezrin). Both talin and ezrin are potential substrates for cleavage by the $Ca^{2+}$ activated proteolytic enzyme, calpain-1. It is possible that this mechanism underlies the membrane unwrinkling events but it is yet to be proved. The major aim of this thesis was to look for evidence that proteolysis and redistribution of these proteins occurred during neutrophil shape change.

This thesis provide confirmatory evidence that ezrin is cleaved during extravasation of neutrophils and also provide evidence that the subcellular location of talin and ezrin protein can serve as an biological marker to identify extravasted neutrophils.

The subcellular locations of talin and ezrin were identified using immunocytochemistry. Both ezrin (87%) and talin (92%) were detected at the cell membrane of neutrophils. This pattern was lost in polarized neutrophils, as well as after an elevation of cytosolic calcium level and also after transmigration through endothelial monolayers *in vitro*. Under these conditions, the detected ezrin and talin was mainly cytosolic. The same translocation was observed in extravasated oral neutrophils and also neutrophils which had extravasted under pathological conditions (gingivitis and osteoarthritis).

GFP-tagged ezrin was expressed in RAW cells, in order to investigate the mechanism behind the relocation of ezrin. It was found to be triggered by an elevation of cytosolic calcium and was irreversible. It was also triggered locally during phagocytosis at the site where the membrane expanded.

Western blotting showed that ezrin (72-69 kDa intact) was cleaved under similar conditions with fragments at 55kDa, 51kDa and 49kDa being generated by elavated calcium and extravasation. This cleavage was sensitive to calcium and calpain inhibition.

It was concluded that ezrin is present in the plasma membrane wrinkles of resting neutrophils, but that changes when the cytosolic calcium level changes, as occur during

extravsation and phagocytosis. Addition to this, any dynamic change in the surface area of the plasma membrane (phagocytosis), cause a relocation of ezrin away from the plasma membrane. Evidence was also provided that ezrin can be uses as a biological marker to identify extravasated neutrophils.

# Contents

# Publications

Kannan, R, **Elumalai, GL** Orofacial and systemic manifestations in 212 paediatric HIV patients from Chennai, South India (2010) **International Journal of Paediatric Dentistry; 20, 47-52.**

**Elumalai, GL**, Dewitt, S, Hallett, MB (2011) Ezrin and talin relocates from the plasma membrane to cytosol during neutrophil extravasation. **Eur J Clin Invest**; 41, 47-47.

**Elumalai, GL,** Lewis, KJ, Dewitt, S, Hallett, MB (2012) Localised release of ezrin during phagocytosis and $Ca^{2+}$ signaling (in prep).

**Elumalai, GL**, Dewitt, S, Hallett, MB (2012) Ezrin proteolysis and cytosolic relocation during neutrophil extravasation (in prep).

**Elumalai, GL,** Rees, J, Waddington, R, Dewitt, S, Hallett, MB (2012) Subcellular distribution of ezrin in oral neutrophils (in prep).

# Abstracts and conference presentations

**EZRIN  Biochemical Memory for Extravasated Neutrophils**

 November 2011    **GL Elumalai**

Postgraduate Research Day, Cardiff University, School of Medicine, Cardiff.


**EZRIN  Biochemical Memory for Extravasated Neutrophils**

 October 2011       **GL Elumalai,** MB Hallet, R Waddington & D Sharon

Postgraduate Research Day, Cardiff University, School of Dentistry, Cardiff.


**Translocation of EZRIN and TALIN during Extravasation of Neutrophils**

September 2011    **GL Elumalai**

I3 IRG Annual Meeting, *New House Country Hotel, Cardiff.*


**Ezrin and Talin relocates from the plasma membrane to cytosol during neutrophil extravasation**

April 2011       **GL Elumalai,** S Dewitt and M Hallett

European Phagocyte Workshop, ESCI Conference, Crete, Greece.


**Membrane linker proteins relocates away from plasma membrane durin neutrophil extravasation**

November 2010    **GL Elumalai,** S Dewitt and M Hallett

Postgraduate Research Day, Cardiff University School of Medicine, Cardiff.


**Talin relocates from the plasma membrane to cytosol during neutrophil extravasation**

July 2010        **GL Elumalai**

 I3 IRG Annual Meeting, Atlantic College, Wales.

# Abbreviations

| | |
|---|---|
| **7TM** | Trans Membrane |
| **ADP** | Adenosine Diphosphate |
| **AM** | Acetotoxymethyl Ester |
| **ATRA** | All Trans Retinoic Acid |
| **BM** | Basement Membrane |
| **BSA** | Bovine Serum Albumin |
| **BSS** | Balanced Salt Solution |
| **C3** | Complement Component 3 |
| **C3bi** | Complement Component 3bi |
| **C5a** | Complement Component 5a |
| **CAM** | Cell Adhension Molecules |
| **C-ERMAD** | C-terminal, ERM-association Domain |
| **CFU-G** | Colony Forming Unit – Granulocyte |
| **CFU-GEMM** | Colony Forming Unit – Granulocyte, Erythroid, Monocyte,Megakareocyte |
| **CFU-GM** | Colony Forming Unit – Granulocyte, Macrophage |
| **CGD** | Chronic Granulomatous Diseases |
| **CLA** | Cutaneous Lymphocyte Antigen |
| **CLSM** | Confocal Laser Scanning Microscope |
| **CNP** | Circulating Neutrophil Pool |
| **CRs** | Complement System |
| **CSF** | Colony Stimulating Factor |
| **CXCR1** | CXC Chemokine Receptor 1 |

| | |
|---|---|
| **CXCR2** | CXC Chemokine Receptor 2 |
| **DAG** | Diacylglycerol |
| **DMEM** | Dulbecco's Modified Eagle's Medium |
| **DMSO** | Dimethyl Sulfoxide |
| **DNA** | Deoxyribonucleic Acid |
| **DS** | Docking Structure |
| **EAPs** | Endothelial Adhesive Platforms |
| **EC** | Endothelial Cell |
| **EDTA** | Ethylenediaminetetraacetic Acid |
| **EGF** | Epidermal Growth Factor |
| **EGFP** | Enhanced Green Fluorescent Protein |
| **EGTA** | Ethylene Glycol Tetraacetic Acid |
| **ER** | Endoplasmic Reticulum |
| **ERM** | Ezrin, Radixin, Moesin |
| **ERMBMPs** | ERM Binding Membrane Proteins |
| **ESAM** | Endothelial Cell-Selective Adhesion Molecule |
| **ESL-1** | E-Selectin-Ligand 1 |
| **FAK** | Focal Adhesion Kinase |
| **FCS** | Foetal Calf Serum |
| **FcγRs** | Fc Portion of γ-Immunoglobulins, |
| **FERM** | 4.1 Protein, Ezrin, Radixin and Moesin |
| **FITC** | Fluorescein Isothiocyanate |
| **FMLP** | *N*-Formylmethionyl-Leucyl-Phenylalanine |
| **FPR** | Formyl Peptide Receptor |
| **G-CSF** | Granulocyte – Colony Stimulating Factor |
| **GFP** | Green Fluorescent Protein |

| | |
|---|---|
| **GM-CSF** | Granulocyte Monocyte – Colony Stimulating Factor |
| **GRO** | Growth-Related Oncogene |
| **HeBs** | Hepes Buffered Saline |
| **HRP** | Horseradish Peroxidase |
| **HSCs** | Haematopoietic Stem Cells |
| **HUVEC** | Human Umbilical Venous Endothelial Cells |
| **ICAM-1** | Inter-Cellular Adhesion Molecule 1 |
| **ICAM-2** | Inter-Cellular Adhesion Molecule 2 |
| **IFNα** | Interferon Alpha |
| **IFNγ** | Interferon Gamma |
| **IgG** | Immunoglobulin G |
| **IL-1** | Interleukin 1 |
| **IL-3** | Interleukin 3 |
| **IL-8** | Interleukin 8 |
| **ILK** | Integrin-Linked Kinase |
| **IP3** | Inositol 1,4,5-trisphosphate |
| **ITAMs** | Immunoreceptor Tyrosine-based Activation Motifs |
| **JAM A.B,C** | Junctional Adhesion Molecule A, B, C |
| **kDa** | Kilodaltons |
| **LAD** | Leukocyte-Adhesion Deficiency |
| **LB** | Lysogeny Broth |
| **LER** | Low Expression Region |
| **LFA1** | Lymphocyte Function-associated Antigen 1 |
| **LPS** | Lipopolysaccharide |
| **LTC** | Cysteinyl Leukotrienes |
| **MAE** | Methyl-Amino-Ethanol |

| | |
|---|---|
| **MBL** | Mannan-Binding Lectin |
| **MIDAS** | Metal Ion–dependent Adhesion Site |
| **MIP** | Macrophage Inflammatory Protein |
| **MLCK** | Myosin Light-chain Kinase |
| **MNP** | Marginated Neutrophil Pool |
| **NADPH** | Nicotinamide Adenine Dinucleotide Phosphate |
| **NO** | Nitric Oxide |
| **NPP** | Neutrophil Progenitor Pool |
| **NSP** | Neutrophil Storage Pool |
| **PAF** | Platelet Activating Factor |
| **PAMPs** | Pathogen-associated Molecular Patterns |
| **PBS** | Phosphate Buffered Saline |
| **PCR** | Polymerase Chain Reaction |
| **PECAM1** | Platelet Endothelial Cell Adhesion Molecule 1 |
| **PH** | Pleckstrin Homology Domain |
| **PI** | Propidium Iodide |
| **PI** | Periodontal Index |
| **PI3K** | Phosphoinositide 3-Kinase |
| **PIP** | Phosphatidylinositol 4-Phosphate |
| **PIP2** | Phosphatidylinositol 4,5-Bisphosphate |
| **PIP3** | Phosphatidylinositol (3,4,5)-Triphosphate |
| **PIPK1γ90** | Phosphatidylinositol (4)-phosphate 5-Kinase Type Iγ |
| **PKCβ** | Protein Kinase C β |
| **PKCγ** | Protein Kinase C γ |
| **PLA2** | Phospholipase A2 |
| **PLCβ** | Phospholipase C β |

| | |
|---|---|
| **PLC-γ** | Phospholipase C γ |
| **PLCγ2** | Phospholipase C γ 2 |
| **PMN** | Polymorphonuclear Leukocyte. |
| **PRRs** | Pattern Recognition Receptors |
| **PS** | Phosphatidyl Serine |
| **PSGL1** | P-Selectin Glycoprotein Ligand 1 |
| **PSI** | Plexin/Semaphoring/integrin) Domain |
| **PTB** | Phosphotyrosine Binding |
| **PVR** | Poliovirus Receptor |
| **RANTES** | Regulated and Normal T cell Expressed and Secreted |
| **Rf** | Relative Mobility |
| **RFP** | Red Fluorescent Protein |
| **RNA** | Ribonucleic Acid |
| **RPM** | Revolutions Per Minute |
| **RPMI** | Roswell Park Memorial Institute Medium |
| **SCF** | Stem Cell Factor |
| **SDS** | Sodium Dodecyl Sulfate |
| **SDS-PAGE** | Sodium Dodecyl Sulfate-Polyacrylamide Gel Electrophoresis |
| **SEM** | Scanning Electron mMcrograph |
| **SERCa** | Sarco/Endoplasmic Reticulum $Ca^{2+}$-ATPase |
| **SiRNA** | Small Interfering RNA |
| **SNARE protein** | Soluble N-Ethylmaleimide Sensitive Attachment Protein Receptor |
| **TBS** | Tris Buffered Saline |
| **TEM** | Transendothelial Cell Migration |

| | |
|---|---|
| **TH17** | T Helper 17 Cells |
| **THATCH** | Tethering C-Terminal Homology Domain |
| **TLRs** | Toll Like Receptors |
| **TM** | Transmembrane |
| **TNFα** | Tumour Necrosis Factor Alpha |
| **TRIS** | Tris(hydroxymethyl)aminomethane |
| **URP1** | Unc-112 Related Protein 1 |
| **UV** | Ultra Violet |
| **VBSs** | Vinculin-Binding Sites |
| **VCAM**-1 | Vascular Cell Adhesion Molecule 1 |
| **VEGF** | Vascular Endothelial Growth Factor |
| **VE-PTP** | Vascular Endothelial Tyrosine Phosphatase |
| **YFP** | Yellow Fluorescent Protein |
| **βTD** | Membrane Proximal β Tail Domain |

# List of Tables

# List of Figures

# CHAPTER 1

## Introduction

## 1.1 Inflammation

Inflammation is a localized, protective response to trauma or microbial invasion that destroys, reduces or "walls off" the injurious agent and the injured tissue. It is characterized in the acute form by the classic signs of dolor, calor, rubor, tumor and function laesa. Microscopically, it involves a complex series of events, including dilation of arterioles, capillaries and venules, with increased permeability and blood flow, exudation of fluids including plasma protein and transendothelial migration of leukocytes into the inflammatory focus. Diseases characterized by inflammation are an important cause of morbidity and mortality in humans. Deficiencies of inflammation compromise the host, whereas excessive inflammation caused by abnormal recognition of host tissue as foreign or prolongation of the inflammatory process, may lead to inflammatory diseases as diverse as atherosclerosis to post-infectious syndromes, like rheumatic diseases (Gallin 1999). The accumulation and subsequent activation of leukocytes are central events in the pathogenesis of most forms of inflammatory disease.

### 1.1.1 History of inflammation

Inflammation has had a long and colorful history, intimately linked to the history of wounds, wars and infection (Gallin 1999; Ley et al. 2007).  The word "inflammation" comes from the latin word inflammare (to set on fire).The history of inflammation and research stretches over 2000 years, with 200 years of research at cellular level and 20 years of research at the molecular level (Ley et al. 2007). The insight that has been obtained not only led to a better understanding of the inflammatory phenomena, but have also benefited the diagnosis and treatment of patients with inflammatory disorders.

The descriptions of inflammation long before the cardinal signs of rubor, tumor, calor and dolor were stamped by Celsus in the 1st Century. Figure 1.1.1 shows the cartoon depiction of the cardinal signs of inflammation which were described by Celsus 2000 years ago. In its genesis, inflammation was defined by a combination of clinical signs and

symptoms not by specific pathophysiology. Two centuries after Celsus, Calen was influential in promoting the humoral view of inflammation. In his model, inflammation (and pus specifically) was part of the beneficial response to injury, rather than a superimposed pathology. This humoral view of inflammation persisted into the 19th century when Virchow added the fifth cardinal sign, function laesa (loss of function) in 1871. By the end of the 19th century, it was accepted that changing cell populations arising from both the blood and local proliferation were a key feature of many models of inflammation.

Advances in microscopy and cell biology in the 19th century gave rise to cell based definitions of inflammation, which revealed the complexity of events that underlies all inflammatory reactions. A prominent German biologist, Neumann, defined inflammation more lossely as a "series of local phenomena developing as the result of primary lesions to the tissues and that tend to restore their health". However, we know that inflammation today is a more complicated cascade. Modern molecular biology  superimposes additional layers of complexity on this commonly accepted model. Firstly, a tissue much be influenced by proinflammatory signaling molecules, even in the absence of inflammatory cell invasion. Secondly, both inflammation and repair can be triggered and modulated by primary events occurring outside the vasculature, such as vibration, hypoxia and mechanical loading.

All the views developed in the last century by Claude Bernard, Cohnheim, Virchow and Metchnikoff with the four signs of Celsus' cardinal signs for inflammation  in the background  represents the pre-history of inflammation (Rocha e Silva 1994). Post-history of inflammation is marked  by Sir Henry Dale and his concept of auto-pharmacology, which describe the inflammation phenomena that depends upon formation, synthesis or release of endogenous active substances, called mediators of physio-pathological phenomena (Rocha e Silva 1994). Subsequent advances in field of inflammation are the identification of different classes of inflammatory mediators, the pathways that control their production and their mechanisms of action.

Although there has been an explosion of knowledge about inflammation over the second half of the 20th Century, our clinical concepts about inflammation have remained essentially unchanged. We now know that inflammation comes in many different forms and modalities, that are governed by different mechanisms of induction, regulation and resolution, still we have long way to go to completely understand the basic of inflammation (Medzhitov 2010). There is no evidence that the pace of discoveries in inflammation research will slow down as the inflammatory components of many chronic and acute diseases are recognized and investigated. Table 1.1.1 enlists the key development in the field of inflammation from 1st Century until 20th Century; this table was adapted from Scott 2004.
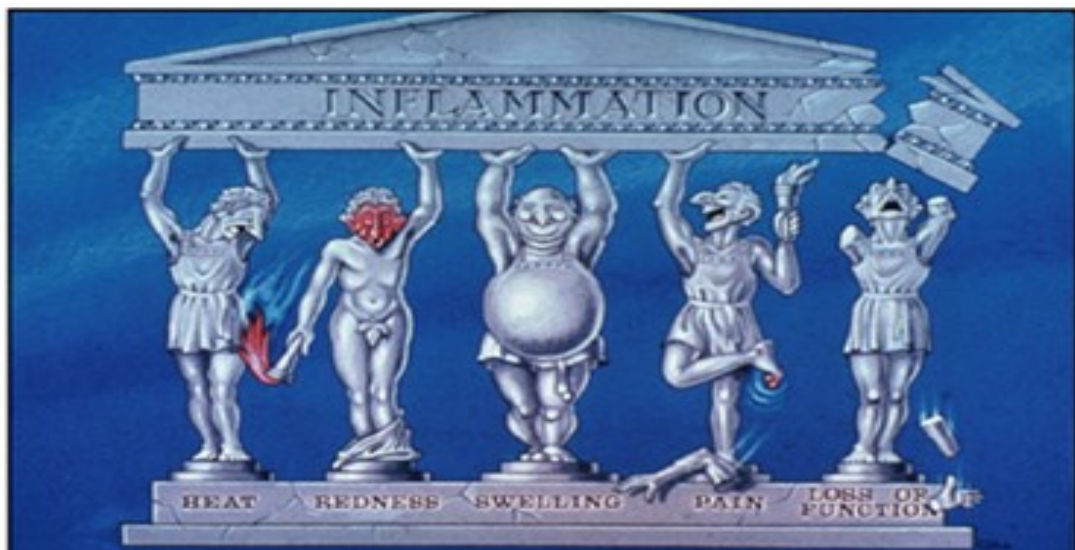


**Figure 1.1.1.** Five Greeks cartoon representing the cardinal signs of inflammation — heat, redness, swelling, pain and loss of function that are as appropriate today as they were first described by Celsus more than 2000 years ago. This figure was adopted from Nature Reviews Immunology, 2002, 2; 787-795.

**Table 1.1.1. Key development in field of inflammation until 20<sup>th</sup> Century  (Scott et al. 2004)**

| Author and year | Quotation | Historical interpretation | Modern significance |
|---|---|---|---|
| Celsus,  1<sup>st</sup> Century AD | Ruboor et tumor cum calore et dolore | First documentation of cardinal signs of inflammation | Emphasized importance of clinical observations than philosophy based medicine |
| Galen 3<sup>rd</sup> Century | Laudable pus | Infection and inflammation are beneficial to repair of wounds | Inflammation was seen as an expression of humoral theory well into the 19<sup>th</sup> Century |
| Virchow,1871 (fifth cardinal sign) | The inflammatory reaction is a consequence of an excessive intake by interstitial cells that filtering through the vessel wall | Inflammation as a pathological proliferation of cells due to leakage of nutrients from vessels | Recognized cellular nature of inflammatory response |
| Cohnheim,1873 | Finally there lies outside the vessel a colourless blood corpuscle and reveled the physiological basis of the four cardinal signs | Blood corpuscles were seen as pathological mechanisms by which infections spread, secondary to vascular injury | First description of diapedesis |
| Arnold, 1875 | Diapedesis | | |
| Weigert, 1889 | Inflammatory exudates | Evidence of humoral theory | |
| Ziegler, 1889 | Involvement of circulatory system and tissue environment in inflammation | | |
| Jules bordet, 1896 | Complements in inflammation | | |
| Paul ehrlich, 1897 | Humoral theory of immunity | Major milestone in history of inflammation | |
| Bernard shaw, 1906 | Cause of inflammation | | |

| | | | |
|---|---|---|---|
| Metchnikoff, 1908 | The prime moves of the inflammatory reaction are a digestive action toward the noxious agent and discovery of phagocytosis of macrophage and neutrophils | Inflammation as a defensive cellular response to pathogens guided by the vessels rather than an aspect of the pathology itself | First to express the view that phagocytes were protective not pathological |
| Krogh, Lewis Zotterman and Mitchell ,1926 | H- Colloid | | |
| Lewis, 1927 | Inflammation as the triple response to injury. And role of Endogenous mediator in inflammation (Triple response). | Inflammation is characterized by the cascular events mediated both by local chemicals and by axons | First recognition of neurogenic inflammation, first physiological characterization of vascular events |
| Menkin, 1938 | Leukotaxin | | |
| Claude Bernard, Ludwig, Dubois-Raymond, 1973 | Physiological regulations of inflammation | | |
| Rocha e Silva, 1974 | Inflammation as a multi-mediated phenomenon of a pattern type in which all mediators would come and go at the appropriate moments increasing cascular permeability attracting leucocytes producing pain local edema and necrosis | Inflammation defined by mediators | Biochemical definition of inflammation |
| Robert Koch and Louis Pasteur, 1979 | Microbial agents as major inducers of the acute inflammatory response | | |

## 1.2 Principles of inflammation

Inflammation is a manifestation of the body's response to tissue damage and infection. Humans and animals have various defensive mechanisms to protect them from different pathogens including viruses, bacteria, fungi, and protozoan and metazoan, parasites; as well as tumors and a number of various harmful agents, which are capable to alter the homeostasis. The basic principle of inflammatory reaction is to bring the cells of the defense and immune system to the site of infection or tissue injury, in order to remove the pathological agent and to protect the host. The detailed processes of inflammation have revealed that it is a complex stereotypical reaction involving a number of cellular and molecular components and important changes in the physiological systems as well. The result of each inflammatory reaction may be beneficial (defending the body against agents that alters the homeostasis) or harmful (damage to surrounding tissues).

According to different criteria, inflammatory reaction can be divided into several categories. The criteria include:

1. *Time* -- hyperacute (peracute), acute, subacute and chronic inflammation;
2. *The main inflammatory manifestation* - alteration, exudation, proliferation;
3. *The degree of tissue damage* - superficial, profound (bordered, not bordered);
4. *Characteristic picture* - nonspecific, specific;
5. *Immunopathological mechanisms*
   - allergic (reaginic) inflammation,
   - inflammation mediated by cytotoxic antibodies,
   - inflammation mediated by immune complexes,
   - delayed-type hypersensitivity reactions.

Either exogenous factors like traumatic, ionizing irradiation, nutritional deficiency, biological agents and caustic agents, endogenous factors like immunological reactions, genetic and neurogenic, cause cell and tissue damage. Thus, specific immune response help in the

healing processor or can leads to harmful outcomes like autoimmune diseases and immunopathological reactions.

Inflammation is often considered in terms of acute inflammation that includes all the events of the acute vascular and acute cellular response (see below); and chronic inflammation that includes the events during the chronic cellular response and resolution or scarring (see below). The earliest, gross event of an inflammatory response is temporary vasoconstriction, i.e. narrowing of blood vessels caused by contraction of smooth muscle in the vessel walls, which can be seen as blanching (whitening) of the skin. This is followed by several phases that occur over minutes, hours and days later, outlined in the table 1.2.

**Table 1.2. Vascular and cellular events associated with inflammatory reactions**

| 1 | Acute vascular response | Few seconds to few minutes | Vasodilation and increased capillary permeability due to alterations in the vascular endothelium, which leads to increased blood flow (*hyperaemia*) that causes redness (*erythema*) and the entry of fluid into the tissues (*oedema*). |
|---|---|---|---|
| 2 | Acute cellular response | Few hours | Appearance of granulocytes, particularly neutrophils, in the tissues. Pus formation. |
| 3 | Chronic cellular response | Next few days | Appearance of a mononuclear cell infiltrate composed of macrophages and lymphocytes. |
| 4 | Resolution | Next few weeks | Scarring or granulomatous tissue. |
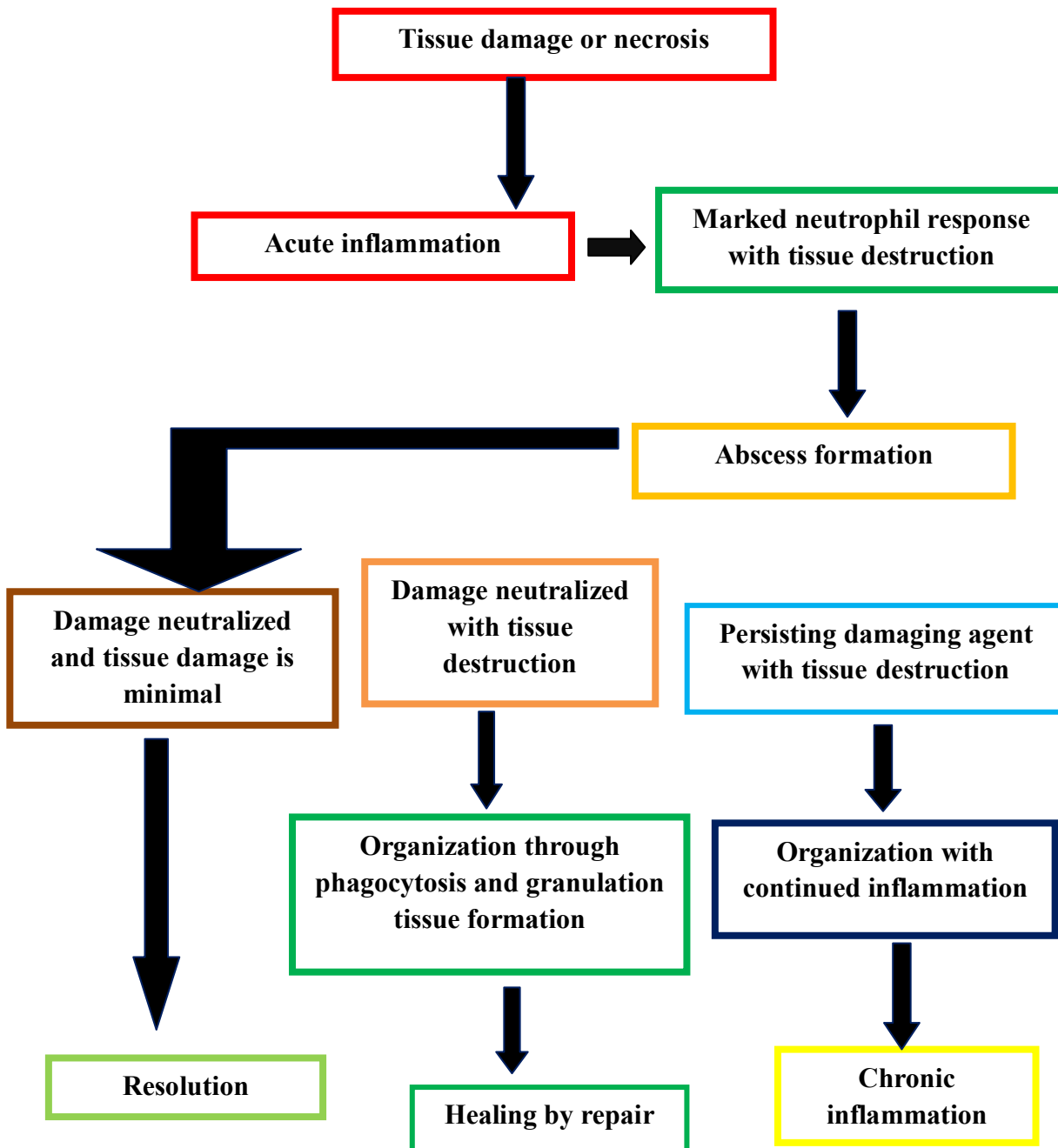
**Figure1.2. Flow chart showing the various outcomes of inflammatory reaction to tissue injury. This reaction can result from sustained tissue insult, failed resolution of the acute inflammation or hypersensitivity immune response. Chronic inflammation often demonstrates slow onset with a persistent cyclical tissue destruction and repair.**

### 1.2.1 Phases of inflammatory reaction to injury and infection

Inflammation is the phylogentically and ontogenetically the body's oldest defense reaction to protect the body against infectious agent, antigen challenge or even just physical, chemical or traumatic damage, it is characteristic by three major events.

1. **Vasodilation** is a classic feature of acute inflammation and is clinically characterized by redness and warmth at the site of injury. The purpose of the vasodilatory response is to facilitate the local delivery of soluble mediators and inflammatory cells. This is mediated primarily by nitric oxide (NO) and vasodilator prostaglandins. Both these mediators causes smooth muscle relaxation which leads to vasodilation. Vasodilatation initially involves arterioles followed by the opening of new microvascular beds. In cases of severe systemic inflammation such as sepsis, induced by the actions of NO and pro-inflammatory cytokines, such as TNF-α (Sherwood and Toliver-Kinsky 2004).

2. **Increased capillary permeability**: Beginning immediately after injury, several different pathways can induce increased vascular permeability as listed below (Wilhelm 1973):

• *Formation of venule intercellular endothelial gaps* is the most common mechanism underlying increased vascular permeability; endothelial cells are induced to contract, thereby opening intercellular gaps. Contraction is elicited by chemical mediators (e.g. histamine), which occurs rapidly after injury and is reversible and transient (15 to 30 minutes); hence it is an immediate-transient response. It involves only small venules (not capillaries or arterioles); these venules will also eventually be sites for leukocyte emigration. The same response can be caused by cytokines, such as interleukin-1 (IL-1) and tumor necrosis factor (TNF-α), but will be delayed (4 to 6 hours) and protracted (24 hours or more).

- *Direct endothelial cell injury.* Severe necrotizing injury (e.g. burns) causes endothelial cell necrosis and detachment that affects venules, capillaries and arterioles; recruited neutrophils may contribute to injury. The damage usually evokes immediate and sustained endothelial cell leakage.

- *Delayed prolonged leakage* begins after a delay of 2 to 12 hours and may last for days; venules and capillaries are affected. The causes of this include mild/moderate thermal injury, x-ray irradiation, or ultraviolet (UV) injury (e.g., sunburn). Direct endothelial injury or secondary cytokine effects (endothelial contraction) may also be implicated.

- *Leukocyte-mediated endothelial injury* results from leukocyte aggregation, adhesion, and migration across the endothelium. Leukocytes release of reactive oxygen species and proteolytic enzymes causes endothelial injury or detachment.

- *Increased transocytosis*. Transendothelial channels form by interconnection of vesicles from the vesiculovacuolar organelle. Certain factors (e.g. vascular endothelial growth factor, VEGF) induce vascular leakage by increasing the numbers of these channels.

- *Leakage from new blood vessels.* During repair, endothelial proliferation and capillary sprouting (angiogenesis) result in leaky vessels. Increased permeability persists until the endothelium matures and intercellular junction form.

Inflammatory responses can be classified into three types, based on the onset of inflammatory reaction and change in vascular permeability. The three types of inflammatory response are listed below (table 1.2.1).

**Table 1.2.1. Types of inflammatory response**

| Type of inflammatory response | Duration | Type of injury | Characteristic | Example |
|---|---|---|---|---|
| Early response | Less than 1 minute | Non-intense injury | Begins in one minute, reaches peak in 3 minutes and last only 5-10 minutes | Heating, cold injury, surgical incision crushing and chemical injury. |
| Immediate response | 1 to 10 minutes | Moderate injury | Begins in the initial minutes after injury, reaches a peak in the first hour and has a duration not exceeding 10 hours. | Thermal injury, ultraviolet injury. |
| Delayed<br><br>Two forms | Less than 1hour | Moderate injury | Follows after increased vascular permeability, | Moderate thermal injury, cold injury, ultrasonic injury, acute bacterial infection. |
| | 2- 10 hours | Severe injury | | Ultraviolet and chemical injury, β and x-radition, iota-toxin and delayed hypersensitivity reaction. |

3. **Oedema and leukocytes migration.** Fluid which accumulates during inflammation is composed of exudate that is caused by alterations in post-capillary venules pressure, which overcomes the osmotic pressure of plasma protein. There are two phases of inflammatory oedema formation. The immediate temporary phase, with a peak

between 8 and 10 minutes and duration about 30 min, develops because of a release of fluid from venules mediated by histamine. This is followed by a immediate prolonged phase, which has characteristics similar to the early phase, but with a longer duration of a few days. The second delayed phase needs a few hours to develop.

In the fluid exudate, all components of plasma, including fibrinogen, kinins, complement, immunoglobulins, etc; and inflammatory cells are present. Exudative infiltrate is responsible for two of the cardinal signs of inflammation. The first is swelling (tumour), and the second is pain (dolor), caused by the increased pressure in tissue. The pain can also result from the acidic pH of exudate, the accumulation of potassium ions and the presence of bradykinin, serotonin or other mediators.

The formation of oedema can also lead to stasis of blood flow, which in turn causes the white blood cells to accumulate along the endothelium and begin to cross the vessel wall. Cellular exudate is formed during the second and the third phases of inflammation. In the earliest stages of inflammation, neutrophils are particularly prevalent, but later monocytes and lymphocytes migrate towards the site of infection, the entire steps involved in migrations of leukocytes is explained later. The cellular composition of exudates, thus, differs depending on the phase of inflammation but can vary with the type of inflamed tissue and factors triggering inflammatory process. Neutrophils are dominant when a pyogenic bacterial infection or local depositions of immune complexes containing IgG are the cause of inflammation. Mononuclear phagocytes represent the main infiltrating cells in subacute and chronic phases of the majority of inflammatory reactions; and in the case of infection with intracellularly parasitizing microorganisms. Eosinophils and basophils are predominant when inflammation has been initiated by immediate allergic reactions or by parasites.

Therefore, a number of different cell types are recruited into the area where damage has occurred; and these are responsible for inactivation and removing of the invading

infectious agents, for removing damaged tissues, for inducing the formation of new tissue; and reconstructing the damaged cell matrix, including basement membranes and connective tissues.

The cellular content in the exudates have specific role in order to resolve the inflammatory situation. For instants, professional phagocytes (neutrophils, eosinophils, monocytes and tissue macrophages) are essential for performing phagocytosis and removing all the microbes and dead cells. Lymphocytes are involved in the specific immune responses, endothelial cell play a major role in the regulation of leukocyte emigration from the blood into inflamed tissue; and platelets with mast cells are involved in the production of early phase mediators. The accumulation of leukocytes in inflamed tissue results from adhesive interactions between leukocytes and endothelial cells within the microcirculation. These adhesive interactions and the excessive filtration of fluid and protein that accompanies an inflammatory response are largely confined to one region of the microvasculature -- postcapillary venules. The contribution of different adhesion molecules to leukocyte rolling, adherence, and emigration in venules will be discussed later. This process is similar for granulocytes, monocytes and lymphocytes, only different chemotactic factors and cytokines may be involved in its initiation and control.

The flowchart shown below, outlines the various cellular and vascular events and different phases involved in any inflammatory events. This chart was adapted from text book of Anatomy and Physiology by Benjamin Cummings 2001, 3rd edition, published by Pearson education.

**Stimuli**
- **Infection or microbial toxins**
- **Trauma**
- **Physical or chemical agents**
- **Tissue necrosis**
- **Foreign bodies**
- **Immune reactions**

**Mast cells degranulate** → **Histamine; PG's; serotonin**

**Endothelial cells** → **Nitric oxide**

**Vasodilatation due to Relaxation of vascular smooth muscles**

**RUBOR CALOR**

**Increase vessel caliber and flow**

**Chemical mediators:**
- **Vasoactive amines**
- **C3a**
- **Bradykinin**
- **LTC4, LTD4, LTE4**
- **Bacterial products**

**Vascular permeability due to Phosphorylation of contractile proteins causing endothelial cell contraction**

**Increase hydrostatic pressure - transudate (low protein**

**Leakage of plasma protein Decrease osmotic pressure Exudates (high protein)**

**Fluid to interstitial space**

**Decrease blood flow**

- **TNF α and IL-1**
- **Histamine, thrombin, PAF**

**Increase expression of selectins , increase expression of integrins**

- **Bacterial products exogenous chemical mediators**

**TUMOR**

**DOLAR (pain) PRESSURE AND SWELLING, LOSS OF FUNCTION**

- **Endogenous chemical mediators LTB4, C5a, chemokines**

**Margination and adhesion of WBC's**

**Transmigration (diapedesis)**

**Leukocyte activation Recognition of opsonis Phagocytosis; reactive oxygen species, lysosomal enzymes** etc

- **Bacterial products exogenous chemical mediators**

**Chemotaxis**

**Removal of inflammatory stimuli, healing, resolution or chronic inflammation**

## 1.3 Neutrophils

Neutrophils play a central role in the inflammatory process, followed by macrophages, eosinophils and mast cells. The neutrophils represent the first line of defence against infecting microbes. It is the most numerous white blood cell, out-numbering all the other white cells put together. It represents the most significant part of the immune system, without which any species would be overwhelmed by infection and unable to survive.

## 1.3.1 History of the study of neutrophils

Early microscopists visualized the white corpuscles of the blood along with the numerous red blood corpuscles. However, it was not until Paul Ehrilich used coloured stains and showed that these white corpuscles were of several types. The nuclear stains showed that the white blood cells had either a clearly defined large single nucleus or apparently smaller numerous nuclei. Ehrlich consequently named these latter cells as polynuclear cells. However, further studies showed that the apparently separate nuclei were, in fact, the large lobes of a single nucleus. The large nuclear lobes were linked by fine interconnecting parts which were difficult to visualize, and gave rise to the original error. In 1898, Ehrlich renaming these cells as cells with polymorphous nuclei. This complex name was adapted by Metchnikoff to produce the more familiar name: polymorphonuclear leukocyte (PMN). Consequently, this name remained in common use today.The stains that Erhlich used also also showed that the PMNs were themselves not a uniform population of cells. The granules within some PMNs stained with basic aniline dyes (basophils); and some other PMNs had granules which stained with acidic dyes, such as eosin (eosinophils). However, the major population of PMNs had granules which stained with neutral stains, and were hence named as neutrophils. However, Metchnikoff (father of neutrophil cell biology) actually called neutrophils, microphages to contast with the larger macrophages.

The role of neutrophils in inflammation was unclear to 19th Century scientists, when it was thought that neutrophils carried "germs" (which were spontaneously generated) to the site of inflammation. However, Waller demonstrated that neutrophils leave the blood vessels by diapedesis, doubting the 19th Century concept. Metchnikoff proved that neutrophils were actually the opponents of infection, describing the process of phagocytosis; and proving that both phagocytosis and diapedesis were the mechanism used by neutrophils to kill the infecting microbes.

Following the acceptance of Metchnikoff's phagocyte theory, the focus of research became the mechanism by which neutrophils achieved the killing of bacteria after phagocytosis. Eichwald in 1864 had demonstrated that pus contained products of proteolysis. However, this was neglected as a killing mechanism because of presence of anti-proteases. The exact mechanism for the killing remained undiscovered for 50 years. It was not until 1933, that it was discovered that phagocytosis was accompanied by a massive burst of oxygen consumption (Baldridge and Gerard 1933). Anger L, showed that neutrophil peroxidase could destroy toxins in the presence of hydrogen peroxide. Selvaraj further established a role of oxygen and Sbarra showed that in low oxygen neutrophils could phagocyte but do not kill microorganisms. Segal and Jones later established the molecular nature of the oxidase as containing a b-type cytochrome by its lack in patients with Chronic granulomatous disorder(CGD) (Hallett MB, 2001)

Advances in signaling within neutrophils have occurred more recently, mainly in the second half of the 20th Century. Karnovsky demonstrated that inorganic phosphate was incorporated into phosphatidylinositol during neutrophil activation and made the first major discovery of the signaling mechanism in neutrophils. The second discovery was that cytosolic free $Ca^{2+}$ signaling which was involved. Woodin and Weinke were the first to demonstrate a direct role for $Ca^{2+}$ (Hallett MB, 2001). They showed that Streptolysin A

activated neutrophils by increasing the permeability of the plasma membrane to $Ca^{2+}$. Table 1.2.1 lists other advances.

**Table 1.3.1: History of discovery of neutrophils (adapted from Hallet MB 1989)**

| Discovery | Discoverers | Date |
|---|---|---|
| Identification of the neutrophils | Ehrlich | 1886 |
| Phagocyte theory | Metchnikoff | 1895 |
| Opsins | Wright & Douglas | 1903 |
| Respiratory burst | Baldridge and Gerard | 1933 |
| Non-mitochondrial oxidase activity | Becker et al, Sbarra & Karnovsky | 1958,1959 |
| Involvement of phosphatides | Karnovsky & Wallach | 1960 |
| Involvement of $ca^{2+}$ ions | Woodin & Weineke | 1963 |

## 1.3.2 Haematopoiesis of neutrophils

The term "haematopoiesis" comes from ancient Greek meaning "to make blood ". All cellular blood components are derived from haematopoietic stem cells. In a healthy adult person, approximately $10^{11}$–$10^{12}$ new blood cells are produced daily in order to maintain steady state levels in the peripheral circulation (Stites 2001). Haematopoietic stem cells (HSCs) reside in the medulla of the bone (bone marrow) and have the unique ability to give rise to all of the different mature blood cell types. HSCs are self-renewing. When they proliferate, at least some of their daughter cells remain as HSCs, so the pool of stem cells does not get depleted. The other daughters of HSC differentiate into three lineages (myeloid, erythroid and lymphoid progenitor cells). However, each can commit to any of the alternative differentiation pathways that lead to the production of one or more specific types of blood cells, but cannot self-renew. This is one of the vital processes in the body. In developing embryos, blood formation occurs in aggregates of blood cells in the yolk sac. As development progresses, blood formation occurs in the spleen, liver and lymph nodes. When bone marrow develops, it eventually assumes the task of forming most of the blood cells for the entire organism. In children, haematopoiesis occurs in the marrow of the long

bones, such as the femur and tibia. In adults, it occurs mainly in the pelvis, cranium, vertebrae, and sternum. In some cases, the liver, thymus, and spleen may resume their haematopoietic function, if necessary. This is called extramedullary haematopoiesis. The figures 1.3.2a and 1.3.2b show the changes in anatomical location of hematopoiesis during human development. Two models have been proposed; a classic model and a myeloid-based model. According to the classic model proposed by Weissman (Wheeler 1993) the hematopoietic stem cells give rise to myeloid-erythroid progenitor cells and lymphoid progenitor cells. However this model is not accepted anymore. The myeloid-based concept has become widely accepted, where the stem cells give rise to myelo-eyrthroid progenitors and myelo-lymphoid progenitors. The figure 1.2.3c is the schematic representation of both these models.

Differentiatied red and white blood cell production is regulated with great precision in healthy humans; and the production of granulocytes is rapidly increased during infection. The proliferation and self-renewal of these cells depend on stem cell factor (SCF). Glycoprotein growth factors regulate the proliferation and maturation of the cells that enter the blood from the marrow and cause cells in one or more committed cell lines to proliferate and mature. Other factors that stimulate the production of committed stem cells include CSF-granulocyte-macrophage (CSF-GM), CSF-granulocyte (CSF-G) and CSF-macrophage (CSF-M). These stimulate CFU-GEMM (colony forming unit-granulocyte, erythroid, monocyte, megakaryocyte) which no longer retain the capacity to self replicate. These cells in turn differentiate into the CFU-GM (colony forming unit – granulocyte, macrophage), which in turn differentiate into CFU-G (colony forming unit– granulocyte), which becomes progressively more committed with each division eventually give rise to neutrophils. These cell lines along with the stem cells comprise the neutrophil progenitor pool (NPP) (Kanwar and Cairo 1993; Wheeler 1993), as shown in figure 1.3.2d.

Neutrophil myelopoiesis is a closely regulated process that begins with the differentiation of puripotent cells into primitive myeloid progenitors, which differentiate into

specific myeloid precursors. Contact with adhesion molecules, hematopoietic growth factor and cytokines promotes the progression of myeloblasts along specific pathways to mature as either neutrophils, eosinophils, basopils or monocytes (Serhan 2010). The coordinated expression of a number of myeloid transcription factor including PU.1, CCAAT enhancer binding protein α and Ω and GF, are necessary for the regulation of neutrophil development. Among the extracellular factors that direct pluripotent stem cells to differentiate into neutrophils, CSF-G plays an essential role. CSF-G had been shown to induce myeloid differentiation, stimulate proliferation of granulocytic precursors and provoke neutrophil release from the bone marrow (Serhan 2010). The biological effects of G-CSF are mediate via its receptor CD114, a member of haematopoietic cytokine receptor family. Other haematopoietic cytokines contributing to neutrophil development *in vivo* include CSF-GM, IL-6 and IL-3. Figure 1.3.2.f is a schematic representation of granulocytopoieisis and the possible factors responsible for regulation of synthesis of neutrophils and other granulocytes. Although incompletely understood, the mechanisms controlling neutrophil homeostasis involve both neutrophil production and clearance (Serhan 2010). Recent observations implicate the SDF-1/CXCR4 signaling system in the process of neutrophil clearance. SDF-1 is a chemokine that is secreted from bone marrow and attracts neutrophils by engaging the CXCR4 receptor. Senescent neutrophils upregulate CXCR4 and obtains the ability to migrate towards SDF-1 and homing to the bone marrow, result in clearance of aging cells from the blood. In the bone marrow, as well as in the spleen and liver, damaged and aging neutrophils are cleared by tissue macrophages. Reduction of neutrophil populations is also effected through the induction of apoptosis.

A feedback loop down regulating neutrophil production has recently been identified. Following phagocytosis of apoptotic neutrophils by tissue macrophages, the latter shut down their secretion of IL-23. In consequence, IL-17 production by TH17 cells is reduced. Lack of IL-17 then results in decrease levels of CSF-G and consequently, reduced

neutrophil development and release (Serhan 2010). In the setting of increased neutrophil populations, this system is poised to maintain neutrophil populations within a constant range (Serhan 2010).. Table 1.2.3 and figure 1.2.3d, shows the various cytokines and regulating factors responsible to produce different granulocytes.
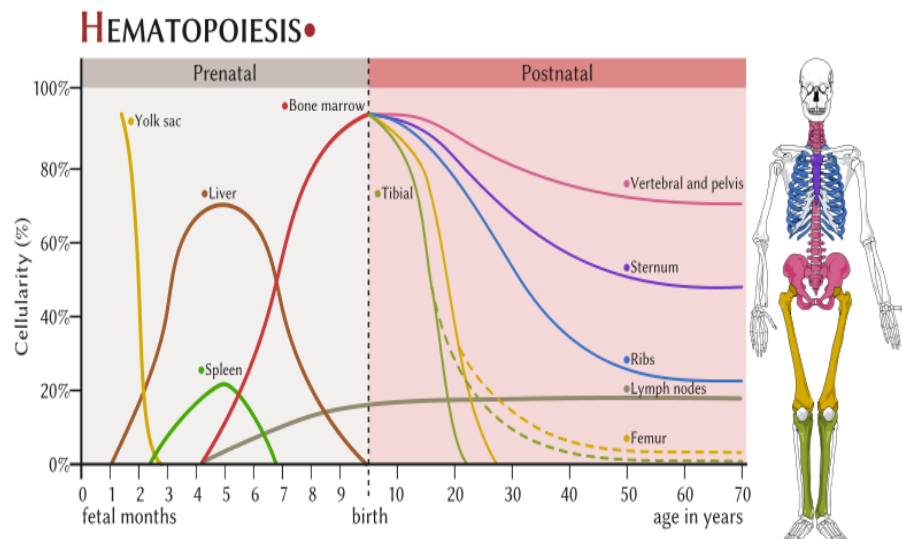
**Figure 1.3.2 a.** Various hematopoiesis sites in human. Yolk sac is the most predominant hematopoiesis tissue in fetus, while bone marrow is the common site for hematopoiesis during postnatal stage. Various bone marrows of long bones remain the predominant site for the production of various blood cells are the common sites in grown adult. This picture is adapted from Wikipedia.
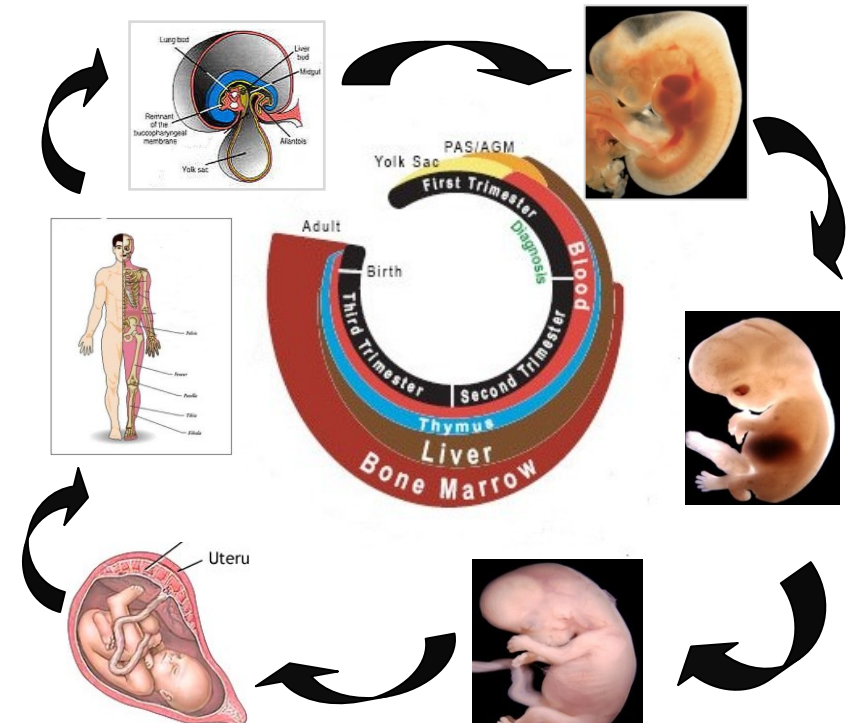


**Figure 1.3.2b.** Hematopoiesis in humans.Schematic diagram showing the predominant hematopoiesis tissues involved in production of different blood cells during various development stage in human life. This picture is adapted from Wikipedia.
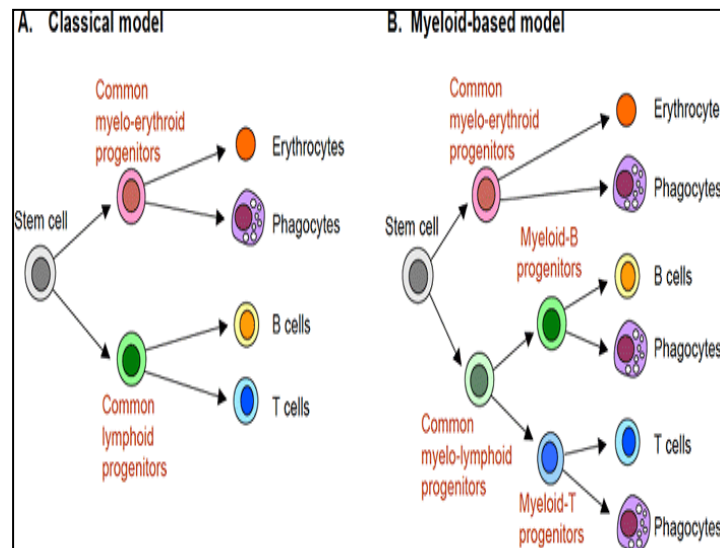


**Figure 1.3.2c.** Models of lineage commitment during hematopoiesis. **A.** Classic model. Hematopoietic stem cells diverge into common myelo-erythroid progenitors and common lymphoid progenitors. **B.** Myeloid-based model. The first branch point generates common myelo-erythroid and common myelo-lymphoid progenitors, and the myeloid potential persists in the T and B cell branches even after these lineages have diverged. This model postulates that specification towards erythroid, T and B cell lineages proceeds on the basis of a prototypical myeloid program. This picuture was adapted from RIKEN Press Release (2008).

**Figure 1.3.2d.** Cytokines involved in hematopoiesis.Diagram including some of the important cytokines that determine which type of blood cell will be created. This picture was adapted from Wikepedia.
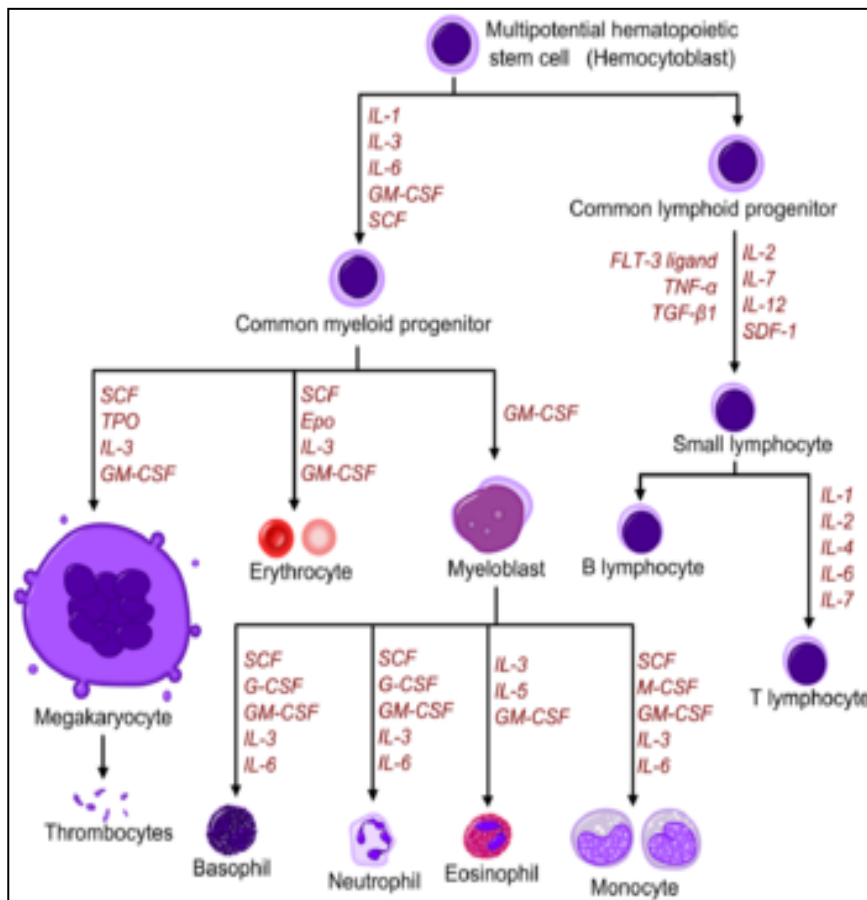


**Figure 1.3.2e.** Production of various blood cells in human. This picture was taken from New world Encyclopedia.
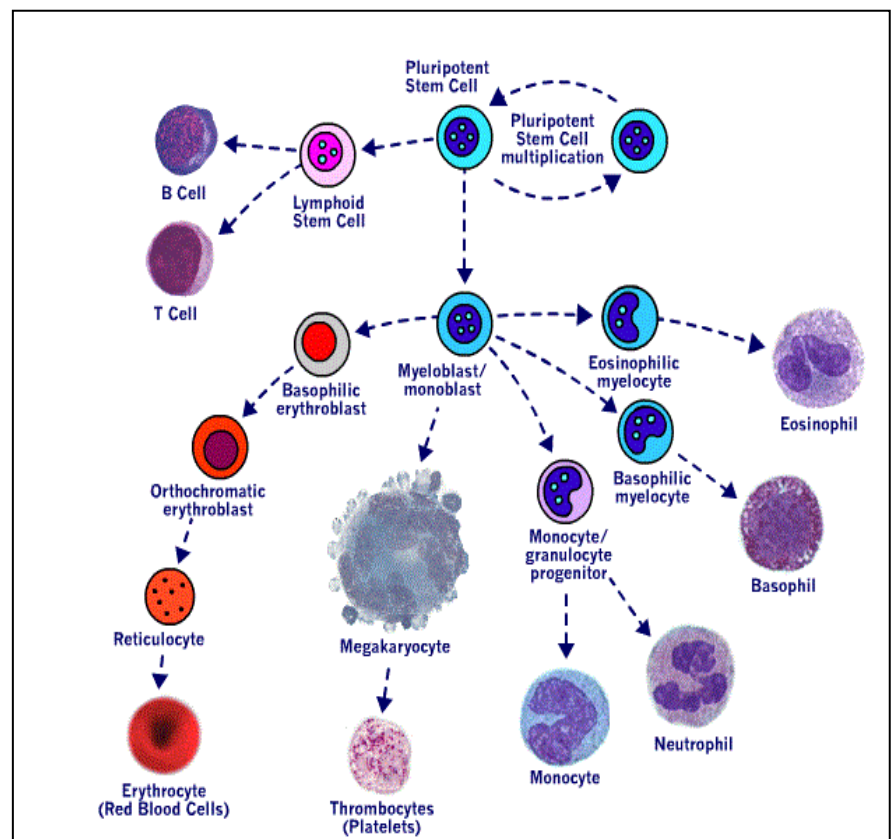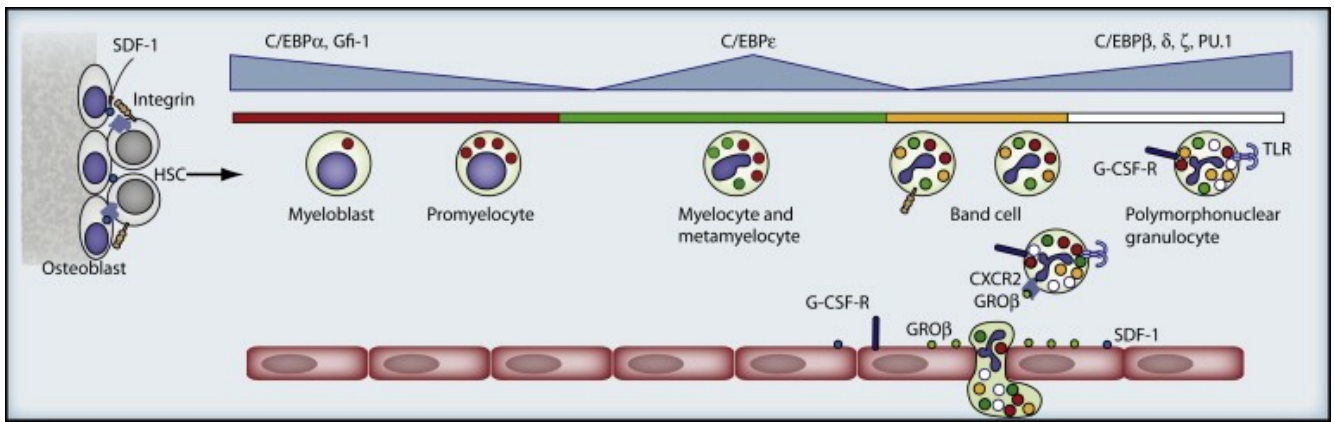
**Figure 1.3.2.f:** Granulocytopoiesis in the bone marrow. Stem cells present in the niches provided by osteoblasts and endothelial cells. The balance between PU.1 and C/EBPα and Gfi-1 expression determines the differentiation of cells into the granulocytic or the monocytic pathways. The different subsets of granules (azurophil (red), specific granules (green), and gelatinase granules (yellow) and secretory vesicles (empty) are formed sequentially during maturation from promyelocytes, determined by the expression of transcription factors indicated on the top of the figure. Retention and release of cells is determined by the balance between CXCR4 (favoring retention) and CXCR2 (favoring release) and their ligands SDF-1, and KC and Groβ, respectively. G-CSF stimulates neutrophil release directly by effects on the neutrophil and indirectly by reducing the SDF-1 expression and enhancing the expression of Groβ on endothelial cells. This picture was taken from Journal of Immunity, 2010, 33(5): 657-70

## 1.3.3 Life cycle of neutrophils

The neutrophils life cycle can be categorized into three phases, the bone marrow phase, followed by a circulating phase and ending with a tissue phase. Within the bone marrow phase, neutrophils originate from self-renewing myeloid stem cells which give rise to myeloblast which inturn differentiate into prometamyeloblast (azurophils granule formation), myelocytes (specific granule formation), metamyelocytes, at which stage the cell division terminates while the development of granules continues. Terminally differentiated neutrophils are released from the bone marrow (figure 1.3.3a; figure 1.3.3b and table 1.3.3a). The entire bone marrow phase for neutrophils last for approximately 14 days. About 60% of all nucleated cells in the bone marrow belong to the myeloid series. The bone marrow comprises a reserve pool of mature neutrophils that contains roughly 20 times the number of neutrophils in the

circulation. During infections, the cells are released sooner (up to $10^{12}$ per day instead of $10^{11}$ per day in normal condition (Kuijpers 2001). The neutrophils released from the bone marrow enter the next phase, the circulating phase. In the circulation, neutrophils have a half-life of 6-9 hours. Neutrophils comprise more than 50% of circulating leukocytes and more than 90% of circulating phagocytes. Within the circulation, PMNs exist in two pools in a dynamic equilibrium: a circulating pool and a marginated pool, the latter believed to be sequestered within the microvasculature of many organs. They move reversibly from circulating pools and margination pool (capillaries of certain tissues like lungs). The main function of marginated neutrophils is to be mobilized rapidly in response to infection or other stress (Hallett, MB,2001). During steady-state granulopoiesis, roughly $10^{11}$ neutrophils are released into the blood stream daily. Tissue phase is the last phase in the life cycle of neutrophils, were these cells leave the blood stream and entre the inflammatory area with help of chemotatic gradients (figure 1.3.3a). The main purpose of this phase is to kill tissue bacteria and fungi. Once they destroy the microorganism, they undergo apoptosis and are cleared by tissue macrophages. In normal body conditions, the neutrophils extravaste in the lungs, the oral cavity and into the gastointestinal tract and are cleared in this way (Hallett, MB, 2001)

In the resting uninfected host, the production and elimination of neutrophils are balanced, resulting in constant number of peripheral blood neutrophils. Neutrophil turn over is under strict control, as demonstrated by the spontaneous apoptosis that neutrophils undergo before their removal by macrophage in the lung, spleen and liver (Hallett, MB, 2001). During pathogical conditions the number of circulating neutrophils dramatically increases even up to 10-fold because of either an accelerated release of neutrophils from the bone marrow combined with a stimulated maturation of immature neutrophils by CSF, or a demargination from lungs or the spleen. Under these conditions, the generation of specific chemotactic

agents triggers the migration of neutrophils to the site of infection, where their phagocytic activities and defensive functions are exerted (Hallett, MB, 2001).

The last three cell stages (the metamyelocytes, band cells and neutrophils. myeloblast) constitute the neutrophil storage pool (NSP). Once the neutrophils are produced they lose the ability to divide and their synthetic machinery becomes almost totally inactivated. The development and formation of neutrophil granules occurs in a sequential process during myeloid cell differentiation (figure 1.3.3a.). Granule formation begins in the early promyelocyte stage, a period during which the majority of nascent granules are rich in myeloperoxidase, an enzyme that catalyzes that formation of hypochlorous acid. These primary granules are also referred to as azurophilic, owing to their affinity for the basic dye azure A. They are functionally similar, although not identical, to lysosomes of other cells. Azurophilic granules maturation is largely complete at the myelocyte stage of neutrophil development, at which point, peroxidase negative granules begin to form. Based on their time of appearance and content, the latter are subdivided into secondary and tertiary granules. Specific granules developed in myelocytes and metamyelocytes are rich in lactoferrin, whereas gelatinase granules form in band stage and lack lactoferrin. A fourth category of granules, secretory vesicles, are smaller than the others and appear during the late stage band nuclear neutrophil segmentation. The content of granules is listed in the table 1.3.3b.
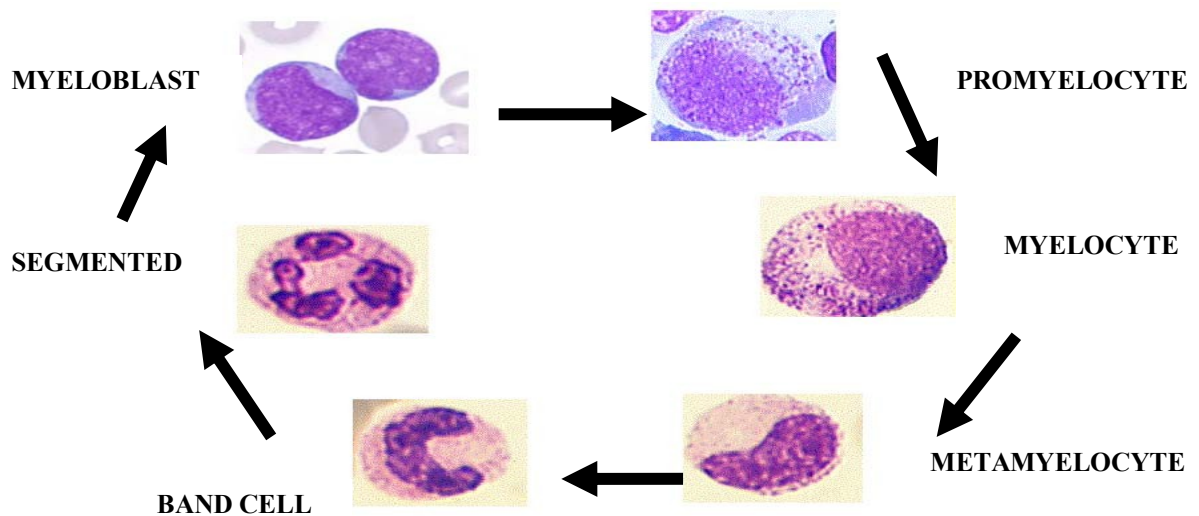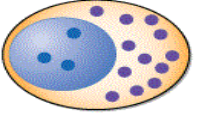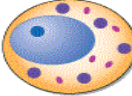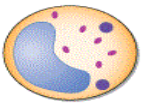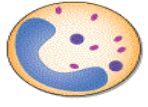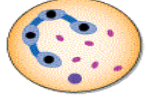
**Figure 1.3.3a.:** Shows the different cell stages during maturation of the neutrophil. The overall maturation scheme of the neutrophilic line consists of nuclear shrinkage and segmentation with concurrent condensation of the chromatin. This process begins with the formation of a functionally immature myeloblast and culminates with the development of a phagocytic-segmented neutrophil. This maturation takes about 15 days and occurs in the bone marrow. Adapted from www.googleimages.com.

**Table 1.3.3a. Stages in neutrophil development and morphological characters** (this table

was taken from Text Book of Physiology by Guyton 12th Edition)

| Stage of neutrophils development | Morphological characteristics |
|---|---|
| MYELOBLAST | Prominent round nuclei, relatively undifferentiated cytoplasm, high nuclear cytoplasmaic ratio, peroxidase found in RER, golgi, matured azurophil granules. (Blue-red in Wright's, 3-5 mitotic divisions). |
| PROMYELOCYTE | Production and accumulation of many peroxidase positive sheroidal ellipsoidal azurophil granules (~05μm) with cystalline centers, peroxidase also in RER and Golgi,peroxisomes appear (catalase). |
| MYELOCYTE | Production and accumulation of peroxidase negative specific granules (0.2 μm spheres, 0.1 x1μm rods) other variable shapes, cell divisions now dilute azurophil granules so that specific granule are 2X more abundant. |
| META MYELOCYTE | Non- dividing, non –secretory. |
| BAND, SEGMENTED | Nuclear morphology changes, mitochondria are lost, surface receptors for activation become expressed 33% azurophil, 67% specific granules. |

| Cell | Stage | Surface Markers | Characteristics |
|------|-------|-----------------|-----------------|
| | MYELOBLAST | CD33, CD13, CD15 | Prominent nucleoli |
| | PROMYELOCYTE | CD33, CD13, CD15 | Large cell Primary granules appear |
| | MYELOCYTE | CD33, CD13, CD15, CD14, CD11b | Secondary granules appear |
| | METAMYELOCYTE | CD33, CD13, CD15, CD14, CD11b | Kidney bean–shaped nucleus |
| | BAND FORM | CD33, CD13, CD15, CD14, CD11b CD10, CD16 | Condensed, band–shaped nucleus |
| | NEUTROPHIL | CD33, CD13, CD15, CD14, CD11b CD10, CD16 | Condensed, multilobed nucleus |

*a*CD= Cluster Determinant; ● Nucleolus; ● Primary granule; • Secondary granule.

**Figure 1.3.3b:** Stages of neutrophil maturation. Schematic diagram of different stages in maturation of neutrophils and its morphologic characters. This picture was taken from Harrison's Principle of Internal Medicine, 17th edition by Fauci AB et al, 2001.

**Table 1.3.3b. Content of neutrophil granules (adapted from Borregaard et al, 1996)**

| Granules | Membrane content | Matix content |
|----------|------------------|---------------|
| Azurophil granules | CD63, CD68. | Acid β glycerophosphatase, acid mucopolysaccharide, α1- antitrypsin, αmannosidase, azurocidin/ CAP37, heparin binding protein, bactericidal permeability, increasing protein, β-glycerophosphatase,β-glucuronidase, cathepsins, defensins, elastase, lysozyme, myeloperoxidase, N-acetyl-β- glucosaminidase, proteinase-3, sialidase. |
| Specific granules | CD15 antigens,CD66, CD67, cytochrome-b558, FMLP-R, fibronectin-R, G-protein α -subunit, Laminin-R, Mac-1 (CD11b/CD18), NB1 antigen, 19kD-protein, 155kD-protein, Rap1, Rap2, thrombospondin-R, TNF-receptor, vitronectin-R. | β2-microglobulin, collagenase, gelatinase,histaminases, heparanase, lactoferrin, lysozyme, plasminogen activator, sialidase, vitamin B12-binding protein. |

| Gelatinase granules | Cytochrome b558, diacylglycerol, deacylating enzyme, FMLP-R, mac-1(CD11b/CD18). | Actytranferase, β2-microglobulin, gelatinase, lysozyme. |
|---|---|---|
| Secretory vesicles | Alkaline phosphatase, CR1 (CD45), cytochrome b 558, FMLP-R, mac-1(CD11b/CD18), uroplasminogen activator-R, CD10, CD13, CC45, FcγRIII(CD16), C1q-receptor, DAF. | Plasma protein, including tetranectin. |

## 1.3.4  Morphology of neutrophils

Neutrophils are small, having a spherical diameter of approximately 10 micrometers (Wintrobe,1981). The cytosol is largely filled with 5 nuclear lobes connect by fine threads. They have hetergenous cytoplasmic granules that are storage pools for mostly cell-specific intracellular enzymes, cationic protein, receptors and discrete proteins. They have a water volume of approximately 346fl (Hempling 1973). The density of a typical neutrophils is 1.08-1.09 (Pertoft et al. 1960), making them denser than most other cells of myeloid lineage. This high density is due largely to the granules, which make up 15-16% of the cell by volume (Schmid-Schonbein et al. 1980) which are themselfs very dense (Bretz and Baggionlini, 1974). As previously described, the nucleus is the chief distinguishing feature of the neutrophils, occupying more than 20% of the cell volume (Schmid-Schonbein et al 1980). The nucleus is multi-lobed, with the number of lobes increasing from 2-5 as the neutrophils age (Kline. 1975, Mcdonald et al. 1978). The neutrophil cytoplasm is packed with three different types of granules (Boxer and Smolen 1988), each containing substances specific to particular functions performed by the cells (table 1.3.4).

By electron microscopy, approximately one third of the cytosol appears to be occupied by these organelles. However, in the living spherical neutrophils, this appears to be an underestimated, with the major part of neutrophil cytoplasm being occupied by nuclear lobes. In contrast, the nucleus plus perisomes, lysosomes and endosomes in live cells occupies only 9% of the cell volume. Another striking feature is that neutrophils contain virtually no mitochondria, and few ER and a golgi-like region which makes up less than 1% of the total volume of the average cell (Hallett 1989). These unique features distinguish the neutrophils from other white blood cells, and their isolation and identification depends on the density and morphology conferred by them.

**Table 1.3.4 Morphology of neutrophils**

| Parameter | Value | Species |
|---|---|---|
| Diameter | 10-15µm | Human |
| Volume | 346fl | Human |
| Organelle volume | | |
| Cytoplasm | 63% | Human |
| Nucleus | 21% | Human |
| Granules | 15.4% | Human |
| Mitochondria | 0.6% | Human |
| Water volume | 274fl | Human |

## 1.3.5 Receptors of neutrophils

Neutrophils also have a specific set of surface markers, including receptors for substance produced in the natural immune response, e.g Fcγ, C5a and C3bi. Another marker abundant on neutrophils surfaces is CD59. Since their interactions with the external milieu are crucial for innate responses, neutrophils have developed a recognition apparatus that is able to specifically bind a wide range of extracellular ligands (Hallett 1989). There are between 0.5-1

million of these receptors per neutrophils. There are also receptors for a range of inflammatory mediators, such as TNFα, interleukins and other cytokines and bacterial formylated peptides (the most commonly used analogue is a FMLP) and lipopolysaccharide (LPS, endotoxin). Following ligation of one or more types of surface receptors, neutrophils generate a number of activation steps, via the generation of a cascade of intracellular "second messengers." (Hallett 1989). These steps are biochemical events, which mediate the transmission of biological information between membrane receptors and various intracellular components, involved in specific effector functions. Consequently, neutrophil receptors are able to regulate a wide range of functions, including adhesion, migration, phagocytosis, survival, cell activation, gene expression induction, proinflammatory mediator release; and target cell killing (Hallett 1989).

The transduction machinery is mainly, but not exclusively, located in the plasma membrane; and is composed of a series of enzymes (i.e. kinases, phosphatases, adenylate cyclase, phospholipases and other enzymes involved in lipid metabolism) or regulatory proteins (G-protein subunits, channel proteins, anchoring and adaptor proteins) (Hallett 1989). This in turn, is regulated by several other second messengers (calcium ions, inositol phosphates, diacyglycerol, phosphatidate, cAMP, and so forth). A non- exhaustive list of neutrophil receptors includes

- Receptors for proinflammatory mediators (i.e. the anaphylotoxin complement component C5a, leukotriene B4 [LTB4], platelet-activating factor [PAF], substance P, and bacterial formylated peptides typified by FMLP);

- Receptors for cytokines such as interferon-γ (IFNγ), IL-1, IL-4, IL-6, IL-10, IL-13, IL-15, IL-18, TNFα, G-CSF, GM-CSF and many others;

- Receptors for chemokines, including those for IL-8/CXCL8 and GROα/CXCL1, called CXCR1 and CXCR2;

- Receptors/adhesion molecules for the endothelium (see later);

- Receptors for tissue matrix proteins and lectins; opsonin receptors, those for the Fc portion of γ-immunoglobulins (FcγRs); and for the major cleavage fragments of the complement system (CRs).

Neutrophils constitutively express the low-affinity FcγRs (FcγRIIA/CD32A and FcγRIIIA/CD16A), and when exposed to IFNγ or G-CSF, the high-affinity FcγR (FcγRI/CD64) as well. CR expressed by neutrophils are CR1 (also known as CD35), which binds to complement components C1q, C4b, C3b, and mannan-binding lectin (MBL); CR3 (α Mβ 2 integrin, CD11b/CD18, or MAC-1), which binds to iC3b, ICAM-1 and some microbes; CR4 (α Xβ 2 integrin, CD11c/CD18), which binds to iC3b (Hallett 1989). By expressing these latter receptors, neutrophils are able to recognize and bind, in a cooperative manner, IgG-opsonized particles and/or complement-opsonized microbes; and then activate their phagocytosis. Neutrophils also express a variety of pattern recognition receptors (PRRs). The latter represent an emerging class of sensors that function by recognizing the so-called pathogen-associated molecular patterns (PAMPs) (Hallett 1989). Neutrophils express all TLRs (with the exception of TLR3), whose activation has been shown to influence many functional responses. For instance, engagement of TLR can (a) modulate neutrophil expression of adhesion molecules; (b) regulate neutrophils recruitment directly through effects on chemokine receptor expression and indirectly through effects on CXCL8 generation by neutrophils themselves; (c) "prime" neutrophils for enhanced ROS production; and (d) prolong neutrophil survival both directly and indirectly (via monocyte) (Hallett 1989).

**Table 1.3.5.Receptors of neutrophils**

| Receptor | Cell response | Signal generated | Activation mechanism | Ligand type |
|---|---|---|---|---|
| 7TMR | Chemotaxis | Calcium, tyrosine | Occupancy | IL-8 |
| PAF | Degranulation | | | C5a |
| G protein SP coupled R | Oxidase activation | Phosphorylation<br><br>cAMP, actin polymerization | | FMLP |
| Selectin-carbohydrate residue | Rolling | | Aggregatoin | |
| Integrin R | Adherence, phagocytois | $Ca^{2+}$, tyrosine | Aggregation | C3bi |
| ICAM-1 | Oxidase activation, shape change | Phosphorylation, actin polymerization, | | |
| FcR immune complex | Adherence,<br><br>shape change | $Ca^{2+}$ , monomeric tyrosine | Aggregation | IgG |
| GCP-linked CD59 | | Calcium, tyrosine phosphorylation | Aggregation | CD16 |
| TNFα R | Priming | Tyrosine phosphorylation | Occupancy and aggregation | TNFα |
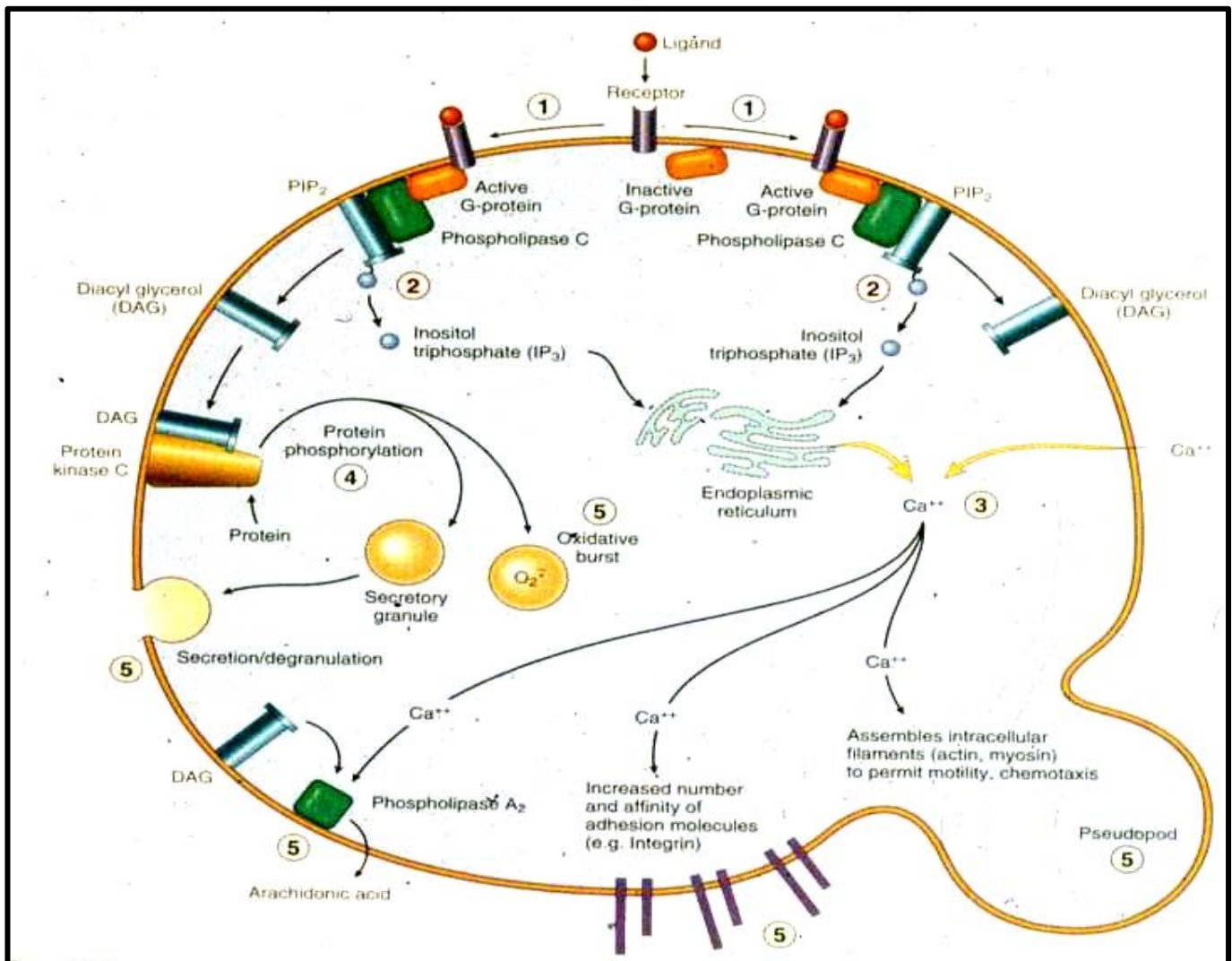
**Figure 1.3.5.** Schematic representation of various signals inside neutrophils. This picture was taken from Journal of Laboratory Investigation, 2000, 80(1): 198-201.

## 1.4 Kinetics of neutrophils

Inflammation is defined as a condition or state that tissues enter as a response to injury or insult (Seely et al. 2003). The neutrophils are the most important and the one of the most

extensively studied cell involved in the inflammatory response. As the principal circulating phagocytes, the neutrophils is the first and most abundant leukocyte to be delivered to a site of infection or inflammation; and is an integral component of the innate immune system (Seely et al. 2003). The kinetics of neutrophils from the circulation to the inflamed area is highly regulated which involves extensive interaction of adhesion molecules and receptors between the endothelial lining and the neutrophils. The migratory properties of white blood cells are indispensable to drive immune responses throughout the body. To ensure migration to the proper locations, the trafficking of leukocytes is tightly regulated. The migration and extravasation of leukocytes across the endothelium that lines the vessel wall occurs in several distinct steps, referred to as the multi-step paradigm, originally introduced by (Butcher 1991) and extended by Springer (1994b). The first step comprises the rolling of the leukocytes over the endothelial cells, mediated by transient weak interactions between adhesion molecules. Subsequently, loosely attached leukocytes are in such close proximity of the endothelium that they can be activated by cytokines, presented on the apical surface of the endothelium. Consequently, the activated leukocytes will spread and firmly adhere to the endothelium and finally migrate through the intercellular clefts between the endothelial cells to the underlying tissue. The recruitment of leukocytes from the blood is one of the most dramatic cellular responses to inflammation; and is central to the physiologic trafficking of leucocytes. The steps which neutrophils undergo in order to reach the inflammatory tissue are explained in detail in this section. Figure 1.4 shows the various steps involved during extravasation of neutrophils and the associated adhesion molecules and receptors.

## 1.4.1 Margination and adhesion (Step 1)

Neutrophils are partitioned in the blood between a circulating pool, present in large blood vessels, in the axial stream of small vessels and a marginating pool. In the absence of

inflammation, the marginating or physiological regional granulocyte pool (Peters 1998) comprises granulocytes transiently arrested in narrow, mainly pulmonary, capillaries. Neutrophils transmigration from the intravascular to the extravascular milieu predominantly occurs in the post capillary venule within the systemic circulation and in the capillary in the pulmonary circulation, tooth gingival junction in oral cavity. (Downey 1993).
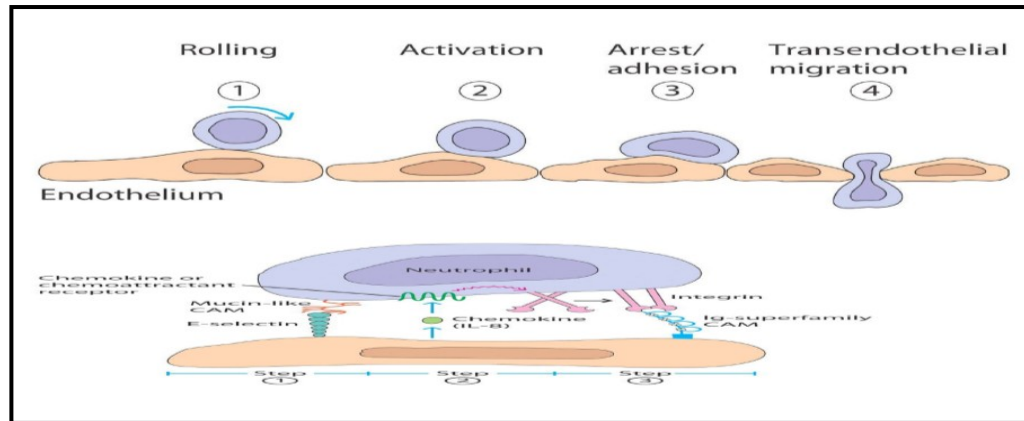


**Figure 1.4a.** Stages and molecules involved in extavasation of neutrophils. The molecules involved during this process are E and P selectin expressed on endothelium and the mucin family on neutrophils. The neutrophils roll over the endothelium. Signals induced by chemoattractant makes the neutrophils to attach firmly over the endothelium. Activation of integrins neutrophil movement is arrested and they finally attach firmly over the endothelial lining and finally enables the neutrophils to cross the endothelial barrier. This picture was taken from Robins Textbook of Pathology 12th Edition, 2001.
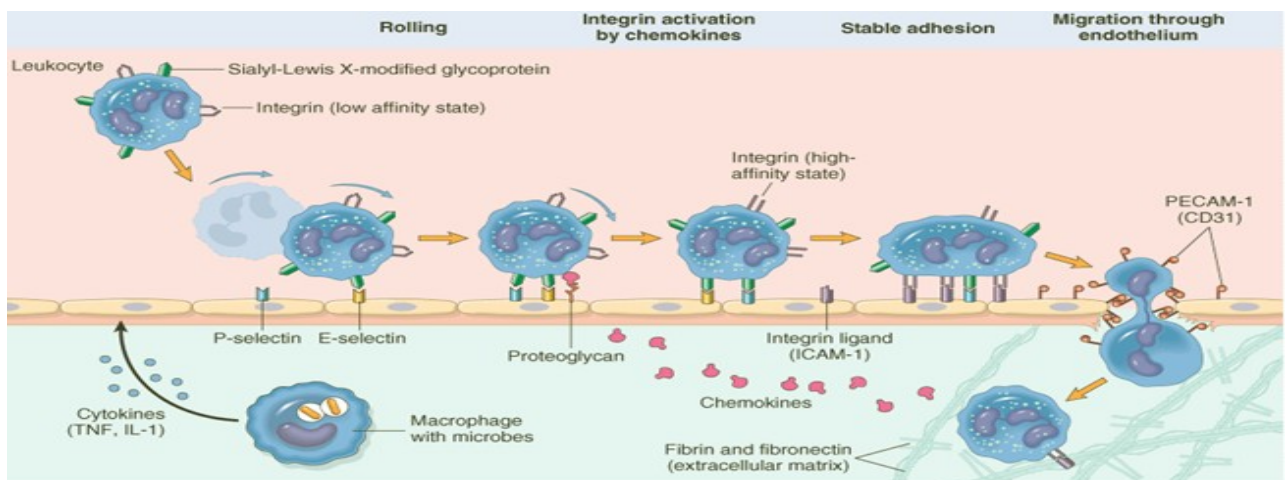


**Figure 1.4b.** Stages during extravastaion of neutrophils. Under inflammatory condition, endothelial cells express E and P selectin, as well as ligands on surface of neutrophils are L-selectin. The relatively weak interaction between selectins and their ligands results in a rolling motion of the neutrophils over the endothelium, slowing the cell down. The rolling neutrophils are activated by binding of its chemokine receptors to chemokines presented on the endothelial surface. Next, integrins are activated causing firm adhesion, which is followed by transmigration of the neutrophils throught the endothelial barrier. This picture was taken from Robbin's Text Book of Pathology, 12th Edition, 2001.

The first step  is margination or movement of the neutrophils from the central stream to the periphery of a vessel, in post-capillary venules. When the vessel diameter is 50% larger than the diameter of the leukocyte, erythrocytes move faster than the larger leukocytes, especially in the centre of the vessel, pushing neutrophils to the vessel periphery (Schmid-Schönbein et al. 1980). This margination allows for a molecular interaction between the cell surface of the neutrophils and endothelial cells to occur, resulting in neutrophils rolling onto the vessel wall. This initial event appears on the endothelium adjacent to the inflamed site, new adhesion molecules are expressed by the endothelium under the presence of inflammatory mediators released by damaged or infected tissues, which result in the local extravasation of leukocytes. In post-capillary venules or in pulmonary capillaries, the slow flow rate, futher reduced by vessel dilation at sites of inflammation, allows a loose and somewhat transient adhesion, referred to as tethering. During this tethering step, neutrophils respond to ligands, mainly chemokines, dispatched on the endothelium surface (Springer 1994a). This weak adhesive interaction between the neutrophils and endothelial cells allows the neutrophils to interact with the endothelium, which in turn results in the extravasation of neutrophils  (Premack and Schall 1996).

## 1.4.2  Adhesion to endothelium (Step 2)

The next step in movement of neutrophils is termed "rolling", which involves both physical and molecular forces. The ability to roll and adhere to endothelial cells is inversely proportional to the vessel shear rate and directly proportional to luminal red blood cell velocity (Blixt 1985; Firrell and Lipowsky 1989; Perry and Granger 1991). Once in proximity to the endothelial cell, a low-affinity adherence occurs and in conjugation with the shear stress of passing erythrocytes, the neutrophils begins to roll along the endothelial lining of the vessels.

The low affinity-rolling step is mediated by selectins and their ligands (table1.4.2). Selectins are a family of glycoprotein surface adhesion molecules and include L-selectin (expressed exclusively on leukocytes), E-selectin (expressed exclusively on endothelial cells) and P-selectin (expressed on platelets and endothelial cells). The ligands for neutrophil L-selectin are multiple sialylated carbohydrate determinates, which are linked to mucin-like molecules (Rosen 1993; Springer 1994c).

These selectin ligands on endothelial cells are inducible with a variety of inflammatory cytokines and lipopolysaccharide (Spertini et al. 1991). In addition to L-selectin-mediated rolling, endothelial cell expression of E-selectin is necessary for normal leukocyte recruitment and rolling (Mulligan et al. 1991; Kanwar et al. 1997). E-selectin appears on endothelial cells one to two hours after cell stimulation by IL-1, TNFα or lipopolysacharides (Lawrence and Springer 1993; Patel et al. 1995). E-selectin counter receptors include PSGL-1 and ESL-1 (E-selectin-ligand 1), a molecule highly homologous to the cystein-rich FGF receptor (CFR) and located on neutrophil microvilli (Sheerin et al. 1997), a location organized by the ERM proteins ezrin, radixin and moesin that connect to the actin cytoskeleton (Bruehl et al, 1997; Steegmaier et al, 1997; Buscher et al, 2010).

Defects in neutrophil selectin ligand expression due to a metabolic defect in a synthetic pathway common to all selectin ligands, leads to faulty neutrophil trafficking (LAD2). P-selectin, readily mobilized in a few minutes to the endothelial cell surface following stimulation by thrombin, histamine or oxygen radicals, interacts primarily with a mucin-like ligand, PSFL-1 (P-selectin glycoprotein ligand-1), located at the tip of leucocyte microvilli (Moore et al. 1995; McEver and Cummings 1997).

The kinetic of neutrophils recruitment in selectin-deficient mice suggests that P- and L-selectin contribute sequentially to leukocyte rolling and shows that L-selectin is involved in

prolonged neutrophil sequestration in inflamed microvasculature (Doyle et al. 1997; Ley et al. 1995; Steeber et al. 1998). Binding of PSGL-1 to P-selectin and E-selectin establishes the initial contact between neutrophils and activated endothelial cells. E-selectin and ESL-1 mediate the slower rolling, while E-selectin binding to CD44 mediates a redistribution of PSGL-1 and L-selectin to form clusters (Hidalgo et al. 2007) concomitant with further reduction in the speed of rolling.

The selectin-mediated bonds form and detach sequentially, but with sufficient strength to mediate attachment only  during the shear stress that is created by the laminar flow of blood in vessels (Ley et al. 2007; Papayannopoulos et al. 2010). Unlike P- and E- selectins, L-selectin is constitutively present on leukocytes. Its binding capacity is, however, rapidly and transiently increased after leukocyte activation (Li et al. 1998). So far, only one inducible L-selectin counter-receptor, specifically expressed on inflamed endothelium has been described, which bears the cutaneous lymphocyte antigen (CLA) (Tu et al. 1999).

In addition to its binding to endothelial ligands, leukocyte PSGL-1 is a counter receptor for leukocyte L-selectin and there is evidence that neutrophils roll, via L-selectin, on previously adherent neutrophils (Bargatze et al. 1994; Alon et al. 1996). This secondary tethering would synergistically enhance leukocyte accumulation on inflamed endothelium. However, other investigators have demonstrated that antibodies to P-selectin will attenuate rolling, but not impact on adherence (Bienvenu and Granger 1993). Blocking L-selectin in animal models reduced neutrophils mediated tissue injury, which  was belived to be dependent upon neutrophils adherence (Mulligan et al. 1994). In addition, soluble L-selectin shed from neutrophils may attenuate TNFα-stimulated neutrophils adherence and subsequent vascular permeability (erri 2002).

These studies suggest that selectins not only mediate rolling, but also impact upon ensuring leukocyte adherence (Witko-Sarsat et al. 2000). Selectins bind sialyl Lewis X carbohydrate structures expressed on their ligands (Somers et al. 2000). The signaling induced by binding of ligands to PSGL-1 and CD44 involves activation of Src family kinases Hck, Fgr and Lyn (Yago et al. 2010), which phosphorylate and activate ITAMs (immunoreceptor tyrosine-based activation motifs) on two adaptor proteins, DAP12 (NDAX activation protein of 12 kDa) and FcRγ (γ chain of immunoglobulin Fc receptors) (Zarbock et al. 2008).

These recruit Syk (spleen tyrosine kinase) that becomes activated by phosphorylation. Activated Syk in turn activates Bruton tyrosine kinase (Yago et al. 2010; Mueller et al. 2010), which mediates the further activation of PLC-γ (phospholipase C γ), PI3K (phosphoinositide 3-kinase) and p38 mitogen-activated protein kinase, resulting in integrin activation and cytoskeletal rearrangements in the neutrophil (Ley et al. 2007; Barreiro and Sánchez-Madrid 2009; Woodfin et al. 2010). Table 1.4.2 lists the adhesion molecules and receptors involved in the extravasation of neutrophils. Figure 1.4.2 is a schematic representation of the interaction of selectins during the extravasation of neutrophils.

**Table 1.4.2.  Neutrophil and endothelial cell adhesion receptors**

| Receptors | Cell | Ligand | Cell type | Purpose |
|---|---|---|---|---|
| L-selectin | Neutrophils | sLe$^a$, sLe$^x$ | Endothelium | Rolling and weak adhesion of neutrophils on endothelium |
| CD11a/CD18 | Neutrophils | ICAM-1, ICAM-2, ICAM-3 | Endothelium | Adhesion of neutrophils on endothelium |

| CD11b/CD18 | Neutrophils | ICAM-1 | endothelium | Adhesion of neutrophils on endothelium |
|---|---|---|---|---|
| | | iC3b | complement | |
| | | fibrinogen | | Phagocytosis |
| | | factor X | | |
| CD11c/CD18 | Neutrophils | iC3b | Complement | Phagocytosis |
| E-selectin | Endothelium | sLe$^x$ | Neutrophils | Firm neutrophils on endothelium adhesion |
| P-selectin | Endothelium, platelets | sLe$^x$ | Endothelium | Firm neutrophils on endothelium adhesion |
| | | PSGL-1 | neutrophils | Firm neutrophils on endothelium adhesion |
| PECAM-1 | Endothelium neutrophils | CD31/$\alpha_v$ | Leukocytes | Diapedesis of neutrophils through endothelium |
| ICAM-3 | Neutrophil | CD11a/cd18 | Leukocytes | Antigen presentation |
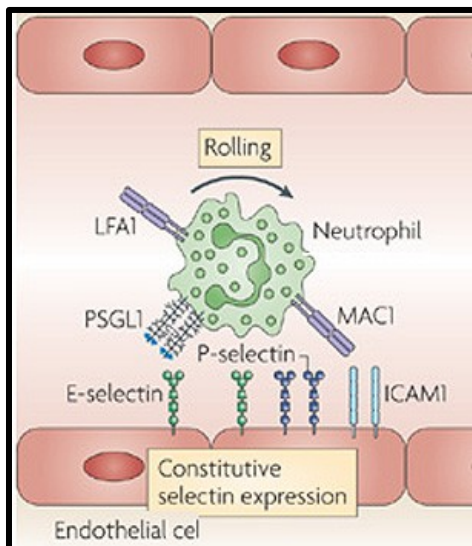


**Figure 1.4.2.** Interaction of neutrophils and endothelial cells. Neutrophils roll on constitutively expressed P-selectin and E-selectin on the dermal vasculature by interacting with ligands, such as P-selectin glycoprotein ligand 1 (PSGL1).  L-selectin, expressed on leukocytes and P-selectin, expressed on activated platelets and endothelial cells, with their common leukocyte ligand, P-selectin glycoprotein ligand-1 (PSGL-1). These rapidly reversible interactions mediate rolling adhesion of leukocytes on vascular surfaces during inflammation. L- and P-selectin bind to the same N-terminal region of PSGL-1 but with different affinities. This picture was adopted Nature Reviews Immunology, 2009, 9: 364-375.

### 1.4.3 Firm adhesion and spreading (Step 3)

During rolling, the cell surface of the neutrophil determines its ability to undergo 'adherence'. In contrast to rolling, which is a dynamic low-affinity adhesive interaction, adherence is a stationary high-affinity (strong) adhesive interaction between the neutrophil and endothelial cell. This interaction is largely mediated by a separate set of adhesion molecules, namely the integrins $\beta_2$ subfamily (CD11a, CD11b, CD11c/CD18) and their ligands (ICAM-1). The importance of integrin-mediated adhesion to neutrophil delivery and host defense was first demonstrated in patients with leukocyte adhesion deficiency type 1 (Anderson and Springer 1987)  and in animal models (Fischer et al. 1983; Anderson et al. 1984; Sligh et al. 1993). The interaction of neutrophils with integrin is unique which differ from monocytes and lymphocytes, which also interact via $\alpha_4\beta_1$ integrin with endothelial VCAM-1.

Integrins are a family of heterodimeric proteins (made up of two different subunits, namely α-subunits and β-subunits) that are expressed on the cell surface; and are integral to the process of cell adhesion. Of this family, the $\beta_2$-integrins are restricted to leukocytes and are essential for normal leukocytes trafficking. They consist of three distinct α-subunits (CD11a, CD11b, and CD11c) that are bound to a common β-subunit (CD18). Although the distribution of $\beta_2$-integrin subclasses differs among leukocyte populations, neutrophils express all three classes (figure 1.3.3). The relative contribution of each α-subunit to leukocyte adherence may vary and depend upon the stimulus leading to adherence and transmigration (Granger and Kubes 1994). Neutrophil integrins interact with complementary surface molecule ligands on endothelial cells in order to generate the high-affinity bond that characterizes adherence. Particularly important to neutrophils, intercellular adhesion molecule (ICAM)-1 on endothelial cells serves as the ligand for both CD11a/CD18 and CD11b/CD18, whereas ICAM-2 is capable of binding CD11a only (Zimmerman 1992).

The regulation of $\beta_2$-integrin avidity (clustering) involves interactions of both α and β chain cytoplasmic tails with the cytoskeleton (Van Kooyk et al. 1999) and the membrane association of cytohesin-1, a guanine nucleotide exchange protein that binds to the cytoplasmic portion of CD18 (Kolanus et al. 1996; Nagel et al. 1998). During the initial rolling on endothelial cells, integrin "activation" signals are also given by chemoattractants displayed on the endothelial membrane and presumably also by the engagement of selectins and their counter-receptors. The ligation of L-selectin (Simon et al. 1995) or PSGL-1 interaction with P-selectin (Yago et al. 1999) signal neutrophil adhesive functions, via CD11b/CD18 integrins (Brenner et al. 1996; Steeber et al. 1997). However, signaling pathways that lead to integrins switching to an active conformation differ with the stimulating agonist and are still incompletely characterized (Capodici et al. 1998; Jones et al. 1998; Blouin et al. 1999).

The $\beta_2$ integrins are unable to interact with their physiological ligands in unstimulated neutrophils, a safety mechanism that controls acute and chronic inflammatory responses. The ligand binding capacity is acquired upon activation signals ("inside-out signaling") that lead to integrins clustering and to a transition of a $\beta_2$-integrin subpopulation to a high affinity state (Rieu and Arnaout 1996; Stewart and Hogg 1996). Various agonists trigger CD11b/CD18 activation in neutrophils, including chemoattractants (PAF, IL8, FMLP, C5a), cytokines and growth factors (TNFα or GM-CSF); and bacterial products (formylated peptides and lipopolysaccarides). Integrins transmit signals triggered by their clustering and multiple engagements with adhesion substrates ("outside-in signaling") into the cell cytoplasm. Neutrophils integrate these integrin engagement and signals, delivered simultaneously by inflammatory cytokines or chemoattractants, to activate a cascade of intracellular events resulting in cell spreading and tight adhesion of neutrophils to the endothelium.

Intergrin activation is also necessary for neutrophil, locomotion, degranulation and oxidative burst. These outside-in transduction pathways also include the activation of various tyrosine kinases (Berton 1999a; Fuortes et al. 1999; Lowell and Berton 1999), CD11b/CD18 promotes antibody-dependent phagocytosis (Todd and Petty 1997) by interacting with Fc$\gamma$ RIIIb. Moreover, activation of integrins plays a vital role in generation of pro-inflammatory mediators (CD14) interaction with CD11bCD18 only occurs in the presence of lipopolysaccarids and binding protein and may play a role in the generation of pro-inflammatory mediators (Zarewych et al. 1996; Petty and Todd 1996; Todd and Petty 1997).
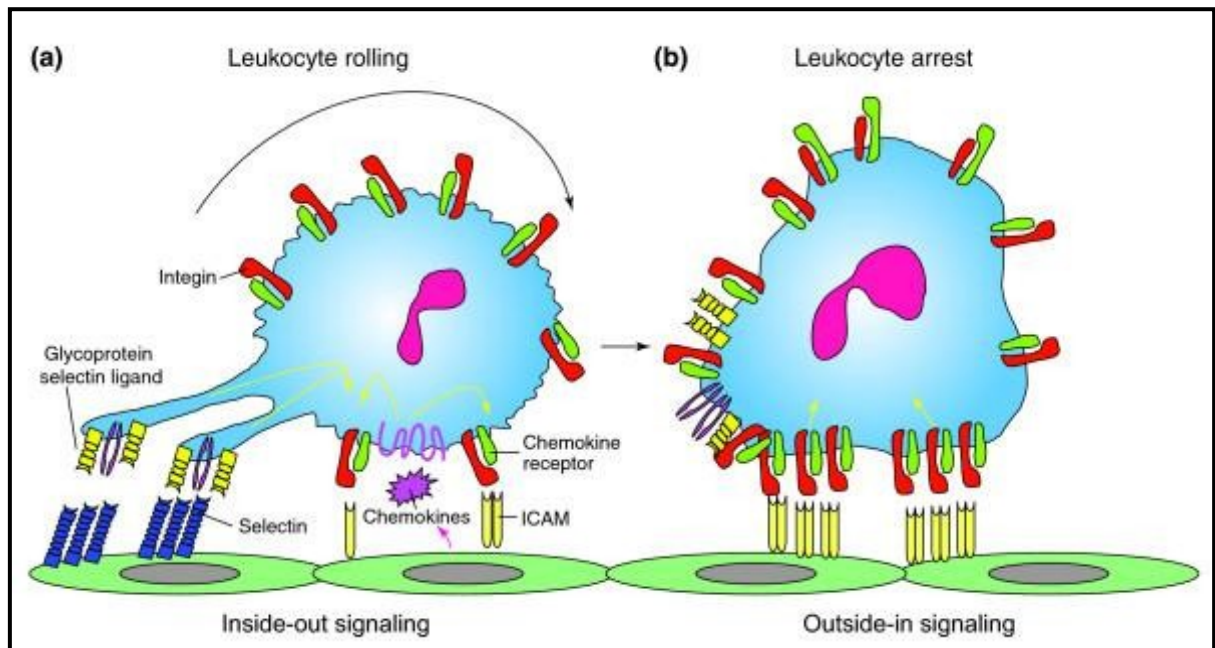


**Figure 1.4.3.** Leukocyte recruitment to the endothelial surface. **(a)** Binding of glycoprotein selectin ligands (yellow and purple) on the leukocyte to selectins (blue) on the endothelial surface, and weak binding of low-affinity leukocyte integrins (green) to ICAMs (pale yellow) on the endothelium facilitates cell tethering and rolling. This binding, together with signals from chemokines (pink), generates inside-out signals (yellow arrows) that shift the bound integrins to a high-affinity ligand-binding state. **(b)** Leukocyte arrest is mediated by clusters of high-affinity integrins (red) binding to ICAMs on the endothelial cells. These focal clusters can themselves signal outside-in to affect functions, such as cell polarization and migration. This picture was taken from Genome Biology 2007, 8(5): 215.4-215.8.

## 1.4.4　　　Extravasation or diapedesis (Step 4)

The mechanism of leukocyte migration across the endothelium is a complex multistep process (Springer 1994b). Extravasation or diapedesis is the final step by which leukocytes migrate, either between two or three adjacent endothelial cells, across the endothelial cell body or through the endothelial cell (Feng et al. 1998). Still, it is not clearly understood which one of the three routes neutrophils take. However, extravasation requires modifications of endothelial cell-to-cell adherent junctions and the disorganization of the junctional components, like VE-cadherin, β-catenin, plakoglobin and the reorganization of actin filaments, which have been observed in the vicinity of regions of firm adhesion between neutrophils and endothelial cells (Del Maschio et al, 1996) .

Two cell adhesion molecules of the Ig-superfamily (CAMs) has been shown to be involved in leukocyte transmigration, the platelet endothelial cell adhesion molecule-1 (PECAM-1 or CD31) and, more recently, the junctional adhesion molecule (JAM) (Muller et al. 1993; Vaporciyan et al. 1993; Martin-Padura et al. 1998). PECAM-1 is expressed both on the neutrophil surface and at the endothelial cell junction and mediates neutrophil extravasation via PECAM-1/PECAM-1 homophilic interactions. A "zipper" model has been proposed to account for a transmigration of leukocytes that maintains the permeability barrier of the endothelial cell monolayer (Muller et al. 1993).   The JAM is selectively concentrated at inter-endothelial tight junctions but is not present on neutrophils.

Finally, PECAM-1 is able to transduce signals into the cell and its dimerization, by antibody cross-linking, increases CD11b/CD18 binding capacity via an inside-out signal transduction that involves PI3-kinase (Berman and Muller 1995; Pellegatta et al. 1998). In addition, it has been shown that adherent leukocytes transmigrate by an increase in intracytoplasmic calcium levels in endothelial cells. This in turn activates MLCK (myosin light-

chain kinase), resulting in myosin skeleton reorganization and retraction of the cell body (Hixenbaugh et al. 1997),  which leads to increases in the gap between the endothelial cells. But this phenomenon takes place only in endothelial cells adjacent to transmigrating leukocytes and facilitates leukocyte migration across the endothelial monolayer (Su et al. 2000).  Figure 1.4.4 represents the two possible routes that neutrophils may take in order to cross the endothelial lining.
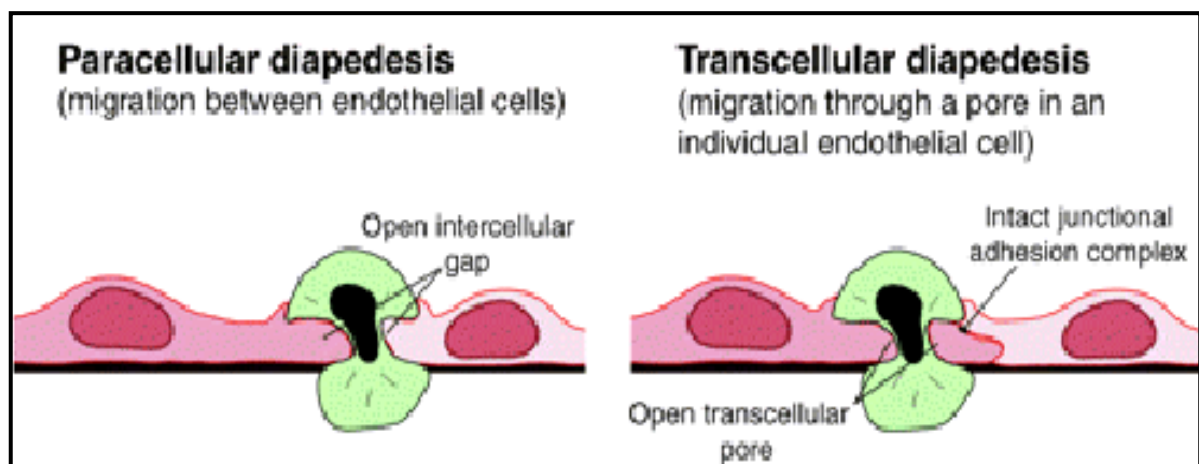


**Figure 1.4.4.** Paracellular and transcellular routes of leukocyte diapedesis. Trafficking of leukocytes throughout the body requires their movement into (intravasation) and out of (extravasation) the vascular and lymphatic circulation. Finally leukocytes cross the endothelial barrier (diapedese) and enter the interstitium.  The process of diapedesis, whether during intravasation or extravasation, can occur by two distinct pathways: paracellular or transcellular. Paracellular diapedesis. Leukocytes and endothelial cells coordinately disassemble endothelial cell-cell junctions and open up a gap between two or more endothelial cells (Muller, 2003). Transcellular diapedesis. Leukocytes migrate directly through individual endothelial cells via a transient transcellular pore that leaves endothelial cell-cell junctions intact. This picture was adapted from Journal of Cell Science, 2009, 1(5); 3025-3035.

## 1.5   New concept in extravasations of neutrophils

Transendothelial migration was described first almost 200 years ago (Ley et al. 2007), but its molecular mechanisms were only discovered recently (Imhof and Aurrand-Lions 2004) and were

not included in the classical adhesion cascade (Butcher 1991; Springer 1994a). In recent years, through more detailed real-time imaging of leukocytes, a number of additional steps have been added to the cascade including "slow rolling" and "intravascular crawling" and a more multifaceted transmigration response (Woodfin et al. 2010). Slow rolling mediates the transition between primarily selectin-mediated rolling to integrin-mediated firm arrest and is induced via selectin signalling and LFA-1 (Ley et al. 2007).

The subsequent firm arrest of rolling leukocytes to the endothelial cells surface involves a complex regulation of integrin-affinity modulation, leading to the interaction of high affinity integrins with their endothelial cells adhesion ligands, as coordinated by surface bound stimulating factors, such as chemokines (Ley et al. 2007; Woodfin et al. 2010). This aspect of the leukocyte adhesion cascade has been extensively researched and reviewed (Ley et al. 2007; Rose 2007; Evans et al. 2009).

Post arrest, the lateral motility of leukocytes on the surface of endothelial cells, intravascular crawling, towards preferred sites of transendothelial cell migration (TEM) (Schenkel et al. 2004; Phillipson et al. 2006) is mediated via the integrin Mac-1; and has been reported as a key determinant of the route of leukocyte TEM, i.e paracellular vs transcellular (Phillipson et al. 2006). With respect to the latter, it is now widely accepted that leukocyte TEM can occur via both paracellular migration through endothelial cells junctions and the previously contentious model of transcellular migration, whereby leukocytes pass through the body of endothelial cells (Carman and Springer 2008; Carman 2009).

In addition, TEM is now accepted to be a component of a more compound leukocyte transmigration response, involving the collective penetration of leukocytes through the three distinct barriers of the venular wall, i.e the endothelium, pericytes and their associated basement membrane (Wang et al. 2006; Voisin et al. 2009). Figure 1.4.4, illustrates the key steps pre-requisite to and associated with neutrophil transmigration.

## 1.5.1 Intravascular leukocyte-endothelial cell interactions pre-requisite to transmigration

1. *Intravascular crawling*

Adherent leukocytes do not necessarily transmigrate at the point of initial arrest, but rather locomote laterally to preferred sites of TEM (Schenkel et al. 2004; Phillipson et al. 2006). This luminal crawling is dependent on $\beta_2$ integrins *in vitro* and *in vivo*; and its blockade increases the incidence of transcellular, as opposed to paracellular, TEM (Phillipson et al. 2006). Details of the mechanisms that mediate the transition from firm arrest to intravascular crawling remain unclear, but recent *in vivo* data suggests a role for the Rho family guanine exchange factor, Vav-1, in this response, which play active roles in the crawling of leuckocytes along the shear flow of the blood (Phillipson et al. 2009). Other molecules and mechanisms recently implicated in leukocyte motility include JAM-A (Weber et al. 2007; Alon and Ley 2008).

JAM-A has been implicated in leukocyte infiltration into inflamed sites in many inflammatory models (Weber et al. 2007), but the precise mechanism through which this occurs remains unclear. The strong endothelial cells junctional expression of JAM-A suggests that endothelial JAM-A may direct the movement of leukocytes through cell-cell junctions, via binding to its leukocyte ligand (Nourshargh et al. 2006; Woodfin et al. 2007a). However, there is also evidence for the involvement of leukocyte JAM-A in neutrophil transmigration *in vivo* and neutrophil JAM-A has been shown to mediate directional leukocyte migration *in vitro* (Corada et al. 2005; Woodfin et al. 2010). Such a role may facilitate leukocyte motility towards and through endothelial cells junctions, as well as leukocyte motility in the extravascular tissue in certain inflammatory scenarios (Woodfin et al. 2010).

2. *Formation of adhesive platforms and docking structures*

Endothelial cells are the critical substrate for the attachment and motility of leukocytes within the vascular lumen, thus actively facilitating the leukocyte transmigration response. The key feature of venular endothelial cells is the expression of endothelial cells adhesion molecules, such as ICAM-1 and VCAM-1, integrin ligands whose expression is enhanced on activated endothelial cells. Recent studies have shown that the expression of these molecules can be further regulated, resulting in the formation of pro-adhesive sites termed "endothelial adhesive platforms" (EAPs) (Barreiro et al. 2008) or sites that promote TEM, termed "docking structures" or "transmigratory cups" (Barreiro et al. 2002; Carman and Springer 2004). The latter are VCAM-1, ICAM-1, moesin, ezrin, tetraspanin and actin-binding protein enriched domains, that protrude from the surface of the endothelium to partially embrace adherent leukocytes (Barreiro 2007). Whilst the formation of "docking structures" appears to be triggered through interaction of endothelial cells adhesion molecules with their leukocyte ligands, the formation of EAPs is determined by the existence of pre-formed tetraspanin (e.g CD9, CD151 and CD81)-enriched microdomains (Barreiro et al 2007). Although the ability of leukocyte integrins to bind to their ligands, through affinity and avidity changes, has long been known to be regulated by conformational changes and membrane clustering (Bing-Hao Luo 2007; Evans et al. 2009).

3. *Transcellular or paracellular route?*

Classically, leukocyte transmigration was viewed as migration between adjacent endothelial cells. But two roads can be taken by neutrophils during transendothelial migration: the transcellular road, whereby neutrophils penetrate an individual endothelial cell, or the paracellular road, whereby neutrophils squeeze between endothelial cells. Studies using electron microscopy have provided evidence that leukocytes can migrate directly through the endothelial cell body (Feng et al. 1998). Irrespective of the routes, the key players involved in

guidance are again the major neutrophil $\beta_2$ integrins, LFA-1 and Mac-1; and their ligands ICAM-1 and ICAM-2. ICAM-1 is concentrated to the recently described tetraspanin-enriched microdomains to form so-called endothelial adhesive platforms. A recent study has shown that the cytoplasmic tail of ICAM-1, together with higher expression levels, is required for high transcellular transmigration (Yang et al. 2005). In fact, the truncation of the cytoplasmic tail of ICAM-1 was shown to direct leukocytes to a paracellular transmigration route. This difference in ICAM-1-dependency may be due to the presence of alternative adhesion molecules in endothelial junctions highlighted by a number of recent studies. An endothelial 'cup-like' structure, called a 'podoprint', has been shown to form around migrating leukocytes during initial stages of transcellular migration of lymphocytes (Carman et al. 2007). These podoprints are composed of ICAM-1 and VCAM-1 in a caveolin-rich structure, possibly linked to the cytoskeleton protein vimentin(Carman and Springer 2004; Nieminen et al. 2006) Mechanically, transcellular migration is driven by internalization of ICAM-1 by the caveolin-rich domains forming channels, through which leukocytes cross the endothelial cell body (Millan et al. 2006). Surprisingly, activated leukocytes also use PECAM-1 for transcellularmigration, whereas non-activated leukocytes ignore PECAM-1 during transmigration (Carman and Springer 2004; Nieminen et al. 2006). A cup-like structure also forms around activated leukocytes, but contains PECAM-1 in addition to ICAM-1. Thus, although mechanisms used for both routes of transmigration seem to differ, common adhesion molecules may be involved. The factors which influence the choice between the two migrating routes, however, remain to be found. Figure 1.5 shows the schematic diagram of the recently added steps in extravasation of neutrophils.

4. *Neutrophil-endothelial cell cross talk and signaling to junctions*

Leukocyte interactions with the endothelial surface trigger cellular and sub-cellular events that initiate and/or facilitate leukocyte passage through the endothelium. This includes

triggering the formation of endothelial cells adhesion molecule clusters in the form of docking structures described above, but also interaction of the associated molecules with the cytoskeleton via adaptor proteins such as vinculin, paxilin and ERM proteins (ezrin, radixin and moesin) (Barreiro 2007; Nottebaum 2008; Wittchen 2009). These events can link leukocyte-endothelial cells interaction to changes in endothelial cells contractility or junctional integrity (Nottebaum 2008; Alcaide 2009). The homophilic binding of VE-cadherin at endothelial cells junctions provides an essential means of regulating the stability of endothelial cells contacts, but also acts as a barrier to transmigrating leukocytes. Stimuli, such as histamine, thrombin, vascular endothelial growth factor and the adhesion of leukocytes via ICAM-1 ligation, can stimulate dissociation of VE-PTP from VE-cadherin; and a subsequent increase in tyrosine phosphorylation of VE-cadherin leading to decreased junctional VE-cadherin interaction and enhanced leukocyte TEM (Allingham et al. 2007; Alcaide et al. 2008).

**Figure 1.5.** Ilustrating the hypothetical sequence of events involved in regulation of neutrophil transmigration. As indicated by recent findings. **A**: Rolling leukocytes adhere and crawl on the luminal surface to the point of transmigration. Adhesive platforms and docking structures facilitate the subsequent TEM response, which may occur via the paracellular or transcellular route. Beyond the endothelium, neutrophils migrate through gaps between pericytes and permissive regions within the vascular basement membrane where expression of certain basement membrane constituents is lower than average. Migration through the basement membrane may involve neutrophil proteases such as neutrophil elastase and β1 integrins such as the laminin receptor α6β1. Once within the three dimensional matrix of the interstitium leukocytes utilise an amoeboid, integrin independent, form of motility. It is hypothesised that different types of inflammatory stimuli trigger different mechanisms of transmigration as illustrated in panels B and C. **B**: Activation of the endothelium by stimuli such as IL-1β stimulates a PECAM-1-, ICAM-2- and JAM-A-dependent transmigration, with each of these molecules mediating a specific step of the transmigration response. **C**: Activation of leukocytes and endothelium with stimuli such as TNFα triggers a transmigration response that is independent of PECAM-1, ICAM-2 and JAM-A, but may involve other junctional proteins such as ESAM. Under these conditions leukocytes may use either the paracellular or transcellular route, with both routes possibly involving invasive protrusions. Adopted from Current Opinion in Hematology 2010, 17(1); 9-17.

## 1.5.2   Neutrophil migration through endothelial cell

**A.** *Paracellular endothelial migration*

The molecular mechanisms mediating the paracellular migration of neutrophils have been worked out in great detail. The main players on endothelial cells are ICAM-1; ICAM-2; platelet endothelial cell adhesion molecule 1; junctional adhesion molecule A, B, and C; endothelial cell-selective adhesion molecule; poliovirus receptor—all belonging to the immunoglobulin superfamily—CD 99; CD 99L2 and VE-cadherin. PECAM-1; JAM A, -B, and -C; ESAM; CD99 and VE-cadherins form homotypic contacts to stabilize the endothelial cell junctions, but with the exception of VE-cadherin and ESAM, these adhesion molecules are also expressed on the neutrophil (PECAM-1, JAM A, CD99) and are capable of binding to proteins expressed on the neutrophil surface; and thus, assist the neutrophils in passage between the endothelial cells.

In addition, a number of molecules at endothelial cell junctions actively facilitate leukocyte transmigration via a paracellular route (eg PECAM-1, ICAM-2, CD99, ESAM and

JAMs) for which there is significant *in vitro* and *in vivo* evidence (Woodfin et al. 2010). Current research is to investigating the specific roles and mechanism of action of these molecules under different inflammatory conditions; and there is emerging evidence for the involvement of endothelial cell junctional molecules in multiple aspects of leukocyte transmigration, as exemplified in Table 1.5.2. All these findings suggested the following sequence of events:

ICAM-1 and ICAM-2 accumulate at the cell-cell junctions mediating neutrophil contact via their $\beta_2$ integrin partners (LFA-1 and Mac-1). ICAM-1 at the endothelial cell junctions guides neutrophils to these structures (Woodfin et al. 2009; Alcaide et al, 2009). Signals from ICAM-1 activate Src and Pyk-2 tyrosine kinases, which phosphorylate VE-cadherin and destabilize the VE-cadherin bonds, probably by preventing VE-cadherin from associating with $\beta$-catenin that mediates binding to the actin cytoskeleton via $\alpha$-catenin ((Ostermann.G 2002; van Buul et al, 2005; Allingham et al., 2007; van Buul and Hordijk, 2008; van Buul et al, 2010a), thus loosening the endothelial cell-cell junctions. ESAM may also play a role in the loosening of the endothelial cell junctions. Lack of ESAM, as demonstrated in the *Esam$^{-/-}$* mouse, results in decreased activity of the Rho signaling pathway in endothelial cells (Wegmann et al, 2006), which is known to destabilize endothelial cell junctions (Stamatovic et al, 2003).

Lack of ESAM results in decreased neutrophil transendothelial cell migration, as observed in both the mouse cremaster model (Wegmann et al, 2006) and in an ischemic-perfusion mouse liver model (Khandoga et al, 2009). ICAM-2 concentrated at the endothelial cell junctions further guides neutrophils to enter the endothelial cell junctions. Neutrophils accumulate at the entrance between endothelial cells if ICAM-2 is blocked or absent; and successful transmigration is inhibited correspondingly (Woodfin et al, 2009). Many knock out mice models have demonstrated the importance of PECAM-1 and JAM-A in paracellular migaration (Woodfin et al. 2010). Upregulation of the laminin receptor $\alpha_6\beta_1$ induced by PECAM-1 signaling assists the further migration through the perivascular basement membrane (Dangerfield et al. 2002;

Woodfin et al. 2009). Endothelial cell PECAM-1 may also interact with the GPI-linkedCD177 (NB1-antigen), which is upregulated on neutrophil surfaces from specific granules to facilitate transmigration (Sachs et al, 2007). The CD177-PECAM-1 interaction facilitates neutrophil transmigration with an efficacy that depends on a dimorphism of the PECAM-1 antigen (Bayat et al, 2010). Other significant advancements relate to the functions and signalling of JAMs listed in the table 1.5.2.a,b &c adapted from Woodfin A. et al. 2007 and Woodfin et al. 2007b
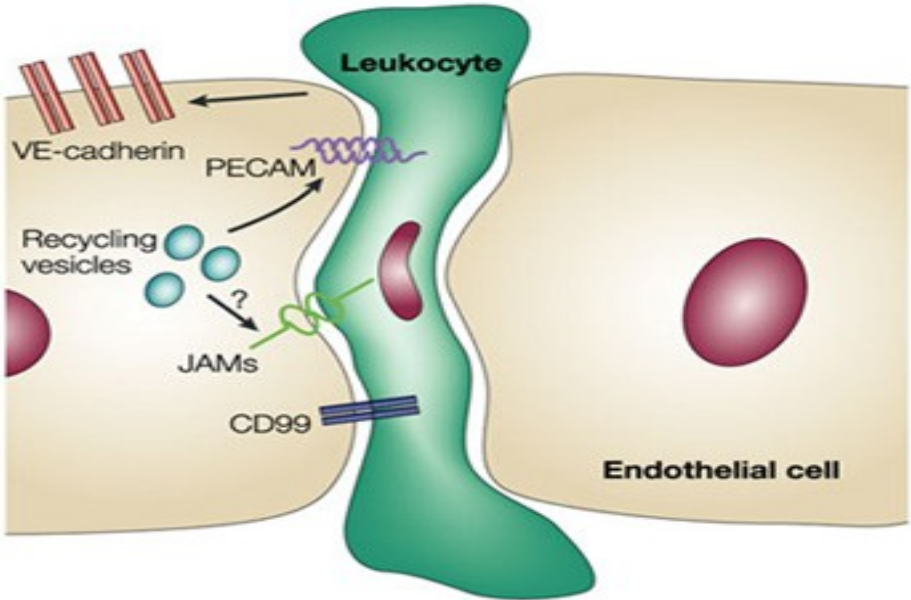


**Figure 1.5.2.a.** Molecules involed in paracellular transmigration of neutrophils. schematic diagram representing various junctional adhesion molecules properly involved during the paracellular transmigration of neutrophils. During their passage through the interendothelial cleft, leukocytes encounter different junctional proteins. During this process, vascular endothelial cadherin (VE-cadherin) tends to redistribute to the endothelial surface, whereas platelet endothelial cell adhesion molecule (PECAM) and junctional adhesion molecules (JAMs) are concentrated along the endothelial cell borders, probably as a result of targeted recycling of specific vesicles. CD99, a membrane protein that is present in endothelial cells and leukocytes, functions independently in directing leukocyte diapedesis through the cleft. Blocking both PECAM and CD99 leads to an additive inhibitory effect on diapedesis. Nature Reviews Molecular Cell Biology, 2004, 5; 261-270.

**Table 1.5.2a. Function of JAM-A**

| JAM-A | Early neutrophil transmigration | Hemophilic interaction with JAM-A and hetrophils interaction with LFA-1(Weber et al. 2007; Woodfin et al. 2007a; Wojcikiewicz. 2009) |
|-------|--------------------------------|-----------------------------------------------------------------------------------------------------------------------------------|
| JAM-C | Neutrophil transmigration | Interaction between endothelial cell JAM-C and leukocyte Mac-1 (Woodfin |

| | | et al. 2007a) |
|---|---|---|

**Table 1.5.2b. Role of various junctional molecules in diapediesis of neutrophils**

| Endothelial cell junctional molecules and specific roles | Associated transmigration response | Reference |
|---|---|---|
| **Leukocyte sub-type specificity**<br><br>PECAM-1 | TEM of monocytes, PMN cells but only some sub-sets of lymphocytes | (Woodfin et al. 2007b) |
| ESAM | Transmigration of PMN, but not lymphocytes | (Woodfin et al. 2007a) |
| CD99L2 | Transmigration of PMN, but not lymphocytes | (Woodfin et al. 2007a) |
| **Stimulus specificity**<br><br>PECAM- 1 | Transmigration-induced by IL-1β, $H_2o_2$ but not TNFα or HCL | (Woodfin et al. 2007b) |
| JAM-A | Responses induced by IL-1β and other cytokine | (Woodfin et al. 2007a) |
| ICAM-2 | Transmigration induced by IL-1β, but not TNFα | (Huang MTet al, Woodfin et al. 2009) |
| **Stage of migration**<br><br>ICAM-2 | Entry to the endothelial cell junction | (Woodfin et al. 2009) |
| PECAM-1 | Leukocyte migration through the endothelium and endothelial cell basement membrane, | (Woodfin et al. 2009) |
| JAM-A | Migration through endothelial cell junction | (Woodfin et al. 2007a; Woodfin et al. 2007b) |
| CD99 | Migration through EC at the stage distal to subsequent to that mediated by PECAM-1 | Schenkel AR, Lou O, 2009 |
| **Trans cellular migration**<br><br>JAMA-A | Associated with transcellular pores | Carman CV, 2009 |
| PECAM-1 | Associated with transcellular pores and contributes to transcellular migration | Carman CV, 2009 |

### B. Transcellular endothelial migration

The transcellular route is believed to be taken by about 20% of neutrophils, but may vary greatly among different tissues and depend on the stimulation of the endothelial cells *in vitro* set-ups (Woodfin et al, 2010). The mechanisms and incidence of transcellular TEM has recently been reviewed in detail, with a particular focus on the role of invasive leukocyte protrusions (Carman 2009). Transcellular TEM has been observed in a broad range of tissues including bone marrow, thymus, lymph nodes, pancreas and the blood brain barrier (Carman 2009); and *in vitro* assays have facilitated mechanistic investigations. They have also established a possible role for podosomes in guiding lymphocytes in crossing the endothelial barrier by locating the thinner peripheral areas of the cell, rather than the perinuclear region (Carman. 2007) (Carman, 2007; Woodfin et al, 2010). The nature and functional role of such leukocyte protrusions requires further investigation. It has also been suggested that SNARE proteins are essential in trafficking and fusion of intracellular organelles and exocytosis of granules and vesicles are essential in this process (Carman et al, 2007). It seems that the lateral migration of neutrophils mediated by Mac-1 favors paracellular migration, and transcellular migration increases from 20% to 80% in the absence of Mac-1, as determined in a mouse cremaster muscle preparation (Phillipson et al, 2008). In that study, the endothelial cell docking structures were demonstrated to progress to domes that finally swept around the neutrophil in a process similar to phagocytosis, thus indicating a very active role of the endothelial cell in transcellular migration.
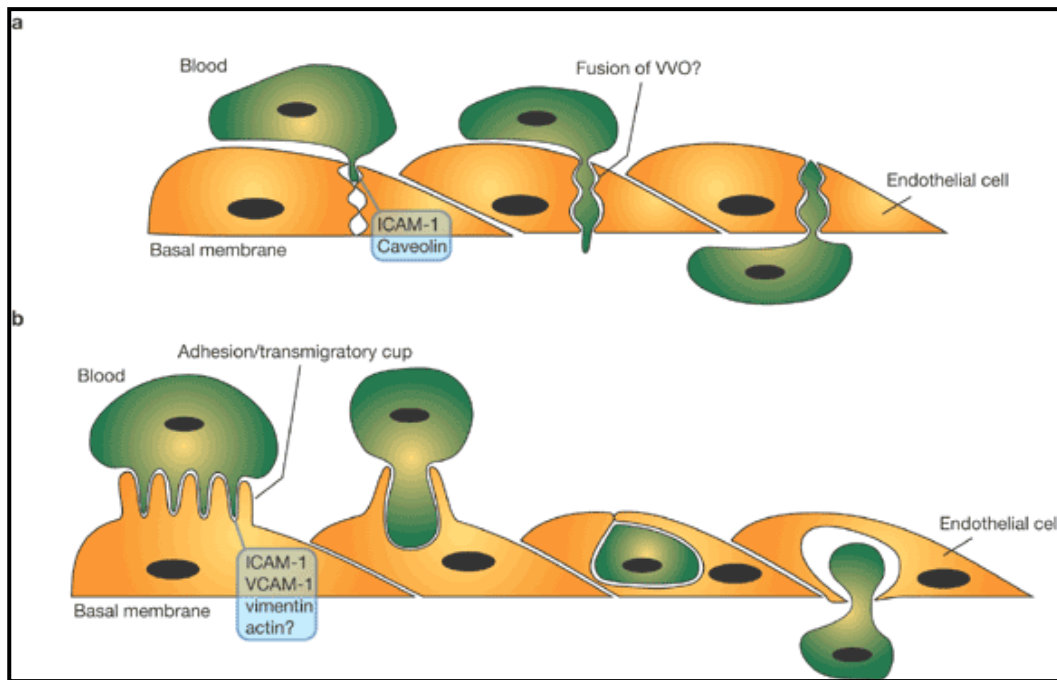
**Figure 1.5.2.b**(**a**). Various molecules involved in extravasation of neutrophils. Leukocytes may actively penetrate the endothelial cell cytoplasm by elongating pseudopods inside vesicles containing caveolin and ICAM-1. These vesicles can fuse with vesiculo-vacuolar organelles (VVOs), forming a channel that allows leukocyte migration through the endothelial monolayer. (**b**) When leukocytes adhere to the endothelial surface, an adhesion/transmigration cup is formed. This docking structure contains microvilli that elongate from both endothelial cells and leukocytes. The microvilli contain adhesion molecules (such as ICAM-1 and VCAM-1) and cytoskeletal proteins (such as vimentin and actin). The adhesion/transmigratory cup may mediate leukocyte phagocytosis and movement towards the basal membrane of endothelial cells.  Adopted from Nature Cell Biology  2006, 8; 105 – 107.

## 1.5.3  Neutrophil migration through venular walls beyond the endothelium

Once past the endothelium, migrating cells face two further barriers; the pericyte sheath and the tough venular basement membrane (Hirschi and D'Amore 1996; Rowe and Weiss 2008). Due to the difficulties associated with the isolation and culture of pericytes, little is known about the role of this cell type in leukocyte transmigration. There are, however, reports on the ability of neutrophils to migrate through the pericyte sheath, via both paracellular (Voisin 2009) and transcellular pathways (Feng 1998); though the associated mechanisms need to be fully elucidated. The mechanisms by which leukocytes penetrate the vascular basement membrane

also remains unclear, but depending on the vascular bed and the leukocyte sub-type could involve leukocyte receptors for basement membrane constituents (e.g β1 integrins, such as α2β1 and α6β1, receptors for collagen IV and laminins, respectively) and leukocyte proteases (e.g neutrophil elastase) (Hallmann,2005; Wang et al, 2006). The neutrophil is highly equipped with proteases capable of breaking down the basal membrane collagens and laminins, such as elastase (azurophil granules), MMP8 (specific granules), MMP9; and the membrane attached matrix metalloproteinase, MT6-MMP (gelatinase granules and secretory vesicles) (Kang et al., 2001). Additionally, it has recently been shown that the venular basement membrane contains pre-formed regions with low expression of certain basement membrane components (e.g laminin-8, laminin-10 and collagen IV), termed low expression regions (LERs), that are preferentially used by transmigrating neutrophils and monocytes (Voisin et al. 2009 ; ( Wang et al. 2006). It is possible that the same retraction of endothelial cells that opens the tight junctions subsequently allows passage through the basal membranes of a cell capable of amoeboid migration, such as the neutrophil, without necessitating degradation of the matrix (Rowe and Weiss, 2008). The complexity and diversity of leukocyte transmigration in different tissues suggests that mechanisms of leukocyte migration through the pericyte and basement membrane coverage of venules may similarly be diverse as governed at the molecular level (e.g composition of the basement membrane) and/or cellular level (e.g the phenotype and density of pericytes) (Woodfin et al. 2010).

## 1.6   Signaling by chemoattractants

In addition to intercellular adhesion, leukocytes require a chemoattractant gradient in order to complete the process of transmigration. Chemoattractants are soluble molecules that confer directionality on cell movement; cells migrate in the direction of increasing concentration of a chemoattractant in a process termed 'chemotaxis'. Neutrophils have long been known to undergo chemotaxis toward damaged or inflamed tissue (Seely et al. 2003). The production of

chemoattractants in the inflammatory environment is from a combination of sources, including bacterial by-products and cell wall constituents, complement factors and chemokines produced by inflammatory and non-inflammatory cells.  The endothelium of inflamed microvessels produces chemoattractants, such as platelet-activating factor (PAF), leukotriene B4 and various chemokines, immobilized via a "presentation molecule" (proteoglycan) on the luminal surface of endothelial cells. Among these chemokines, interleukin 8 (IL-8) specifically attracts neutrophils (Premack and Schall 1996; Rollins 1997)  and were unable to promote lymphocyte transmigration through endothelium (Roth et al. 1995) and has been demonstrated well in animal models (Sekido et al. 1993; Folkesson et al. 1995; Matsumoto et al. 1997). There is evidence that microvascular endothelial cells not only synthesize IL-8 in response to IL-1 or LPS, but also store IL-8 in Weibel-Palade bodies and release it upon stimulation by histamine or thrombin (Utgaard et al. 1998; Wolff et al. 1998).  Moreover, tissue-derived IL-8 is internalized by endothelial cells of postcapillary venules and small veins, transcytosed in a abluminal-to-luminal direction via plasmalemmal vesicles (caveolae); and presented at the tips of microvilli of the endothelial cell luminal surface (Middleton et al. 1997). Not only neutrophils and endothelium produce IL-8, monocytes, smooth muscle cells, epithelial cells and fibroblasts are also capable of generating IL-8 when they are stimulated with a pro-inflamatory agonist such as IL-1 or TNF-α (Seely et al. 2003). Chemoattractants serve not only to direct leukocytes to specific areas of inflammation, but also recruit specific subpopulations of leukocytes to inflamed tissue, such as neutrophils in response to acute bacterial infection, eosinophils at sites of chronic allergic inflammation or parasitic infection; and monocytes in chronic inflammatory diseases (Seely et al. 2003).

Chemoattractant mediators may thus be classified based on their spectrum of leukocyte activity (Table 1.6.a). Classical chemoattractants include N-formylated peptides produced by bacteria, such as FMLP, polypeptides (e.g. C5a) and lipids (e.g. leukotriene-B4), which act as

chemoattractants for various non-specific leukocyte populations (Schiffmann, 1975; Fernandez 1978; Ford-Hutchinson  1980). Extensive *in vitro* and *in vivo* investigation has identified IL-8 as a principal factor in neutrophil delivery (Huber 1991; Mulligan 1993; Smart  1994a; Smart 1994b).

Other chemokines that are specific for neutrophils include epithelial cell-derived neutrophil activating peptide; neutrophil activating peptide-2; growth-related oncogene (GRO)-α, GRO-β and GRO-δ; and macrophage inflammatory protein (MIP)-2α and MIP-2β. These chemokines are structurally similar and consist of the first two cysteine (C) amino acid residues separated by a separate amino acid (X); and are referred to as CXC chemokines or α chemokines (Premack and Schall 1996). Separate families of chemokines are known as CC chemokines, because the first two-cysteine residues are in juxtaposition. Monocyte chemoattractant protein-1, -2 and -3; MIP-1α and MIP-1β; and RANTES (regulated upon activation, normal T cell expressed and secreted) are members of the CC family, (or either expressed and secreted) predominantly oriented toward monocytes (Strieter RM 1994). Thus, chemoattractants help to explain how leukocytes localize to specific inflammatory sites and how specific leukocyte populations are recruited to those sites (Seely et al. 2003). Leukocyte delivery is further regulated by chemoattractant receptors that exhibit specificity for both the type of leukocyte on which they are expressed and the ligand to which they bind. The specificity of chemoattractant-induced leukocyte chemotaxis is related to differential expression of chemokine receptors, a superfamily of G-protein-coupled receptors with seven transmembrane regions (Yokomizo et al. 1997).

Although chemokine receptors share similar structures, they differ in their ligand specificity (Table 1.6.b). For example, IL-8 receptor A (CXC R1) and IL-8 receptor B (CXC R2) have a 78% identical amino acid sequence and both bind IL-8. However, although IL-8 receptor A is specific for IL-8, IL-8 receptor B has multiple agonists, including other CXC

chemokines, such GRO-α, GRO-β, GRO-δ, neutrophil-activating peptide-2; and epithelial cell-derived neutrophil activating peptide-78 (Seely et al. 2003). Neutrophil transmigration appears to depend to a greater degree on IL-8 receptor A than on IL-8 receptor B, because antibodies directed against IL-8 receptor A inhibited the majority (78%) of IL-8 induced chemotaxis (Hammond et al. 1995; Ahuja and Murphy 1996). In contrast, IL-8 receptor B has been implicated in the transendothelial migration of T cells (Babi 1996).

In addition, chemoattractant receptors are expressed on specific leukocyte subsets (Table1.6.c), CXC chemokine receptors are primarily restricted to neutrophils (Springer 1994c). Thus, chemokine receptors display both ligand and leukocyte specificity. These complex rules defining the interactions between specific chemoattractants and leukocytes are the mechanisms that allow the host response to deliver specific subsets of leukocytes to localized areas of infection or inflammation (Seely et al. 2003). Chemoattractant receptors not only mediate the process of chemotaxis, but changes in receptor expression within the inflammatory environment confer changes on cell function.

Ligation of chemoattractants to receptors activates phospholipases, via heterodimeric G proteins, resulting in intracellular $Ca^{2+}$ release, $Ca^{2+}$ channel opening and activation of conventional proteine kinase C isoforms (Premack and Schall 1990; Brockhaus et al. 1990). Tyrosine kinases (mainly Lyn of the Srk-family) (Ptasznik et al. 1996; Welch and Maridonneau-Parini 1997; Berton 1999b) and the GTP-binding protein Ras (Worthen et al. 1994)) are also activated. Ras activation triggers the MAPK/ERK cascade, which appears to be involved in various chemoattractant-induced neutrophil functions (Pillinger and Abramson 1995; Krump et al. 1997; Nick et al. 1997). Activation of small GTP-binding proteins of the Ras, Rac, and Rho families regulate actin-dependent processes, such as membrane ruffling, formation of filopodia and stress fibers, mediating cell adhesion and motility (Cox et al, 1997; Nobes and Hall, 1999, Benard et al, 1999;). Moreover, Rho family members relay signals from chemokine receptors

to the outside-in activation of integrins. The $Ca^{++}$- and DAG-independent protein kinase C-$\zeta$ has recently been proposed as a downstream effector of Rho signaling in this process (Laudanna et al, 1996, 1998).

Finally, chemoattractant receptors, via their coupled G-protein heterodimers, activate PI3-kinase, which is involved in the pathways leading to degranulation and NADPH-oxidase activation (Okada et al, 1994; Klippel et al, 1996; Thelen and Didichenko, 1997). The role of PI3-kinase in neutrophil adhesion promoted by G-protein-coupled receptors is not clearly defined (Akasaki et al, 1999; Shimizu and Huntiii, 1996). Specific PI3-kinase inhibitors block chemoattractant-induced neutrophil locomotion or homotypic aggregation, but have no effect on integrin CD11b/CD18 expression and activation triggered by these agonists (Niggli and Keller 1997; Capodici et al. 1998; Jones et al. 1998). Cross-talks between chemoattractant receptors and their signaling pathways may result in desensitization to one chemoattractant by another. In particular, signals delivered by "end target-derived" chemoattractant; such as formyl peptides, released by bacteria or by mitochondria from dying cells, or complement C5a, produced in their immediate surrounding are dominant and override "regulatory cell-derived" attractants, such as bioactive peptides (LTB4) or chemokines (IL-8) (Kitayama et al. 1997; Foxman et al. 1999). This will allow, for example, leukocytes recruited by endothelial-derived chemoattractants to migrate away from the endothelial agonist source towards their final target within a tissue.

In summary, the kinetics of neutrophils are highly regulated and involves multiple steps which involves interaction between neutrophils and endothelial cells. Involvement of adhesion molecules on both the cells cannot be ignored. Selectins, expressed by activated endothelial cells and leukocytes, bind to ligands on opposing cells. These interactions mediate leukocyte capture from flow and tethering to endothelium. The high dissociation/association rates of

selectins allow leukocytes to roll in the direction of flow and sense activation signals on the endothelial wall. Chemokines presented on luminal surfaces trigger rapid activation of leucocyte integrins, leading to rolling arrest and firm adhesion. Secondary adhesion events are mediated by leukocyte integrins [LFA-1 (leukocyte function-associated antigen 1), VLA-4 (very late antigen 4) and Mac-1], which bind to endothelial adhesion molecules, such as ICAM-1 and VCAM-1. (Figures 1.6).
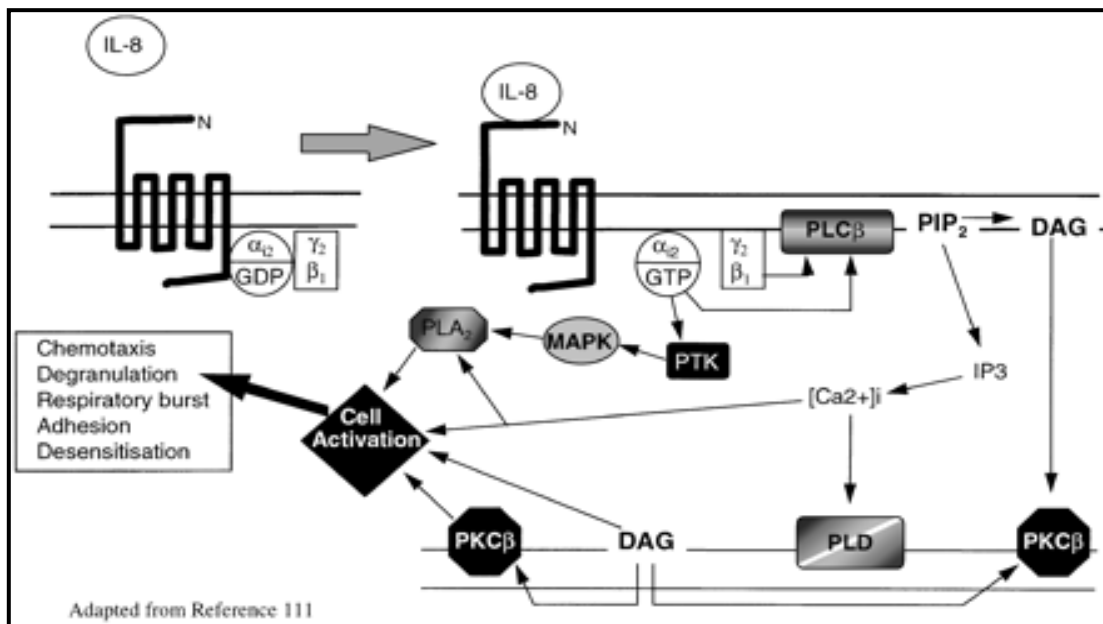


**Figure 1.6.** Model of chemokine receptor activation and signal transduction for IL-8 and neutrophils.IL-8 binding to CXCR1 or CXCR2 causes guanosine triphosphate displacement of guanosine diphosphate in the $G\alpha_{i2}$subunit, which allows dissociation of $G\alpha_{i2}$ from $G\beta\gamma$. $G\beta$ activates phospholipase C ($PLC\beta$), which cleaves $PIP_2$ into the second messengers DAG and $IP_3$. DAG activates $PKC\beta$, whereas $IP_3$ causes the release of calcium from intracellular stores. The rapid rise in intracellular calcium activates PLD. Meanwhile $G\alpha_{i2}$directly activates PTK. These activate MAP kinases and phosphorylate serine and threonine residues on the C-termini of CXCR1 and CXCR2, leading to receptor inactivation. MAP kinases activate phospholipase $A_2$. DAG, intracellular calcium, PKC and phospholipase A2 (PLA2) all interact with specific cell activation mechanisms, leading to cell motility, degranulation, release of superoxide anions and modification of integrin avidity. Adopted from Journal of Immunity, 2012, 5; 705-716.

**Table 1.6a. Neutrophil chemoattractants**

| Neutrophil specific | Neutrophil  non-specific |
|---|---|
| IL-8 | C5a |
| Granulocyte chemotactic protein (GCP)-2 | Tumor necrosis factor (TNFα) |
| Epithelial cell-derived neutrophil attractant (ENA)-78 | Monocyte chemoattractant protein (MCP)-1, MCP-2, MCP-3, MCP-4 |
| Neutrophil-activating peptide (NAP)-2 | f-Met-Leu-Phe (FMLP) |
| Growth-related oncogene (GRO)-α, GRO-β, GRO-γ | Macrophage chemotactic and activating factor (MCAF) |
| Macrophage inflammatory protein (MIP)-1, MIP-2 | Platelet-activating factor (PAF) |
| | Regulated upon activation, normal T cell expressed and secreted (RANTES) |
| Platelet factor (PF)-4 | I-309 |
| Mast cell-derived chemotactic factor | Casein |
| 5-Hydroxyeicosatetraenoic acid | Leukotriene-B$_4$ (LTB$_4$) |

**Table 1.6b.  Neutrophil chemoattractant receptors and their ligands**

| Class | Receptors | Ligands |
|---|---|---|
| C-X-C receptors | CXCR1 (IL-8 receptor A) | IL-8 |
| | CXCR2 (IL-8 receptor B) | IL-8, GRO, NAP-2, ENA-78, GCP-2 |
| | CXCR3 | Mig, IP-10 |
| | CXCR4 | SDF-1 |
| C-C receptors | CCR1 | MIP-1α, MIP-1β, MCP-3 |
| | CCR2A, CCR2B | MCP-1, MCP-3 |
| | CCR3 | Eotaxin, RANTES, MCP-3 |
| | CCR4 | MIP-1α, RANTES, MCP-1 |
| | CCR5 | MIP-1α, MIP-1β, RANTES |
| | CCR6 | MIP-3α |
| | CCR7 | ELC |
| | CCR8 | I-309 |
| Non-C-X-C | C5aR | C5a |
| | FMLPr | FMLP |

ELC, Epstein-Barr virus-induced molecule 1 ligand chemokine (CCL19); ENA, epithelial cell derived neutrophil activating peptide; FMLP, f-Met-Leu-Phe; GCP, granulocyte chemotactic protein; GRO, growth-related oncogene; IP, inducible protein; IP-10, interferon- γ inducible protein; MCP, monocyte chemoattractant protein; Mig, monokine induced by interferon- γ (CXCL9); MIP, macrophage inflammatory protein; NAP, neutrophil-activating peptide; RANTES, regulated upon activation, normal T cell expressed and secreted; SDF, stromal derived factor.

**Table 1.6c. Human neutrophil states: adhesion, chemotaxis, apoptosis and function**

| PMN state | PMN receptors | PMN functions |
|---|---|---|
| Circulating PMN (resting bloodstream PMN, collected by venipuncture) | Adhesion receptors: constitutive expression of L-selectin, PECAM-1 | PMN–endothelial cell interactions: baseline PMN rolling, adhesion on activated endothelium and transmigration |
| | Chemoattractant receptors: constitutive expression of IL-8 receptor A, IL-8 receptor B, C5aR | Chemotaxis: will undergo chemotaxis to PMN-specific and leukocyte nonspecific chemoattractants<br><br>Function: minimal PMN respiratory burst (ROI$^\bullet$) and microbicidal activity (proteolytic enzymes). |
| | Apoptosis receptors: constitutive expression of TNF-α receptor I, Fas, FasL | Apoptosis: constitutive apoptosis (PMN half-life ~6 h) |
| Primed PMN (PMN stimulated with priming agent *in vitro*) | Adhesion receptors: increased expression of CD11b, L-selectin, PECAM-1, ↔FMLPr | PMN–EC interactions: unclear impact on rolling, adhesion, diapedesis |
| | Chemoattractant receptors: ?IL-8 receptor A, ?IL-8 receptor B, ↔C5aR | Chemotaxis: no change in chemotaxis Function: when activated, display increased respiratory burst and microbicidal activity after activation |
| | Apoptosis receptors: ?TNF-α receptor I, ?Fas, ?FasL<br><br>Other: CD14, PAFr ↑LTB$_4$r, ↑PAFr | Apoptosis: delayed constitutive apoptosis |
| Activated PMN (PMN stimulated with activating agent *in vitro*) | Adhesion receptors: ↑ CD11b, ↑ FMLPr, ?L-selectin, PECAM-1 | PMN–endothelial cell interactions: ↑ PMN rolling and adhesion, ?transmigration |

| PMN state | PMN receptors | PMN functions |
|---|---|---|
| | Chemoattractant receptors: IL-8 receptor A, ↓↓ IL-8 receptor B, ↔C5aR | Chemotaxis: ↔chemotaxis to C5a, LTB$_4$/ZAS; ↑ ?chemotaxis to FMLP<br><br>Function: ↑ respiratory burst (ROI˙) and microbicidal activity (proteolytic enzymes); ↑ phagocytosis |
| | Apoptosis receptors: unknown Other: ↓ C3br, ↓ 1C3b | Apoptosis: delayed apoptosis |
| Exudate PMN (PMN collected from dermal exudate milieu *in vivo*) | Adhesion receptors: ↑ CD11b, ↑ Mac-1, ↓ L-selectin, ↓ PECAM-1 | PMN–EC interactions: unknown |
| | Chemoattractant receptors: ↓ IL-8 receptor A, ↓ IL-8 receptor B, ↑ C5ar<br><br>Function: ↑ FMLPr | Chemotaxis: ↑ baseline chemotaxis, ↓ chemotaxis to IL-8, ↑ chemotaxis to C5a<br><br>Function: ↑ respiratory burst (ROI˙), ↑ microbicidal activity and phagocytosis |
| | Apoptosis receptors: ↓ binding to TNF-α, ?↓ TNF receptor I, ↔Fas, FasL | Apoptosis: ↓ constitutive apoptosis; ↓ TNF-α-induced, but not Fas-induced apoptosis |
| Septic PMN (PMN collected from circulation in septic patients *in vivo*) | Adhesion receptors: ↓ L-selectin, ?CD11b, ?FMLPr, ?PECAM-1 | PMN–EC interactions: unknown |
| | Chemoattractant receptors: ↓ IL-8 receptor A, ↓ IL-8 receptor B, ↓ C5aR | Chemotaxis: ↓ chemotaxis to IL-8 and C5a<br><br>Function: ? ↑ respiratory burst (ROI˙), ?↑ microbicidal activity and phagocytosis |
| | Apoptosis receptors: ↓ TNF-α receptor I, ?Fas, ?FasL | Apoptosis: ↓ constitutive apoptosis; ↓ TNF-α-induced, but not Fas induced, apoptosis |
| Unresponsive or apoptotic PMN | Adhesion receptors: ↓ L-selectin, ?CD11b, ?PECAM-1 | PMN–EC interactions: no interaction |

| PMN state | PMN receptors | PMN functions |
|---|---|---|
| | Chemoattractant receptors: unknown | Chemotaxis: ↓ chemotaxis<br><br>Function: ↓ respiratory burst (ROI˙), ↓ phagocytosis |
| | Apoptosis receptors: ? ↓ TNF receptor I, ?Fas, ?FasL<br><br>Other: ↓ PAFr | Apoptosis: unresponsive PMN undergo apoptosis. and apoptotic PMN are unresponsive |

?, unknown/controversial; EC, endothelial cell; FasL, Fas ligand; FMLP, f-Met-Leu-Phe; LT, leukotriene; PAF, platelet-activating factor; PECAM, platelet–endothelial cell adhesion molecule; PMN, polymorphonuclear leukocyte; ROI, reactive oxygen intermediates; TNF, tumor necrosis factor; ZAS, zymosan activated serum.

## 1.7   Surface morphology of neutrophils

All inflammatory tissue is characterized by infiltration by neutrophils, macrophage, monocytes and lymphocytes. In order to achieve this, these inflammatory cells interact with endothelium and undergo a change from a spherical to a flattened morphological. This change in morphology is required not only for firm adhesion, but is also  necessary for transmigration through the endothelium, whether by migration between the endothelial cells or paracellular migration (Carman and Springer 2004 ;Dewitt and Hallett 2007). This morphology change requires a large expansion of the surface area of the leukocytes. The review by Robert Kay and colleagues (Kay et al. 2008) discussed this important topic of the 'surface-area problem' — the mechanism by which the apparent surface area of the chemotactic cell expands (and contracts). It has been argued that without the ability to expand its surface membrane area, cell polarization, pseudopod formation, phagocytosis and chemotaxis would not be possible; and thus actin polymerization and other cytoplasmic changes are subordinate to membrane expansion (Dewitt and Hallett 2007; Hallett and Dewitt 2007) .

Kay and colleagues suggest that 'folds' in the cell surface as possible reservoirs of additional membrane were unlikely; and focus on endocytic cycling as the potential mechanism. However, they have underestimated the surface-area problem for neutrophils that increase their surface by far more than the 20–30% increase in surface area in amoeba. Many electron microscopic studies of neutrophils (Bessis 1973; Hallett et al. 2008) reveled that this cell type has an extensive wrinkled surface which would double the apparent cell surface area (Hallett et al. 2008). Furthermore, the wrinkles disappear during expansion of the apparent surface area by osmotic swelling; and quantification shows that this membrane reservoir produces an additional surface-area increase of approximately 100% (Ting-Beall et al. 1993).

The unwrinkling of the membrane may have been demonstrated in other experimental models, such as antibody-coated beads (Shao and Hochmuth 1996) and micropipette suction (Evans et al. 1993; Herant et al. 2006). All these models showed not only unwrinkling of neutrophils cell membrane (producing extra membrane), but also increase in surface area. Mathematical modelling of the kinetics and forces that are required suggests that this extra membrane results from the unfurling of plasma-membrane wrinkles, which are held in place by a 'molecular velcro' ( Herant et al. 2005; Herant et al. 2006 ) . Significantly, the force required to 'unwrinkle' the membrane is significantly reduced during phagocytosis (Herant et al. 2005), which suggests that the velcro holding the wrinkles together can be released by intracellular signals that are associated with phagocytotic stimulation. Hallett et al have suggested that these signals might include the cleavage of proteins that hold the wrinkles in place (Hallett et al. 2008); and involve $Ca^{2+}$ activation of $\mu$-calpain (Dewitt and Hallett 2002). Although Lawson et al showed that endocytic cycling occurs (as a way of replacing integrin to the front of neutrophils (Lawson and Maxfield 1995), Hallett et al suggested that wrinkled cell

surface  (Hallett et al. 2008) must not be discounted as a possible solution to the surface-area problem.

As the spherical geometry is the minimum surface area required to enclose a certain volume, it is obvious that the volume of the cell must decrease, or its surface area must increase during this transformation from spherical to non-spherical shape (Dewitt and Hallett 2007). In fact, the surface area of the cell appears to increase during flattening onto the endothelium. For cells like neutrophils, where the intracellular organelles such as the nucleus and granules occupy a large percentage of its volume, there is little possibility of a volume change in any case. The increase in surface area, however, is surprisingly large, with an increase by more than 100% (Dewitt and Hallett 2007). This extra reserviour of plasma membrane may be provided by the unfolding of the wrinkles present on the cell membrane of the neutrophils (figure 1.7a & b).

### 1.7.1    Possible methods of membrane expansion

The possibility of stretching the plasma membrane has been ruled out because the cohesion of the phospholipid bilayer depends on the hydrophobic interaction of the fatty acid chains excluding water (Dewitt and Hallett 2007). Any "stretching" effect on the bilayer, which laterally separates the lipid molecules would allows water molecules between the lipid and would  rupture of the bilayer (Hamill and Martinac 2001; Dewitt and Hallett 2007; Hallett and Dewitt 2007). The proteins in a biological membrane may permit a little additional stretch, but it has been shown experimentally (and theoretically calculated) that biological membrane and simple phospholipid bilayers can expand by no more than  about 4% before rupturing (Hamill and Martinac 2001).
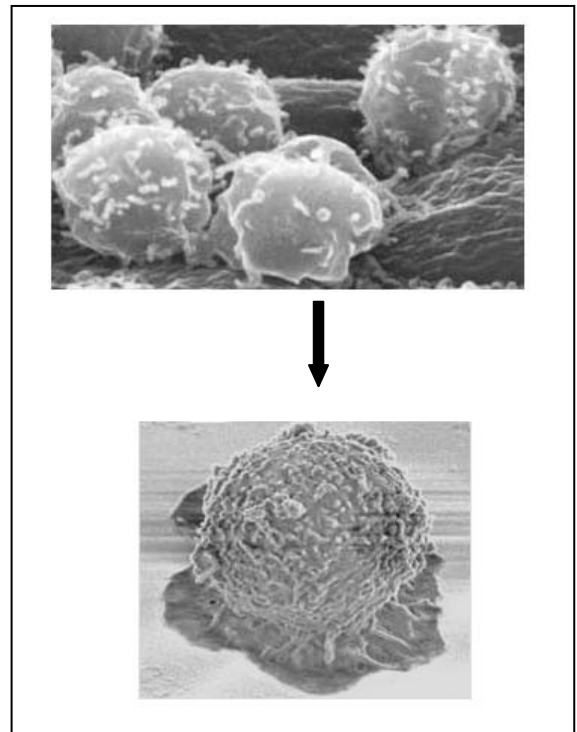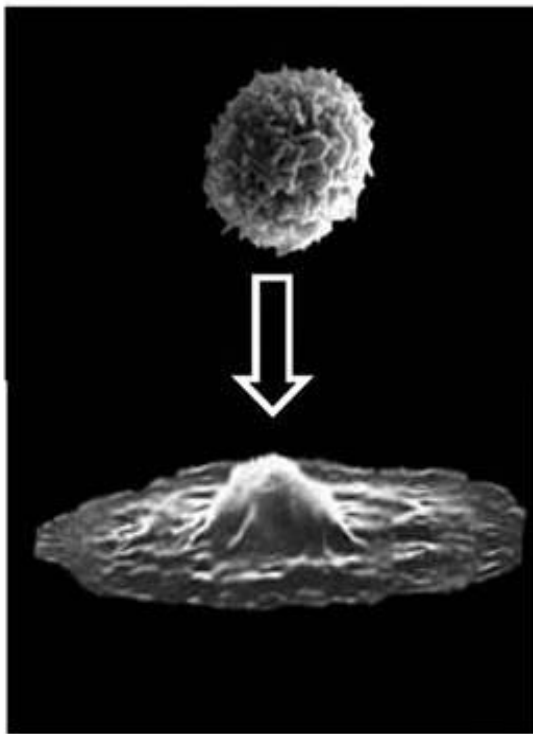
**Figure 1.7a & b.** The electron microscopic picture of neutrophils. The picture shows the wrinkled plasma membrane and unfolding of these wrinkles as the neutrophils spread. Figure was adapted from Nature Reviews Molecular Cell Biology 2008, 9; 662-665.

There is, thus, far too little stretch in the plasma membrane to account for the expansion of surface area required for cell flattening during adhesion to the endothelium. The intracellular membranes which enclose secretory granules within the cell has also been excluded as potential source of membrane resreviour during, the polarization of neutrophils. There are two problems with this source of membrane (Dewitt and Hallett 2007; Hallett and Dewitt 2007). The first problem is that fusion of the membrane of the granule with the plasma membrane would also release the contents of the vesicle (superoxides, hydrolases, degradative enzymes in neutrophils) into the extracellular space, which will damage the tissue surroundings (Sengelov et al. 1995).

Moreover, it would need more then 2500 vesicles to fuse with cell membrane per polarization. A single granule with a diameter of 0.2 μm (1/50th the diameter of a neutrophilic

phagocyte) would contribute only 0.04% additional membrane area, in order to obtain 100% increase in surface area (Nüsse and Lindau 1988; Eiserich et al. 2002; Dewitt and Hallett 2007). Such a massive release of granular material does not occur during extravasation. Moreover, release of all the granular content in the vicinity of the endothelium could also be catastrophic (Dewitt and Hallett 2007).

A scanning electron micrograph (SEM) of a neutrophil or macrophage shows that these cells have numerous surface wrinkles and folds, which means immediately that the that the actual surface area of these cells is greatly in excess of that of a sphere of the same diameter. This gives the possibilty that the extra membrane required during shape change of neutrophils is provided by the unfolding of the wrinkled plasma membrane. It is therefore important to understand how the wrinkles are formed and regulated (figure 1.7a & b).

### 1.7.2    Molecular velcro of membrane wrinkles

A series of elegant biophysical studies about the properties of the neutrophil plasma membrane has been performed using suction of the plasma membrane into micropipettes (Evans et al. 1993; Herant et al. 2005, 2006). Their findings show that a moderate amount of suction can expand the membrane into the mouth of the micropipette by up to about 5% of the membrane area; and further expansion is possible by applying a greater force (Herant et al. 2003; Dewitt and Hallett 2007; Hallett and Dewitt 2007). These measurements are consistent with there being a limited amount of "slack" in the wrinkles. Additional force is required to "unwrinkle" the remainder of the membrane, as if the wrinkles are held together by a molecular "velcro-like" mechanism (Herant et al. 2003).

Presumably, the "molecular velcro" is sufficiently strong to hold the wrinkles in place against the osmotic pressure tending to swell the cells. However, when neutrophils are

activated to expand their plasma membrane, the amount of available slack membrane increases, and the force required to un-velcro the wrinkles is reduced significantly (Herant et al. 2005). As the velcro holding the wrinkles in place has lost its grip under this condition, the membrane in the wrinkles would now become available to accommodate the change in shape as the cell flattens out (Hallett and Dewitt 2007)(Fig. 1.7a & b) . The loss of surface wrinkles in neutrophils when they flattened out is apparent in SEMs and can be seen in classic textbooks. Dewitt et al and Hallett et al (2007) have explained the nature of the molecular velcro and suggest how its grip may be loosened.

The wrinkled plasma membrane is not unique to neutrophils and macrophages; and it is seen across the surfaces of myeloid cells. These linear ridges, projecting about0.8 μm high and 0.1 μm wide, with lengths of 10–15 μm (Burwen and Satir 1977), which  on lymphocytes are termed "microvilli"; can be seen in transmission electron microscopy images (Tohya and Kimura 1998). These wrinkles and microvilli are permanent (or at least long-lived) structures, which influence the distribution of some surface molecules, like L-selectin (on the wrinkles) and integrin molecules (valleys between wrinkles). The lymphocyte microvilli have parallel actin filaments running within their long axis (Tohya and Kimura 1998), to which the cytoplasmic tail of selectins is bound via a linker molecule, ezrin (Ivetic et al. 2002; Ivetic 2004).

In neutrophils, there is a well-defined cortical network of polymerized actin, but the molecules involved in maintaining the surface wrinkles are not yet fully established but probably include membrane linker proteins like talin and ezrin. Two general models has been suggested (Dewitt and Hallett 2007; Hallett and Dewitt 2007) (fig 1.7.3), dependent on linkage to the cytoskeleton via ezrin or talin. In both models, a wrinkled membrane could be formed by cross-linking actin to membrane proteins. The two models are not, of course, mutually

exclusive, but the "velcro" may be attached to the cytoskeleton outside the wrinkles (fig 1.7.3a) or within the wrinkle (fig 1.7.3b). These models also depend on the actin-membrane linkage via L-selectin and $\beta_2$-integrin; and would explain their non-homogenous distribution on the cell surface, i.e., their exclusion or inclusion from the wrinkled membrane (Dewitt and Hallett 2007; Hallett and Dewitt 2007).

### 1.7.3    Unfolding of wrinkled membrane – role of calcium

It has been established for over 20 years that a large rise in cytosolic-free $Ca^{2+}$ accompanies macrophage and neutrophil spreading (Kruskal et al. 1986; Jaconi et al. 1991). It has also been shown that uncaging cytosolic $Ca^{2+}$ or inositol 1,4,5-trisphosphate ($IP_3$) to provide controlled $Ca^{2+}$ elevation causes an acceleration in the rate of flattening (Marks and Maxfield 1997; Pettit and Hallett 1998). This is similar to the relationship between $Ca^{2+}$ and membrane expansion during pseudopod extension around the particle during phagocytosis (Dewitt and Hallett 2002), where acceleration was dependent on µ-calpain activity (Molinari and Carafoli 1997; Dewitt and Hallett 2002).

This is a $Ca^{2+}$-activated protease (Molinari and Carafoli 1997;Goll et al. 2003), which cleaves substrates *in vitro* and *in vivo*. The flattening of lymphocytes during adhesion via ß2-integrin is dependent on the activity of calpain (Stewart et al. 1998; Leitinger et al. 2000). As a number of the substrates of calpain are cytoskeletal proteins involved in membrane linkage (Franco and Huttenlocher 2005), this would provide a mechanism for releasing the grip of the molecular velcro. The calpain cleavage site lies between a 4.1/ezrin/radixin/moesin (FERM) domain, binding to membrane-associated proteins; and an actin-binding domain, linking to the cytoskeleton (Dewitt and Hallett 2007; Hallett and Dewitt 2007) (fig 1.7.3.e).

Activation of calpain by elevated $Ca^{2+}$ would thus lead to the uncoupling of the link between the membrane and the underlying actin cytoskeleton and permit additional membrane to become available for cell flattening (Figure 1.7.4). However, there must be some selectivity in the activation of calpain, as activation of a (relatively) non-specific protease within the cytosol of a healthy cell would be disastrous. *In vitro*, activation of μ-calpain requires unusually high $Ca^{2+}$ concentrations, its dissociation constant is about 30μM (Michetti et al. 1997), whereas physiologically, global cytosolic $Ca^{2+}$ signals reach a maximum of about 1 μM.

In fact, the selectivity may arise from the existence of a subplasma membrane microdomain of high $Ca^{2+}$. The $Ca^{2+}$ concentration near the plasma membrane exceeds 50 μM during the influx of $Ca^{2+}$ from the extracellular medium, although the concentration in the bulk cytosol remains below 1 μM (Davies 1996; Davies and Hallett 1998). When uncaging $Ca^{2+}$, it was necessary to elevate bulk, cytosolic-free $Ca^{2+}$ to levels above the saturation point of the indicator, estimated to be about 50 μM (Pettit and Hallett 1998; Hillson 2006; Dewitt and Hallett 2007). However, the more physiological signal induced by uncaging $IP_3$ (which induces release of $Ca^{2+}$ from stores and then physiological $Ca^{2+}$ influx) induced neutrophil flattening at physiological $Ca^{2+}$ concentrations in the cytosol (Dewitt and Hallett 2002).

This again suggests that calcium –influx driven microdomains of high $Ca^{2+}$ exist in the cell. The $Ca^{2+}$ concentrations within individual wrinkles may reach the highest level, as there is a larger localized surface area to volume ratio (Brasen et al. 2010). In addition, it has been reported that calpain translocates to the plasma membrane (Gil-Parrado et al. 2003), perhaps by virtue of its C2-like domain. Together, these phenomena would limit calpain activity to the strategically required location and target subplasma membrane proteins. It is, in fact, known that cleavage of talin, an important calpain substrate, occurs during physiological $Ca^{2+}$ influx in

neutrophils (Sampath et al. 1998), suggesting that when activated by $Ca^{2+}$ influx, calpain-mediated proteolysis has specificity.

Furthermore, a number of important calpain substrates, including ezrin, Wiskott-Aldrich syndrome protein and myosin X, undergo μ-calpain-dependent cleavage in myeloid and lymphoid cells (Shcherbina et al. 1999; Shcherbina et al. 2001; Sousa and Cheney 2005). In non-immune cells, calpains have also been implicated in the local control membrane surface area leading to membrane protrusions (Franco et al. 2004).
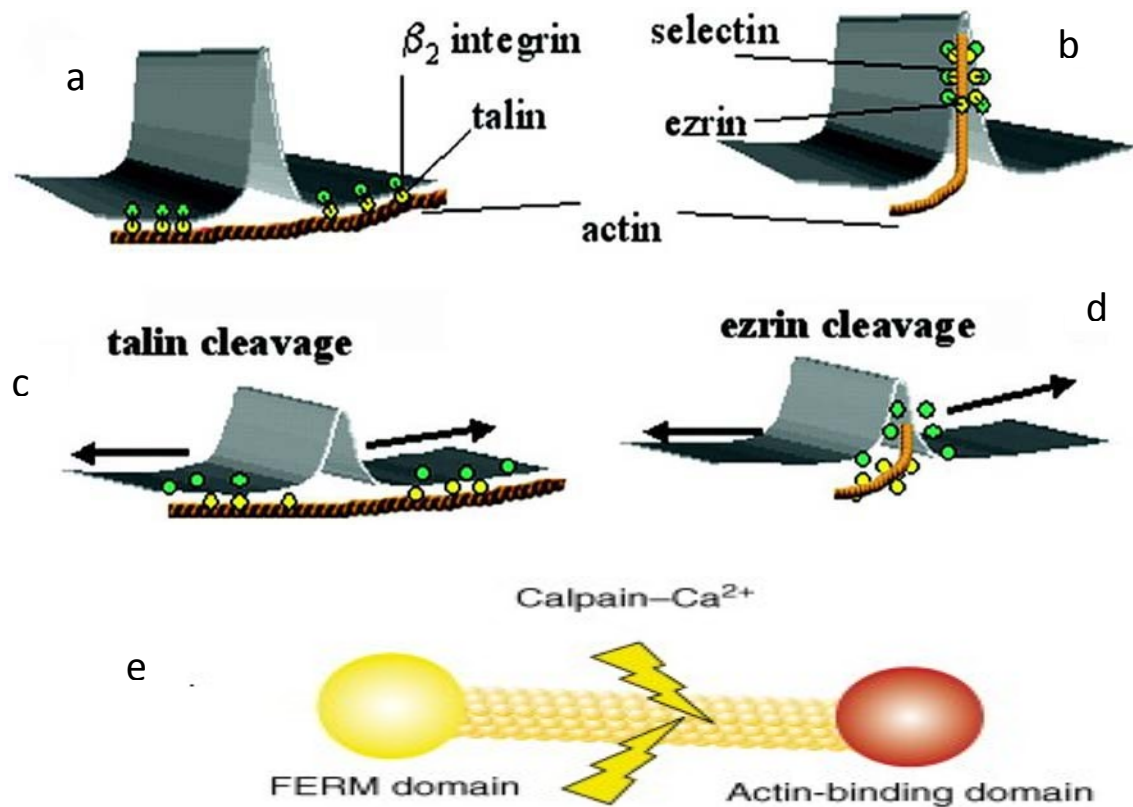


**Figure 1.7.3.** Mechanism for wrinkle release. In (a) and (b), two possible configurations are shown in which the wrinkles are held in place by (a) integrin–talin–actin across the wrinkle valleys and (b) selectin–ezrin–actin within the wrinkle. The effect of (c) talin or (d) ezrin cleavage on releasing the wrinkle is also shown. (e) The structural relationship of the FERM and actin-binding domains to the calpain cleavage site is shown. This relationship is seen in talin and ezrin. The proposed effect of $Ca^{2+}$ activation of calpain on releasing plasma membrane from wrinkles and may enable to accommodate the change in shape and associated increase in surface area. This figure is adopted from Journal of Leukocyte Biology, 2007, 81(5); 1160-1164.

## 1.8 Membrane linker proteins

Membrane actin linker proteins would have a key role in the formation and maintenance of cell surface wrinkles. The FERM (4.1 protein, ezrin, radixin and moesin) is band 4.1 superfamily is  a group of proteins that potentially links actin to phospholipid membranes (Isenberg et al. 2002). To this group belong talin, the erythrocyte membrane protein 4.1 (Rees et al. 1990),  ezrin, radixin, moesin (Bretscher et al. 1997); and some tyrosine phosphatases (Belliveau et al. 1995) . The ERM is made of globular head domain, FERM domain in the amino terminus, followed by a long region of high α-helical linker region and terminats in a carboxy-terminal domain, known as the C-terminal, ERM-association domain (C-ERMAD);  that has the ability to bind the FERM domain or filamentous actin (F-actin) (fig 1.8.1a).

The globular FERM domain is composed of three subdomains, characterized by similarity to: (1) the ubiquitin fold, α-helix bundle structure classified as an acyl-coenzyme A binding protein-like fold, (2) a seven-stranded β-sandwich with one long α-helix, classified as a phosphotyrosine-binding domain; and (3) a pleckstrin-homology domain. The C-terminal domain, on the other hand, adopts an extended structure and is composed of one β-strand and six helical regions comprised of 34 amino acid that provide the major actin binding sites, However, two additional sites in the middle region of the tail and in the N-terminal domain was also  sites for actin binding (Bretscher A 2002; Smith WJ 2002).

Other than providing a binding site for actin, the C-terminal covers an extensive area on the FERM domain surface and covers the intergrin binding site. ERM proteins are maintained in a dormant, inactive conformation through the interaction between FERM and the C-terminal domains (Bretscher A 2002; Smith WJ 2002). The release of the C-ERMAD from the FERM domain is necessary for their full activation and exposes binding sites in the FERM domain and the F-actin-binding site of the C-ERMAD (fig 1.8.a). Current ideas indicate that the ERM

protein in dormant state act like a spring, when the affinity between the FERM domain and the C-ERMAD is reduced, the molecule pops open, allowing it to connect the membrane to the underlying actin cytoskeleton. However, the entire mechanism for activation for ERM is yet to be studied, but it may be activated phospholipids and kinase. The proteins of this family which are elevant to neutrophils include talin and ezrin (Bretscher A 2002; Smith WJ 2002).

### 1.8.1    Talin

Talin is a widespread protein that is found in a variety of mammalian cells, where it is concentrated in focal cell adhesions (Burridge and Connell 1983) and ruffling membranes (DePasquale and Izzard 1991). In vertebrates, two talin genes, talin 1 and talin 2, have been reported (Monkley et al. 2001; Senetar and McCann 2005; Domadia et al. 2010) . Talin consists of multiple domains having distinct functions (Roberts and Critchley 2009). In platelets, talin redistributes from the cytoplasm to the plasma membrane upon activation, leading to secretory events and platelet coagulation via integrins (Beckerle et al. 1989) , a complex process that is not fully understood.

Each domain in the talin have distinct functions (Roberts and Critchley 2009) and Several divergent binding epitopes have been mapped along the entire sequence of 2541 amino acids (Rees et al. 1990), suggesting that talin may be a multifunctional protein. Talin has a globular N-terminal head region and a flexible rod domain, which can be dissociated by the protease calpain 2 (fig 1.8.1.a). The head contains a FERM (protein 4.1, ezrin, radixin, moesin) domain (subdivided into F1, F2 and F3 subdomains), which has binding sites for the cytoplasmic domains of β-integrins and as well as for filamentous actin (F-actin) (Critchley and Gingras 2008). The head also binds to two signalling molecules that regulate the dynamics of focal adhesion, namely PIPK1γ90 [a splice variant of phosphatidylinositol (4)-phosphate 5-kinase type Iγ] and focal adhesion kinase (FAK), although it is not clear whether

binding to FAK is direct(Critchley and Gingras 2008). The N-terminal head region (residues 1–400), is composed of the FERMdomain containing F1, F2, and F3 domains, with a further extension towards N-terminus termed the F0 domain (Domadia et al. 2010).

The head region of talin functions as an activator of integrins by binding directly to the cytoplasmic region of the b tails (Tadokoro et al. 2003; Anthis et al. 2009). Structural study reveals that talin F3 contains a phosphotyrosine binding (PTB) fold that interacts with the membrane proximal NPxY motif of the b3 cytoplasmic tail (García-Alvarez et al. 2003). The talin F2 and F3 domains are important for the activation of integrins, but the F0 and F1 domains are also required for the activation of integrins a5b1 and aIIbb3, despite differences in the level of activation (Bouaouina et al. 2008). The talin rod (the C-terminal of talin: residues 482–2541) defines a long helical rod region with multiple bundles of α-helices (Roberts and Critchley 2009).

The helical rod region is primarily involved in binding to cytoskeletal proteins F-actin and vinculin (Roberts and Critchley 2009); and it is also involved in maintaining an inactivated talin (Goult et al. 2009). In the tail of talin, an additional integrin-binding site at least two actin-binding sites and several binding sites for vinculin, which itself has multiple partners, has been identified. Recently, binding sites for two independent transmembrane proteins, laylin (Borowsky and Hynes 1998) and integrin β-subunit cytoplasmic domain (Calderwood et al. 1999), have been identified in this fragment. The C-terminal helices of two talin monomers form an anti-parallel dimer, although the relative position of the two subunits within the dimer is uncertain (Critchley and Gingras 2008). Calpain cleavage before amino acid residue 434 yields two major domains, an N-terminal head portion of 47-kDa and a 190-kDa rod domain containing the C-terminus (Isenberg et al. 2002). The 47-kDa head fragment is believed to be of major importance for talin's association with the plasma membrane (Isenberg et al. 2002).

Phospholipid binding has also been show to be exclusively mediated by 47 kDa domin (Niggli 1994) (fig 1.8.1b).
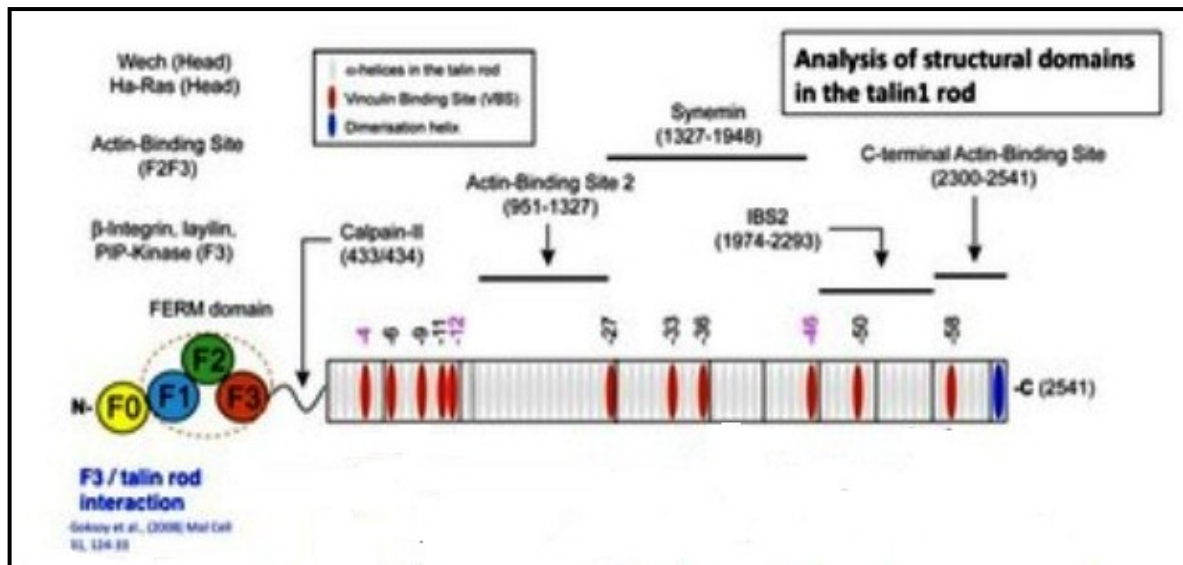


**Figure 1.8.1a.** Domain structure of talin. The N-terminal talin head (1–400) contains a FERM domain comprising F1, F2, and F3 domains preceded by the F0 domain. The talin rod (482–2541) contains 62 amphipathic α-helices, the most C-terminal of which is required for talin dimerization (*blue*). The position of the various ligand-binding sites is indicated, including the intramolecular interaction between F3 and the talin rod. Adopted from Journal of Cell Science, 2008, 121; 1345-1347.
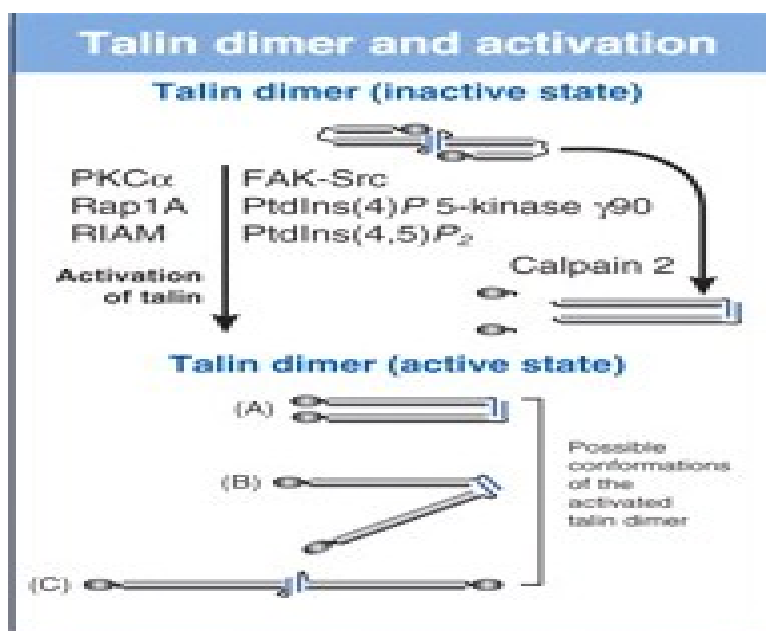


**Figure 1.8.1b.** Possible orientations of the subunits in the talin dimer. Journal of Cell Science, 2008,121; 1345-1347.

### 1.8.1.1 Interactivities of talin rod with actin cytoskeleton

The talin rod domain comprises 62 amphipathic α-helices, which form a series of helical bundles. Studies using peptide arrays show that around ten of these helices can bind to a hydrophobic pocket in the vinculin head. Predictably, the key vinculin-binding residues in talin are also hydrophobic, but these are usually buried within the helical bundles (Campbell and Ginsberg 2004; Gingras et al. 2005). Indeed, talin binds to vinculin with low affinity and it is unclear how vinculin accesses the vinculin-binding sites (VBSs) in talin. It is possible that force exerted on the integrin-talin-actin complex by actomyosin contraction exposes the VBSs in talin and enables vinculin to bind to and stabilize the complex, possibly by crosslinking talin to F-actin (Ziegler et al. 2006; Humphries et al. 2007).

Binding of talin to F-actin is intimately linked to talin dimerisation. The actin-binding site (ABS) in the C-terminal region of the talin rod comprises a five-helix bundle and a C-terminal helix that is required for dimer formation. Together, these constitute a talin/HIP1R/Sla2p actin-tethering C-terminal homology (THATCH) domain (Gingras et al. 2008). Interestingly, actin only binds to the THATCH dimer and the dimerisation domain itself appears to contribute to binding. Electron microscopy shows that the THATCH dimer binds to three actin monomers along the long pitch of the same actin filament and does not crosslink F-actin. Presumably, the actin-bundling activity of talin is explained by the presence of at least two other ABSs in talin (Critchley and Gingras 2008).

### 1.8.1.2 Interaction between talin and integrin

`Integrins are formed by non-covalently bound α and β subunits. In mammals, 18 α and 8 β subunits combine in a restricted manner to form 24 specific dimers, which exhibit different ligand-binding properties. Integrin subunits have large extracellular domains (approximately

800 amino acids)that contribute to ligand binding, single transmembrane (TM) domains (approximately 20 amino acids) and short cytoplasmic tails (13 to 70 amino acids, except that of β4). All three domains are required to regulate the affinity of integrins. β2 and β3 integrins can change affinity on a subsecond time scale and many of the paradigms of integrin structure and function were deduced from studies of these integrins. However, it is not clear whether they can be generalized to all integrins (Hynes 2002).

The extracellular domain of the heterodimer consists of a ligand-binding head domain standing on two long legs (fig 1.8.1.2), α integrin subunits contain a seven-bladed β-propeller domain that forms the head. Half of the α subunits contain an I domain (also referred to as a von Willebrand factor A domain), which when present is nearly always the ligand-binding site. The I domain possesses a conserved metal ion–dependent adhesion site (MIDAS), which binds divalent cations required for ligand binding by integrins. The β subunit is composed of a hybrid domain that connects to the βI domain, which is analogous to the I domain of the α subunit, a PSI (plexin/semaphoring/integrin) domain, four epidermal growth factor (EGF) domains; and a membrane proximal β tail domain (βTD). In integrins without an I domain, ligands bind to a crevice between the αβ subunit interface, where they interact with a metal ion–occupied MIDAS within the β subunit and the propeller domain of the subunit (Meyer et al. 2006). Despite the controversial role of the salt bridge in maintaining integrins in a low-affinity state, high integrin affinity is thought to be associated with separation of the α and β cytoplasmic tails. Many proteins bind directly to integrin tails, yet only talin and kindlins can regulate integrin affinity. The role of these NxxY motifs–binding proteins in integrin activation and function will now be discussed in detail.

The integrin-binding site for the talin head was mapped to the membrane-proximal NPxY motif, a common binding motif for PTB domain–containing proteins (Calderwood et al 1999;

Calderwood 2002; Uhlik 2005). Mutations within the NPxY motif of both β1 (Bouaouina et al. 2008) and β3 (Tadokora et al. 2003) integrins, as well as mutations in the talin PTB domain ( Wegener et al 2007), abolish talin binding and decrease integrin affinity. Insights into how talin increases integrin affinity came from experiments showing that the talin head effectively out competes the αIIb tail for binding to the β3 tail (Vinogradova et al. 2000). Fluorescence energy transfer (FRET) experiments in cells confirmed that the talin head induces separation of the integrin tails (in this case αLβ2), which is concomitant with increased basal integrin ligand binding (Kim et al. 2003).

Cells depleted of talin1 by small interfering RNA (siRNA) cannot respond to common activation stimuli (Tadokoro et al. 2003). Furthermore, genetic experiments (Monkley et al. 2000; Brown et al. 2002; Cram et al. 2003; Petrich et al. 2007) demonstrated that talin1 ablation universally leads to integrin-adhesion defects. Even though there are several protein with PTB domain such as Dok1 (Calderwood et al. 2002), tensin (McCleverty et al. 2007), and Numb (Calderwool et al. 2002), binds with NPxY motif, non other then talin can modulate integrin affinity. This might be because the talin head has an additional binding site on the β integrin tail in the membrane proximal region, where the α and β integrin tails interact (Patil et al .1999; Vinogradova et al. 2002), whereas Dok1 binds only to the region surrounding the NPxY motif ( Oxley et al. 2008).

Crystallographic data has clarified that talin-dependent integrin activation involves binding of the talin F3 subdomain to the β3 integrin tail at two locations, in order to induce the displacement of the α integrin tail and facilitate tail separation (Wegener et al. 2007). The talin F3 subdomain contains an extra loop of amino acids that binds to membrane-proximal sequences in the β3 integrin tail. Thus, it was proposed that talin first encounters the β integrin tail by binding the NPxY motif through its PTB domain; and the loop sequence subsequently

interacts with membrane proximal sequences within the β tail to displace the α integrin tail and separate the TM domains. Although the talin head increases integrin affinity, full-length talin is required to cluster integrins into focal adhesions (Legate et al .2009), which are hubs that relay signals from integrins to different cellular compartments. Cells that do not express talin are unable to undergo sustained spreading, which indicates an adhesion defect (Zhang X et al. 2008).

Expressing the talin1 head in these cells partially restored the spreading defect, but focal adhesions were still absent, demonstrating that the clustering of integrins into larger adhesion structures depends on both the head and rod of talin. These studies also showed that talin is essential for coupling the actin cytoskeleton to adhesion structures and established talin as a key adaptor linking the cytoskeleton to the extracellular matrix (Zhang et al. 2008). Mutational analysis of talin indicates that a functional dimerization motif is both necessary and sufficient to localize talin to focal adhesions (Semetar 2006; Smith J et al. 2007). Because talin contains two β integrin–binding sites, one within the FERM and the other within the rod domain, the talin homodimer has up to four integrin-binding sites, which may enable talin to act as an integrin crosslinker in order to promote clustering.

Consistent with this hypothesis, cleavage of the talin head from the rod domain by the protease calpain induces focal-adhesion disassembly (Franco  et al .2004).Because integrin activation has to be strictly controlled, talin-integrin binding is tightly regulated (Fig1.8.1.2.2a). NMR studies revealed an autoinhibitory interaction between the talin C-terminus and the PTB domain that blocks the integrin-binding pocket (Goksoy et al.2008). Therefore, when talin function is not required it may be maintained in an autoinhibited state. Activation of talin is still not clear, however, it probably involves binding to the lipid second messenger phosphotidylinositol-4,5-bisphosphate [PtdIns(4,5)$P_2$] because this lipid elicits a

conformational change that disrupts the autoinhibitory interaction and enhances integrin-talin binding (Martel et al. 2001; Goksoy 2008).

Although phosphoinositide binding can enhance the affinity of many PTB domains for their substrates (Uhlik et al. 2005), this does not hold true for the isolated talin head. Talin binds to PIPKIγ and directs it to focal adhesions (Di Paolo et al. 2002; Ling et al. 2002). Thus, a feed-forward loop may exist to enhance talin recruitment to sites of adhesion formation.Talin-integrin interactions are also controlled through phosphorylation of the β integrin tail. The Tyr within the β1 and β3 integrin NPxY motif can be phosphorylated by src family kinases (Chen 1992c; Law et al. 1996) and when mutated to Phe, it reverses the integrin-dependent spreading and migration defects in viral-Rous sarcoma oncogene (v-src)– transformed fibroblasts ( Chen 1992).

The interaction between talin and β integrin tails is regulated by a phosphorylation switch mechanism. Structural analysis showed that the talin PTB–integrin NPxY interaction occurs through acidic and hydrophobic interactions (Di Paolo et al. 2002) and cannot accommodate the introduction of a phosphate group. Accordingly, the affinity of the talin F3 subdomain for a phosphorylated β3 tail peptide is reduced compared with that of the unphosphorylated peptide (Oxley et al. 2008). Therefore, phosphorylation could inhibit integrin activation by maintaining an inhibitory complex on inactive integrin tails or by blocking talin binding directly. Mutations and truncations of the β3 integrin tail C- terminal to the talin-binding site decrease integrin affinity for ligands (Chen et al.1992; Chen et al. 1994; Xi et al. 2003; Ma et al 2006), which raises the possibility that additional factors also alter integrin affinity status. Indeed, recent work shows that talin is not the only master regulator of integrin activation and that the kindlin family of proteins, which bind to this region of β1, β2, and β3 integrins, are as

important as talin in mediating this function (Ma et al. 2008; Montanez et al. 2008; Moser et al. 2008).
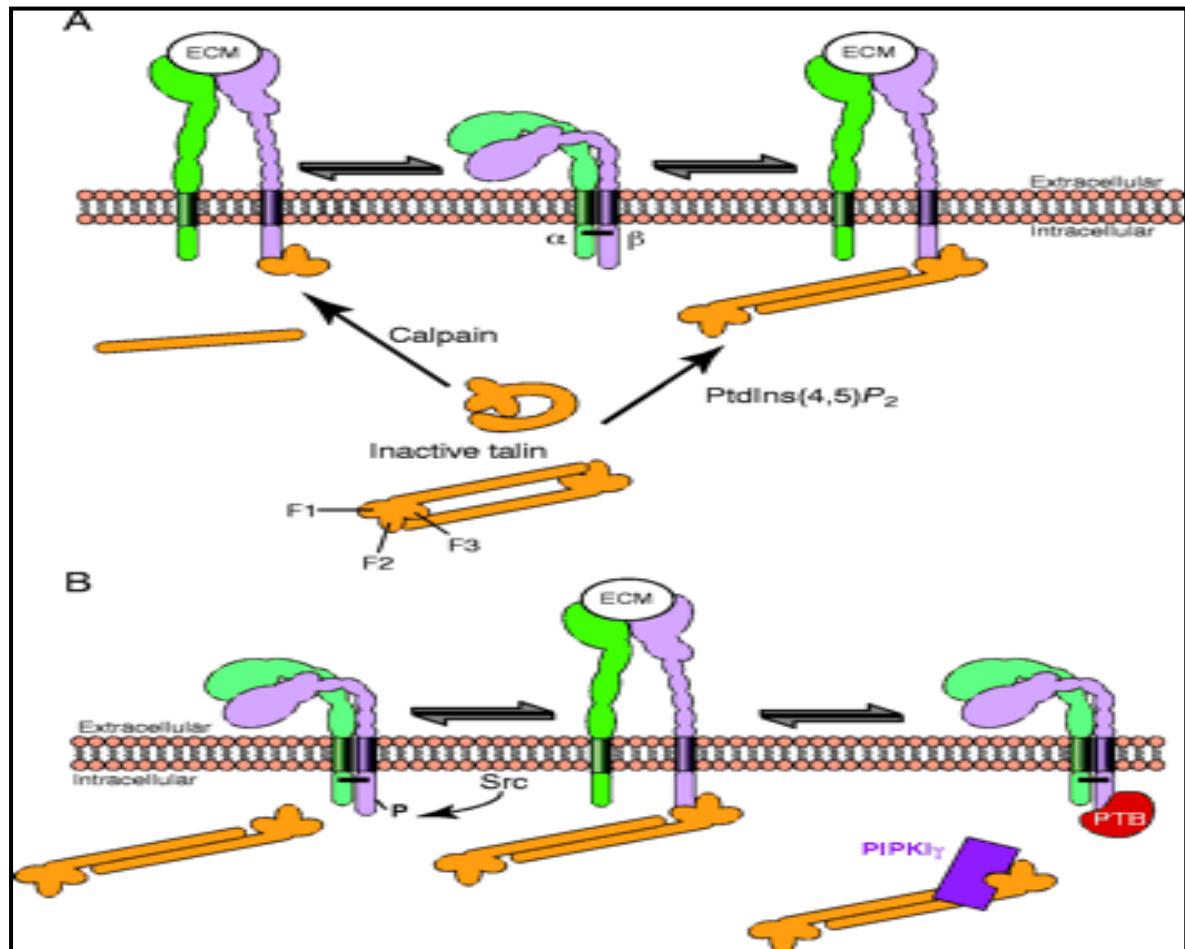


**Figure 1.8.1.2.2.** Potential mechanisms regulating talin-mediated integrin activation. Talin binding to integrin β tails induces conformational changes in the extracellular domain, increasing their affinity for ligands (the nature of the conformational changes remains controversial and the model shown represents only one of several possibilities). Mechanisms that regulate talin binding may therefore control integrin activation. The putative salt bridge stabilizing the interaction between membrane-proximal regions of the α and β tails in the inactive conformation is illustrated as a black bar. The three-lobed FERM domain within the talin head is indicated. (A) Stimulation of talin binding. Two hypothetical models of inactive talin are shown, where regions of the rod mask the β tail-binding site in the F3 subdomain. Calpain cleavage or PtdIns(4,5)$P_2$ binding unmasks the binding site, potentially activating integrins. (B) Inhibition of talin binding. Src-mediated tyrosine phosphorylation (P) of integrin NPxY motifs, and competition with other β tail-binding proteins (e.g. PTB domain proteins), or other talin-binding proteins (e.g. PIPKIγ-90), may prevent integrin-talin interactions, so inhibiting integrin activation. Hence, dynamic interplay between the stimulatory and inhibitory pathways might determine the integrin activation state. Adopted from Journal of Cell Science, 2004, 117; 657-666.

## 1.8.2 Kindlin

Kindlins are related to talin. They belong to a family of evolutionarily conserved FER domain–containing proteins named after the gene mutated in Kindler syndrome, a rare skin blistering disease. There are three kindlin family members in mammals: kindlin-1 [Unc-112 related protein 1 (URP1)], kindlin-2 (Mig2), and kindlin-3 (URP2) (Siegel et al .2003). Kindlin-1, which is predominantly expressed in epithelial cells, is found in tissues such as skin, intestine and kidney; kindlin-2 is expressed in most tissues, with highest amounts in skeletal and smooth muscle cells; and kindlin-3 expression is restricted to cells of hematopoietic origin (Siegel et al. 2003; Jobard et al. 2003; Ussar et al. 2006).

All three proteins localize to integrin-dependent adhesion sites; kindlin-1 and -2 localize to focal adhesions and kindlin-3 localizes to podosomes, which are integrin-dependent adhesion sites found in hematopoietic cells. Two human diseases caused by kindlin gene mutations have characteristic features of defective integrin function. Kindler syndrome, which is caused by the loss of kindlin-1, is a rare genodermatosis characterized by an epithelial cell-adhesion defect followed by poikiloderma and cutaneous atrophy (Siegel et al. 2003; Jobard et al. 2003). Kindlin-2 deficiency is embryonically lethal in zebrafish and mice, but has not been described in humans. Kindlin-3 deletion causes severe bleeding that is reminiscent of Glanzmann thrombasthenia, a disorder arising from defects in αIIb or β3 integrin subunits. The platelet integrins cannot bind ligands and platelet aggregation is defective, despite normal amounts of talin (Moser et al. 2008). Only very limited information is available on the functions of kindlins. Kindlin-3 has been reported to influence integrin-mediated strengthening of cell adhesion (Shi, et al. 2007; Dowling 2008) and to cooperate with talin in inducing integrin activation (Ma, et.al. 2008).
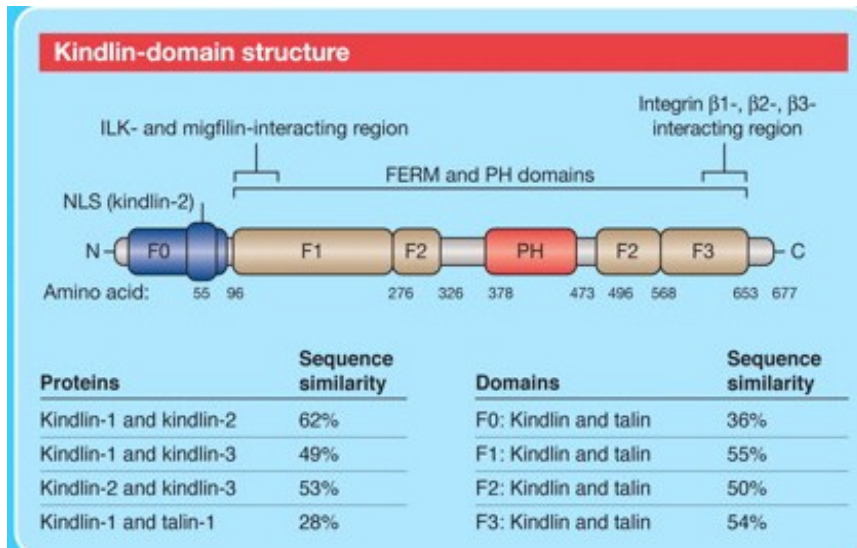
**Figure 1.8.2a.** Kindlin domain structure and binding partners. (A) Domain architecture of kindlins. All members of the kindlin protein family show identical domain architecture (top). Arrows indicate the regions of kindlins that interact with β1-integrin and β3-integrin, ILK or migfilin. The interactions with ILK and migfilin are based mainly on the studies of kindlin-2 and UNC-112. (B) Overlay of the kindlin-2 F3 subdomain model structure (blue) and the talin F3 subdomain structure (green) in complex with the β1-integrin peptide (red) showing a conserved PTB fold. ILK, integrin-linked kinase; PTB, phosphotyrosine binding; UNC-112, uncoordinated protein 112. Adopted from Journal of Cell Science, 2010, 123; 2353-2356.
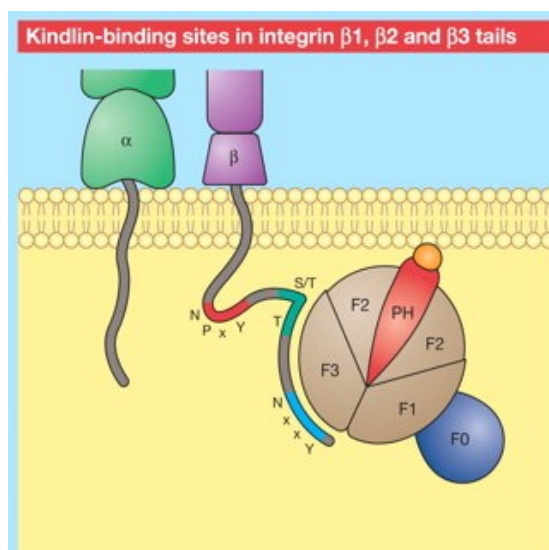


**Figure 1.8.2b.** Schematic diagram showing the binding site of kindling with intergrin. They bind via their F3 subdomains to the membrane-distal NxxY motif of β integrin cytoplasmic tails. Figure adopted from Journal of Cell Science, 2010, 123; 2353-2356.

### 1.8.2.1. Kindlins as regulators of integrin activation

Kindlins are essential components of the integrin adhesion complex. Mutations in kindlin-3 were implicated in a rare leukocyte-adhesion deficiency (LAD) type III (LAD-III), which results from severe defects in leukocyte and platelet integrin activation (Kuiljper et al. 2008; Mory et al. 2008; Svensson et al. 2009 ). Genetic and siRNA depletion of kindlin-1, -2 and -3 in mice and cells provided definitive experimental proof that kindlins are essential regulators of integrin function because the conformational shift of integrins from the low- to high-affinity state does not occur in the absence of kindlins (Ma et al. 2006; Moser et al. 2008; Ussar et al. 2008). Both kindlin and talin depletion cause impairment of platelet aggregation which implies that both proteins are required to regulatory integrin affinity (Nieswandt et al. 2007; Petrich et al. 2007).

Furthermore, leukocytes lacking kindlin-3 are unable to transmigrate across the vessel wall into inflamed tissues because of an integrin-mediated adhesion defect (Moser et al. 2009). The phenotypes of these mice resemble LAD-III patients, which led to the identification of mutations in kindlin-3 as a cause of this disease (Kuijper et al. 2009; Svenson et al. 2009) Kindlin-mediated integrin activation requires a direct interaction between kindlin and β integrin tails. The kindlin and talin FERM domains show high levels of sequence similarity (Koleker et al. 2004). However, the kindlin FERM domain exhibits the structural hallmark of being split into two halves by a pleckstrin homology (PH)–domain insertion in the F2 subdomain (Fig 1.8.2.1a, b & c). Molecular modeling of the kindlin-2 F3 subdomain that uses the talin F3 subdomain as a structural template suggests that it also resembles a PTB domain capable of recognizing β integrin tails (Shi et al. 2007). Biochemical experiments confirmed the predicted interaction of kindlins with the cytoplasmic tails of β1, β2, and β3 tails (Kloeker et al. 2004; Shi 2007; Ma et al. 2008; Montanez et al. 2008; Moser et al. 2008; Moser et al. 2009).

Kindlin-1 and kindlin-2 PTB-domain mutations abolish their interaction with the β1 integrin tail (Usar et al. 2008; Shi et al. 2007) and impair the ability of kindlin-1 to activate integrins (Moser et al. 2008). Unlike talin, kindlins bind the distal NxxY motif on the β1, β2, and β3 tails (Fig.1.8.2.1) (Ma et al. 2008; Montanez et al. 2008; Moser et al. 2009; Moser et al. 2008; Ussar et al. 2008; Shi et al. 2007 ) additional sequences may also be involved in kindlin binding. Although the intervening sequence between the two NxxY motifs in the β1 and β3 integrin cytoplasmic tails are dispensable for talin binding, mutation of a double Thr or Ser/Thr within this sequence impairs kindlin binding (Moser et al. 2008). Because kindlins and talin bind distinct regions of the β integrin tail, they may cooperate to regulate integrin affinity (Ma et al. 2008; Montanez et al. 2008; Moser et al. 2009; Calderwood et al. 2002; Calderwood et al. 1999).

Although kindlins are not sufficient to shift integrins to a high-affinity state, they facilitate talin function. The amount of talin expressed in cells determines the efficacy of kindlins in promoting this function because overexpressing kindlin-2 in cells with relatively little talin  (Han et al. 2006) has little or no effect on integrin affinity modulation; and coexpression of the talin-head domain with kindlin-1 or -2 results in a synergistic increase in αIIbβ3 affinity. Conversely, talin depends on kindlins to promote integrin affinity because talin-head overexpression failed to increase αIIbβ3 affinity in CHO cells in which kindlin expression was reduced by siRNA. Thus, kindlins require talin and talin is not sufficient to increase integrin affinity. Kindlins also function as cytoskeletal linker molecules in outside-in signaling. Kindlin-1 and -2 bind to integrin-linked kinase (ILK) and the filamin-binding protein migfilin, both of which link kindlins indirectly to the actin cytoskeleton (Tu. et al. 2003; Zhang et al. 2006; Montanez et al. 2008). Both proteins localize to cell-matrix adhesions in a kindlin-dependent manner, demonstrating that kindlins are central linker proteins mediating the assembly of integrin-dependent adhesion complexes (Tu. et al. 2003; Zhang et al. 2006; Montanez et al. 2008). Kindlin-3–deficient platelets exposed to

divalent $Mn^{2+}$, which shifts integrins into the high-affinity state independent of intracellular cues, can adhere to fibrinogen or collagen-coated surfaces. However, subsequent platelet spreading is impaired, which indicates that integrin-dependent cytoskeletal rearrangements do not occur in the absence of kindlin-3 (Moser et al. 2008). These observations suggest that kindlins remain associated with the adhesion complex and fulfill essential functions as bidirectional signaling molecules.
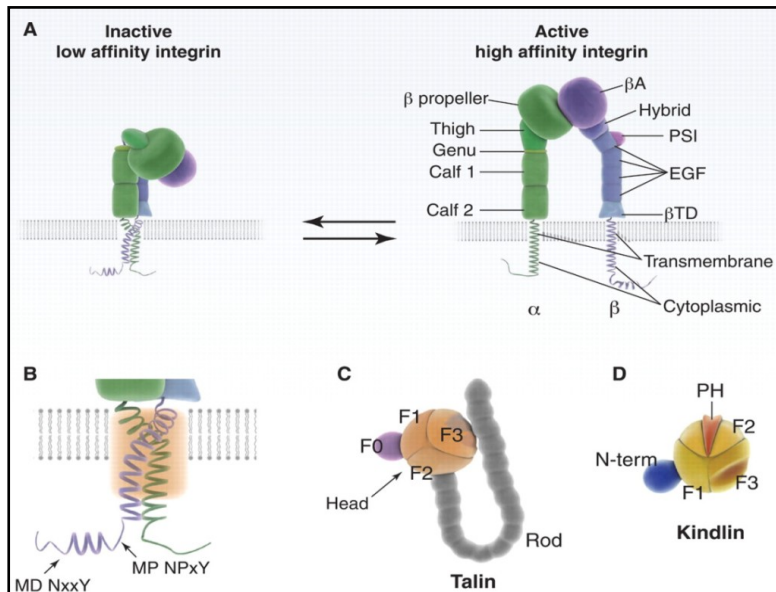
**Figure 1.8.2.1a.** Integrin architecture and schematic representation of integrin activation. Specific contacts between the ectodomains, the TM, and cytoplasmic domains keep the integrin in its bent conformation. Separation of the integrin legs, transmembrane, and cytoplasmic domains occurs during integrin activation, resulting in an extended integrin conformation. The α subunit is shown in green and the β subunit in violet. (**B**) A closer look at the interacting site (orange rectangle) between the transmembrane and membrane proximal cytoplasmic domains of the α and β subunits. The membrane proximal (MP) and distal (MD) NPxY/NxxY motifs within the β tail are indicated. (**C** and **D**) Schematic drawings of the integrin-activating proteins talin (C) and kindlin (D). The FERM domains are depicted as balls subdivided into three subdomains, F1 to F3. Kindlins contain a PH domain inserted into the F2 subdomain. Domain sizes are not to scale, and talin is shown as a monomer for simplicity. This diagram was adapoted from, S*cience*, 2009, 324; 895-899.
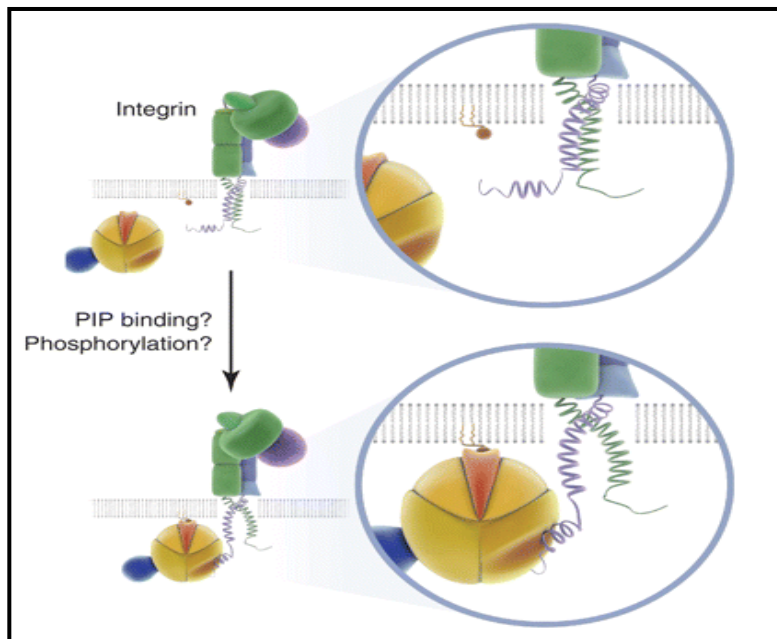


**Figure 1.8.2.1b:** Hypothetical model of kindlin recruitment and binding to the β integrin cytoplasmic tail. Phosphoinositide binding to the PH domain and/or phosphorylation might activate kindlin proteins and recruit them to the membrane, where they bind via their F3 subdomains to the membrane-distal NxxY motif of β integrin cytoplasmic tails. This diagram was adapoted from S*cience*, 2009, 324; 895-899.
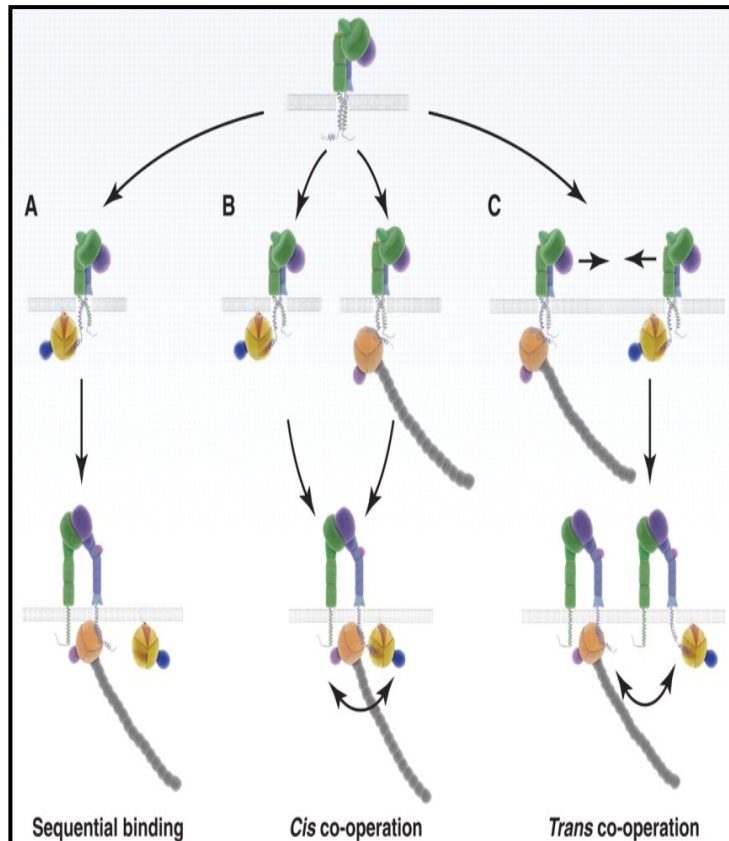
**Figure1.8.2.1c.** Putative crosstalk mechanisms between talin and kindlin during integrin activation. (a) Model for the sequential binding of kindlin and talin to the integrin tail. Kindlin binding to the MD NxxY motif facilitates talin binding to the MP NPxY motif, which results in the displacement of kindlin from the β tail and final integrin activation. (b) Because of the distinct binding sites for talin and kindlin at the β integrin tail, simultaneous binding may be possible. The order in which each protein binds to the integrin tail is not known. (c) Communication between talin and kindlin in tran*s*, where each protein is bound to a different integrin tail, can also be envisioned. In this model, talin and kindlin binding to integrin tails results in the formation of integrin nanoclusters and a subsequent talin-kindlin crosstalk. This diagram was adapoted from *Science,* 2009, 324; 895-899.

## 1.8.3 Ezrin

Ezrin is also a member of the FERM family and is of special interest to the maintenance of cell surface morphology. Ezrin is the p81 substrate of the epidermal growth factor (EGF) receptor tyrosine kinase; and was first purified from epithelial intestinal brush border microvilli. It is also a calpain substrate. Initially, the hypothesis of an interaction of ERM proteins, including ezrin, with the plasma membrane was due to the presence of the FERM domain, which is involved in the interaction between band 4.1 and glycophyrin C (Correas, et al. 1986). Algrain et al. (1993) did the first experiments reinforcing this hypothesis, showing by transfection experiments that the amino-terminal domain of ezrin associates with the plasma membrane whereas the carboxy-terminal domain associates with the cytoskeleton (fig 1.8.3a).
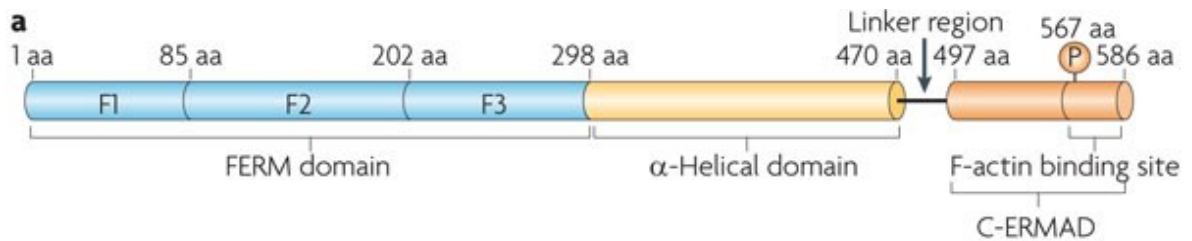
**Figure1.8.3a.** Structure of ERM family of proteins. All ERMs (ezrin, radixin and moesin) have a similar domain structure. The domain organization of ezrin is shown here. The amino‑terminal FERM domain (blue) consists of three subdomains: F1, F2 and F3. The central ~150 residue region (yellow) is predicted to have a high α‑helical content and propensity to assemble into a coiled coil. This is followed by a linker region that is Pro‑rich in ezrin and radixin, but not in moesin; and the protein terminates in the carboxy‑terminal ERM‑associated domain (C‑ERMAD; orange), which contains thefilamentous actin (F‑actin) - binding site. Adopted from Nature Reviews Molecular Cell Biology, 2010,11; 276-287.

The molecules which bind with ERM and plasma membrane are named ERMBMPs (ERM binding membrane proteins) (Yonemura and Tsukita, 1999). These proteins are subdivided in two classes: one involved in the direct attachment of ERM to the plasma membrane and the other in an indirect mechanism. Table 1.8.3 lists the two classes of ERM associated protein.

### Table 1.8.3. ERM associated proteins

| Interactions | Functional outcome | Cells/ tissues | references |
|---|---|---|---|
| *Direct attachment* | | | |
| CD44 | Cell motility and formation of uropodia | epithelial cells and fibroblasts | Tsukita, et al.1994 |
| ICAM-2 | Cell motility and formation of uropodia | lymphocytes | Helander, et al.1996 |
| Syndecan 2 | Transduction of signals from extra cellular matrix | Family of transmembrane heparan sulfate proteoglycans | Granes, et al. 2000. |

| | | | |
|---|---|---|---|
| PA2.26 | Reorganization of the actin cytoskeleton and a redistribution of ezrin concomitantly to a change in cell morphology. | Carcinoma cell lines, fibroblasts, epithelial cells of the choroid plexus, mesothelial cells and endothelia of lymphatic vessels | Scholl, et al. 1999 |
| **Indirect attachement**<br><br>EBP50 | Adaptor protein | Polarized cells | Reczek, et al. 1998 |

As ERM proteins are actin binding proteins, they may control actin assembly directly. This would be consistent with ERM proteins, notably ezrin, being highly abundant (almost 1:1 to actin) in dynamic membrane structures, such as in gastric parietal cell membranes or microvilli (Berryman, et al. 1995). In addition to the C-terminal F-actin-binding site, a second site within residues 280–309 of ezrin mediates binding to G-actin as well as to F-actin (Roy, et al.1997). Intriguingly, deletion of the conserved 30 N-terminal residues of ezrin inhibited both the actin-binding and membrane extension properties identified in the 280–309 ezrin domain (Martin, et al.1997). Indeed, ezrin and other ERMS are candidates to control directly the elongation of actin microfilaments.

The two amino acid sequences (1–29 and 280–309) essential for actin-binding and membrane extensions in ezrin are highly conserved in other ERM proteins, including merlin/schwannomin. This protein is also concentrated in actin-rich structures1–3 but does not possess the C-terminal. At least in vitro, both the actin-binding and the membrane binding sites of full-length native ERM proteins appear to be masked. As mentioned above, the carboxy-terminal half of ezrin binds to actin filaments with relatively high affinity (Badour, et al. 2003; Lee, et al. 2003; Cao, et al. 2005). At physiological ionic strength, full-length ERM proteins have very low affinity to the cytoplasmic domain of EMAP *in vitro*, whereas the amino-terminal halves of ERM proteins lacking carboxy-terminal halves bind to the same with high affinity (Gautreau, et al. 2002).

Considering that a significant amount of monomeric ezrin is detected as a soluble form in the cytoplasm (Schwartz-Albiez, et al. 1995 and McClatchey, et al. 2003), these findings led to the proposal of an intramolecular head-to-tail association model for ERM protein activation and inactivation (fig1.8.3b). In native ERM proteins, the amino- and carboxy-terminal halves may mutually suppress each other's functions, namely membrane- and actin-binding, respectively, through an intramolecular head-to-tail association.

Actually, the amino-terminal half of an ERM protein is directly associated with the carboxy-terminal half *in vitro* (Kikuchi 2002) and the amino-terminal half of ezrin suppresses the dominant-negative effect of the carboxy-terminal half of ezrin *in vivo*. This arrangement suppresses the formation of cellular protrusions by inhibiting the function of ezrin (Kupfer and Singer 1989). Intermolecular head-to-tail association of ERM proteins is found in viva (Schwartz-Albiez, et al. 1995; McClatchey, et al. 2003); and the intermolecular and intramolecular interfaces between the amino- and carboxy-terminal halves appear to be distinct.

A specific feature of ERM proteins is the proposed change in conformation that could drive the translocation of the protein from a soluble pool to a membrane-skeleton-associated form (fig 1.8.3b). There has been no formal demonstration of such a change, but it almost certainly occurs *in vivo*. The change was predicted following the discovery of the self-association properties, the mapping of the N- and C-ERMADs, various structure–function studies performed in different cell-expression systems and the identification of binding sites that were apparently masked in the purified soluble proteins. Opening of the full-length molecule should result in unrestricted binding of proteins, such as EBP50 and RhoGDI or Dbl, in the N-ERMAD; and F-actin in the C-ERMAD.

In various experimental cell and tissue systems, ERM association with the membrane skeleton always correlates with an enhanced state of ERM phosphorylation. Conversely, dephosphorylation induced by various means triggers the reversion of ERM proteins to a soluble form and promotes the disassembly of the membrane-skeleton structure (Mackay, et al. 1997;

Tran Quang, et al. 2000). Ezrin undergoes phosphorylation at Tyr and Ser/Thr sits. Serine/threonine phosphorylation may be a key signal for the activation of ERM proteins.

Two papers have described that ERM proteins specifically bind to phosphatidylinositol4-phosphate (PIP) and phosphatidylinositol 4, 5-bisphosphate (PIP,) (Barret, et al. 2000; Gautreau, et al. 2002). As described above, native full-length ERM proteins have very low affinity for the cytoplasmic domain of EMBP's at physiological ionic strength. PIP elevated this binding affinity, suggesting that phosphoinositides are also key factors for the activation of ERM proteins (Gautreau, et al. 2002). The possible upstream factors required for activation of phosphorylation and phosphoinositide synthesis are Rho, one of the small GTP-binding proteins, is now considered to be a general regulator of actin-based cytoskeletal organization, especially of actin-filament-plasma-membrane associations. Recent *in vitro* and *in vitro* analyses suggest an intimate relationship between the Rho signalling pathway and activation of the actin-membrane cross-linking ability of ERM proteins (Gautreau, et al. 2002) .

The *in vitro* binding of ERM proteins to the cytoplasmic domain of EMBP's in the presence of crude cell homogenate is enhanced by GTPyS and completely suppressed by C3 toxin, a specific inhibitor of Rho (Matsui, et al. 1998). Furthermore, Rho guanine nucleotide dissociation inhibitor (GDI), an important regulator of Rho, is tightly associated with ERM complexes in viva (Bretscher, et al. 2002). In addition, Myc-tagged Rho introduced into MDCK cells colocalizes with ERM proteins (Matsui, et al. 1998). Several intensive studies have been performed to identify the direct target of Rho, showing that Rho regulates phosphatidylinositol turnover (Nakamura et al 1999). For example, Rho activates PIP 5-kinase, which elevates the PIP level in membranes. Rho also regulates the activity of some serine/threonine kinases (Nakamura, et al.1999). It is possible that these kinases phosphorylate ERM proteins. It is thus fascinating to speculate that, through the activation and inactivation of ERM proteins, Rho can regulate the actin-based. By forming a cross link between plasma membrane and actin, ERM proteins involved both in the

morphogenesis of the membrane structures on which they are concentrated and in cell adhesion, involving molecular mechanisms that are not yet understood fully (Mangeat, et al. 1999). Functional inactivation of ERM proteins has provided some clues to their roles (table 1.8.3b). Overall, these data indicates that ERM proteins are cytoskeletal proteins with pleiotropic functions. In addition to a structural role as membrane–cytoskeleton linkers, they also regulate cell adhesion.
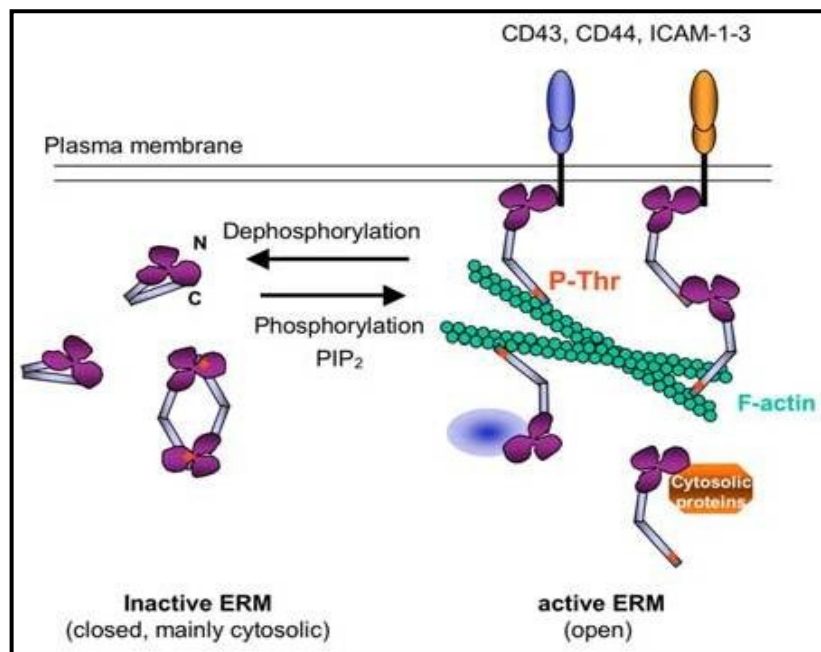


**Figure 1.8.3b.** Two forms of Ezrin. Ezrin is activated through phosphatidylinositol 4,5‑bisphosphate (PtdIns(4,5)P2) binding and phosphorylation of Thr567, which reduces the affinity of the N‑terminal FERM domain for the C‑ERMAD. This unmasks binding sites for F‑actin and the cytoplasmic tails of specific membrane proteins, such as CD43 (also known as SPN), CD44, intercellular adhesion molecule 1 (ICAM1), ICAM2, Na+–H+ exchanger 1 (NHE1; also known as SLC9A1), syndecan 2 and β‑dystrophin. Furthermore, the adaptor protein ERM‑binding phosphoprotein 50 (EBP50; also known as NHERF1) can also bind the FERM domain. This picture was taken from Frontiers in Bioscience, 2006,11; 207-211.

**Table 1.8.3b. Experimental established functions of ERM proteins**

| Experimental Studies | Methods Used | Inference | Reference |
|---|---|---|---|
| Suppression of expression of ERM in Thymoma cells | Antisense oligonucleotides | Disappearance of all membrane structures | Takeuchi, et al. (1994) |
| Suppression of expression of ERM in mouse epithelial cells | Antisense oligonucleotides | Cell-matrix and cell- cell adhesion inhibited | Takeuchi, et al. (1994) Bretscher, et al (1997) |
| Application of antisense to primary neurons *in vitro* | | Promotes stabilizing the formation of neurite outgrowths and axonal growth cones | Paglini, et al. (1998) |
| Inactivation of Ezrin in Rat-1 fibroblast and a V-fos transformed cell line | Chromophore-assisted laser inactivation | Inhibition of membrane protrusion and reversible membrane retraction. | Helander, et al. (1996) |
| Inactivation of Ezrin cytosolic pool in rat-1 cells | Chromophore-assisted laser inactivation | Massive cell retraction that originated from the non-irradiated leading edge of the cells | Lamb, et al. (1997) |
| Overproducing in insect cell line | | Delay in cell detachment after viral infection | Martin, et al. (1995) |
| Assessment of resistance of mouse cell line expressing ICAM-2 cell surface molecules to natural killer cells | Trasfection with cDNA encoding human ezrin | Became sensitive to IL-2 and cause formation of uropods and relocation of ICAM-2 to the surface of uropods which leads to target-cell recognition | Helander, et al. (1996) |
| Inducing over production of ezrin during cell migration and tubulogenesis | | Drastic improvement in tubulogenesis and cell migration | Gary and Bretscher. (1995) |
| Stable expression of an N-terminal ezrin | | Absence of apical microvilli, decrease in tubulogenesis and cell migration | Crepaldi, et al. (1997) |

## 1.9 Membrane linker proteins and calpain

Calpain is a calcium-activated, intracellular cysteine protease distributed widely in animal cells (Hayashi et al. 1999). There are two ubiquitous calpain isozymes, μ-calpain and m-calpain, that are activated at micromolar and millimolar Ca2+ concentrations, respectively. Both calpains share similar biochemical characteristics, except for the calcium concentration required for activation; and their amounts vary from one tissue to another. Both calpains are composed of a large catalytic (80kDa) subunit and a small regulatory (30kDa) subunit; and each subunit contains a calmodulin like domain at the c-terminus (Croall and Demartino 1991; Kawasaki and Kawashima 1996). Upon $Ca^{2+}$ binding to the calmodulin-like domains, calpains become active and begin to autolyze. In the case of μ-calpain it is belived that the restricted autolysis in the large subunit that accompanies the increase in calcium sensitivity is itself the activation steps. Hayashi et al. (1999) have provide evidence that μ-calpain binds to the cytoplasmic surface of cell membranes as an 80kDa proenzyme and is converted autolytically to the 76kDa form via a 78kDa intermediate on the membrane. In neutrophils, μ-calpain is the predominate form (Inomata et al. 1989). Even though the physiological function of calpain is yet to be revealed, it has been suggested to play an important role in cellular events that occur in response to mobilized Ca2+. Like talin, ezrin is also a substrate for proteolysis by calpain.

The hypothesis that different sensitivity to calpain provides a basis for selective termination of the specialized linker structures of ezrin and moesin is supported by theoretical considerations and experimental evidence. Since the ability of ezrin and moesin to function as linker proteins requires sites in the N-terminus that bind plasma membrane proteins and sites in the C-terminus that bind the actin cytoskeleton (Algrain et al. 1993), proteolytic cleavage has the capacity to disrupt membrane-cytoskeleton linkages. Evidence

strongly suggesting that calpain sensitivity suffices as a basis for terminating the linker function of ezrin is provided by studies in gastric parietal cells in which ezrin cleavage by calpain was linked to inhibition of proton secretion (Yao 1993). In endothelial cells, ezrin cleavage by calpain was associated with stimulation of locomotion and abolition of ezrin's ability to associate with β-actin (Shuster et al. 1995). Ezrin and moesin in blood lymphocytes exhibit a divergent response to $Ca^{2+}$ signaling. Whereas ezrin was cleaved, moesin remained intact. Similar results were obtained when lymphocytes were activated with the more physiological stimulus anti-CD3 mAb.

These findings suggest that moesin, but not ezrin, retained the ability to function during and subsequent to $Ca^{2+}$ signaling. Indeed, ezrin and moesin may function sequentially to support different morphological structures required as lymphocytes differentiate, i.e. early acting ezrin in resting cells and moesin contributing to surface projections in lymphocytes that have undergone $Ca^{2+}$ signaling and activation. Circulating lymphocytes are spheroidal cells with a surface dominated by slender microvilli that serve to monitor the vascular wall (von Andrian etal 1995). As part of the early response to proliferation-inducing stimuli, lymphocytes undergo cytoskeletal remodeling and become polarized (Oslzowny etal 1998, Stewart et 1998, Gray 1993).

In resting lymphocytes, ezrin and moesin were found by fluorescent microscopy to co-localize in surface microvilli, and these structures were rapidly disassembled on cell activation.. Since ezrin and moesin can form heterodimers *in vivo* (Gary  and Bretscher 1993), early acting linker structures in resting lymphocytes may be composed of both ezrin and moesin, yet be disassembled upon lymphocyte activation by calpain proteolysis of only ezrin. In support of this theory, fluorescent microscopy revealed weak ezrin staining

homogeneously distributed in the cytosol, and moesin found as the sole ERM protein in the uropods of polarized activated T-lymphoblasts (Serrador et al. 1997).

In summary, ezrin and moesin represent the ERM proteins in blood cells. Cleavage of ezrin by calpain and insensitivity of moesin to this protease are documented as biochemically distinguishing features. Calpain-dependent cleavage of ezrin and persistence of moesin is demonstrated in the early response of intact lymphocytes to proliferation-inducing stimulation. Together, these findings suggest that different susceptibility to calpain contributes to the specialized non-redundant functions of ezrin and moesin.

## 1.10 Aims

Neutrophils change shape to migrate across the endothelial cell line to infiltrate any inflammatory area. It has been suggested that this change in shape of the cell may be because of unfolding of wrinkles present on the plasma membrane of neutrophils. These wrinkles are probably held in place by a group membrane linker proteins like talin and ezrin, which are know to form a link between the cell membrane and actin. These proteins are also proteolytically cleaved by the calcium activated proteolytic enzyme called calpain. Theoretically, it is possible that proteolytic cleave of membrane linker proteins in neutrophils may cause unfolding of wrinkles which in turn provides the extra reservoir of plasma membrane which neutrophils may use to extravaste across the endothelial lining.

The aim of the work presented in this thesis is to identify the subcellular position of membrane linker protein in neutrophils, to establish whether they are proteolytically cleaved during neutrophil activation. This would also establish a possible biological marker in extravasted neutrophils. This thesis also present a cell model for investigating the dynamic of ezrin proteolysis during cell shape change.

# CHAPTER 2

## Materials and Methods

## 2.1    General materials

## 2.1.1    Reagents used

Table 2.1.1 List of reagents used in the study

| Reagent name | Pharmaceutical company |
|---|---|
| Acetic acid | Fisher Scientific, Leicestershire, UK |
| Acridine orange | Sigma Chemical, Poole, UK |
| ALAN | Calbiochem, UK |
| Amaxa nucleofector solution V | Lonza, Cologne, Germany |
| Asante red | TEFLabes, Inc, Austin, UK |
| BCA protein assay | Thermo scientific, UK |
| Bio-Rad DC protein assay kit | Bio-Rad Laboratories, Hemel Hempstead, (UK) |
| Biotinylated protein ladder | Cell Signaling Technology |
| Bovine serum albumin (BSA) | Sigma Chemicals, Poole, Dorset, UK. |
| $CaCl_2$ | Sigma Chemicals, Poole, Dorset, UK. |
| Coomassie brilliant blue | Sigma Chemicals, Poole, Dorset, UK. |
| Dextran | Sigma Chemicals, Poole, Dorset, UK. |
| Dimethyl sulphoxide (DMSO) | Sigma Chemicals, Poole, Dorset, UK. |
| EDTA | Sigma Chemicals, Poole, Dorset, UK. |
| EGTA | Sigma Chemicals, Poole, Dorset, UK. |
| Ethanol | Fisher Scientific, Leicestershire, UK |
| Fetal calf serum (FCS) | Fisher Scientific, Leicester, UK |
| Ficoll-paque | Amersham Biosciences, Uppsala, Sweden |
| Filter paper | Whatman International Ltd, Maidstone,UK |
| Fluorescein isothiocyanate (FITC) | Sigma Chemicals, Poole, Dorset, UK. |
| Fluro-4-AM | Invitrogen, Carlsbad, California, USA |
| FMLP | Sigma Chemicals, Poole, UK |
| Formaldehyde | Fisher Scientific U.K. Ltd, Leicester, UK. |
| Fura-2 dextran | Invitrogen, Carlsbad, California, USA |
| Fura-2-AM | Molecular Probes, Eugene, Oregon, USA |

| | |
|---|---|
| Giemsa stain | Raymond A Lamb, UK |
| Glycine | Melford Laboratories Ltd, Suffolk,UK |
| Heparin sodium (5000 IU/ml) | CP Pharmaceuticals Ltd, Wrexham, UK |
| Hepes | Fisher Scientific U.K., Leicester, UK. |
| HiMark™ pre-stained high molecular weight protein standard | Invitrogen, UK |
| Horse serum | Vector Laboratories Inc., Burlingame, USA |
| Hybond nitrocellulose membrane | Amersham Bioscience UK Ltd, Bucks, UK |
| Ionomycin | Calbiochem, UK |
| KCl | Sigma Chemicals, Poole, Dorset, UK. |
| $KH_2PO_4$ | Sigma Chemicals, Poole, Dorset, UK. |
| Machery-nagel nucleobond® extra maxi kit | Abgene, Surrey, UK |
| Methanol | Fisher Scientific U.K. Ltd, Leicester, UK. |
| $MgSO_4$ | Sigma Chemicals, Poole, Dorset, UK. |
| $Na_2CO_3$ | BDH Laboratory Supplies, Poole, UK. |
| $Na_2HPO_4$ | Sigma Chemicals, Poole, Dorset, UK. |
| NaCl | Sigma Chemicals, Poole, Dorset, UK. |
| $NaHCo_3$ | Fisher Scientific U.K., Leicester, UK. |
| NaOH | Sigma Chemicals, Poole, Dorset, UK. |
| $NiCl_2$ | Sigma Chemicals, Poole, Dorset, UK. |
| NuPAGE® anti-oxidant | Invitrogen, UK |
| NuPAGE® LDS sample buffer(4x) | Invitrogen, UK |
| NuPAGE® novex 3%-8% tris-acetate Gel 1.5 mm, 15 well | Invitrogen, UK |
| NuPAGE® sample reducing agent (10x) | Invitrogen, UK |
| NuPAGE® tris-acetate SDS running buffer (20X) | Invitrogen, UK |
| Phosphate buffer (pH 6.8) tablets | BDH Laboratory Supplies, Poole, UK |
| Protease inhibitor cocktail | Sigma Aldrich, Poole, UK |

| | |
|---|---|
| Protein A/G PLUS-agarose | Santa Cruz biotechnology, inc, Heidelberg, Germany |
| RPMI | Sigma Chemicals, Poole, UK. |
| Sodium dodecyl sulphate (SDS) | Melford Laboratories Ltd, Suffolk,UK |
| SuperSignal west pico chemiluminescent | Thermo Fisher Scientific , Rockford, USA |
| Supersignal$^{TM}$ west dura system | Pierce Biotechnology, Inc, Rockford, IL, USA |
| Thapsigargin | Sigma Chemicals, Poole, UK |
| Tris base (tris-hydroxymethyl)-aminomethane) | Melford Laboratories Ltd, Suffolk,UK |
| Triton$^®$ X-100 | Sigma Chemicals, Poole, UK |
| Trypan blue | Sigma Chemicals, Poole, UK |
| Trypsin | Sigma Chemicals, Poole, UK |
| Tween 20 (polyoxyethylene sorbitan monolaurate | Sigma Chemicals, Poole, UK |
| U73122- PLC inhibitor | Sigma Chemicals, Poole, UK |
| Zymosan A | Sigma Chemicals, Poole, UK |
| ZymosanA bioparticles opsonizing reagent | Molecular Probes, Eugene, USA |

## 2.1.2    Equipments used in this study

| | |
|---|---|
| 96-well and 6-well; flat well bottom; TC-treated; working volume: 0.1-0.2mL; | Fisher-Scientific, UK |
| BCA protein assay | Thermo scientific , Uk |
| Bio-Rad DC protein assay kit | Bio-Rad Laboratories, Hammelmpstead, UK |
| Cell culture inserts for 24 well plates (ThinCert$^{TM}$) | Greiner Bio-One GmbH, Germany |
| Cellometer auto T4 plus SK-1800 | Nexcelom Bioscience, Lawrence, USA |

| | |
|---|---|
| Cellometer cell counting chamber slides | Nexcelom Bioscience, Lawrence, USA |
| CLSM confocal microscope (SP2) | Leica, Milton Keynes, UK |
| CLSM confocal microscope (SP5) | Leica, Milton Keynes, UK |
| Color silver stain kit | Thermo scientific, UK |
| Culture flasks ($25cm^2$ and $75cm^2$ | Greiner Bio-One Ltd, UK |
| ECL PLUS western blotting detecting system | GE Health Care, UK |
| Eppendorf 5629 micromanipulator | Eppendorf, Hamberg, Germany |
| Eppendorf Femtojet pressure controller | Eppendorf, Hamberg, Germany |
| Eppendorf Injectman micromanipulator | Eppendorf, Hamberg, Germany |
| Falcon tube | Fisher-Scientific, Leicestershire, UK |
| IC100 Intensified CCD camera | PTI, Surbiton, U.K. |
| IC100 Intensified CCD camera | PTI, Surbiton, U.K. |
| Micropipette capillaries | Sutter Instruments, USA |
| Micropipette Puller P2000 | Sutter Instruments, USA |
| Microscope stage heater | Linkam Scientific Instruments, U.K. |
| Neubauer haemocytometer counting chamber | *Mod-Fuchs Rosenthal, Hawksley*, UK |
| Nikon Eclipse inverted microscope | Nikon, UK |
| Nikon Eclipse inverted microscope | Nikon, UK |
| Novex® Semi-Dry Blotter | Invitrogen , UK |
| Olympus BX5I Microscope | Olympus, U.K. |
| Pre-pulled femtotips<br><br>Phagocytosis - tip diameter 1$\mu$m<br><br>SLAM - tip diameter 0.5$\mu$m<br><br>Part-cell labelling - tip diameter 5 mm | Manufactured in house |
| Pre-pulled femtotips - Phagocytosis- tip diameter 1$\mu$m | WPI, UK. |
| Roller mixer | Stuart, Wolf-Laboratories, York, UK |
| Supersignal ™ west dura system | Pierce Biotechnology, Inc., Rockford, IL, USA |
| The Xcell sure lock™ protein electrophoresis cells(mini-cell) | Invitrogen,UK |

| Universal containers | Greiner Bio-One Ltd, UK |
|---|---|
| UVIpro gel documentation system | Wolf Laboratories, UK |
| UVITech imager | UVITech Inc., Cambridge, UK |
| Micromanipulator | Eppendorf .Inc , UK |
| WPI micromanipulator | WPI, USA |

.

## 2.1.3  Software used in this study

| Image Master 1.4b8 | PTI, Surbiton, UK |
|---|---|
| Microsoft Excel 2000 | Microsoft, Redmond, USA. |
| Paintshop Pro Version 4.15 SE | Jacs Software Inc. |
| Microsoft PhotoEditor 3.0 | Microsoft, Redmond, USA. |
| Microsoft Paint Version 5.1 | Microsoft, Redmond, USA. |
| Adobe Photoshop 7.0, | Adobe Systems Inc, USA |
| Microsoft Word 2007 | Microsoft, Redmond, USA. |
| UVIpro Acquisition Software | UVITEC, Cambridge, UK |
| UVIband Software Package | UVITEC, Cambridge, UK |
| Image J | NIH, U.S.A |
| Gif Animatior (32-bit) | Alchemy Mindwork Inc, Canada |

## 2.2    Cell lines used

Ten different cell lines were used in this study, in order to find a positive control for talin, kindlin and ezrin. HL60 cell lines were acquired from the European Collection of Animal Cell Culture (ECACC, Salisbury, UK) PZ-HPV-7 were obtained from the American Type Culture Collection (ATCC, Rockville, USA), PNT-2C2 were kindly given to us by Professor Norman Maitland (University of York, York, UK). Full details of these cell lines are supplied in table 2.2. DMEM and RPMI media supplemented with 10% fetal calf serum and antibiotics was used to regularly maintain the cells.

**Table 2.2 Cell lines used in this study**

| Cell line | Origin | Cell morphology | Tissue type | Features |
|---|---|---|---|---|
| PZ-HPV-7 | 70 year old Caucasian male | Epithelial | Non tumourogenic epithelial cell line transformed through HPV18 transfection | Derived from normal adult prostatic epithelial cells |
| PNT2C2 | 33 year old Caucasian male | Epithelial | Normal prostatic epithelial cell line, immortalised with SV40 DNA | |
| HL 60 (ECCACC No: 88112501) | PHLS, Salisbury, UK | Neutrophil | Blood or bone marrow | Derived from patient with myeloid leukaemia |
| RAW 264.7cells | LGC Standards, UK | Monocyte-marcrophage Cell line | Mouse muscle | Established from a tumor induced by Abelson murine leukemia viru |
| MAC cells | LGC Standards, UK | Lymphocytes | Mouse muscle (myloma) | Established from a tumor induced by Abelson murine leukemia virus |
| MCF7 | LGC Standards, UK | Lymphocytes | Mouse muscle (myloma) | Immunoglobulin; monoclonal antibody; against human mammary tumor cells |
| PLB-985 cells | LG Standars, UK | Neutrophils | Peripheral blood | From human acute myeloid leukemia |
| 3T3 cells | LGC Standards, UK | Fibroblast | Mus musculus (mouse) | Embryo |
| HUVEC | ICLC, Genova, Italy | Endothelium | Umbilical cord | Human Caucasian |
| HeLa | ICLC, Genova, Italy | Epithelial –like morphology | Human cervix | Carcinoma |

## 2.3    Antibodies used

### 2.3.1    Primary antibodies

Complete information of the various primary antibodies used in the research is given in
table below.

**Table 2.3.1. List of primary antibodies**

| Antibody name | Source | Molecular weight (kDa) | Supplier | Product code |
|---|---|---|---|---|
| Anti-kindlin3 | Mouse polyclonal antibody | 76 | Abcam, Inc | AB 67928 |
| Anti- talin head group (H-300) | Rabbit polyclonal antibody | 206 | Santa Cruz Biotechnology, Inc. | SC-15336 |
| Anti-talin tail group (8-D4) | Mouse monoclonal antibody | 190 | Santa Cruz Biotechnology, inc. | SC-59881 |
| Anti- ezrin (3C12) | Mouse monoclonal antibody | 81 | Santa Cruz Biotechnology, inc. | SC-58758 |
| Anti – actin ( phalloidin) | Mushroom conjugated with tetra methyl rhodomine | 78 | Sigma-Aldrich Company Ltd. Pool, UK | P2141 |
| Phycoerthythrin or fluorescein labelled antibody to CD11b | Raised against human and mouse CD11b | | Miltenyi Biotec , UK | 130-081-240 |
| Fluorescein-labelled antibody to CD18 | Raised against human and mouse CD11b | | Miltenyi Biotec, Uk | 130-081-201 |

## 2.3.2    Secondary antibodies

The secondary antibodies used for western blotting technique were horseradish peroxidise (HRP)-conjugated goat anti-mouse IgG and goat anti-rabbit IgG both supplied by by Santa-Cruz Biotechnology (Santa-Cruz, USA). Those used for immunocytochemistry were either goat anti-rabbit IgG or goat anti-mouse IgG conjugated either with FITC or CY3 supplied by Santa-Cruz Biotechnology (Santa-Cruz, USA) and  Zymed laboratories. Inc, UK. Details regarding secondary antibody used in this study is given in the table 2.3.2.

**Table 2.3.2.: List of secondary antibodies used in this study.**

| | | | | |
|---|---|---|---|---|
| Anti- rabbit  IgG FITC conjugated | Goat antibody | Depended on primary | Santa cruz Biotechnology, Inc. | SC- 2012 |
| Anti- mouse IgG- FITC conjugated | Goat antibody | Depended on primary | Santa Cruz Biotechnology, Inc | Sc-  2047 |
| Anti- mouse IgG- CY3 conjugated | Goat antibody | Depended on primary | Zymed laboratories,Inc. | Lot : 80140333 |
| Anti- rabbit  IgG CY3 conjugated | Goat antibody | Depended on primary | Zymed laboratories,Inc | Lot no:80642005R |
| Anti-rabitt (whole molecule) IgG peroxidase conjugate | Goat antibody | Depended on primary | Santa Cruz Biotechnology, Inc | Sc- 2004 |
| Anti-mouse (whole molecule) IgG Peroxidase conjugate | Goat polyclonal antibody | Depended on primary | Santa Cruz Biotechnology, Inc | Sc- 2005 |

## 2.4 Solutions and reagents

### 2.4.1 Neutrophil isolation

***Venous blood neutrophil isolation***

*Balanced Salt Solution (BSS)*

BSS, (0.13M-NaCl, 2.6mM-KCl, 8.0MM-$Na_2HPO_4$ and 1.83mM-$KH_2PO_4$, pH 7.4), was conveniently made in 5L batches with double distilled water, using following quantities 40g-NaCl, 1g-KCl, 5.75g-$Na_2HPO_4$ and 1.0g–$KH_2PO_4$. This was then adjusted to pH 7.4 using NaOH, aliquoted and heat autoclaved 20Psi for 30mins.

*Hepes Buffered Krebs medium (HBK)*

HBK, (120mM-NaCl, 4.8mM-KCl, 25mM-Hepes, 1.2mM-$KH_2PO_4$, 1.2mM-$MgSO_4$), 1.3mM-$CaCl_2.2H_2O$ and 0.1% bovine serum albumin (fraction V), pH7.4, was made up in the following stock solutions with double distilled water 1.2M-NaCl (35.2g/500ml), 2.5M-Hepes (29.8g/50ml), 0.48M-KCl (3.58g/100ml),0.12M-$KH_2PO_4$ (1.63g/100ml), 0.12M-$MgSO_4.7H_2O$ (2.95g/100ml), 0.13M-$CaCl_2.2H_2O$(1.9g/100ml), stored at 4$^°$C until needed, diluted accordingly and made up to in 100ml aliquots with the addition of a 100µl of frozen 10% solution of bovine serum albumin (fraction V). This was then adjusted to pH7.4 using NaOH.

*Dextran*

6 grams of dextran (80k) was dissolved in 100ml of BSS. This is used for erythrocyte sedimentation.

***Oral salivary neutrophils isolation***

*Phosphate Buffered Saline (PBS)*

PBS, 0.58M-$Na_2HPO_4$, 0.17M-$NaH_2PO_4$, 0.68M-NaCl, pH 7.4, was made up in as 1L of 10x stock with double distilled water as follows: $Na_2HPO_4$ (82.33g), $NaH_2PO_4$ (23.45g), NaCl (40.0g). This was stored at 4$^°$C until needed and diluted 1:10. The buffer had a pH of 7.3-7.4.

***Neutrophil isolation from gingival crevicular fluid***

The gingival crevicular fluid collected from the isolated tooth was emptied into a 50µl of 1% phosphate buffered saline which had 1µl of heparin (i.e. 250IU). Later, the cells were fixed in

suspension using 100µl of 4% formaldehyde. Then these cells were processed for immunocytochemistry in order to identify the subcellular position of various membrane linker proteins of interest.


### 2.4.2    Solutions used for cell culture and protein work

*0.05M EDTA*

1g KCl, 5.72g $Na_2HPO_4$, 1g $KH_2PO_4$, 40g NaCl and 1.4g EDTA was dissolved in 5L distilled water, adjusted to a pH of 7.4, autoclaved and stored until further use.

*Trypsin (25mg/ml)*

This solution was made up by dissolving 500mg trypsin in 0.05M EDTA, before being mixed and filtered through a 0.2µm minisart filter (Sartorius, Epsom, UK). This solution was then aliquotted into samples of 250µl and stored at -20°C until further use. When required for cell culture work, one of these aliquots was further diluted in 10ml 0.05M EDTA and used to detach cells.

*Balanced Saline Solution (BSS)*

79.5g NaCl, 2.1g $KH_2PO_4$ (BDH Chemical Ltd, Poole, UK), 2.2g KCl (Fisons Scientific Equipment, Loughborough, UK) and 1.1g of $Na_2HPO_4$ (BDH Chemical Ltd. UK) was dissolved in 10L of distilled water, and the pH amended to 7.2, using 1M NaOH (Sigma-Aldrich, Inc. UK)

*Neutrophils lysis buffer*

50mM of Hepes (200µl of 10x stock solution), 150mM of NaCl (200µl of 10x stock solution), 10% glycerol (200µl), 1% Triton X100 (200µl), 1.5mM $MgCl_2$ (200µl of 10x stock solution), 5mM of EGTA (200µl of 100x stock solution), 5mM EDTA (200µl of 100x stock solution), 1mM of $Na_3VO_4$ (200µl of 100x stock solution), 1.5mM NaF (200µl of 100x stock solution), 0.1%SDS (1ml of 10% stock solution).

*Cell lysis buffer*

This was made up by dissolving 2mM $CaCl_2$, 0.5% Triton X-100, 1mg/ml aprotinin, 1mg/ml leupeptin and 10mM sodium orthovanadate in 50ml double distilled water. The solution was then stored at 4°C until further use.

*Protease inhibitor cocktail*

A mixture of protease inhibitors with broad specificity for the inhibition of serine, cysteine, aspartic proteases and aminopeptidases. Contains 4-(2-aminoethyl)benzenesulfonyl fluoride (AEBSF), pepstatinA, E-64, bestatin, leupeptin and aprotinin, with no metal chelators. Supplied by Sigma-Aldrich, UK.

*Stripping buffer*

7.5g glycine, 0.5g SDS and 5ml of Tween20 made up to 500ml with double distilled water and pH of 2.2 by using HCL. Used for reprobing membranes for talin tail group.

*Running buffer (for SDS-PAGE)*

NuPAGE® Tris-Acetate SDS running buffer (20X) from Invitrogen, UK. was used for electrophoresis NuPAGE® Novex tris-acetate gels are made with high-purity, strictly quality-controlled reagents: Tris base, acetic acid, acrylamide, bis-acrylamide, TEMED, APS and highly purified water. They do not contain SDS. To perform electrophoresis this solution was further diluted to 1X concentration by adding double distilled water.

*Sample reducing buffer*

NuPAGE® Reducing Agent (10x) from Invitrogen, UK was used to reduced protein samples for protein gel electrophoresis. It contains 500 mM dithiothreitol (DTT) at a 10X concentration.

*Sample loading buffer*

NuPAGE® Novex LDS sample buffer from Invitrogen, UK was used which provide the best separation and resolution of small to medium-sized proteins by utilizing a neutral pH environment which minimizes protein modifications.

*Antioxidant*

The NuPAGE® Antioxidant is a proprietary reagent that helps maintain proteins in a reduced state during protein gel electrophoresis. The NuPAGE® Antioxidant is added to the running buffer in the upper (cathode) buffer chamber. The NuPAGE® Antioxidant migrates with reduced proteins during gel electrophoresis, preventing the proteins from reoxidizing and keeping the proteins in a reduced state. It protects sensitive amino acids, such as methionine and tryptophan, from oxidizing.

*Transfer buffer*

1.82g of 0.03M Tris, 1g of 2% SDS (w/v), 7.51g of 0.2M of Glycine and 50ml of 10% methanol was dissolved in 500ml of distilled water.

*Tris-acetate gel*

Precasted NuPAGE® Novex 3-8% triacetate gel, with 15 well and 1.0mm in thickness (Invitrogen, UK) was used. It is made with high-purity, strictly quality-controlled reagents: Tris base, acetic acid, acrylamide, bis-acrylamide, TEMED, APS and highly purified water.

*Tris Buffered Saline (TBS)*

24.228g Tris and 80.06g NaCl was dissolved in 1L of distilled water in order to make a 10x TBS (0.5M Tris, 1.38M NaCl, pH 7.4) stock solution. The pH was then adjusted to 7.4 using HCl and stored until further use.

*Ponceau S stain*

Supplied directly by Sigma-Aldrich, Inc. UK

*Coomasie blue stain*

100g Coomassie Brilliant Blue (Sigma-Aldrich, Inc. UK) was dissolved in 100ml acetic acid (Fisher Scientific, Leicestershire, UK) and 250ml ethanol (Fisher Scientific, Leicestershire, UK), which was then added to 650ml distilled water.

*Coomasie blue destain*

500ml of methanol was mixed with 100ml acetic acid and then added to distilled water to make up a final volume of 1L.

*Amido black staining*

0.5% amido black solution was prepared by dissolving 2.5g of amido black 50ml of acetic acid and 125ml of ethanol, in 325ml of distilled water.

*Amido black destainer*

100ml of 10% acetic acid, 250ml of 25% of ethanol dissolved in 1liter of distilled water.

*Silver staining kit*

Supplied by Thermo Scientific, USA.

Fixating solution (for silver staining the Nupage gel).

50ml of 50% ethanol and 5ml of 5% acetic acid added in to 100ml of distilled water.

## 2.4.3 Solution used for purification of plasmids

*LB broth*

10g tryptone, 10g NaCl and 5g yeast extract was dissolved in 1L of distilled water. The pH of the solution was then adjusted to 7.0 and after being autoclaved was left to cool. Antiobiotics were then added and the solution stored at room temperature.

*Elution buffer*

To prepare 8ml elution buffer, 1ml 8x PBS was mixed with 2ml 2M imidazole and topped with distilled water to a volume of 8ml. The pH was then adjusted to pH 7.4-7.6, and the final solution filtered.

*Machery-nagel nucleobond midi kit*

The NucleoBond® midi kit was purchased from Abgene, UK. The kit contain resuspension buffer, lysis buffer, neutralization buffer, equilibration buffer, wash buffer, elution buffer RNaseA (lyophilized), NucleoBond Xtra Midi colums and filters, NucleoBond finalizers, 30ml, 1ml syringes and TRIS buffer.

*Amaxa nucleofection*

A total of $2x10^6$ cell/ml of RAW 264.7 were counted, centrifuged and resuspended in 100µl of Nucleofector kit V (according to the manufacturer protocol). 8µg of ezrin plasmid (pH421-GFP) was added to the cell suspension and then transferred to a sterile cuvette (provided by the manufacture). Program D-023 was used to insert ezrin plasmid (ph421-GFP) into RAW 264.7 cell line by nucleofection. Cell were recovered in 500µl pre-warmed DMEM before being divided between 3 glass bottom dishes (Fisher Scientific, Leicester, UK), each containing 500µl pre-warmed DMEM. Cells were incubated at 37ºC in 5% $CO_2$ for 3 hours, before they were observed under the Confocal laser scanning microscopy(CLSM) to assess the transfection frequency and protein distribution.

## Plasmid pH421

The plasmid details were obtained from Addgene data base

| | |
|---|---|
| Gene/insert name | Ezrin |
| Alt name | EZR |
| Insert size | 1758 |
| Species | H. sapiens (human) |
| GenBank ID | NM_003379 |
| Entrez Gene | EZR (CVL, CVIL, VIL2, MGC1584, FLJ26216, DKFZp762H157) |
| Fusion protein or tag | GFP |
| Terminal | C terminal on backbone |
| Vector backbone: | pEGFP-N1 |
| Vector type | Mammalian expression |
| Backbone size w/o insert | 4700 |
| Cloning site 5' | EcoRI |
| Site destroyed during cloning | No |
| Cloning site 3' | SalI |
| Site destroyed during cloning | No |
| 5' Sequencing primer | GTGCACAAGTCTGGGTAC |
| 3' Sequencing primer | GTGAGCTACCATGTCCAG |
| Bacterial resistance | Kanamycin |
| Growth strain | DH5α |
| Growth temperature (℃) | 37 |
| High or low copy | High copy |

| Selectable markers | Neomycin |
|---|---|

## 2.4.4 Solutions used for immunocytochemistry

*40%formaladehyde:* diluted to 4% formaldehyde by adding 1X PBS. Used for fixing neutrophils and other cells.

*10X Triton:* diluted to 0.1% concentration using PBS.Used for permeabilization of neutrophils.

*Horse serum:* diluted to 4% using 1X PBS. Used for blocking non-specific binding of antibody.

*Primary and secondary antibodies* used to detect the subcellular position of membrane linker protein are given in table 2.3.1 and table 2.3.2.

*Confocal microscopy* was used to detect the subcellular location of membrane linker protein.

## 2.5    General methods

## 2.5.1   Isolation of neutrophils from human blood

Neutrophils were isolated from the heparinized blood of healthy adult volunteers as described by Hallett et al. (1990).

1. Heparinised blood (100$\mu$l/20ml blood; final concentration of 20IU per ml of blood) was mixed with 5ml Dextran (6% 80KDa in BSS) and allowed to sediment at room temperature for 30-45 minutes at 25$^{\circ}$C.

2. After sedimentation, the middle layer (buffy coat) containing white cells and plasma, was carefully removed and centrifuged (1900rpm, 2 minutes). Red blood cells were removed by hypotonic lysis, by resuspending the cells in 1ml double distilled water for 10 seconds, then restoring the osmolarity by diluting to 25ml with pH 7.4 BSS. This was centrifuged at 1900rpm for 2 minutes.

3. Polymorphonulcear leukocytes was separated from the other white blood cells, such as lymphocytes and monocytes, on the basis of densities, by Ficoll-Paque density gradient centrifugation. The pellet was resuspended in 5ml Hepes buffered Krebs (HBK) medium (+Bovine serum albumin) and overlaid on to 5ml of Ficoll-Paque. After centrifugation (1000rpm, 25 minutes), the supernatant was removed and the pellet containing the neutrophils (fig 2.5.1) washed to remove any Ficoll by resuspending in HBK, centrifuging (2000rpm, 1minute) and resuspending in HBK (1ml). The cell number, type and viability were then assessed by cell counting, typan blue exclusion, nuclear staining, phagocytosis assay and by assessing neutrophils response to FMLP by measuring calcium signalling. The average cell concentration produced from 20 ml of blood was found to be approximately 2-3x $10^7$, of which 90% were seen to be polymorphonuclear leukocytes by nuclear staining. The cells were then kept on ice for further use.

## 2.5.2 Isolation of extravasted neutrophils – *in vivo* method

### 2.5.2.1 Isolation of salivary neutrophils

Salivary neutrophils were isolated from healthy volunteers with no clinically diagnosable oral inflammatory conditions and were used as a source of extravasted neutrophils. The original oral rinse techniques described by Ashkenazi and Dennison (1989) and Cheretakis et al. (2005) were modified for use in this project. The subjects were asked to rinse their oral cavity for 1 minute with 10ml of 4X PBS and samples were collected for 4 – 5 minutes. The samples were pooled into a universal container. Neutrophils were isolated by centrifuging the samples at 1900rpm for 2 minutes. To the pellet 1ml of HKS solution was added and the samples were either used immediately or kept on ice until required.

**Figure 2.5.1.** Isolation of neutrophils from venous blood. Schematic diagram shows the various steps involved in isolation of neutrophils from venous blood
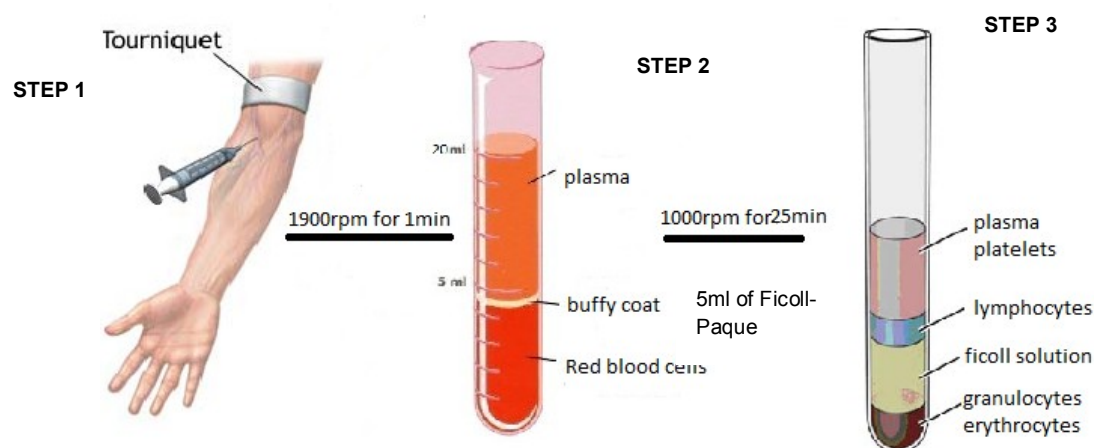


## 2.5.2.2 Isolation of neutrophils from gingival crevicular fluid

Capillary tube technique was followed to collect gingival crevicular fluid from both clinically inflamed gingival, as well as from clinically healthy gums. First, the tooth with clinical signs of acute gingivitis was identified and isolated using cotton roles. Following this, a sterile 4 cm glass capillary tube with a internal diameter of 2- 3 mm which could accommodated 10μl of fluid, was inserted into the entrance of the gingival crevice of the isolated tooth for 5 minutes and gingival crevicular fluid was collected for 15 to 20 minutes. The amount of fluid collected was measured by placing each capillary tube with the collected gingival cervicular fluid against a measuring ruler. Later, the collected fluid was emptied into a sterile eppendorff tube which contained 1μl of heparin (250IU) diluted in 50μl of 1X PBS. Using 4% formaldehyde, the cells were fixed in suspension. The cells were then force on to a glass cover slip using microtome (5000rpm for 5 minutes). These cells were later stained with specific primary antibody using

immunocytochemistry, as described in Section 2.5.6.1. This technique was used by Skapski (1976), Courts et al. (1977), Wilton 1977).

### 2.5.3 *Ex vivo* isolation of neutrophils after transendothelial migration

Transendothelial migration was performed to collect neutrophils that were extravasated under experimental condition. In this setup, neutrophils isolated from blood were allowed to pass through a monolayer of human umbilical vein endothelial cells (HUVEC cell line) which were grown in a sterilized insert and placed over 6 well cell culture plate. The cells that are collected at the bottom of the well represented extravasated neutrophils. Immunocytochemistry and western blotting techniques were used to detect membrane liner protein, talin, ezrin and kindlin. Cell tracker conjugated with FITC or CY3 was used to differentiate between the two groups of neutrophils in a mixed sample. The protocol described by Greiner Bio-One Ltd. and the technique described by Lyck et al. (2006) and Luscinskas et al. (2008) was used in this project.

*Preparation of HUVEC cell line*

HUVEC cells were cultured in $25cm^2$ and $75cm^2$ culture flasks (Greiner Bio-One Ltd. Gloucestershire, UK) with a loosely fitted cap in incubators at 37°C, 98% humidification and 5% $CO_2$. Cell confluence was visually assessed using a light microscope. If the cells were not confluent, the flasks were left in the incubator to grow until they reached sub-confluency (2-3 days). All handling of cells was carried out aseptically, using a Class II Laminar Flow Cabinet with autoclaved and sterile equipment. Once the cell reached a confluency of approximately 80-90%, the medium was aspirated and the cells briefly rinsed with sterile EDTA in order to remove any remaining serum which has an inhibitory effect on the action of trypsin. Adherent cells were then detached from the tissue culture flask using 1-2ml of Trypsin/EDTA (0.01% trypsin and 0.05% EDTA in BSS buffer) by incubating the cells at $37^0$C for approximately 5 minutes. Once detached, the cell suspension was then poured into 20ml universal containers (Greiner Bio-One

Ltd, Gloucestershire, UK) before being centrifuged at 1,600 rpm for 5 minutes, in order to pellet the cells.The excess liquid was then aspirated and the cell pellet resuspended in an appropriate amount of medium. The cells were either counted for use in immediate experimental procedures or transferred into fresh tissue culture flasks for re-culturing.

*Preparation of insert and neutrophils*

ThinCert™ cell culture inserts with porous membrane size of 3µm supplied by Greiner Bio-One, UK) were used.  Each insert was supplied with 6 multi-welled cell culture plates.. Three inserts were used as control in order to establish the influence of TNFα on the extravasation of neutrophils across the endothelial cell line. Each insert were coated with 100µl of 1:200 dilution of matrigel and allowed to dry at room temperature. After this each insert was rehydrated by rinsing twice with 200µl of DMEM tissue culture medium. Both outer and inner compartment of the setup was filled with DMEM medium in such a way that the level of the medium in both compartments was at the same level (fig 2.5.3A & B). 100µl of HUVEC ($1x10^5$cells/ml or $1x10^4$cells/ml) were added to each insert and left in the incubator for 3 to 4 days to adhere and become confluent. Once the cells reach confluency, 13nM/ml TNFα was added to the outer compartment of the test inserts (i.e excluding the inserts which were used as control). TNFα was used to upregulate ICAM1 in the endothelial cell line. The setup was left in the incubator overnight. $1x10^5$ neutrophils /ml of DMEM medium was added to each insert and left to adhere for 30 minutes in the incubator, so that all the neutrophils will settle down along the endothelial cell lining (fig 2.5.3A &B). The remaining isolated neutrophils from the venous blood were suspended in 1ml of DMEM and kept in the incubator. This sample represents non-extravasted neutrophils. The DMEM medium from the outer compartment of the insert was replaced with fresh medium mixed with 1µM of FMLP, prepared from 1mM stock solutions. Each time, the level of the medium in the two compartments were checked and maintained at same level.This setup was left in the incubator for 45 minutes and the cells which cross the endothelial cell layer were

collected from the outer compartment, either on a glass cover slip (to use for immunocytochemistry) or in suspension (for western blotting technique).
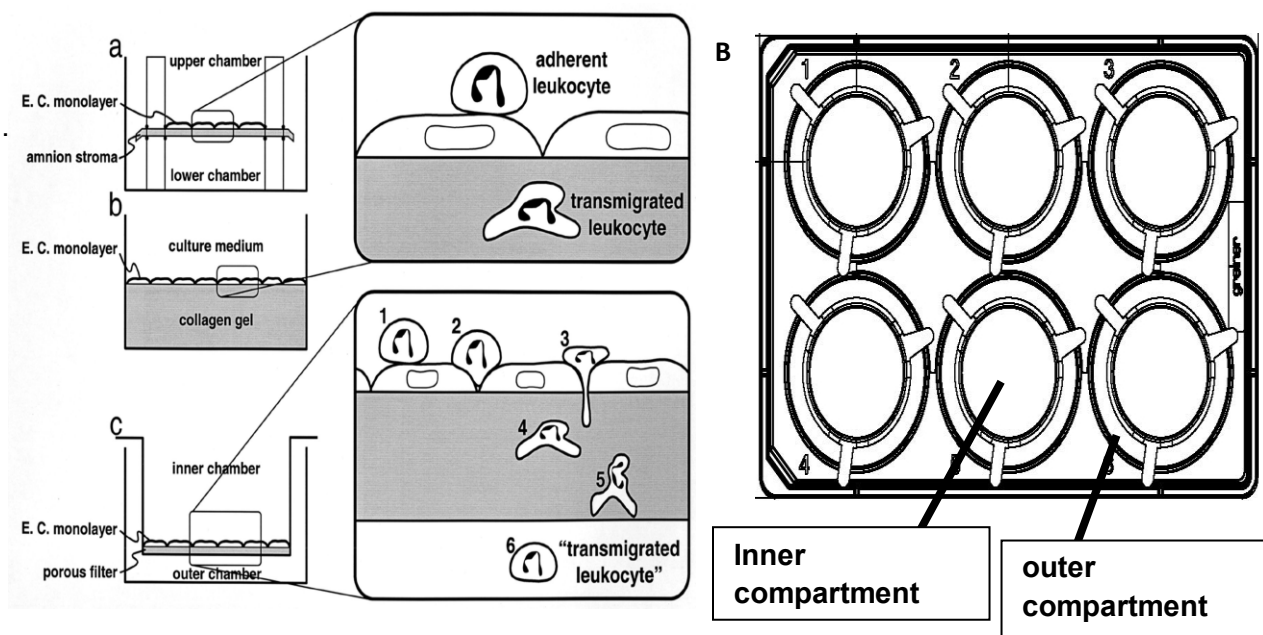


Figure 2.5.3.a. Schematic diagram of the transendothelial migration assay. 1x10$^5$ neutrophils/ml were added over the insert wich has coated with a monolayer of TNFα-treated endothelial cells. 1µM of *FMLP* was used to set in a chemical concentration gradient which enables the neutrophils to cross the endothelial monolayer. The migrated cells were collected on a glass cover slip placed at the bottom of the outer well or collected in suspension. The entire experiment was performed set at 37°C for45 minutes- 1 hou. The collected cells were then fixed and stained with respected primary antibodies. Figure 2.5.3.B. shows the aerial view diagram of the transendothelial migration assay. The inner compartment has the harvested monolayer of endothelial cells, to this compartment isolated neutrophils and *FMLP* was added. Migrated neutrophils were collected from the outer compartment.

## 2.5.4  Assessment of viability of isolated neutrophils

Viability experiments were carried out on neutrophils isolated from venous blood and saliva using trypan blue exclusion techinique, as well as calcium signaling efficiency in these cells using FMLP as a stimulus. Viability of these two groups of neutrophils were also assessed by evaluating the capacity of phagocytosis and chemotactic response in single cells, as well as in populations of neutrophils.

### 2.5.4.1 Trypan blue exclusion

This method relies on the observation that dead cells or cells with damaged membranes become stained by a deep blue color, due to their inablilty to exclude the dye.

1. 10 µl of cells in HBK were placed on a microscope slide and mixed with an equal volume of trypan blue stock (0.2% w/v in PBS). This was incubated for 2-3 minutes at room temperature.

2. The cells were then examined by light microscopy and the number of blue cells per field were counted and expressed as a percentage of the total.

    Using the above mentioned technique, typical viabilities of neutrophils isolated from venous blood was 95-99% and 90% for salivary neutrophils.

### 2.5.4.2 Evaluation of Phagocytosis in neutrophils

Phagocytic competence of populations of neutrophils was assessed by incubating cells with opsonized zymosan, before fixing and staining cells; and calculating the percentage of phagocytic cells. Phagocytic competence of single neutrophils was assessed by recording the ability of neutrophils to engulf an opsonised zymosan particle using a micropipette and micromanipulator. Zymosan particles (10mg/ml) were opsonised either with human serum or purified human C3bi.

#### 2.5.4.2.1 Phagocytosis assessment in neutrophil population

1. Neutrophils were allowed to adhere to glass slides for 10 minutes at 37ºC.

2. Non-adhered material was washed away and fresh HBK/BSA medium applied.

3. 100µl of 0.1mg/ml C3bi opsonised zymosan particles was added to the neutrophils and slides incubated at 37ºC for 7, 15 or 30 minutes.

4. After incubation, non-adhered material was washed away with HBK/BSA and cells were fixed and stained using Giemsa staining kit for 15 minutes, according to the manufacturer's protocol.

5. Slides were mounted with glass coverslips, allowed to dry, and assessed by light microscopy for phagocytic uptake (ie. number of cells having undergone phagocytosis and number of particles internalized per cell). See fig 2.5.4.2.1a & b. Out of 200 neutrophils isolated from venous blood counted nearly all the cells had atleast 1zymosan partical. Similar finding was found in neutrophils isolated from saliva.

Figure 2.5.4.2.1a. Phagocytosis assessment in blood neutrophils. Light microscopic picture of phagocytosis by neutrophils isolated from venous blood (incubation - after 7 minutes)
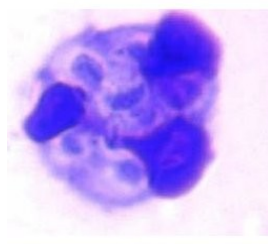


Figure 2.5.4.2.1b. Phagocytosis assessment in salivary neutrophils. Light microscopic picture of phagocytosis by neutrophils isolated from saliva- after 7 minutes
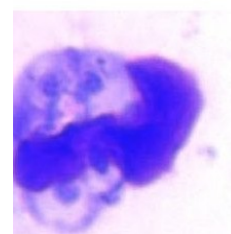


### 2.5.4.2.2 Phagocytosis assessment in single neutrophils - micropipette manipulator

The micropipette manipulator supplied by Eppendorf (Hamburg, Germany,) has two components: the injectman which moves the micropipette in three dimensions; and the femtojet which creates negative pressure inside the glass micropipette. This pressure enables

you to pick one opsonised zymosan and place it at close proximity to the selected neutrophil. Video studio movie wizard was used to record the entire phagocytosis event.

1. Neutrophils were allowed to adhere to glass slides for 10 minutes at 37ºC.

2. Non-adhered material was washed away and fresh HBK/BSA medium.

3. 10µl of 0.1mg/ml C3bi opsonised zymosan particles was added to the neutrophils and a healthy neutrophil was selected using light microscopy.

4. Using the micropipette manipulator, a zymosan particle was picked up and delivered to the selected neutrophils and the entire event was recorded using movie wizard video studio software.

 Similar steps described above were followed to evaluate the phagocytosis capacity of salivary neutrophils. Both groups of neutrophils were efficient at engulfing opsonised zymosan particles. This confirms that isolated neutrophils were healthy and retained their functional ability.

### 2.5.4.3 Cytosolic free Ca$^{2+}$ measurement in neutrophils

Fura-2 was used for this experiment. Fura-2 is a calcium chelator that displays a marked shift in fluorescent excitation spectrum when it binds to Ca$^{2+}$. Both Ca$^{2+}$ bound and unbound forms of Fura2 are fluorescent and two wavelengths are usually selected either side of the isoemissive point which represent the two different Ca$^{2+}$ binding state of the probe (340nm and 380nm). When Fura2 is unbound, it fluoresces maximally with 380nm excitation. When it  binds to Ca$^{2+}$, the spectrum shifts so that the 380nm signal decreases, but the fluorescence excited at 340nm increases. The emission wavelength for both Fura2 states is 505nm (fig 2.5.4.3B). Ratiometric fluorimetry uses these properties of Fura2 to quantify the changes in the cytosolic concentration of free Ca$^{2+}$. Both free and bound Fura2 molecules in cells are monitored by a high

power light source that alternates between 340nm and 380nm; and the 505nm light that is emitted by the two separate excitation wavelengths is collected. Computer software is programmed to calculate the ratio between the bound (340nm) / free (380nm) Fura2. When the free $Ca^{2+}$ concentration increases in cells, the amount of unbound Fura-2 decreases as it binds to the free $Ca^{2+}$. There, is therefore, a decrease in the signal produced by 380nm light, which is mirrored by an increase in the signal from the 340nm light, resulting in an increase in the bound: free (340/380) Fura2 ratio (fig 2.5.4.3C & D).

1. Fura-2 loaded neutrophils were allowed to adhere for 2-3 minutes to glass cover slips maintained at 37°C, using a temperature controlled microscope stage heater.

2. The coverslip was washed twice with HBK/BSA solution to remove unbound cells, debris and excess Fura-2-AM in the solution; and approximately 100$\mu$l HBK (BSA) returned to the coverslip.

3. Fura-2 is a calcium chelator that displays a marked shift in its fluorescent excitation spectrum when it binds to $Ca^{2+}$ (fig 2.5.4.3A).

4. Cells were viewed under a 100X objective of an inverted microscope (Nikon), and the excitation wavelengths (340nm and 380nm) selected using a rapid monochromator (Delta RAM, PTI, Surbiton, UK), which was connected to a Nikon Eclipse inverted microscope. The images at each excitation wavelength were collected using an intensified CCD camera (IC100 PTI, Surbiton, UK) and the ratio image calculated using Image Master software (PTI, UK). Ratio images were acquired with 16 frame averaging and threshold background subtraction at a rate of at least 0.6 frames/second. The ratiometric ($Ca^{2+}$) images were pseudo-colored according to the scale shown in fig 2.5.4.3 (blue to green) and the average ratio value of the pixels was calculated and plotted over the time course. The stimulus was added to the cells under view whilst recording continuously. The calcim signal was effectively absorbed in neutrophils isolated from both blood and saliva.

**Figure 2.5.4.3 Fura Red as calcium indicator**
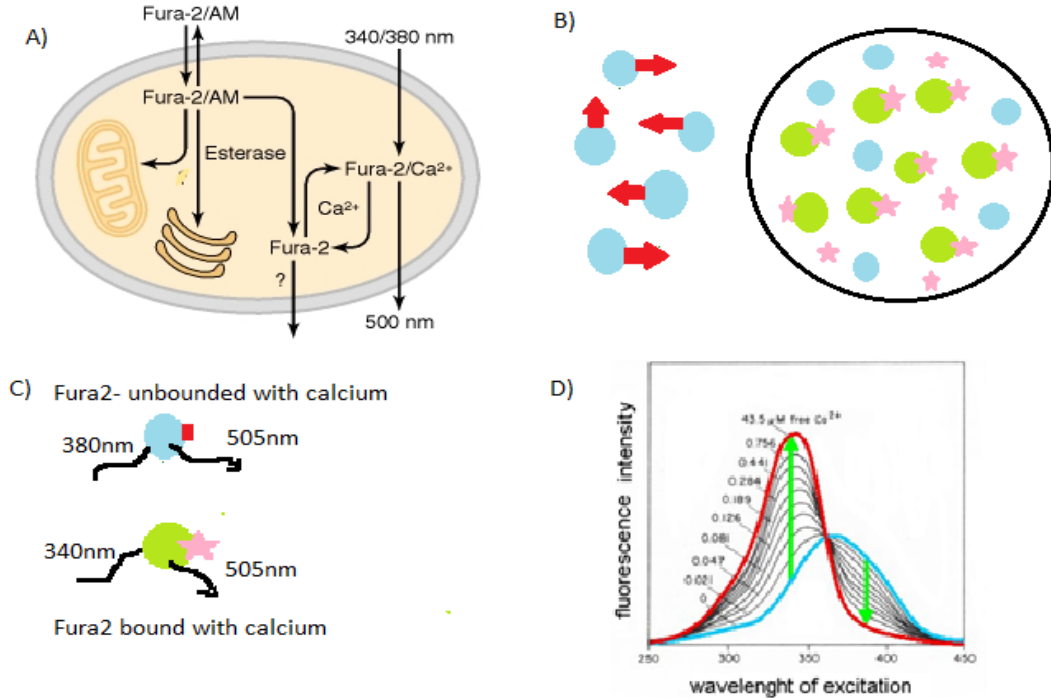


Figure 2.5.4.3. Cytosolic calcium change measured by fura2 probe. The Fura2 probe can be used to ratiometrically measure changes in the cytosolic free $Ca^{2+}$ concentration in cells. (A) Cells are loaded with Fura2 as its AM-ester which is able to cross the cell membrane. Intracellular esterases cleave the AM component allowing Fura2 to bind to available free cytosolic $Ca^{2+}$ (pink star) (B). (C) The excitation and emission spectra for $Ca^{2+}$ bound Fura2 and $Ca^{2+}$ free Fura2 is shown. The excitation spectrum for unbound fura2 displays a left shift when it binds to $Ca^{2+}$. Fluorescence of both states is detected at 505nM. (D) Two wavelengths are selected either side of the isoemissive point (I) to differentially excite the 2 states of the Fura2 probe. 380nm is used to excite $Ca^{2+}$-free Fura2 and 340nm selected for $Ca^{2+}$ saturated Fura2. Increasing $[Ca^{2+}]i$ results in an increase in the number of $Ca^{2+}$-bound-fura2 molecules at the expense of free Fura2. This causes a change in the detected fluorescence intensity for the 2 excitation wavelengths and can be measured as an increase in the ratio of 340/380nm excitation.

### 2.5.4.4  Evaluation of chemotaxis efficiency of neutrophils

A transendothelial migration assay was used to test the chemotaxis efficiency of both salivary neutrophils, as wells as venous blood neutrophils. Two separate transendothelial migration assays were setup as described in Section 2.5.3. Each experimental setup had two inserts treated with TNFα and two not treated with TNFα as a control. $1x10^5$cells/ml of neutrophils isolated form venous blood, as well as from saliva, were added to each insert and left in the incubator for 45 minutes -1 hour. 1µM of FMLP was added to the outer compartment to create difference in concentration gradient.  Neutrophils that had crossed the monolayer of endothelial cells were collected onto a glass coverslip placed at the bottom of the outer compartment. After fixing and staining these neutrophils with Giemsa stain, the number of cells per field was counted separately under light microscope (table 2.5.4.4). Both groups of neutrophils were able to extravasate through the monolayer of endothelial cells which gives sufficient evidence that both groups of neutrophils were functionally active and healthy. Moreover, there was significant difference in number of migrated salivary neutrophils counted in each insert pair that were not treated with, TNFα when compared to the number of migrated venous blood neutrophils (table 2.5.4.4). This difference might indicate the presence of cytoplasmic memory in these cells as they would have crossed both the venous blood endothelial, as well as oral epithelial cells, before shedding into the oral cavity. The result provided below was from venous blood obtained from one subject. This experimental set up was repeated 5 times using venous blood obtained from various individuals and each time similar finding was noted.

**Table 2.5.4.4. Chemotaxis efficiency of neutrophils.**

| Neutrophils | Number of neutrophils counted TNFα treated insert (2 inserts) | Number of neutrophils counted Without TNFα treated insert (2 nserts) |
|---|---|---|
| Venous blood neutrophils | 16253 | 134 |
| Salivary neutrophils | 11174 | 1876 |

## 2.5.5 Cell culture, maintenance and storage

### 2.5.5.1 Preparation of growth media and cell maintenance

Cell lines listed in table 2.2 were either grown in Dulbecco's Modified Eagle's medium (DMEM/ Ham's F-12 with L-glutamine, E15-813, PAA Laboratories,UK) is supplemented with 10% heat inactivated Foetal Bovine Serum (PAA Laboratories, UK) and an antibiotic cocktail. Roswell Park Memorial Institute medium (RPMI medium) supplemented with 10% heat inactivated FCS, 5mM glutamine, 100µg/ml streptomycin and 100µg/ml penicillin at 37ºC in 5% $CO_2$.

- HL60 cells lines and PLB cell lines are immature immortalized myeloid cells and immortalized, so they were grown continuously in RPMI medium supplemented with 10% heat inactivated FCS, 5mM glutamine, 100µg/ml streptomycin and 100µg/ml penicillin at 37ºC in 5% CO2.

- 3T3 cells, RAW264, Hela, PZ-HPV-7, PNT-2C2, MAC and MCF7 cell lines were grown in DMEM supplemented with 10% heat inactivated FCS, 5mM glutamine, 100µg/ml streptomycin and 100µg/ml penicillin at 37ºC, 5% $CO_2$.

1. All the cell lines were cultured in $25cm^2$ and $75cm^2$ culture flasks (Greiner Bio-One Ltd, UK) with a loosely fitted cap in incubators at $37^0C$, 98% humidification and 5% $CO_2$.

2.   Cell confluence was visually assessed using a light microscope and approximating the percentage of cells covering the surface of the tissue culture flasks.  If needed for experimental work, the cells were left to grow until they reached sub-confluence (2-3 days).  All handling of cells was carried out aseptically, using a Class II Laminar Flow Cabinet with autoclaved and sterile equipment.  Cells were routinely sub-cultured when they had reached a confluence of 80-90% (5-7 days), as explained in section 2.3.2.

3.   Once the cells had reached a confluency of approximately 80-90%, the medium was aspirated.

4.   3T3, NIHcells, RAW264, PZ-HPV-7, PNT-2C2, MAC cells and MCF7 cells lines are adherent cells and were detached from the tissue culture flask using plastic cell scapers.

5.   Once detached, the cell suspension was then poured into 20ml universal containers (Greiner Bio-One Ltd, UK) before being centrifuged at 1000 rpm for 15 minutes, in order to pellet the cells.

6.   The excess liquid was then aspirated and the cell pellet resuspended in an appropriate amount of medium and the cells were used in immediate in experimental procedures or transferred into fresh tissue culture flasks for re-culturing.


### 2.5.5.2    Cell storage and cell resuscitation

1. For long term storage cells were frozen in either 10% DMSO, 90% medium supplemented with FCS (HL60, NB4 3T3 and RAW cells) or FCS with 10% DMSO (MyPH8B6 cells). $5\times10^6$ (1 confluent flask) cells were frozen per cryovial.

2. A stock solution of 20% DMSO in medium was prepared.  Cells were centrifuged at 1600rpm for 4 minutes and resuspended in 500μl medium and added to cryovial along with

500μl stock medium and DMSO solution, so that final concentration of DMSO is 10% and cells are exposed to DMSO for as little time as possible. Cryovials were frozen down slowly (1ºC per minute) in -80ºC freezer overnight. Cells are then moved to the liquid nitrogen stores for long term storage.

3. To defrost cells were thawed quickly under warm running water and transferred into 15 ml pre-warmed RPMI/DMEM to dilute the DMSO. Cells are allowed to recover for approx 20 minutes in 37º/5% $CO_2$ incubator. Cells were centrifuged at 1600rpm for 4 minutes and then resuspended in 5 ml warm RPMI/DMEM and placed in a flask.

## 2.5.6  Methods of detection of membrane linker protein

### 2.5.6.1  Immunocytochemistry

Immunocytochemistry was used to assess the presence of talin, kindlin and ezrin protein (ie. cytoskeletal linker proteins) in neutrophils by using monoclonal mouse or polyclonal rabbit antibody as primary antibody and secondary antibody conjugated with FITC or Cy3b were used to visualize the bounded primary antibody under confocal microscope.

1.      100μl of isolated neutrophils were added onto glass cover slip and allowed to adhere at 37ºC for 10 minutes.

2.      Unbounded cells and cell debris were removed by washing the cells twice with HBK solution.

3.      The cells were fixed for 15 minutes at room temperature using 100 μl of 4% formaldehyde, prepared from a stock of 40% formaldehyde using 1X PBS buffer.

4.     Excess of formaldehyde was removed by washing the slide with 1XPBS buffer three times

5.     The cells were permeabilized for 4 minutes using 100µl of 0.1% Triton dissolved in 1XPBS and excess solution was removed by washing the slide with PBS buffer.

6.     100µl of 4% horse serum was used to block any non-specific binding sites and left at room temperature for 2 hours Cells were then washed twice with 4% horse serum.

7.     Primary antibody was diluted at a concentration of 1:100 using 4% horse serum and left overnight at 4ºC.

8.     After overnight incubation, the slides were washed three times with 4% horse serum and 100µl of secondary antibody (1:20 concentration) was added and left at room temperature for 1 hour in a dark foil.

9.     The slides were washed twice with 1XPBS and left at 4°C until observing under a confocal microscope.

## 2.5.6.2  Sodium dodecyl sulphate polyacrylamide gel electrophoresis (SDS PAGE)

## 2.5.6.2.1  Protein extraction and preparation of cell lysates

Once cells had reached an adequate confluence, the cells were scraped off using BSS and a cell scraper.  The cell suspension was then transferred into a universal tube.This was followed by centrifugation at 2,000rpm for 5 minutes, before the supernatant was poured off and the cell pellet resuspended in 200-300µl (depending on pellet size) of lysis buffer. Protease inhibitor were added and left on ice for one hour. At 15 minutes intervals, the samples were vortexed in order to increase the efficiency of lysis. The samples were then heated at 100ºC for 15-20 minutes, followed by centrifugation at 140,000rpm for 5 minutes. The pellet was discarded 10X

NuPAGE reducing agent and 4X NuPAGE sample buffer was added to the supernatant. These were then either quantified for SDS-PAGE as explained below, or stored in -20ºC until further use.The above mentioned steps were followed for extracting protein from neutrophils isolated for saliva, as well as from the blood. The neutrophil cell lysates were not stored in -20ºC, but rather directly quantified for SDS-PAGE.

## 2.5.6.2.2 Protein quantification and preparation of samples for SDS-PAGE

In order to standardise the protein sample concentration for western blotting, the amount of protein in each sample was quantified by following the protocol outlined in the Bio-Rad DC Protein Assay kit (Bio-Rad Laboratories, Hamel Hempstead, UK). In a 96 well-plate, 10mg/ml of bovine serum albumin (BSA) standard (Sigma Ltd, UK) was serially diluted in lysis buffer to a concentration of 0.005mg/ml and used to set up a standard curve of protein concentration. 5µl of either protein sample or standard was then pipetted into fresh wells before 25µl of 'working reagent A' (prepared by adding 20µl of reagent S per millilitre of reagent A) and 200µl of reagent B was added to each well. After mixing the samples, the plate was left at room temperature for 30-45 minutes, in order to allow the colorimetric reaction to take place.  Once this was complete, the absorbance of each of the wells was measured at 620nm, using the ELx800 Plate Reading Spectrophotometer (Bio-Tek, Wolf Laboratories, York, UK). Using the absorbance of the standards, a standard curve was set up and by comparing this to the absorbancies of the samples, sample concentration was determined.  The samples were then diluted in an appropriate amount of lysis buffer in order to normalise them to the protein extracted from the neutrophils. To this, 4x Lamelli sample buffer concentrate and 10x reducing agents in a ratio of 1:1 before the samples were denatured by boiling at $100^0$C for 5 minutes; and either loaded onto an SDS-PAGE gel or stored at -20°C until further use.

## 2.5.6.2.3 Sodium dodecyl sulphate polyacrylamide gel electrophoresis.

The method of SDS-PAGE used during this course of research was based on that of Laemmli(1970).

1.      The system used to carry out SDS-PAGE in this study was the The Xcell sure Lock™ Protein Electrophoresis Cells (mini-cell) supplied by Invitrogen, UK (fig 2.5.6.2.3i).

2.       Precast NuPAGE® Novex 3%-8% tris-acetate gels 1.5 mm, 15 well were used for protein separation. Each gel was supplied in clear pouch with 10ml of packing buffer which contain low levels of residual acrylamide monomer and 0.02% sodium azide (fig 2.5.6.2.3.II)

3.      The gel was washed with double distilled water and locked in the Xcell tank.

4.       Gels were run in NuPAGE® running buffer (Invitrogen) diluted 1:20, prepared by mixing 25ml of the running buffer stock solution with 500ml of distilled water. 200ml of this mix was taken separately in a glass beaker. To this, 500µl of NuPAGE® antioxidant reagent (Invitrogen) was added. The NuPAGE® tris-acetate discontinuous buffer system involves three ions:

- Acetate (-) is supplied by the gel buffer and serves as a leading ion due to its high affinity to the anode as compared to other anions in the system. The gel buffer ions are Tris+ and Acetate- (pH 7.0).

- Tricine (-) serves as the trailing ion from the running buffer. The running buffer ions are Tris+, Tricine and dodecylsulphate (-) (pH 8.3).

- Tris (+) is the common ion present in the gel buffer and running buffer. The Tris-acetate system also operates at a significantly lower operating pH of 8.1 during electrophoresis.

5. Running buffer with antioxidant was added to the middle compartment of the electrophoresis tank and the rest of the buffer was poured in the outer compartment as

per manufacturers' instructions. 500µl of Nupage$^{®}$ antioxidant reagent (Invitrogen, UK) was also added to the gel tank.

6. Gels were run for 1 hour at 150V constant and at current of 40-55 mA/gel (start); 25-40 mA/gel (end).

**Figure 2.5.6.2.3i**. Picture of The Xcell sure lock™ protein electrophoresis tank system.
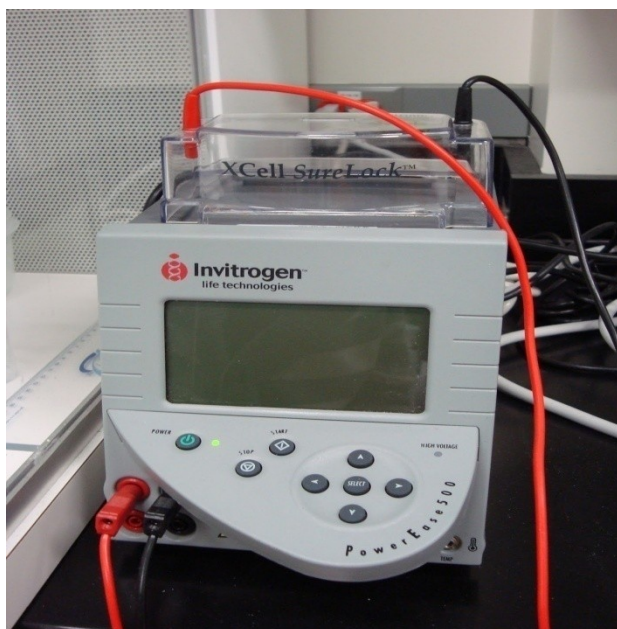




Figure 2.5.6.2.3II. Picture of NuPAGE® Tris-acetate mini gel.



BUFFER CORE

FRONT

BACK

LEVER

PRE-CAST GEL

PRE-CAST GEL OR
DUMMY GEL CASE

GEL TENSION WEDE
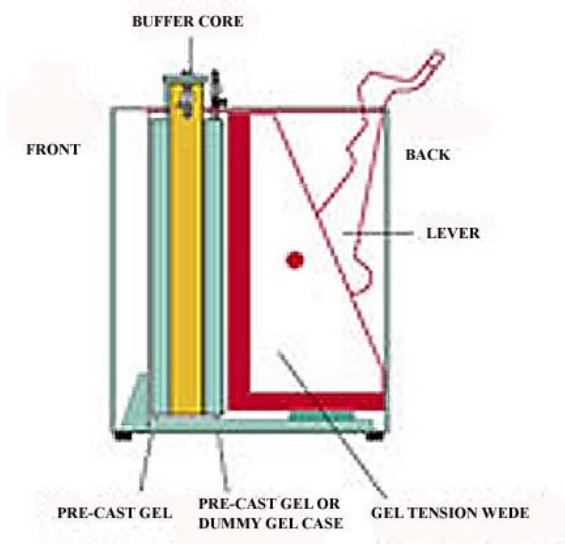
## 2.5.6.2.4 Preparation of pre-stained molecular weight marker

1. *HiMark™ pre-stained protein standard*

HiMark™ pre-stained protein standard from Invitrogen, UK, consists of 9 protein bands in the range of 30-460 kDa; and is designed for use with NuPAGE® Novex 3-8% Trisacetate (fig 2.5.6.2.4a & b). It allows easy visualization of protein molecular weight range during electrophoresis and evaluation of western transfer efficiency. 10- 12µl of this marker was added to the gel during electrophoresis.

Figure 2.5.6.2.4a                                          Figure 2.5.6.2.4b
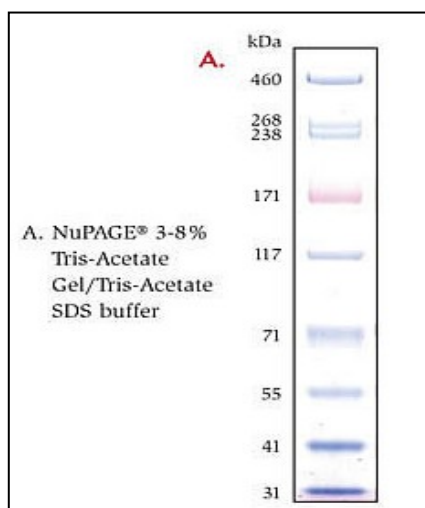
HiMark™ Pre-stained Protein Standard          Biotinylated protein ladder system
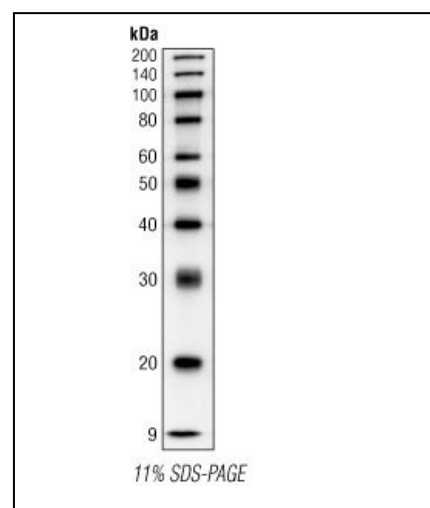


2. *Biotinylated protein ladder system*

This protein ladder was bought from Cell Signaling Technology, UK and was used to visualize the ladder during chemiluminescent western detection procedures (fig 2.5.6.2b). The biotinylated protein ladder was supplied  in 65mM Tris-HCl (pH 7.0 at 25°C), 35mM NaCl, 1mM $Na_2EDTA$, 2%SDS (w/v), 1mM NaN3, 40mM dithiothreitol (DTT), 0.01% (w/v) phenol red and 10% glycerol. Store at −20°C. The protein ladder consists of 10 proteins ranging in apparent molecular weight from 9 to 200kDa. The 9 kDa protein is derived from aprotinin purified from bovine lung. The proteins from 20-50

kDa are paramyosin fragments; the higher molecular weight proteins are fusions of maltose binding protein (MBP) with paramyosin or paramyosin/lacZ fragments. Anti-biotin, HRP-linked Antibody *was* Supplied in 10 µM sodium HEPES (pH 7.5 at 25°C), 150 mM NaCl, 100 µg/ml bovine serum albumin (BSA) and 50% glycerol. Before loading the ladder into the NuPAGE gel, the biotinylated protein ladder was thawed on ice. After mixing well, the desired amount of the protein ladder (10 µl) was aliquotted into a separate tube. The ladder was heated to 95-100°C for 2 minutes and after a quick microcentrifuge spin, was loaded directly onto the gel. Before adding the secondary antibody, anti-biotin HPR antibody was added to the secondary antibody at a dilution of 1:1000; and protein probing steps described later in this section were followed.

## 2.5.6.2.5 Western blotting: transferring proteins from gel to nitrocellulose membrane

1. Once SDS-PAGE was completed, protein samples were transferred to Hybond™ ECl™ P 0.45µm nitrocellulose blotting membrane. The electrophoresis equipment was disassembled and the gel along with the casing was placed in the running buffer until the western blotting model (XCell II™ blotting module from Invitrogen) was set (Fig 2.5.6.2.5a, b & c).

2. 5 sponges, 4 piece of Whatman number 1 filter paper (GE Healthcare, UK) and 1 piece of blotting membrane was soaked in transfer buffer for 30 minutes prior to electroblotting.

3. Transfer buffer was prepared by dissolving 1.82g 0.03M Tris, 1g 2% SDS (w/v), 7.51g of 0.2M glycine and 50ml of 10% methanol in 500ml double distilled water.

4. Three of the sponges that were soaked in transfer buffer were placed into the blotting module, followed by two soaked pieces of Whatman number 1 filter paper.

5. The gel was separated from the plastic casing and was placed on top of the filter papers, followed by Hybond blotting membrane. Finally two more sponges and two more filter papers were placed on top of the blotting membrane, 'sandwich'. Proteins were transferred for 1 hour at 30V and 220mA.

Figure 2.5.6.2.5a, b, and c. Western blotting system and setup

a



b

**C**



Cathode

Anode

Gel cast between glass plates.
Notches cast in top of gel to receive samples

western blotting mold

Gel

Transfer Membrane

Filter Paper

Pads

Support Grid

Buffer

**Direction of transfer**
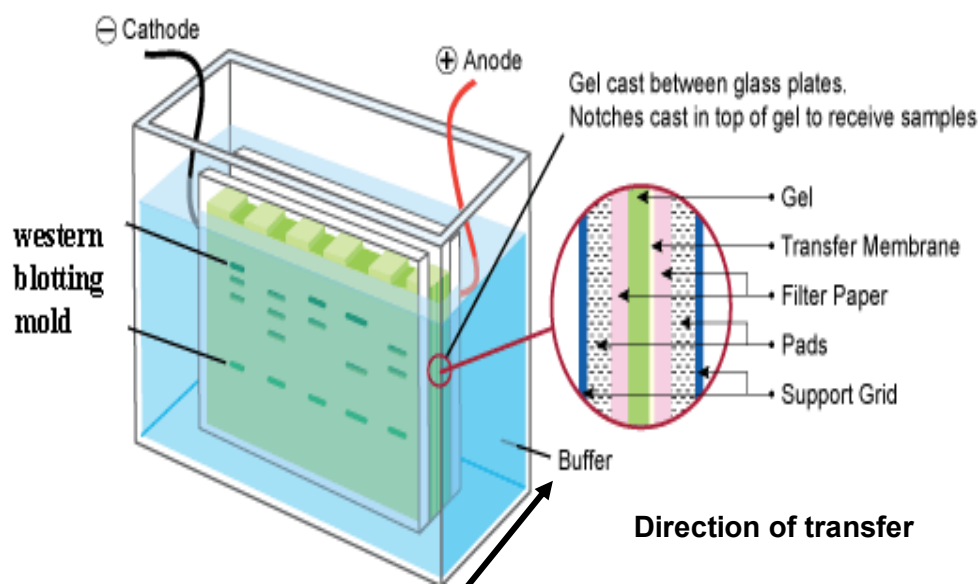
**Figure 2.5.6.2.5a, b & C.** Photographic picture of XCell II™ blot module from Invitrogen was used to transfere the protein from the gel into the membrane. Figure 2.5.6.3b: Photographic picture showing the way the module is place into the XCell Sure lock™ system. Figure 2.5.6.3c. Schematic diagram representing the western blotting set up, the protein runs from cathode (gel) to anode (membrane), wet blotting technique was followed. The gel and membrane was sandwiched between two spongs and two Whatmans filter paper and sealed inside the XCell™Blot module and set at 30V and 220mA for 1hour.

## 2.5.6.2.6 Protein staining

*Staining membranes in ponceau S*

Ponceau S is a reversible and re-usable protein stain that does not interfere with any subsequent immunoprobing.  Its main use is to confirm that protein transfer from the polyacrylamide gel to the nitrocellulose membrane has been successful but can also be used to aid in membrane sectioning for multiple immunoprobing.  The protocol was carried out as follows:

- After the transfer was completed and before probing began, the membrane was immersed in Ponceau S solution for a few minutes at room temperature.

- The solution was then washed off with distilled water until the bands become visible. If required, the membrane was then cut into several sections using a sharp and clean scalpel.

- Once the Ponceau S was completely washed off, it placed in 10% milk solution.

*Coomasie blue staining of polyacrylamide gels*

Coomasie blue is used to stain polyacrylamide gels following SDS-PAGE. This allows for visualisation of protein bands if no immunoprobing is required and can be used as a way of semi-quantifying the volume of the protein bands. The protocol was carried out as follows:

- The gel was immersed in Coomassie blue stain for approximately 30 minutes before being repeatedly washed in destain solution until the background staining disappears, and the protein appears as blue bands. The gel can then be photographed or analysed.

## 2.5.6.2.7 Protein detection using specific Immuno-probing

- Once any staining was completed, the membrane was transferred into 50ml falcon tubes (Fisher-Scientific, Leicestershire, UK), ensuring that the membrane surface that had been in contact with the gel was facing upwards. 10% milk blocking solution was then added to the membranes and incubated for an hour at room temperature on a roller mixer (Stuart Wolf-Laboratories, York, UK).

- Once this was done, the 10% milk solution was poured off and replaced with fresh 10% milk solution; and the falcon left in the fridge for 14 hours.

- Next day, the milk in the falcon was replaced with fresh 10% milk and left in the roller for an hour.

- Then the membrane was washed three times with 3% milk (3 grams of milk power in 100ml of tris-buffered saline with 200µl of tween 20. Each wash lasted for 10 minutes

- This was followed by incubation of the membranes for an hour at room temperature, with primary antibody diluted 1:1000 (for talin) or 1:100(for ezrin) in 5ml of 3% milk solution.

- After pouring off the primary antibody solution, any remaining unbound antibody was washed off three times in 3% milk solution at 15 minute intervals.

- Once washing was completed, the membranes were further incubated with 5ml of 1:1000 HRP-conjugated secondary antibody (of the same species) diluted in 3% milk. This was carried out for an hour at room temperature on a roller mixer.

- This was followed by two 15 minute washes in 10ml of 3% milk solution; and two 15 minute washes with  Tween TBS (0.1% Tween 20 in TBS) in order to wash off any unbound secondary antibody.

- A final two 15 minute washes with solely TBS was carried out so as to remove any residual detergent, before placing the membrane in weighing boats containing TBS solution, ready for chemiluminescent detection.


### 2.5.6.2.8 Chemiluminescent protein detection

Chemiluminescent protein detection was carried out using the Supersignal ™ West Dura system  from Pierce Biotechnology Inc., Rockford, USA (fig 2.5.6.6a), which consists of a highly sensitive chemiluminescent substrate that detects the horseradish peroxidise (HRP) used during the western blot.  The protocol was carried out as follows:

- The two reagents provided were added in a 1:1 (normally 4ml of each for a mini gel) ratio into the weighing boat containing the membrane to be analysed.  After 5 minute

incubation at room temperature with constant agitation, the membrane was carefully removed from the solution using forceps.

- Any excess solution on the membrane was then drained over a piece of tissue paper and transferred into a fresh weighing boat.  The chemiluminescent signal was detected using a UVITech Imager (UVITech Inc., Cambridge, UK) (fig 2.5.6.2.8b), which contains both an illuminator and a camera linked to a computer which then captured and stored the image.

- Each membrane was subjected to varying exposure times until the protein bands were sufficiently visible.  These images were then captured and further analysed with the UVIband software package (UVITEC, Cambridge, UK) which allowed for protein band quantification.

- In this study, β-actin was used as a housekeeping gene and run alongside any other proteins to be detected, so as to allow for additional normalisation of the samples and to compensate for any other negligible inaccuracies which may have occurred during the process.  The cytokeletal protein β-actin is used due to its highly abundant and conserved nature within eukaryotic cells; and is one of the most widely employed and accepted internal controls in scientific research.

In order to confirm reliability of the results, each western blot was carried out three times and the protein bands quantified and standardised separately, followed by calculation of mean values and graphical presentation of the results.  Each sample was blotted along with prestained high molecular weight marker supplied by Invitrogen, UK.

Figure 2.5.6.2.8a &b: Supersignal™ West Dura system  and  Chemiluminescent signal
   Deduction system
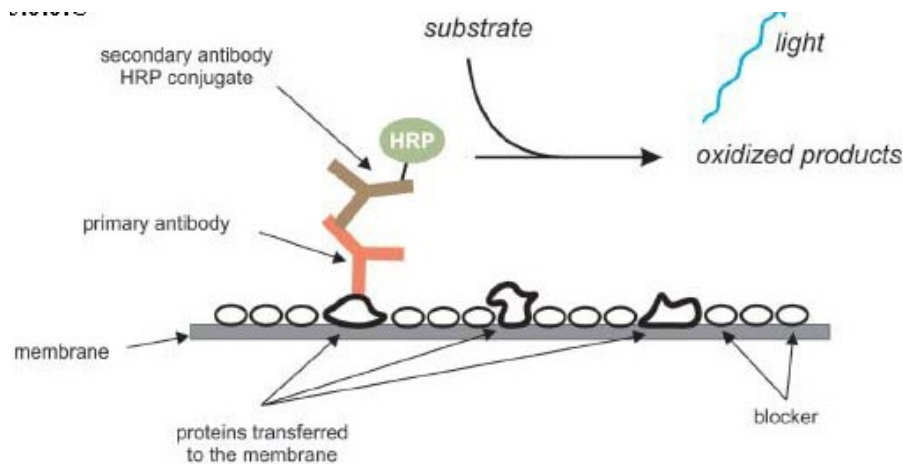




Figure 2.5.6.2.8c. Principle of chemiluminescent. A secondary antibody, conjugated to horseradish peroxidase (HRP) binds to a primary antibody directed towards the protein of interest. The blot is incubated with a chemiluminescent substrate, which is converted by HRP into a light emitting luminescents which is detected and recorded by the UVI band detecting system.

## 2.5.6.2.9 Determination of molecular weight of unknown protein

Determination of the molecular weight of an unknown protein was made by comparing the unknown proteins relative mobility (Rf) with that of several prestained high molecular weight markers (Invitrogen). After the membrane had been exposed to the chemilluminescent probe, the distance from the bottom of the well and to the position of the red tracking dye was measured using Image j Software. This is done before the membrane was stained. After staining the distance of each protein, including the markers from the bottom of the well was measured. Thus the relative mobility, (Rf), relative to the solvent front was calculated:-

Rf = migration distance of protein from bottom of the well/ total distance travelled by the tracking dye

After calculating a plot of log of molecular weight of each of the protein standards against their respective Rf values showed a linear relationship. Unknown molecular weight were estimated via linear regression analysis on the calibration curve thus obtained using the following equation in the form of y= mx+c were :-

Y= log mwt of unknown protein

M= gradient of the calibration curve

X= Rf value of unknown protein

C= interception of curve with x axis

## 2.5.6.2.10 Method for reprobing the membrane after chemiluminenscent detection

After using the chemiluminescent protein detection system (Pierce Biotechnology Inc., Rockford, USA), it was possible to reprobe a membrane several times. This was important as valuable membrane samples could be reprobed several times with a variety of antibodies. Using the following method derived by Kaufmann et al. (1987), it is possible to completely remove both primary and secondary antibodies and reprobe the membrane several times.

1. After immunodetection, the membrane was placed in a falcon tube and 5ml of stripping buffer with pH of 2.2, made by mixing 7.5g glycine, 0.5g SDS, 5ml Tween 20 added to 500ml of double distilled water. This was left in the roller to mix for 30 minutes.

2. After this the membrane was washed three times with TBS Tween 20(100ml of TBS with 200µl of Tween 20). Each wash lasted for 10 minutes.

3. Then, the membrane was then soaked in 10% milk and left in the roller spin for an hour. Then, this milk was replaced with fresh 10% milk and left in the fridge overnight.

4. Then next day fresh 10% milk was added to the membrane and left in the roller spin for and one hour. The membrane was processed as described in section 2.5.6.2.5.

## 2.5.6.2.11 Irreversible staining of western blotting membrane

After immunoprobing and detection, in order to compare the resultant Supersignal™ West Dura system with the total protein on the transfer blot, the anionic dye amido black was used. Protein bands showed up as dark bands on a light blue background.

This staining method was not compatible with the immunodetection of proteins and so permanent staining of membranes did not allow the membrane to be reprobed.

1.      Amido black working solution was prepared by dissolving 100mg of napthalene black in 100ml of 10% acetic acid and 25% propanol solution. The membrane was immersed in this solution for an hour on a shaker.

2.      After this amido black destaining solution prepared by dissolving 100ml of 10% acetic acid, 250ml of 25% of ethanol dissolved in 1Liter of double distilled water. The membrane was left in this solution overnight on the shaker.

## 2.5.6.3  Preparing immunoprecipitates

Immunoprecipitation was used to extract all the targeted membrane linker protein from the neutrophil samples, in order to get the sequence of the cleaved and intact portion of the target protein using mass spectrometry. The process involves adding a specific antibody targeted against a protein of interest within a cell lysate.  This then mixed with sepharose or agarose bonded staphylococcal protein A, protein G or both, in order to collect the ensuing protein-antibody complexes. These complexes were then centrifuged to induce precipitation, run on an SDS-PAGE gel and evaluated using immunoprobing.  The process is carried out as follows:

-      Neutrophils isolated from venous blood here lysed as described in section 2.5.6.2b. Before adding NuPAGE sample buffer and NuPAGE reducing agent, primary antibody targeted against a protein of interest was added to the cell lysate samples, before being incubated at 4°C for 1 hour on a rotating wheel.

-      Following incubation, 50μl of conjugated A/G protein agarose beads (Santa Cruz Biotechnology, supplied by Insight Biotechnologies Inc, UK) was added to each

sample and placed back on the wheel for another hour or overnight, in order to allow for the antibody-protein complexes to bind to the beads.

- Centrifuging at 8,000rpm for 5 minutes then acts as a way of removing any unbound protein or excess antibodies present in the supernatant. The protein pellet was subsequently washed twice with 300µl lysis buffer before being resuspended in 40-60µl of 10x sample buffer and boiled for 5 minutes. The resulting samples were then run on SDS-PAGE gels as explained below.

## 2.5.6.4 Mass spectrometry

*A) Sample preparation*

The immunoprecipitate samples were prepared as explained in section 2.5.6.3 and were run using The Xcell Sure Lock™ protein electrophoresis cells (mini-cell) supplied by Invitrogen,UK, using Precast NuPAGE® Novex 3%-8% tris-acetate Gel 1.5 mm. The technique described in section 2.5.6.2 was followed. Once the electrophoresis is complete:

1. The gel was fixed by using 100ml of fixative solution (50ml methanol, 10ml acetic acid, 40ml deionized water) and left in shaker at room temperature for 10 minutes.

2. Once the gel had fixed, Colloidal Coomassie Blue Staining Kit from Invitrogen was used to stain the gel following the manufacturers protocol, explained in brief below.

3. After the gel was fixed, staining solution was prepared by using methanol (20ml), Stainer A (20ml) mixed in 55ml of deionized water. This mix was added to the gel and left in the shaker at room temperature for 10 minutes.

4.      To this setup, 5ml of stainer B was adder and the gel left overnight in the shaker at room temperature. Protein bands start to appear within 2-3 hours in this set up but was left over night for better results.

5.      The following day, the stainer solution was washed away with deionised water and the gel was scanned before the spots were picked.

B) *Trypsin digestion of the sample*

Trypsin digestion was done in order to recover the peptide from 1DE or 2DE gels for analysis by mass spectrometry. Spots were cut manually using Ettan Spot picker pipette. Spots were picked from the mid-portion of the protein band on the gel, for multiple plugs /spots they were picked from either end of the protein band along with mid-portion. Each plug was treated separately. Plugs were also picked from the protein ladder as a quality control. In this project we took plugs from β-galactosidase (16.3kDa); phosphorylase B (97.4kDa); bovine serum albumin (66.3kDa); glutamate dehydrogenase (55.4kDa); lactate dehydrogenase (36.5kDa); or carbonic anhydrase (31.0kDa).

Each plug was placed separately in a 96 well-plate and the position of the spots on the plate noted. Once the spots were picked the gel was again scanned for discussing the results of the mass spectrometry.

The reagents listed in the table 2.6 were prepared and used for preparation of peptides from the picked plugs. Acetonitrile and solutions of acetonitirile require storage in glass containers. The rest of the reagents were prepared freshly.

**Table 2.6. Reagents used for trypsin digestion of the sample**

| Compound | Molecular weight | Amount per ml | Amount to make |
|---|---|---|---|
| **100mM  ammonium bicarbonate** $NH_4HCO_3$ in water. **Made up 2 days in advance of use.** | 79.06 | 7.91mg | 396mg in 50ml |
| **25mM ammonium bicarbonate** $NH_4HCO_3$ in water. *Made up fresh.* | - | - | 10ml of 100mM stock and 30ml of water |
| **10mM dithiothreitol DTT** (in 25mM $NH_4HCO_3$). *Made up fresh.* | 154.2 | 1.542mg | 1.542mg in 1 ml |
| **55mM iodoacetamide** (in 25 mM $NH_4HCO_3$). *Made up fresh.* | 185.0 | 10.175mg | 10.175mg in 1ml |
| **100mM sodium thiosulphate** in water. *Use within 2 weeks.* | 248.2 | 24.83mg | 248.3mg in 10ml |
| **30mM potassium ferricyanide** in water. *Made up fresh.* | 329.2 | 9.976mg | 9.976mg in 1ml |
| **µ-cyano-4-hydroxycinnamic acid** (in 50% (v/v) acetonitrile in 0.1 % (v/v) trifluoroacetic acid (TFA). *Made up fresh.* | | 5mg | 5mg in 1ml |

# CHAPTER 3

## The role of talin in neutrophil morphology change

## 3.1 Introduction

It is a well known fact that neutrophils rapidly change shape from spherical to a flattened morphology in order to achieve firm adhesion to the endothelial lining. Also during transmigration through the endothelium, irrespective of whether it is through the endothelial cell or between the endothelial cells (Ley et al. 2007), flattening onto the endothelial lining cells is a crucial first step. This morphology change is associated with a massive increase in the surface area of the leukocytes (Dewitt et al. 2007). It has been suggested that the extra reservoir of plasma membrane needed in order to adapt to the change in shape and surface area is provided by unfolding of wrinkles present in the plasma membrane of the neutrophils. The various possible mechanisms that might cause unfolding of membrane wrinkles in neutrophils have been discussed in detail in section 1.7.1.

### 3.1.1 Membrane linker proteins in cell surface wrinkles

The wrinkles found on the plasma membrane of the neutrophils resemble "microvilli" seen in lymphocytes (Shao et al. 1998). These wrinkles may be held in place by protein such as talin, kindlin-3 and ezrin. These proteins act as membrane-cytoskeletal linkers which form a bridge between membrane proteins, such as L-selectin and $\beta_2$ integrin; and the underlying actin cytoskeleton. This bridge may be formed between areas of plasma membrane outside the wrinkles or between the plasma membrane which form the wrinkles (fig 3.1.1) (Dewitt et al. 2007).

## 3.1.2 Mechanism which release membrane wrinkles

It has been shown that uncaging cytosolic calcium (Pettit and Hallett, 1998) or IP$_3$, triggers an elevation of cytosolic Ca$^{2+}$ (Dewitt et al. 2007) causes an accelerated rate of neutrophil flattening. This suggests that an elevation of cytosolic Ca$^{2+}$ is involved in the flattening of the wrinkled membrane present on the cell membrane of neutrophils. Moreover, a similar relationship between cytosolic Ca$^{2+}$ and membrane expansion has been established during pseudopodia extension (Dewitt and Hallet 2002). Under these conditions, unfolding of wrinkles was dependent on the activity of µ-calpain, a calcium-activated protease (Dewitt and Hallet 2002), µ-calpain cleaves substrates *in vitro* and within the cells. Talin and ezrin are the substrates which get proteolysed by calpain in vitro (Dewitt et al. 2008). If this occurs within neutrophils, this would cause cleavage of cross-linking between the cell membrane and cytoskeleton, which would provide a mechanism for releasing the wrinkles on the surface of neutrophils. The calpain cleavage site in both talin and ezrin lies between the FERM domain, binding to membrane-associated protein and an actin-binding domain, linking to the cytoskeleton. Moreover, under inert condition, the integrin binding site of talin (F3 domain in the head group) is covered by the tail end of talin (C-terminal) (fig 3.1.2a, Moser et al. 2009). In a similar way to talin, ezrin may also exist in a self-inhibited form when the cells are inactive (Critchley D et al. 2008; Moser et al. 2009). Cleavage of talin by calpain exposes the integrin binding site which binds to the cytoplasmic domain of intergin. This proteolysis of talin by µ-calpain not only enables binding of the talin N-terminal to integrin but also increases its binding affinity from 6-fold to 100-fold (Yan 2001; Franco et al. 2004; Calderwood et al. 2004). So the proteolytic actions of µ-calpain on talin enable talin to form a bridge between the β$_2$ intergin and underlying actin cytoskeleton. Activation of µ-calpain by calcium would thus lead to the coupling of the link formed by talin between the membrane and the underlying actin

cytoskeleton. By itself, this would not necessarily provide addition membrane to be released from wrinkled region of the plasma membrane.
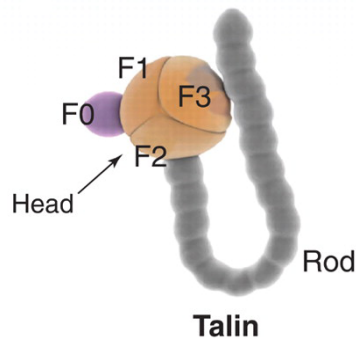


**Figure 3.1.2a.** The molecular structure of talin. This diagram shows the inactive state of talin, where the integrin binding site is masked by the C-terminal (rod end of talin). The FERM domain forms the head which has three subdomain, F1-F3. This picture is taken from Science, 2009, 324; 895-899.

Kindlin3 is similar to talin and shares many structural similarities, both having a FERM domain with three subdomains (figure 3.1.2.b). It also regulates the activation of integrin (PTB fold in F3 subdomain). However, there are several features which distinguish the FERM domains within kindlin from that of talin, including the location of FERM domain (in the C-terminal in kindlin) (Larjava et al. 2008), the presence of a pleckstrin-homology domain (bisecting the F2 subdomain) and kindlin binds to the membrane-distal NxxY motif of β- integrin while talin binds on the membrane proximal NPxY motif of β integrin (fig 3.1.2 .c & d) (Yan 2001; Moser et al. 2009). It has been proposed that attachment of kindlin to integrin enhances the integrin binding affinity of talin, but this concept is yet to be confirmed. A role for kindlin as a regulator and activator of integrin has been established in platelet and in mouse PMN; and is associated with LAD in humans, where neutrophil spreading is affected (Plow et al. 2009; Karakose et al. 2010).

Figure 3.1.2b. Molecular picture of kindling. This diagram shows the FERM domain (kindlin) depicted as a ball subdivided into three subdomains, F1 to F3, a PH domain inserted into the F2 subdomain. Fig 3.1.2c & d. Molecular picture showing the interaction of kindlin (c) and talin (d) with the cytoplasmic domain of β integrin. Talin binds to the membrane proximal NPxY motif of integrin while Kindlin binds to membrane distal NxxY motif of integrin. This picture was taken from Science, 2009, 324; 895-899.

## 3.2 Aims

The aims of the work described in this chapter were therefore to investigate whether the subcellular location of talin and kindlin was altered during neutrophil morphology changes, especially during spreading, polarization, phagocytosis and trans-endothelial migration.

## 3.3 Methods

### 3.3.1 Labeling neutrophils to study the relationship of the linker protein with actin

Neutrophils were isolated as described in section 2.5.1. After incubation with the primary antibody specific for either talin subdomain or kindlin-3 and then secondary fluorescently-conjugated antibody, the coverslip was washed twice with 1XPBS inorder to remove any excess secondary antibody and 2.5μl of rhodamine phallodin (Invitrogen INC) was added

in 100µl of the neutrophil sample and left at room temperature for 20 minutes. Excess phallodin reagent was removed using 1X PBS. Rhodamine phallodin is an high affinity probe for F-actin made from mushroom toxin conjungated to an orange-fluorescent dye, tetramethyl rhodamine (TRIC). The approximated fluorescent excitation and emission is 540-565nm. Image J pluging colocalization software was used to determine where talin and kindlin exists in relation to actin and integrin CD11b. In this project venous blood was collected form 73 volunties who had no medical conditions and were not under any medications. Salivary samples were collected from 107 volunties who had no inflammatory oral condition, no dental caries and had no systemic diseases conditions.

### 3.3.2 Labeling the neutrophils with CD11b antibody

Neutrophils from venous blood were isolated as described in the section 2.5.1 and were fixed and probed for the sub domains of talin and kindlin-3, as described in section 2.5.6.1. CD11b monoclonal antibody conjugated with phycoerythrin (Miltenyi Biotec Inc, Germany) was used to detect the integrin in the neutrophils isolated from the venous blood. This antibody reacts with the 170kDa αM subunit of CD11b/CD18 heterodimer and recognizes the human, mouse and non-human primate CD11b antigen. 1µl of this antibody was added to 100µl of the isolated neutrophils in suspension and these cells were incubated at -4ºC for 30 minutes. Then, these cells were left over the cover slip for 7 minutes to allow the neutrophils to adhere to the glass cover slips. Formylated pepetide (1µM FMLP) was used as a stimulus to polarize the neutrophils. 1µl of FMLP was added to these cells and the left for 5 minutes at room temperature. 1XPBS buffer was used to remove excess FMLP before the cells were fixed, and permeablised and probed for the linker proteins.

### 3.3.3 Labeling polarized neutrophils to study the location of membrane linker protein

100µl of neutrophils isolated from venous blood ($1 \times 10^6$ cells/ml) were allowed to adhere over the glass cover slip for 5-7 minutes. After washing away all the dead and unattached neutrophils. 1µM of FMLP was added and incubated at room temperature for 5 minutes. Excess of FMLP was removed by washing the cover slip with krebs buffer and the cells fixed and probed for talin and kindling, as discussed in section 2.5.6.2.1.

### 3.3.4 Estimating the molecular weight of talin – Western blotting

To measure the molecular weight of talin, immunoblotting technique was used. Neutrophils isolated from blood were lysed using lysis buffer. The techniques and composition of reagents used to prepare the samples to run electrophoresis using NuPAGE® 3-8% tris-acetate precast mini gel system and western blotting using Invitrogen's XCell II™ Blot Module is discussed in detail in section 2.5.6.2. Neutrophil samples were run along with cell lysate of HL60, RAW cells, MCF7, PZHPV7, HECV, PNTC7 and MAC cells (as a control sample to determine the sensitivity and specificity of the talin primary antibody) under denaturing condition. Once the cell lysates were prepared, the amount of protein present in each sample was quantified using BSA assay technique, as described in section 2.5.6.2.2. The amount of protein present in each sample used to detect the molecular weight of talin is given below (graph 3.3.4 a) and the final working protein concentration used to run electrophoresis is given in the table 3.3.4b. The difference in amount of protein in each cell lysate was equalized by adding cell lysis buffer. About 20µl of each sample mixed with sample buffer (NuPAGE® Novex LDS sample buffer) and reducing agent (NuPAGE® Reducing Agent (10x), were loaded into the mini gel and run for 1hour at 150V, at constant current of 55mA.
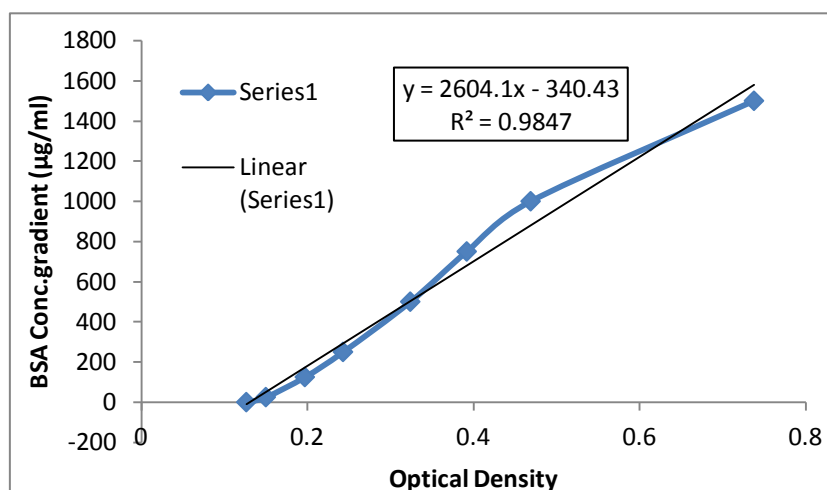
**Graph 3.3.4a:** BSA assay to quantify the amount of protein present in the sample

y = 2604.1x - 340.43
R² = 0.9847

In order to make the proteins accessible to antibody detection, they are transferred by electroblotting from the gel onto a nitrocellulose membrane, as the  protein binds depending upon hydrophobic interaction as well as charge interactions between the membrane and protein and prevents reoxidation of reduced samples during protein transfer. The immunoblotting was carried out for an hour at 30 V, at constant current of 220mA.  The entire procedure involved during electroporesis and immunoblotting is in depth in section 2.5.6.2.5.

**Table  3.3.4b.** Final concentration of protein used to run electrophoresis- talin

| Samples | HL60 | MCF7 | NEUTRO | MAC | PZHPV7 | PNTC7 | RAW | HECV |
|---|---|---|---|---|---|---|---|---|
| Optical density 1 | 0.157 | 0.232 | 0.175 | 0.192 | 0.338 | 0.233 | 0.334 | 0.327 |
| Optical density 2 | 0.23 | 0.413 | 0.179 | 0.182 | 0.323 | 0.414 | 0.346 | 0.221 |
| Average | 0.1935 | 0.3225 | 0.177 | 0.187 | 0.3305 | 0.3235 | 0.34 | 0.274 |
| Concentration (µg/ml) | 1314.9 | 4674.2 | 885.2 | 1145.6 | 4882.5 | 4700.2 | 5129.9 | 3567.4 |
| Concentration (µg/µl) | 1.3 | 4.7 | 0.9 | 1.1 | 4.9 | 4.7 | 5.1 | 3.6 |

After the protein was transferred on to the membrane, the uniformity and overall effectiveness of transfer of protein from the gel to the membrane was checked by the ponceau S dye membrane staining, as discussed in section 2.5.6.2.6. The protein transfer is detected using immunodetection technique (section 2.5.6.2.8) during this last process, the target protein is detected using a specific antibody targeted against talin and appear as a band on the film. The position of the bands was dependent on the molecular weight of the target protein (talin), whereas the band intensity depends on the amount of target protein present (talin). This is achieved after the transferred membrane has been blocked inorder to avoid non-specific interaction of the antibody; and was followed by probing the membrane with the primary antibody, to detect the tail group of talin, by incubating the membrane at 4°C overnight with the talin antibody. After the unbound primary antibody was washed away, the membrane is exposed to secondary talin antibody (goat anti-mouse IgG-HRP from Santa Cruz biotechnology, Inc) at a dilution of 1:2000 which is linked to horseradish peroxidase, The membrane is incubated with this secondary antibody for an hour at room temperature. A chemiluminescent agent (Super Signal West Dura Extended Duration Substrate Solution From Thermo Scientific, UK) is used as a substrate that will luminescent when exposed to the HRP on the secondary antibody. This reaction produces luminescence in place and in proportion to the amount of probed protein. The light is then detected by photographic film. The generic step-by-step procedure is provided in section 2.5.6.2.7 & section 2.5.6.2.8.

## 3.4   Results

### 3.4.1   Distribution of talin in neutrophils

In order to investigate the subcellular location of talin in neutrophils isolated from blood, an anti-talin antibody which was directed against the tail of tailn was used. To test the sensitivity and specificity of the primary antibody, neutrophils were fixed and incubated overnight (i) without the

primary anti talin antibody and (ii) without both primary and secondary talin antibody. There was little or no fluorescent staining under these conditions (fig 3.4.1A from a1-b2), and it was thus concluded that autofluorescence from the cytoplasmic components of neutrophils would not interfere with specific detection of talin. With anti-talin and secondary detection antibody, approximately 92% of neutrophils had peripheral cell membrane staining (fig 3.4.1a). Talin in platelets was also detected by this antibody. (fig 3.4.1a c1-d2).

In order to determine whether the subcellular location of talin changes during physiological stimulation, neutrophils were stimulated with FMLP (1µM) before fixation. Under these conditions, talin was detected at the plasma membrane. In cells which had formed pseudopodia, talin had accumulated within the pseudopodia and was lost from other plasma membrane locations. (fig 3.4.1b). In order to determine whether such a localized effect was observable with other morphological events, neutrophils were stimulated to undergo phagocytosis by incubating them with C3bi opsonized zymosan particles. Under these conditions, talin was detected on the phagosomal membrane and on the membrane of the forming phagocytic cup (fig 3.4.1c). These findings indicate that when neutrophils are in a resting state, talin is uniformly distributed at the cell plasma membrane but when they locally expand their surface area at sites of pseudopodia formation during polarization or phagocytosis, talin location co-incides with regions of plasma membrane expansion.
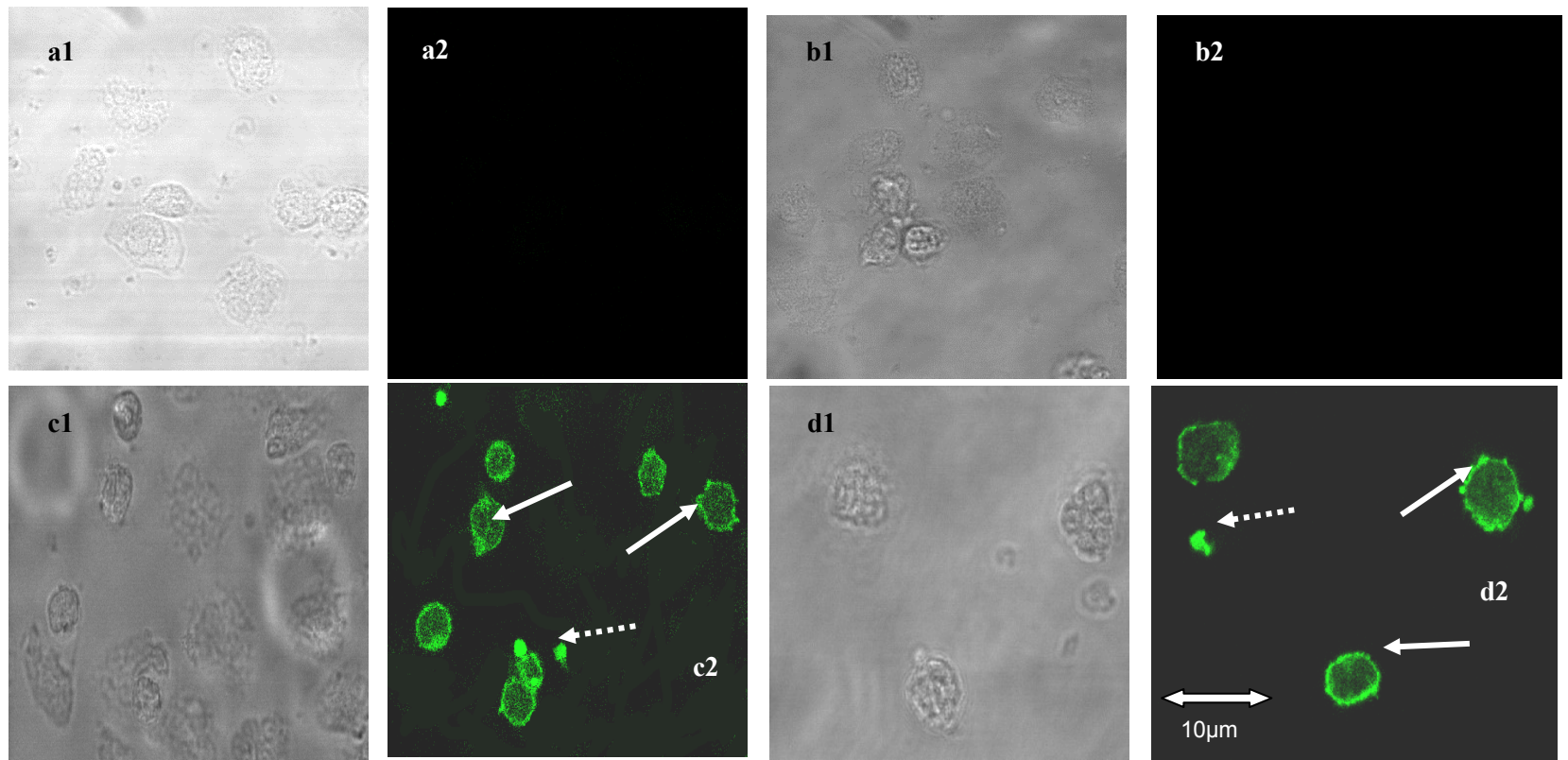
**Figure 3.4.1a. Antibody staining of tail group of talin in neutrophils isolated from blood**. Neutrophils were allowed to spread over the glass coverslip. (a1, a2) Isolated neutrophils were incubated overnight without primary and secondary tail talin antibody to test for autofluorescence, which was absent (b1, b2). In order to test the specificity of the tail talin antibody, neutrophils were incubated in the absence of primary anti-talin antibody, but with the secondary antibody step. Again there was an absence of fluorescence.When incubated the remaining isolated neutrophils with both primary antibody for tail group of talin and secondary antibody (fig c1,c2, d1 and d2), it was found that in nearly 92% of neutrophils, the tail group of talin was seen evenly distributed along the periphery of the cell membrane (indicated by white arrow mark) and several platelets were identified as positive for the tail group of talin (indicated by white dotted arrow in fig c2 and d2).
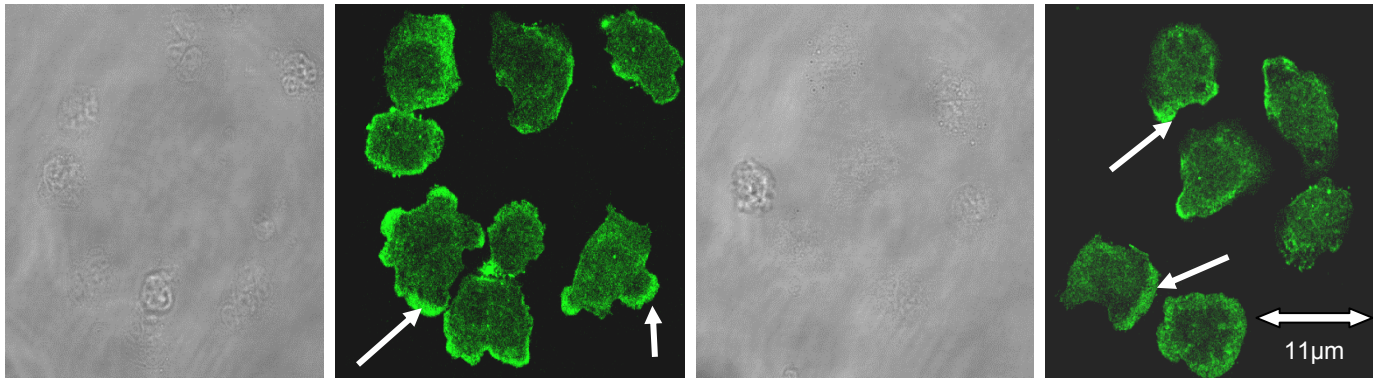
**Figure 3.4.1c. Antibody staining of tail group of talin polarized neutrophils.** Neutrophils were allowed to spread over the glass coverslip and before fixing them, they were incubated at room temperature with 1µM of FMLP for 5 minutes and probed for the tail group of talin. Nearly all polarized neutrophils had talin localized only along the lamellipodia (indicated by arrows).
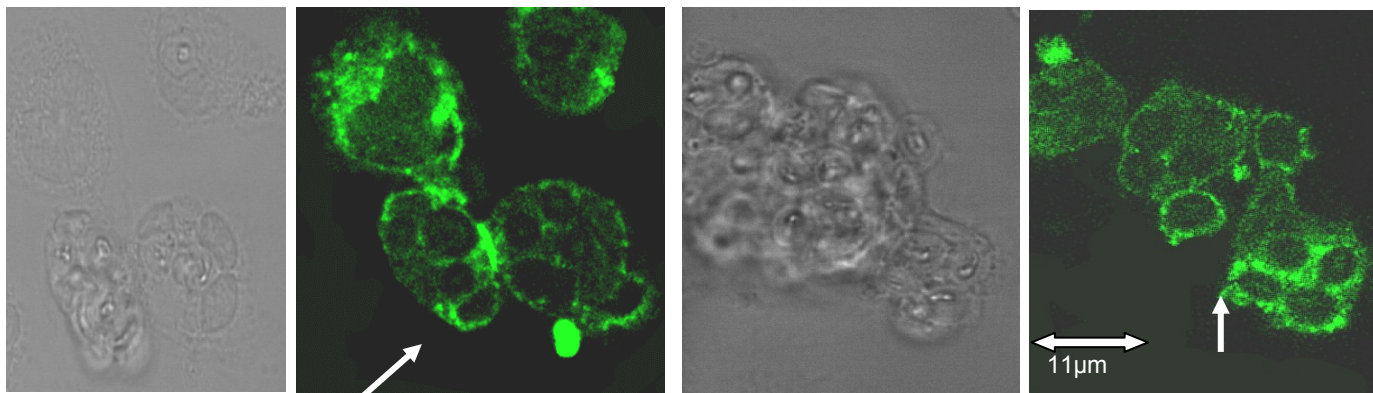


**Figure 3.4.1.2c. Antibody staining of tail group of talin in neutrophils that have undergone phagocytosis.** Neutrophils were incubated at 37ºC with C3bi opsonized zymosan for 20 minutes before fixing and probing them for talin. The tail group of talin was seen only along the phagocytic cup and also along the phagosomes (indicated by arrows), indicating the tail group of talin changes its subcellular position in phagocytic neutrophils.

### 3.4.2 The relationship between talin, actin and CD11b in neutrophils

It was important to discover whether this change in subcellular location of talin was related to the position of CD11b and/or cytoskeletal actin, as talin forms cross links between the membrane protein (CD11b) and cytoskeletal actin. The neutrophils were prepared and labeled with CD11b (section 3.3.2) and actin, as described in section 3.3.1. FMLP was used to activate the neutrophils before they were fixed. Images of neutrophils stained for talin and either CD11b or actin were analyzed using colocalization Image J plugin software. The subcellular location of both CD11b and actin was very highly correlated with the subcellular location of talin in polarized neutrophils (p=0.0017) (Fig 3.4.2a; Fig 3.4.2b). This finding suggests that talin distribution may simply reflect the localization of actin and integrin and thus not give additional information about its role in membrane expansion.
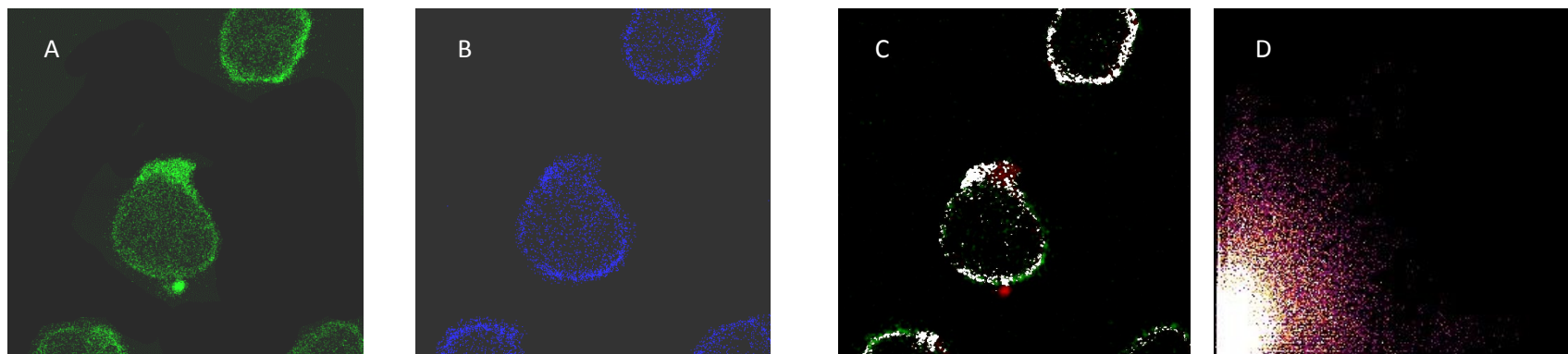
| pearsons pr | over lap (ration of green and blue pixels) | k1 (overlap r of green channel) | k2 (overlap r of blue channel) | Slope(intensity between green and blue pixels) | intercept |
|---|---|---|---|---|---|
| 0.023086 | 0.904135 | 1.255371 | 0.65117 | 0.0312 | 79.9321 |

| pearsons pr | over lap r (ration of green and blue pixels) | k1 (overlap r of green channel) | k2(overlap r of blue channel) | slope(intensity between green and blue pixels) | intercept |
|---|---|---|---|---|---|
| 0.171865 | 0.849093 | 0.656294 | 1.09853 | 0.0629 | 81.6332 |
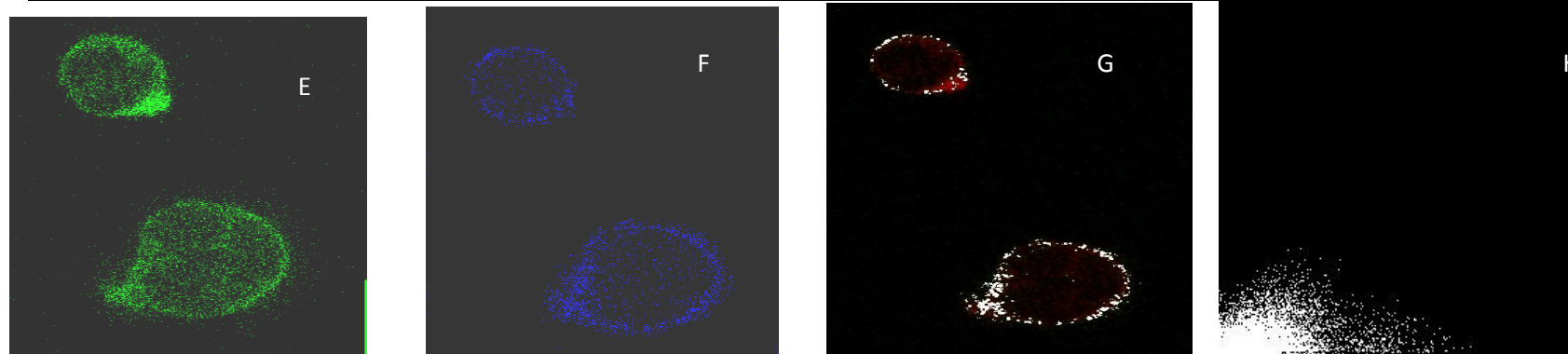
**Figure 3.4.2a: shows evidence of the relationship between the tail group of talin and CD11b.** Neutrophils were incubated at room temperature for 15 minutes with CD11b antibody conjugated with phycoerthythrin before adding 1µM of FMLP and fixing them. The tail group of talin was seen as high intensity staining along the laminopodia of the neutrophils (A & E-similar to the result obtain in the previous experiment), which corresponds to the antibody staining for CD11b (fig B & F). In order to confirm this visual finding, both the selected images were smoothed out and back ground noises removed using image J. Colocalization analysis was done, where  first the both blue and green signals from the images are made to overlap each other (dye overlay technique –qualitative colocalization technique), and the pixels which coincide are represented as yellow or white pixels (figure C&G) and the frequency plots (figure D&H) displays the relationship between the red and green pixels as an intensity– scatter plot, where the X-axis represents the pixels from the tail group of talin(green) and the y-axis represents the CD11b antibody (blue). Nearly 80% of pixels from both green fluorescence (tail group of talin) and the blue florescence (CD11b) overlapped each other and pearson coefficient value of 0.17 was obtained, which shows both tail group of talin and CD11b had a high probability of  colocalization.
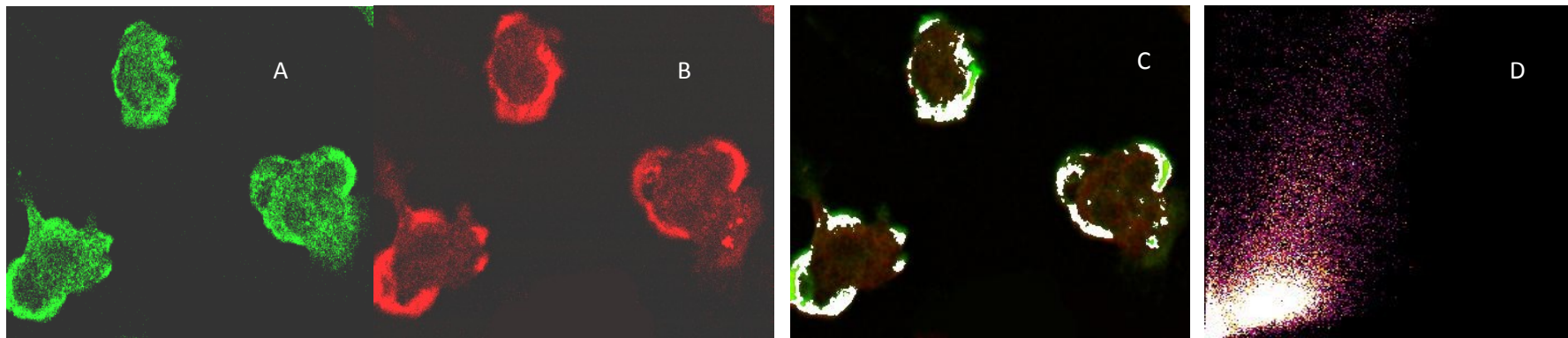
| pearsons pr | over lap r (ration of green and red pixels) | k1(overlap r of green channel) | k2(overlapr of red channel) | Slope (intensity between green and red pixels) | intercept |
|---|---|---|---|---|---|
| 0.233102 | 0.928616 | 1.943452 | 0.4437095 | 0.5216 | 97.5239 |



| pearsons pr | over lap r (ration of green and red pixels) | k1(overlap r of green channel) | k2 (overlapr of red channel) | Slope (intensity between green and red pixels) | intercept |
|---|---|---|---|---|---|
| 0.286374 | 0.936381 | 1.340012 | 0.654329 | 0.5387 | 87.9316 |
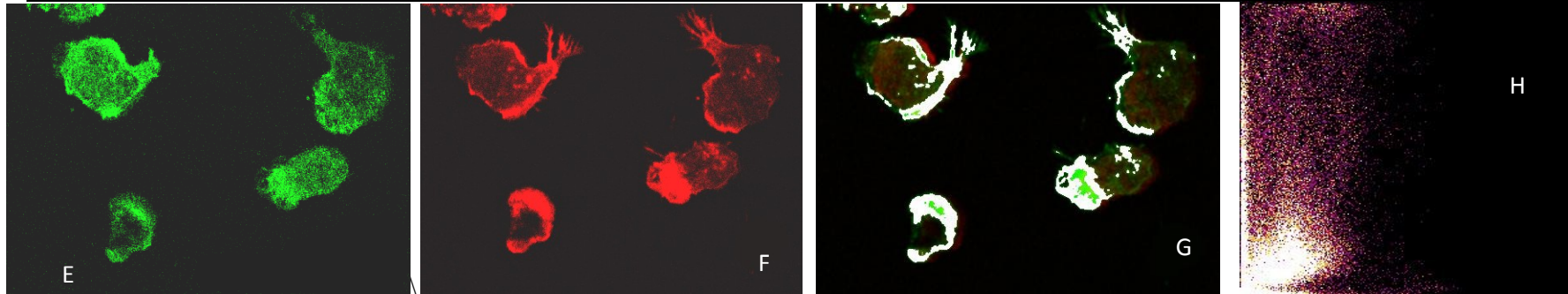
**Figure 3.4.2.b. Shows evidence of the relationship between tail group of talin and actin.** After incubation with antibody to the tail group of talin, neutrophils were stained with phalloidin for 20 minutes at room temperature inorder to stain the actin cytoskeleton. *FMLP* was again used as physiological stimulus. High intensity staining for the tail group of talin (A & E) was seen along the laminopodia of neutrophils (similar to the results obtain in previous experiments), which corresponded to the phalloidin staining of actin cytoskeleton (fig B & F). In order to confirm this visual finding, the selected images were smoothed out and back ground noises removed using Image J. Colocalization analysis was done, were first the both red and green signals from the image were made to overlap each other (dye ovelay technique – qualitative colocalization technique) and the pixels which coincide are represented as yellow or white pixels (fig C & G) and the frequency plots (fig D & H) displays the relationship between the red and green pixels as an intensity–scatter plot, were the X-axis represents the pixels from the tail group of talin (green) and the y-axis represents the phalloidin staining of actin cytoskeleton (red). Nearly 80% of pixels from both green florescent (tail group of talin) and the red florescent (actin) overlapped each other and a pearson coefficient value of 0.2 was obtained, which shows both tail group of talin and actin cytoskeleton are colocalized with each other.

### 3.4.3 Distribution of talin in neutrophils after extravasation *ex vivo*

In order to establish whether the change in subcellular location of talin during neutrophil FMLP induced polarization on glass would occur under more physiological conditions, neutrophils were examined after they had undergone trans-endothelial migration ex vivo. The transendotheial migration assay was performed, as described in section 2.5.3 (fig 3.4.3a). The neutrophils which had crossed the endothelial monolayer had lost the characteristic plasma membrane staining and instead talin was detected in the cytosol (fig 3.4.3b & c). In order to be certain that the staining conditions were not in someway responsible for this dramatic difference, the location of talin in transmigrated and non-migrated neutrophils were compared in cells on the same side and thus, stained under identical condition. Cells which had migrated across the endothelium were stained with cell tracker to distinguish them from cells which had not. This approach demonstrated that neutrophils which had undergone transmigration had lost talin from its plasma membrane location. When the difference in the intensity of talin between cell membrane and cytosole in both the group of neutrophils was quantified, there was a significant difference in the intensity of talin between the two group of cells (graph 3.4.3 1 to 3). This gave strong evidence that the subcellular location of talin changes from cell membrane to the cytosol as the neutrophils cross the endothelial monolayer under experimental *(ex vivo)* conditions. This loss of detectable talin from the plasma membrane was consistent with cleavage of talin in such a way that the head of talin (the region recognized by the antibody) was no longer associated with either plasma membrane or the cortical actin network.

**FIGURE 3.4.3**

**TRANS ENDOTHELIAL**

**ASSAY**

Insert with monolayer of HECV cell

Migrated neutrophils-
**(positive for cell tracker dye)**

**Non-migrated neutrophils**

CELL MEMBRANE
CYTOPLASM

Difference in intensity between cell membrane and cytosole

No of cells counted

**Migrated neutrophils**

GRAPH 2

plasma membrane
cytoplasm

Difference in intensity between cell membrane and cytosole

No of cells counted

**Figure 3.4.3. Subcellular location of the tail group of talin as neutrophils extravasted under *ex vivo* conditions.** A) Schematic representation of the transendothelial migration assay setup (described in section 2.5.3). Migrated neutrophils were loaded with cell tracker dye conjugated with PE to differentiate between these two groups of cells. The non-migrated and migrated neutrophils were then mixed on a glass cover slip, then fixed and probed for the tail group of talin. Non migrated neutrophils retained the tail group of talin at the cell membrane (fig B & C), while the migrated cells lost the peripheral talin staining, giving evidence that talin relocated away from the plasma membrane as neutrophils undergoes *exvivo* extravasation.

Difference in fluroscence between migrated and non migrated neutrophils - tail group of talin

GRAPH 2

Non-migrated neutrophils

Migrated neutrophils



GRAPH 3

Standard deviation ofnon-migrated and migrated cells

Standard mean of error of non-migrated and migrated cells
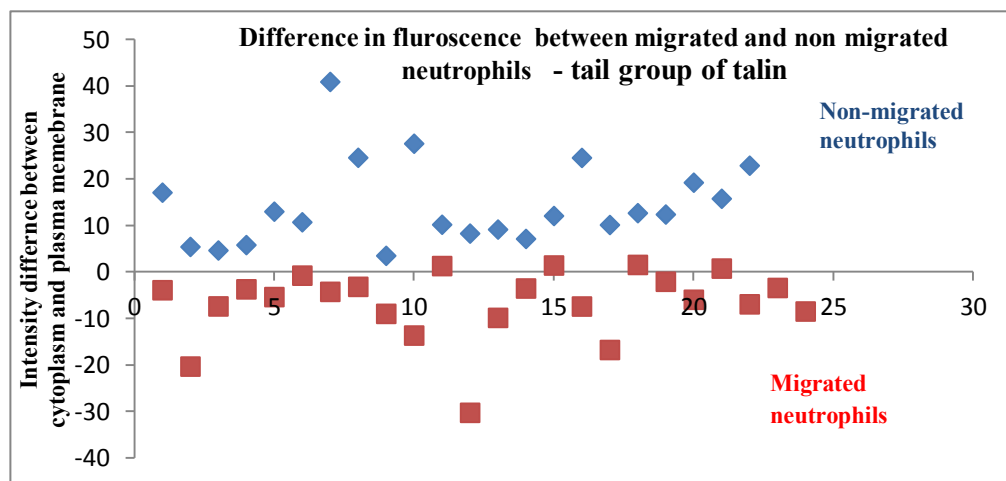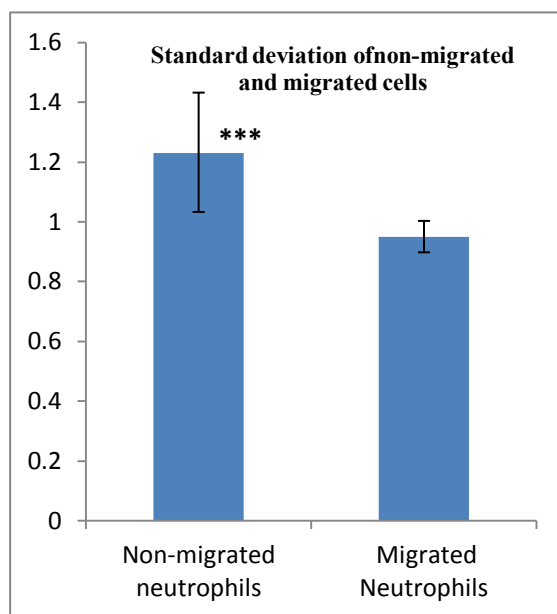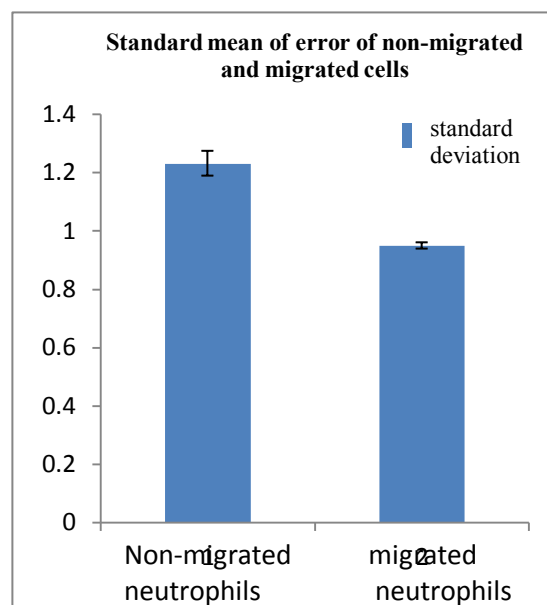
| Neutrophils (mean gray value) | Average difference | Standard deviation | Z test and T-test |
|---|---|---|---|
| Non-migrated cells | 14.49627273 | 9.100626301 | <0.001 |
| Migrated cells | -6.66341667 | 7.455793096 | <0.001 |

Image J was used to quantify the difference in the fluorescent intensity of tail group of talin between the cytosole and the plasma membrane in both migrated as well as non migrated cells (Graph 1-3) and confirmed there was a statistically significant difference in the intensity of tail group of talin between the migrated and non migrated cells. This gave evidence that talin relocates away from the cell membrane into the cytsol as the neutrophils extravasated under experimentalcondition).

### 3.4.4    Distribution of talin in neutrophils after extravasation *in vivo*

To test whether talin relocation accompanies transendothelial migration, the subcellular location of talin in neutrophils which had extravasated *in vivo* and thus, under physiological condition were examined. Neutrophils were isolated from saliva, as explained in section 2.5.2.1. Salivary neutrophils are an excellent representation of extravasted neutrophils under physiology condition and are easily accessible. It was found that approximately 92% of salivary neutrophils lacked cell membrane talin staining (Fig 3.4.4A1- B2). Quantifying the difference in fluorescence intensity between the cytosol and plasma membrane, confirmed that talin is distribution in the cytosol of salivary neutrophils, while the blood neutrophils had a plasma membrane location of talin (graph 3.4.4 1 &2).  Inorder to establish if this finding was due to the pH of saliva or any oral environment conditions, 100µl of blood neutrophils were loaded with cell tracker (conjugated with phycoerthythrin), mixed with 100µl of salivary neutrophils and both the group of neutrophils were fixed together by 4% formaldehyde. The blood neutrophils (positive for cell tracker) retained talin at the plasma membrane, while nearly all salivary neutrophils (negative for cell tracker) had cytoplasmic staining of the tail group of talin (fig 3.4.4 C1-C2). To make sure that the dye (cell tracker) that was used to differentiate between the two group of cells was not blocking the relocation of talin away from the plasma membrane, the reverse labeling experiment was performed by loading the salivary neutrophils with cell tracker conjugated with phycoerthythrin. As before salivary neutrophils had cytosolic talin while  blood neutrophils had talin at the plasma membrane (fig 3.4.4D1-D2).  There was a statistically significant difference in the amount of membrane talin between salivary neutrophils and blood neutrophils (graph 3.4.4.3-4 & 5). This gives evidence that talin relocated away from the plasma membrane into the cytosol, as the neutrophils extravasated under physiological condition.
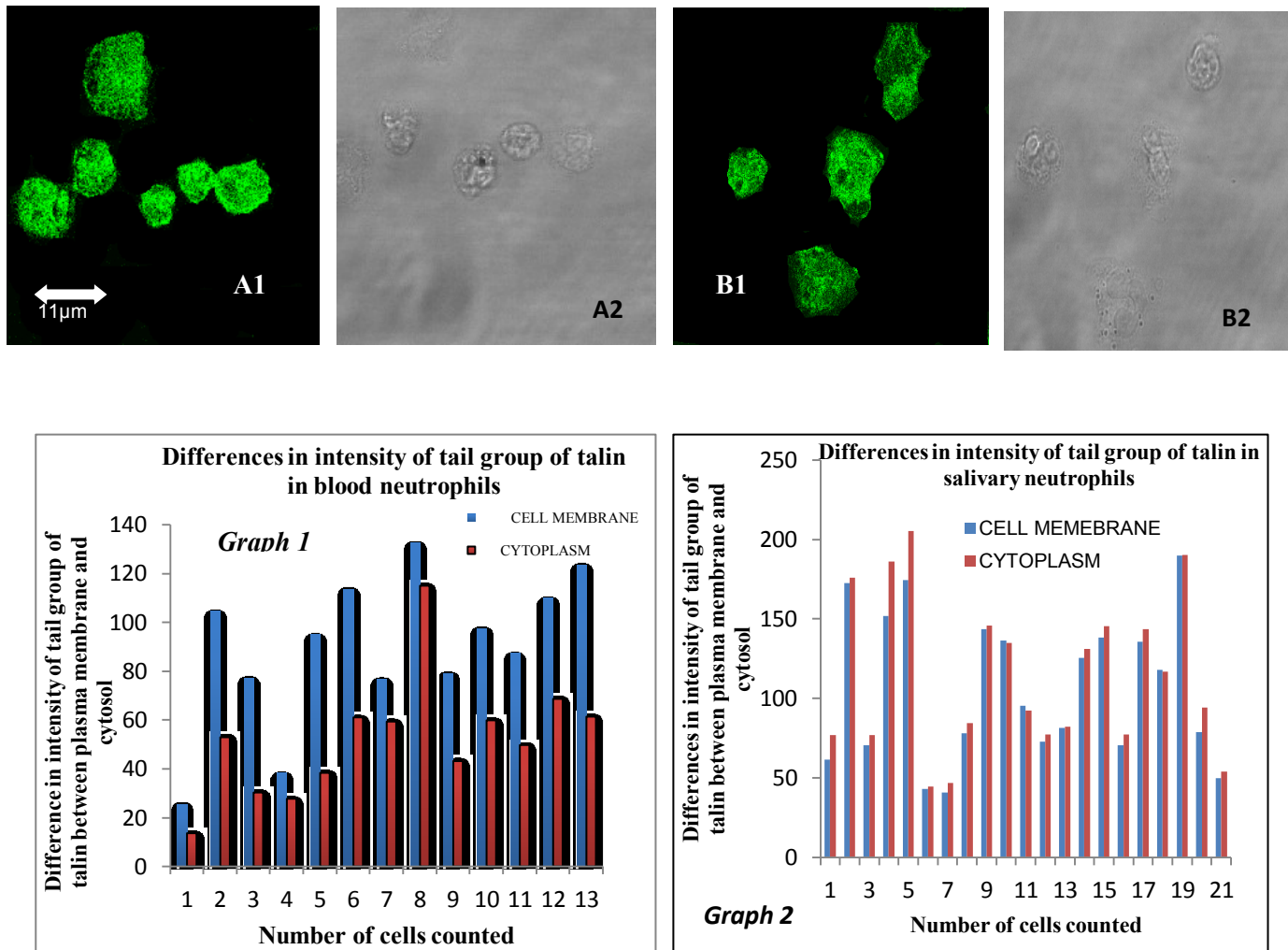
**Figure 3.4.4a. Subcellular location of the tail group of talin in extravasated neutrophils under physiological conditions.** Neutrophils isolated from saliva are a good representation of physiological neutrophildiapedesis. Cells were fixed and stained for the tail group of talin,revealing that nearly all salivary neutrophils lacked the peripheral plasma membrane position of talin; and rather had cytosolic location (fig A1- B2). This indicated that as the neutrophils underwent extravasation, the tail group of talin relocated away from the plasma membrane into the cytosol. ImageJ was used to quantify the intensity of the tail group of talin between the cytosol and plasma membrane in both sailvary neutrophils and blood neutrophils, (fig 3.4.1.5. graph 1 & 2), and confirmed there was a significant difference (p>0.001) in the intensity of talin in both groups of cells.
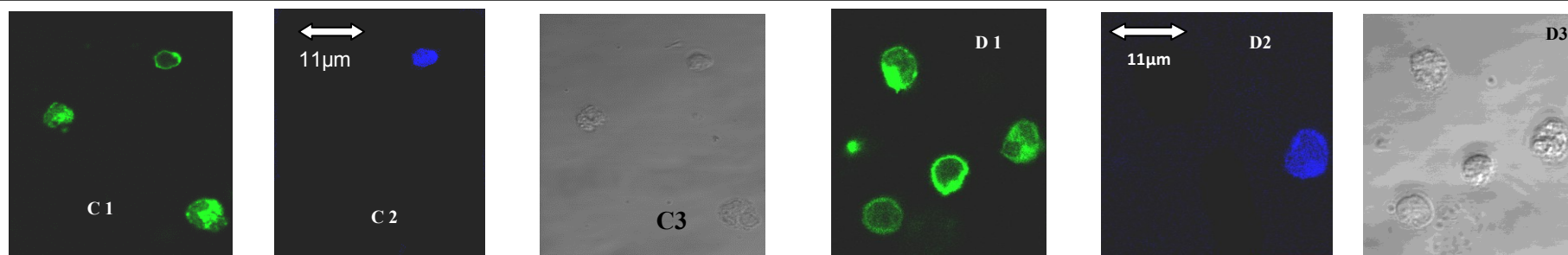
**Figure 3.4.4b.** Shows the consistent subcellular position of ezrin in salivary neutrophils. To find whether the physiological condition in the oral cavity influences the cytosolic location of tail group of talin, both blood neutrophils (loaded with cell tracker-**blue**) and salivary neutrophils were mixed and fixed on the same glass coverslip and probed for the tail group of talin. Cells which were positive for cell tracker (blood neutrophils-**blue**) had talin located at the plasma membrane (fig C1) while the cells which were negative for cell tracker (salivary neutrophils) (fig C2) had cytosolic location of talin. In order to make sure that the dye which used to identify the two groups of neutrophils was not interfering with the change in subcellular position of talin, instead of loading the blood neutrophils with cell tracker, salivary neutrophils were stained with cell tracker (**blue**) but the there was no change in subcellular location of tail group of talin in both the group of neutrophils
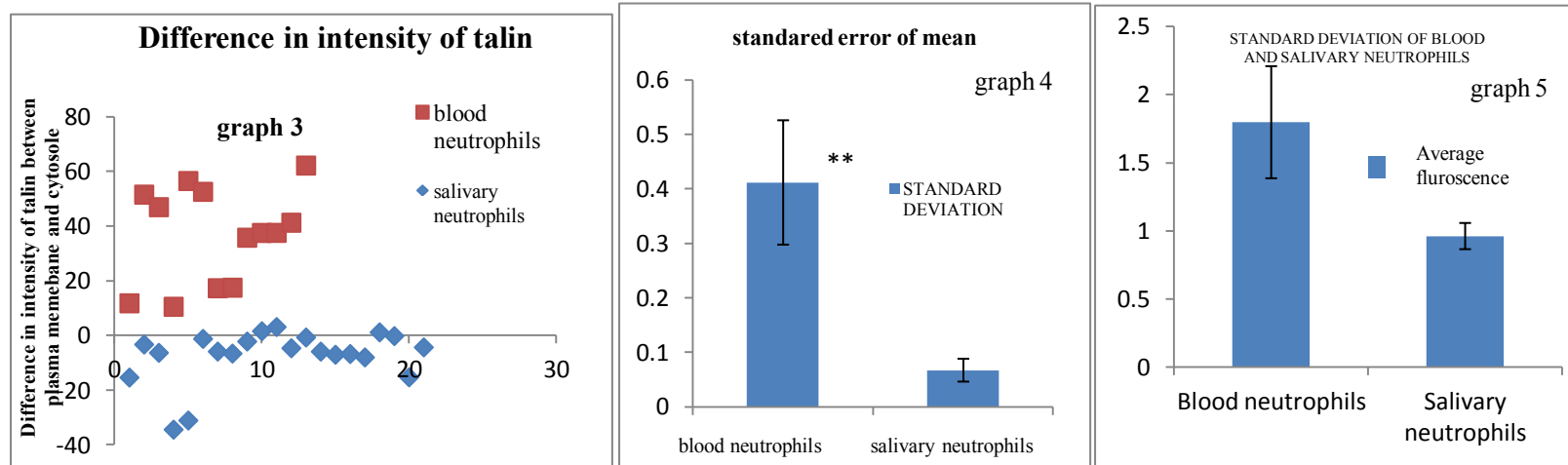






| Neutrophils (mean gray value) | Average difference | Standard deviation | Z test |
|---|---|---|---|
| Blood neutrophils | 36.82 | | 1.88738E-14 |
| | | 17.54 | |
| Salivary neutrophils | -7.32 | | 0.999729436 |
| | | 9.70 | |

**Graph 3.4.4.** Using Leica software, the intensity of tail group of talin was measured in both salivary neutrophils and blood neutrophils and when the difference between the plasma membrane and cytosol was measured between the two group of neutrophils, a statistically significant difference was noted in the location of tail group of talin between salivary neutrophils and blood neutrophils (graphs 3, 4 & 5).

### 3.4.5 Detection of the head group of talin in fixed neutrophils

The data for the loss of talin at plasma membranes was consistent with the cleavage of talin in such a way that the tail of talin (as identified by the antibody used) was no longer associated with the plasma membrane. In order to investigate whether this was the case, the location of the head group of talin was investigated. If the head and tail regions of talin occupied different cellular locations, this would provide evidence for cleavage of talin. However, the antibodies which recognized the head group of talin failed to stain talin in resting neutrophils (fig 3.4.5). Interestingly, the antibody detected the head group of talin in platelets (Fig 3.4.5C2 & D2). When stimulated with FMLP, again the head group of talin was not detectable in neutrophils, but was seen in platelets (Fig 3.4.5C2 & D2). This finding shows that the head group of talin in the neutrophils (but not in platelets) was inaccessible to antibody or unable to bind due to stereotypic hindrance, perhaps because the head of talin was hidden deep inside its binding partner or the cell membrane. If this where the case, it must be concluded that  the release of the tail of talin from the plasma membrane was not accompanied by 'exposure' of the head of talin to allow its detection by antibody. (Fig 3.4.5 D2).

### 3.4.6 Detection of the subcellular location of kindlin in neutrophils

Kindlin-3 is membrane of the same 'family' as talin and is structurally similar to the head of talin. In order to test whether the proposal that the talin head was inaccessible to antibody staining, kindlin-3 was thus used a surrogate. It was found that kindlin-3 also could not be detected in neutrophils (Fig 3.4.6C2), while it could be detected in platelets (Fig 3.4.6D2). Kindlin-3 could also be detected in HeLa cells (Fig 3.4.6E1) which had a characteristic plasma membrane staining. It was, therefore, clear that the antibody was effective in other cells types and again suggested that the FERM domain which is present

in both kindlin-3 and the head group of talin was either buried deep inside the plasma membrane inneutrophils or other location such that stereotypic hindrance prevented antibody binding of neutrophils.
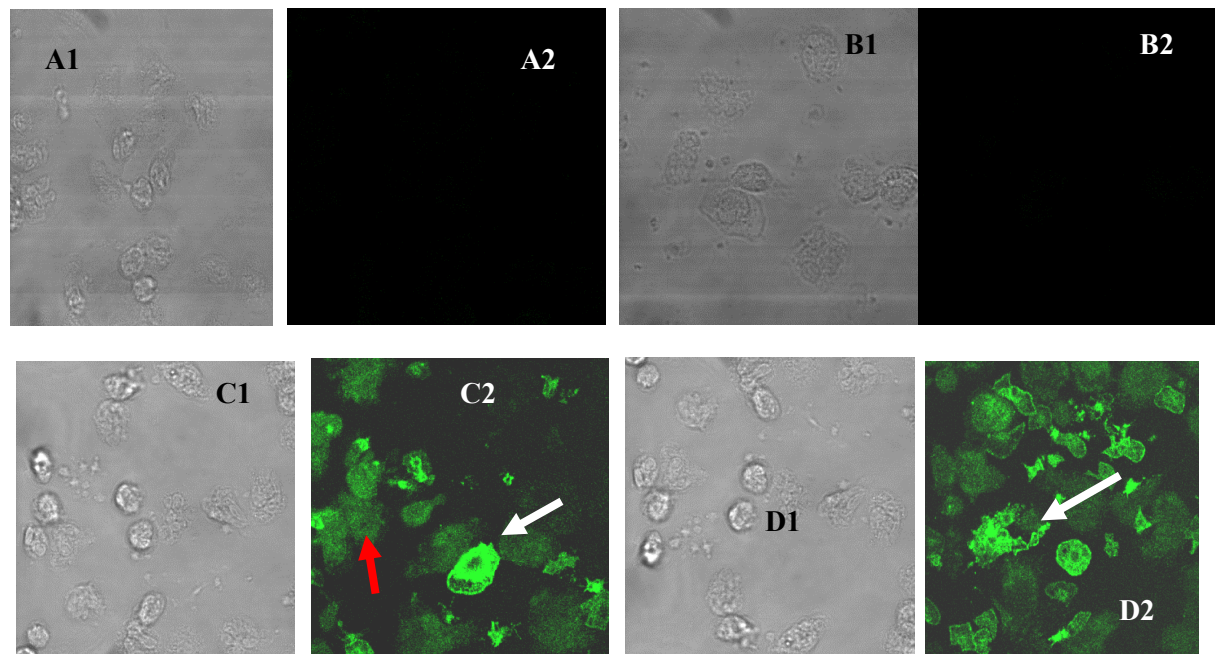


**Figure 3.4.5. Detection of the subcellular location of the head group of talin in neutrophils isolated from venous blood.** Neutrophils which were isolated from 10ml of venous blood were allowed to spread over the glass cover slip for 5 minutes. These neutrophils were then incubated on the glass cover slip with 1µM of *FMLP* for 5 minutes.Excess of *FMLP* was washed with 1X PBS before fixing and probing these neutrophils for the head group of talin. Inorder to test the sensitivity and specificity of the primary antibody for head group of talin, neutrophils were fixed in absence of primary antibody (fig A1 & A2) or in the absence of primary as well as secondary antibody, in order to rule out the auto-fluorescence nature of the cytoplasmic components of neutrophils (fig B1 & B2). When probed for the head group of talin, all the platelets were positive for the head group of talin (indicated by white arrow) was located along the cell membrane of these platelets (fig C1 & C2). However, it was not detectable in the neutrophils (fig D1 & D2). The arrow mark indicates the subcellular location of head group of talin in neutrophils (fig D1 & D2) and in platelets (fig C1 & C2).
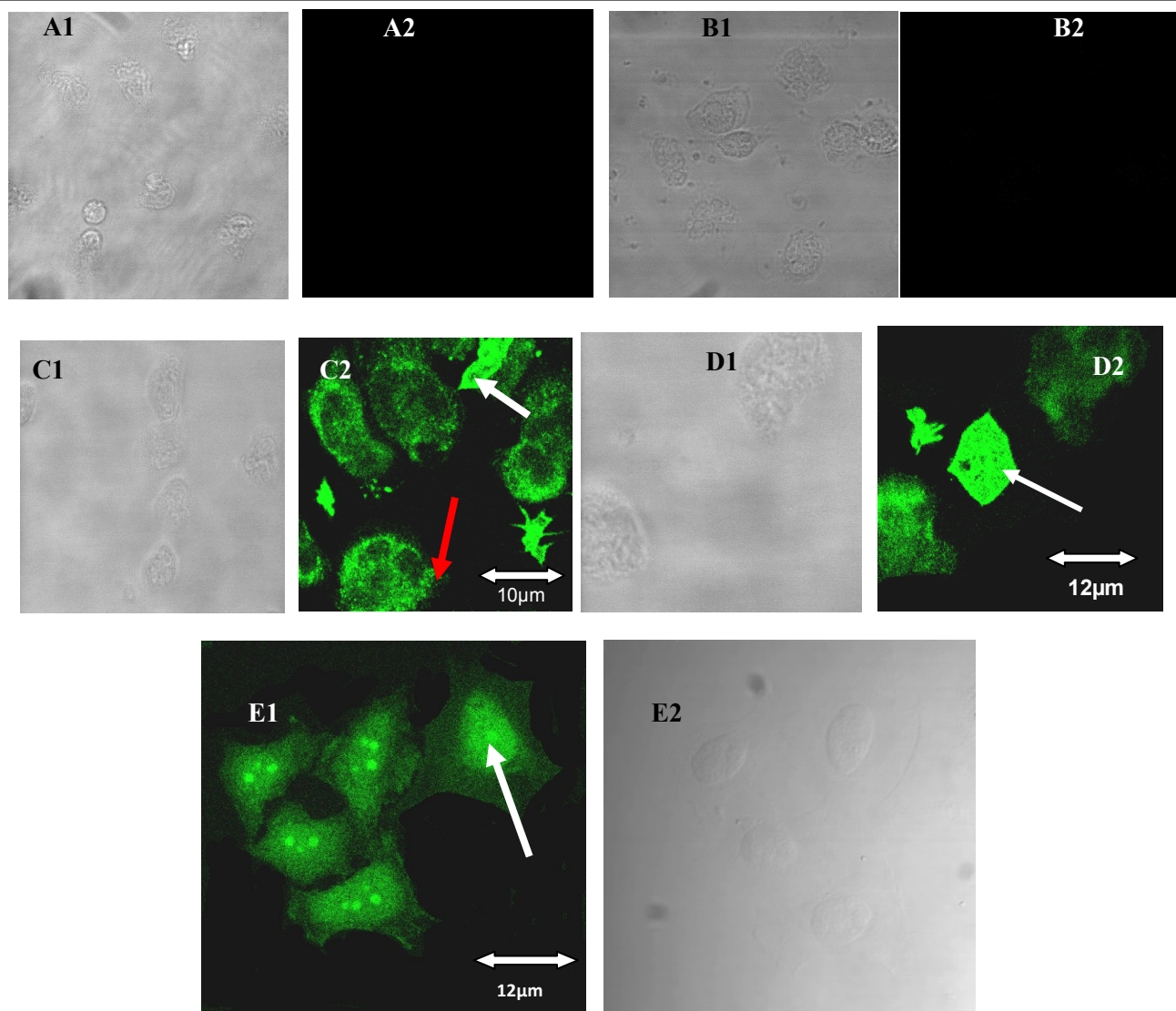
**Figure 3.4.6. Subcellular location of kindlin-3 in neutrophils isolated from venous blood.** Neutrophils isolated from venous blood were stimulated with 1μM of *FMLP* for 5minutes at room temperature before they were fixed and probed for kindlin-3. Nearly all the neutrophils were negative (arrow) for kindlin—3 (fig C1 to D2), while the platelets had cell membrane staining of kindlin-3 (white arrow) (fig C1 to D2). Moreover, to test the specificity and sensitivity of primary anti-kindlin-3 antibodie, HeLa cells were fixed and probed for kindlin-3. The majority ofHeLa cells were positive for kindlin3 (white arrow) (fig E1 & E2). The arrow mark indicates the subcellular location of kindlin-3 in platelets (fig D2) and HeLa cells (fig E1) and also indicates the negative staining of kindlin-3 in neutrophils (fig C2). Figs A1 & A2 are the control samples where the neutrophils were incubated without the primary antikindlin-3 antibody; and figures B1 & B2 indicate the absences of auto-fluorescence in neutrophils (no primary or secondary antibody). This give evidence that the primary antikindlin-3 antibody is sensitive and specific for detecting.

### 3.4.7 Determining the molecular weight of talin in neutrophils isolated from blood

The inability to detect the head group of talin by immunohistochemistry meant that that approach would not be useful in establishing whether talin cleavage had occurred. A molecular approach (western blotting) was therefore adopted to measure the molecular weight of full length talin and establish whether it was truncated (by cleavage) during neutrophil activation. Section 3.3.4 explains the western blotting technique, followed to determine the molecular weight of talin. The primary antibody that was used for western blotting was 8D4 (Santa Cruz Biotechnology, Inc). This was raised against talin of chicken, but detects the intact talin molecule from a number of species and also its proteolytic product 190kDa fragment of human and rat. The talin was detected as two separate bands in all the cell lysate, used except in the neutrophil cell lystate (fig 3.4.7a). After marking on the film the position of the stained protein standard bands from the membrane, Image J was used to plot the log of each molecular weight of the protein standards (y-axis) against their corresponding relative mobility (x-axis). Relative mobility (Rf) is the term used for the ratio of the distance the protein has moved from its point of origin (top of the gel) relative to the distance the tracking dye or a low molecular weight marker has moved (the gel front).  The regression line of the standard curve to obtain values for slope and y-intercept. The molecular weight (size) of talin was estimated using its Rf and the following modified equation:

*log molecular weight = (slope)(mobility or Rf of the target protein) + y-intercept*

 The talin detectable as two separate band had molecular weight of 231kDa (1$^{st}$ band) and 224kDa (2$^{nd}$ band), which corresponds to the expected 230kDa molecular weight of talin, in all the control samples (fig 3.4.7 table 1 & graph 1). It was not clear why talin could not be detected

in neutrophils, but detection of talin tail group by immunohistochemistry clearly showed that talin was expressed.

## Figure 3.4.7. Determining the molecular weight of talin



**A)** 1st protein band

2nd protein band

No detectable band in neutrophil

**Graph 1** Estimating the molecular weight of protein bands

$y = -1.297x + 2.6687$
$R^2 = 0.9694$

log of mol weight

Linear (log of mol weight )
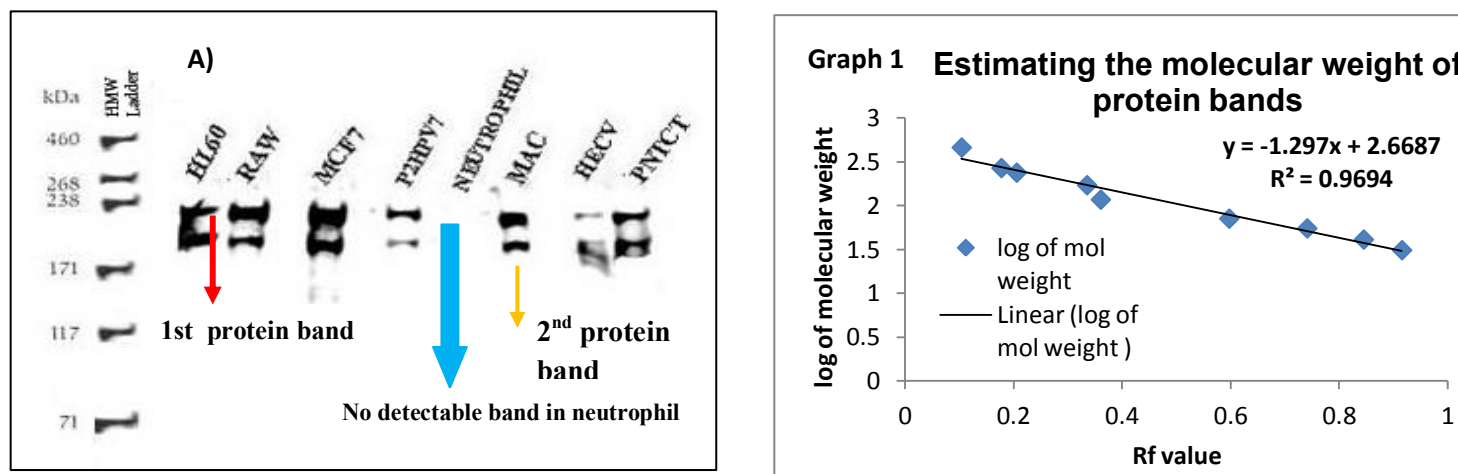
## Table 3.4.7(1). Determining the molecular weight of the (talin) protein bands using image J programme

| Cell lysate | Distance travel by 1st band(mm) | Distance travel by 2nd band(mm | Rfvalue for 1st band | Rf value for 2nd band | Log of mol.weight for 1st band | Estimated mole weight for 1st band (kDa) | Log of mole.weight for 2nd band | Estimated mole weight for 2nd band (kDa) |
|---|---|---|---|---|---|---|---|---|
| HL60 | 83 | 87.01 | 0.2338028 | 0.245098592 | 2.365458 | **231.9** | 2.350807 | **224.2** |
| RAW | 82.2 | 86.15 | 0.2315493 | 0.242676056 | 2.368381 | **233.5** | 2.353949 | **225.9** |
| MCF7 | 80.01 | 89 | 0.2253803 | 0.250704225 | 2.376382 | **237.8** | 2.343537 | **220.5** |
| PZHPV7 | 82.01 | 86.01 | 0.2310141 | 0.24228169 | 2.369075 | **233.9** | 2.354461 | **226.1** |
| MAC | 83.3 | 88 | 0.2346479 | 0.247887324 | 2.364362 | **231.3** | 2.34719 | **222.4** |
| HECV | 81.03 | 86.01 | 0.2282535 | 0.24228169 | 2.372655 | **235.8** | 2.354461 | **226.1** |
| PZHPV7 | 83.02 | 89 | 0.2338592 | 0.250704225 | 2.365385 | **231.9** | 2.343537 | **220.5** |

**Figure: 3.4.7.** On immunoblotting the cell lysates, talin was detected as two separate band in all the cell lysate other than neutrophils. Using image J the distance traveled by each protein band from including the protein ladder standard was determine and using the formula above, the molecular weight of all the protein band was calculated. The molecular weight of the 1st protein band of talin was around 231kDa (indicated by arrow) and the estimated molecular weight of the 2nd protein band (indicated by arrow) was 226kDa.

## 3.5 Discussion

Talin and kindlin-3 are well-known membrane linker proteins, which form crosslinks between membrane associated protein like integrin and the under lying actin cytoskeleton. It has been proposed that wrinkles which are seen on the cell membrane of neutrophils are held in place by these membrane linker proteins. As a substrate for the calcium-dependent enzyme μ-calpain, it is possible that proteolysis of talin might cause the unfolding of wrinkles on the surface of neutrophils and provide an extra reservoir of membrane which the neutrophils might use to accommodate the change in shape and increase in surface area associated with extravasation. It is possible that taliin and kindlin-3 might be a 'biological memory' in extravasted neutrophils. When neutrophils isolated from venous blood were fixed and probed for the tail group of talin, nearly all resting neutrophils had peripheral membrane staining which relocated to the laminopodia in polarized neutrophils. This gave a clue that talin might be involved when the cell changes its shape. The peripheral distribution of the tail group of talin was lost in neutrophils which had extravasted both under experimental conditions and under physiological condition (salivary neutrophils). This relocation of the tail group of talin from the cell membrane into the cytosol as the neutrophils changed its shapes and during extravasation, indicates that the tail group of talin has a role to play in neutrophil morphology changes. When the neutrophils were probed for head group of talin, it was not detectable in neutrophils and this was same with kindlin-3 which also belongs to the FERM family and is similar to talin both structurally and functionally. It was also not possible to measure the molecular weight of talin in neutrophils. This might be due to sterotypic hiderance or talin might be present deep inside the cell membrane of the neutrophils which might not be possible for the antibody to bind. Even though the subcellular location of talin changes from plasma membrane to the cytosol as the neutrophils change shape, neither talin nor kindlin 3 can be used as a biological marker to identify extravastated neutrophils, as its subcellular position was shown to be associated

with integrin (CD11b) and actin cytoskeleton and moreover, it is difficult to measure their

molecular weight as they are not available for the antibody to bind.

# CHAPTER 4

## The role of ezrin in neutrophil morphology

## change

## 4.1 Introduction

The ezrin/radixin/moesin (ERM) protein family act as linkers between cortical actin filaments and plasma membranes. ERM proteins have attracted a great deal of interest. They are involved in formation of microvilli, cell adhesion sites, ruffling membranes and cleavage furrows (Bretscher, 2002; Bonilha, 2007). They have also been shown to be regulated by the Rho signaling pathway, as explained in depth in section 1.8.3.

The ERM family consists of three closely related proteins, ezrin, radixin and moesin. Ezrin (~82kDa) is involved in maintaining cellular projections like microvilli (Saotome, 2004) and was first isolated from chicken intestinal brush borders as a component of microvilli. Molecular cloning revealed that ezrin was identical to cytovillin, which was enriched in microvilli of human placental syncytiotrophoblasts. ERM proteins consist of three domains: a globular N-terminal membrane-binding domain (FERM domain or N-ERMAD), followed by an extended α-helical domain and a positively charged C-terminal actin-binding domain (C-ERMAD). Moreover, ezrin is proteolysed by the calcium-dependent proteolytic ezyme calpain.

The ERM proteins are structured in such a way that intramolecular interaction between the N-terminal and C-terminal domains masks protein–protein interaction sites maintaining the protein in an inactive state in the cytoplasm (Bretscher et al. 1997). Ezrin gets unfolded and becomes activated in response to binding the phospholipid PIP2 and phosphorylation of a conserved threonine residue within the C-terminal domain. When ERMs are activated, the N-terminal FERM (four-point-one, ezrin, radixin, moesin) domain can bind directly to the cytoplasmic portion of transmembrane proteins, such as CD44 and ICAMs, or indirectly through a cytoplasmic membrane scaffolding protein, EBP50. The central region of the ERMs contains an α helical domain that has been shown to be important for PKA association and the C-terminal domain contains a filamentous

actin/FERM binding domain important for regulating F-actin and intramolecular interaction (fig 1.8.3).

ERMs are believed to function in a variety of cellular and developmental contexts, including organization of the apical cortex in differentiating epithelial cells, stiffening of the cell cortex during cytokinesis, epithelial integrity; and lumen morphogenesis in epithelial tubes (Louvet–Vallée, 2000). Since ezrin, like other ERM protein, has a structure which includes actin binding and plasma membrane binding regions, it may function as a cross-linker between actin filaments and the plasma membranes. It might, therefore, have a role to play in holding the plasma membrane wrinkles in place on the surface of neutrophils. Furthermore, since ezrin is a substrate for μ-calpain, it is possible that unfolding of wrinkles may occur when calpain is activated. This would enable the neutrophils to increase their apparent surface area and so permit the rapid cell morphology changes which are required for neutrophil spreading, transendothelial migration and phagocytosis. If ezrin plays such a role, its subcellular distribution may act as a biological marker to identify extravasted neutrophils.

## 4.2  Aims

The aim of the work presented in this chapter is to establish the subcellular location of ezrin in unstimulated neutrophils and whether this changes during phagocytosis, transendothelial migration and in response to elevated cytosolic calcium concentration.

1. To determine the subcellular location of ezrin in *ex vivo* extravasated neutrophils.

2. To determine the subcellular location of ezrin in *in vivo* extravasted neutrophils.

3. To determine the effect of a change in the cytosolic calcium concentration on the subcellular location of ezrin.

4. To determine the effect of subcellular location of ezrin for change in cytosolic level of calcium and effect of calpain and calpain inhibitor.

## 4.3    Methods

### 4.3.1    Detection of ezrin in fixed neutrophils

In order to study the subcellular location of ezrin in neutrophils which were isolated from venous blood, 100µl of $1 \times 10^6$cells/ml of neutrophils were allowed to adhere to the glass coverslip for 10 minutes at 37°C; and the cells were fixed and permeabilised, as described in section 2.5.6.1. 4% Horse serum was used as a blocking reagent and the cells were incubated with this for 1-2 hours at room temperature. After washing, the cells were incubated with primary anti ezrin antibody (diluted 1/100 in 4% horse serum) overnight at 4°C. The anti-ezrin antibody (ezrin 3C12) is a mouse monoclonal antibody raised against amino acids 362-585 of ezrin of human origin. After overnight incubation, the cells were washed with blocking agent (4%horse serum) to remove any left over primary antibody. To this, anti-mouse secondary antibody conjugated with FITC was added at the concentration of 1:20 and incubated at room temperature for 1hour. Before viewing the cells under the confocal microscopy, excess secondary antibody was removed by washing the cells with sterile 1X PBS buffer.

### 4.3.2    Elevation of cytosolic calcium

To  increase the calcium level in neutrophils,  a cocktail mixture of 1µM of thapsigargin (an inhibitor of SER calcium pumps which prevent uptake of calcium into storage sites within the cells), 1µM of ionomycin (to increase the influx of calcium into the cells)  and 13mM calcium chloride (to elevate extracellular calcium level). This cocktail mixture of high calcium was added to neutrophils (venous blood neutrophils) which were isolated in

presences of 1mM of EGTA, These cells were later fixed and stained with ezrin antibody, as discussed in section 4.3.1.

### 4.3.3 Evaluating the effect of calpain on ezrin

Calpain inhibitor I ,also know as ALLN , Ac-LLnL-CHO, MG-101, N-Acetyl-Leu-Leu-Norleu-al, N-Acetyl-L-leucyl-L-leucyl-L-norleucinal, was used to determine the effect of calpain on ezrin in neutrophils. ALLN has a empirical formula $C_{20}H_{37}N_3O_4$ and a molecular weight of 38.35kDa. It inhibits calpain I ($K_i$ = 190 nM), but also calpain II (Ki = 220 nM), cathepsin B ($K_i$ = 150 nM) and cathepsin L ($K_i$ = 500 pM). Neutrophils isolated from the venous blood were incubated at 4ºC for 30 minutes with 1µM ALLN and these neutrophils were allowed to adhere to the glass cover slip and fixed and probed for ezrin, as described in section 4.3.1.

### 4.3.4 Effect of extravasation on the subcellular position of ezrin

Transendothelial migration assays were performed as described in detail in section 2.5.3. Neutrophils isolated from venous blood were allowed to cross a monolayer of endothelial cells, which were grown in a tissue culture insert. 1µM of FMLP was added to the outer chamber of the insert, in order to create a chemotactic gradient. The migrated neutrophils were collected on a glass coverslip and 100µl of a $1 \times 10^5$ cells/ml cell suspension of non-migrated neutrophils loaded with 1mM of cell tracker conjugated with phycoerthythrin dye; was added to the same coverslip. The cells were allowed to adhere to the coverslip, were fixed and then were probed for ezrin antibody, as described in section 4.3.1.

## 4.4 Results

### 4.4.1 The subcellular location of ezrin in venous blood neutrophils

Neutrophils were prepared and stained with ezrin antibody, as described in section 4.3.1. To test the sensitivity and specificity of primary antibody, neutrophils were fixed and

incubated overnight without the primary anti ezrin antibody, or with no anti-ezrin antibody and secondary antibody. This enables the level and location of the auto-fluorescence signal to be determined. This was very low and no correction was observed with ezrin specific staining. Ezrin was located at the neutrophil periphery in the majoriy of cells examined (65/77) (fig 4.4.1A1). On close examination, it was seen that this peripheral staining of ezrin was not uniform, but was absent from areas of the cell membrane where there were cell protrusions (fig4.4.1B1). This suggested that ezrin might be involved during changes in neutrophil morphology. In order to test this, localised pseudopodia were stimulated to form by inducing phagocytosis of C3bi opsonised zymosan particles. Again, the peripheral staining of ezrin was absent in the protrusion which form the phagocytic cup, as well as around formed phagosomes (fig 4.4.1F1- H1). This gave further evidence that ezrin moves away from the cell membrane as the neutrophil changes its shapes and when the plasma membrane undergoes dynamic changes.

**Figure 4.4.1.Subcellular position of ezrin in neutrophils isolated from venous blood**
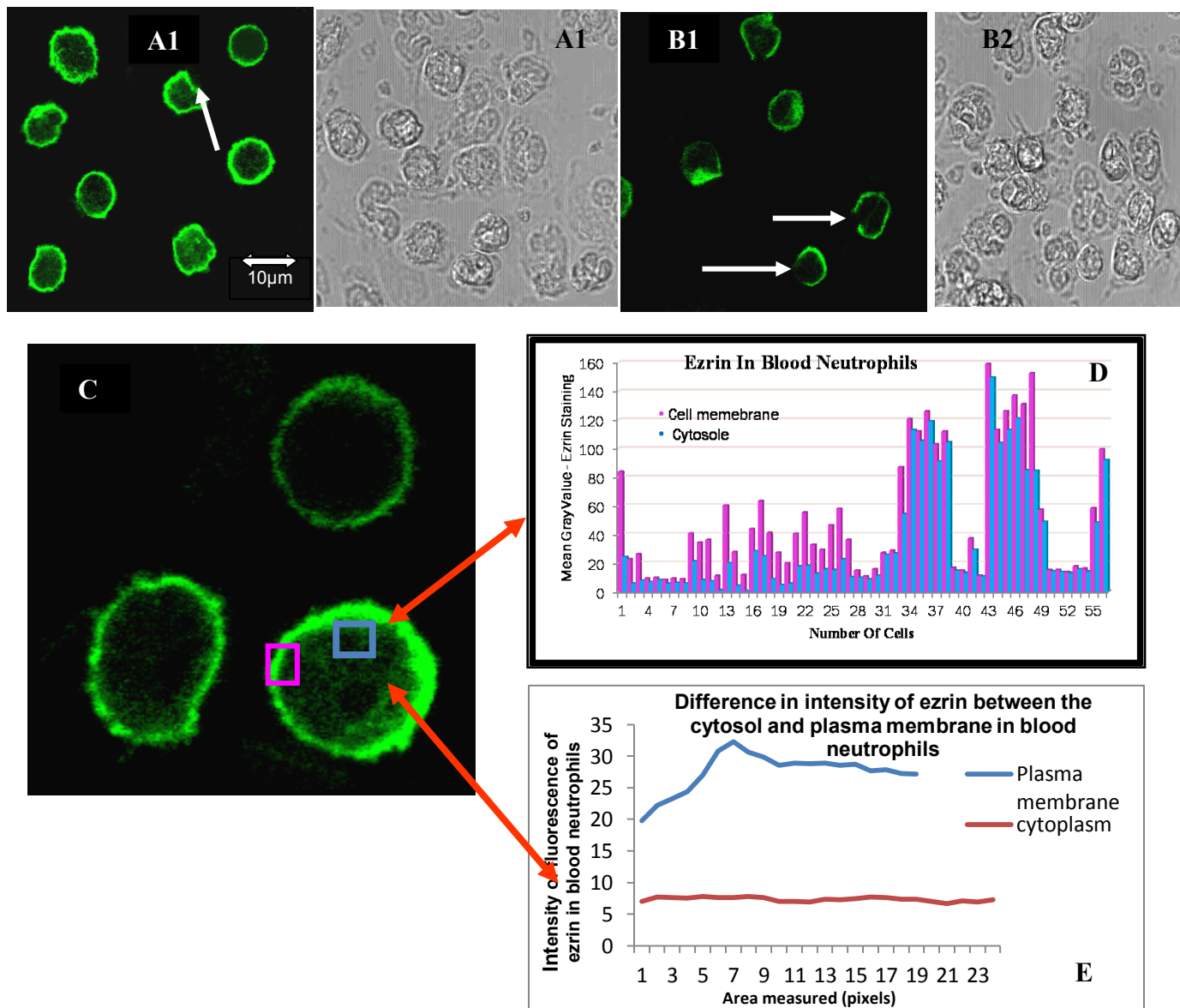


100µl of a suspension of $1\times10^6$cells/ml neutrophils were fixed and probed for ezrin. The majority (65/77) neutrophils observed had cell membrane staining of ezrin (fig A1). This staining was irregularly distributed around the cell membrane, as shown in fig B1(arrow marked) and there were areas in the cell membrane which were devoid of ezrin (arrow marked). Image J was used to measure the difference in intensity of fluorescence of ezrin between the cell membrane and cytsol, the area to be measured was selected as shown in the Figure C which shows an example of the areas selected and measured. Out of 77cells counted, 65 cells ezrin staining at the membrane (fig D) and often the intensity of fluorescence in cytosol was half as intense as the cell membrane (fig E) out of the remaining 12 cells counted, the neutrophils showed no difference in the intensity of ezrin between the cytosol and plasma membrane. The irregular peripheral staining of ezrin might give evidence that ezrin changes its subcellular position, when the neutrophils changes its shape or when there is dynamic change in the plasma membrane.

**Figure 4.4.1. Effect of the subcellular position of ezrin as the plasma membrane changes its dimension**
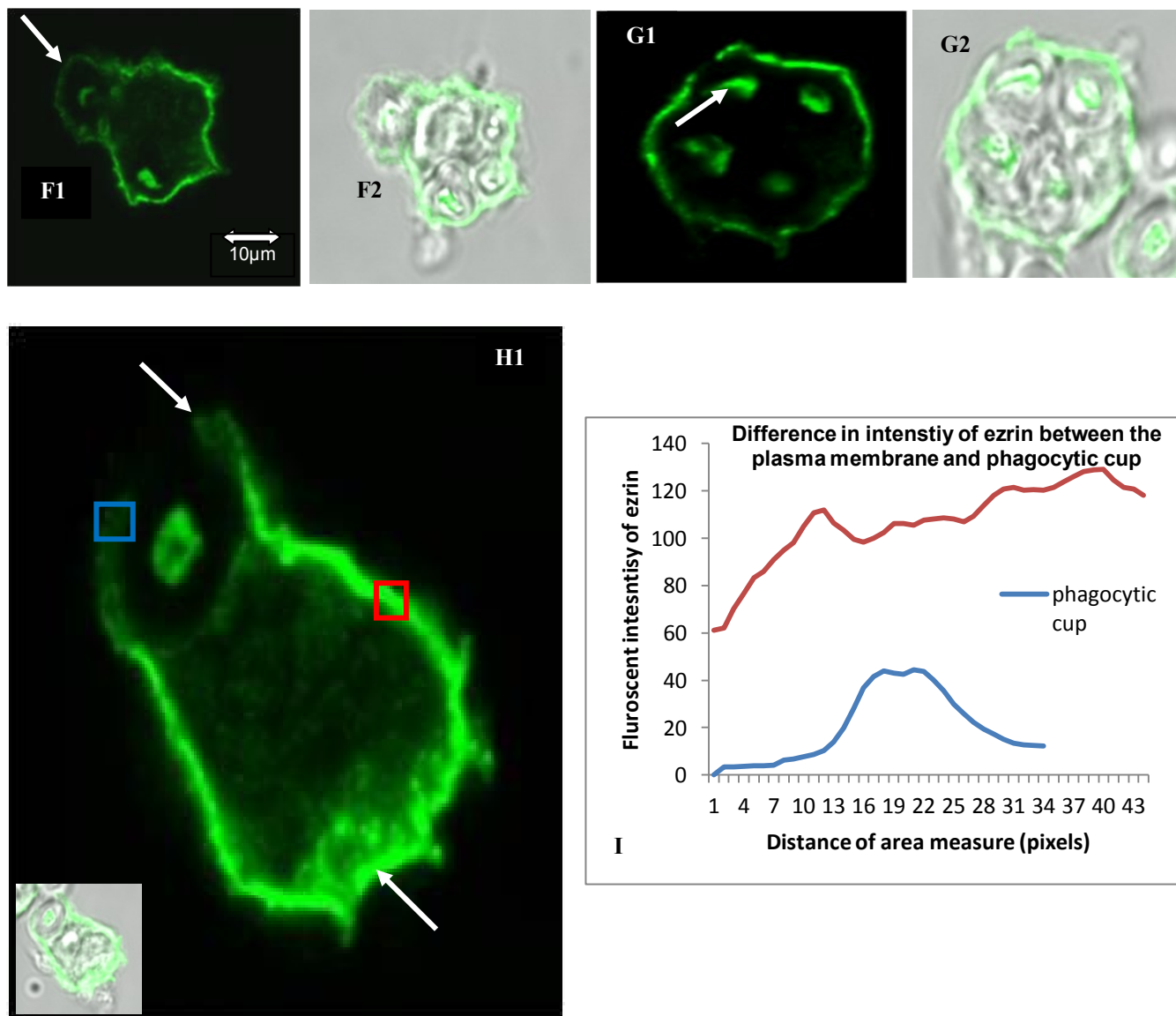


100µl of a suspension of 1x10$^5$ cells/ml neutrophils isolated from venous blood were allowed to undergo phagocytosis by incubating these cells with 100µl of 0.1mg/ml C3bi opsonised zymasan particals at 37$^{\circ}$C for 15minutes. When these cells were fixed and stained for ezrin, the membrane staining of ezrin was lost around the phagosomes membrane as well as along the membrane of the phagocytic cup (fig 4.4.1.F1,G1& H1). This gave an indication that ezrin relocates away from the cell membrane when there is change in dimension or change in shape of the cells. When the fluorescent intensity of ezrin around the phagocytic cup and the rest of the plasma membrane was measured, the intenisty of ezrin around the plasma membrane was twice as intense than around the phagocytic cup (graph I). The Image J programme was used to measure the intensity of ezrin.

## 4.4.2 The subcellular location of ezrin in transendothelial migrated neutrophils *ex vivo*

As ezrin changes its subcellular location from the peripheral membrane into the cytosol when there is a change in cell shape, the question arises whether a similar change occurs in other neutrophil activities, such as during transendothelial migration. Transendothelial assays were, therefore, performed to address this. In contrast to unstimulated neutrophils, nearly all the transendothelial migrated neutrophils (55/57) had a cytosolic subcellular position of ezrin (fig 4.4.2 A1 & A2). This was obvious in double-stained cells, where non-migrated neutrophils, were identified under the same fixation and staining conditions, but retained ezrin at the plasma membrane (positive for cell tracker, fig 4.4.2 A1 & A2). In order to make sure that the cell tracker is not blocking this change in subcellular location of ezrin between these two groups of neutrophils, instead of loading the non-migrated neutrophils with cell tracker, the neutrophils that had crossed the endothelial monolayer were loaded with cell tracker conjugated with phycoerythrin. Migrated cells again retained the cytoplasmic location of ezrin (fig 4.4.2 B1 & B2) while the non-migrated cells retained the plasma membrane staining (fig 4.4.2 B1 & B2). This finding confirms that the membrane linker protein ezrin relocated away from the plasma membrane into the cytosol as the neutrophils extravasated under exvivo conditions. When the difference in the fluorescence intensity of ezrin between the non-migrated and the migrated neutrophils was measured (fig 4.4.2, graph 1 & 2), there was a distinct and statistically significant difference in the distribution of ezrin between these two group of cells fig 4.4.2, graph 3, 4 & 5).
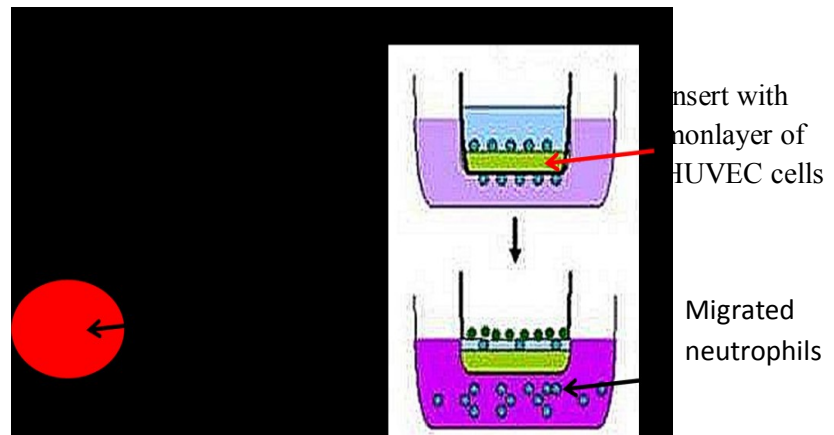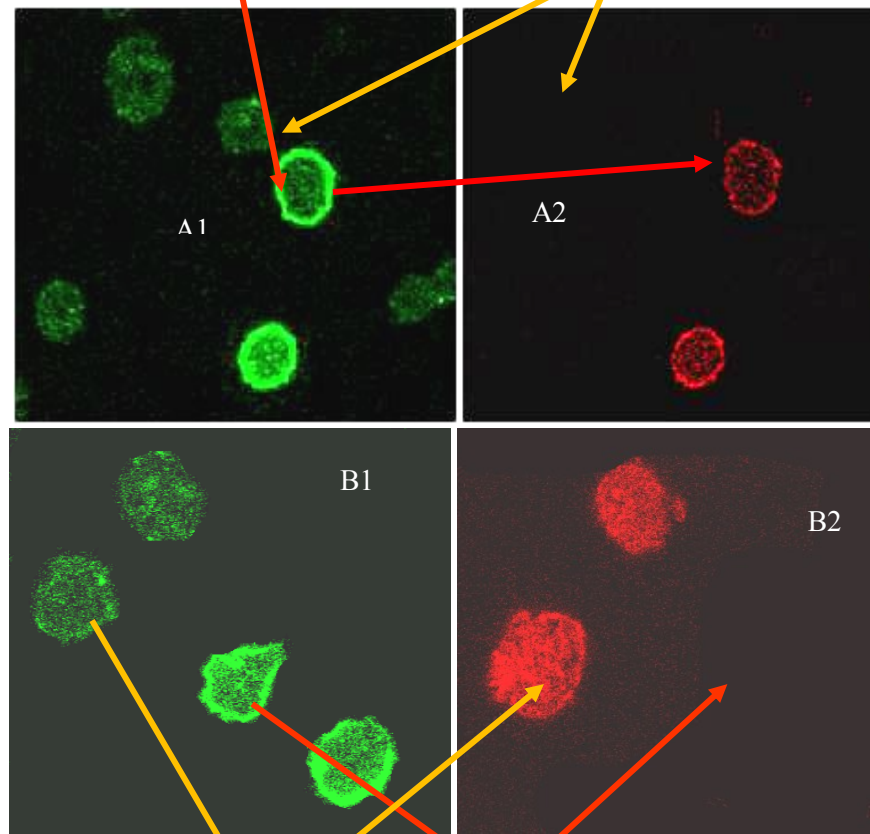
**Figure 4.4.2.** Subcellular location of ezrin in extravasated neutrophils *ex vivo.* Neutrophills isolated from venous blood ($1 \times 10^5$ cells/ml) were stimulated to cross a monolayer of endothelial cells (HUVEC cells grown over an insert) under the influence of chemical gradient set by 1μM of FMLP (top diagram). In order to differentiate between the two groups of neutrophils, the non-migrated neutrophils were loaded with cell tracker conjugated with phycoerythrin by incubating these cells with the 1μM of the dye at room temperature for 15 minutes. Both the non-migrated cells (positive for cell tracker) as well as migrated cells (100μl ) were mixed and fixed on a glass cover slip and probed for ezrin (A1, A2). The non-migrated cells had peripheral staining of ezrin and were positive for cell tracker, while the migrated cells lost the cell membrane staining of ezrin and were negative for cell tracker. To confirm that this change in subcellular loaction of ezrin was not influenced by the cell tracker dye used, the transendotheial migration assay was done in reverse: migrated cells were stained with the dye and mixed and fixed with nonmigrated neutrophils and when probed from ezrin, the non-migrated neutrophils (negative for cell tracker) had plasma membrane staining of ezrin, while the migrated neutrophils (positive for cell tracker) had cytosolic location of ezrin (B1,B2).

**GRAPH 1**

### Difference in intensity of fluorescence of ezrin in non migrated neutrophils

CELL MEMBRANE

CYTOPLASM

Difference in fluorescent intensity betweeen cell membrane and cytosole

Number of cells

**GRAPH 2**

### Difference in intensity of fluorescence of Ezrin in migrated neutrophils

cell membrane

cytoplasm

Difference in fluorescent intensity between n the cell membrane and cytosole

Number of cells

**GRAPH 3**

### scatter plot

diff- migrated   diff- nonmigrated

Differnce in intensity of ezrin bwteen the cell membrane and cytosole

Number of neutrophils counted

**GRAPH 4**

Non-migrated neutrophils
Migrated neutrophils

Standared Error of mean

*** ***

Neutrophils

**GRAPH 5**

Non-migrated neutrophils
Migrated neutrophils

Standared deviation

*** ***

Neutrophils

Graph 1: Comparison of intensity of ezrin between the cell membrane and the cytosol in non-migrated neutrophils. Cell membrane intensity of ezrin was more than the cytosol.

Graph 2: Comparison of intensity of ezrin between the cell membrane and the cytosol in migrated neutrophils. Cytosolic intensity of ezrin was more than the plasmamembrane.

Graph 3: Graphical representation of the difference in subcellular location of ezrin in migrated and non-migrated cells

Graph 4 and 5: Showthe statistical significancein the distribution of ezrin betweenthe migrated and non-migrated cells

**Figure 4.4.2.** The intensity of ezrin between the cell membrane and cytosol was measured (ImageJ) in the migrated and non-migrated cells. The intensity of ezrin was consistently greater in the cytosol than the cell membrane in the migrated neutrophils (graph 1), whereas the reverse was seen in the non-migrated cells (graph 2). There was a significant difference in the distribution of ezrin in the two groups of neutrophils (graphs 3-5). This indicates that ezrin relocated from the cell membrane into the cytosol as the neutrophils extravasated under experimental conditions.

## 4.4.3 The subcellular location of ezrin in extravasted cells

The relocation of ezrin away from the plasma membrane into the cytosol in tran-endothelially migrated neutrophils was established under experimental conditions. In order find evidence of a similar phenomenon under physiological conditions, neutrophils were isolated from saliva, as described in section 2.5.2.1. Approximately 87% of salivary neutrophils had lost the peripheral membrane staining of ezrin and had the characteristic cytosolic location of ezrin (fig 4.4.3 A1 & B1), seen previously in experimentally induced transmigration. The difference in the fluorescent intensity of ezrin between the cell membrane and cytosol in each salivary neutrophil was measured and showed that the cytoplasmic staining of ezrin was greater than the cell membrane (graph 1 & 2). It was important to exclude the possibility that the oral environmental conditions like the salivary buffer system, pH of the saliva, or the techniques used to isolate these neutrophils were not influencing the cytoplasmic position of ezrin. Neutrophils from venous blood were therefore mixed with the salivary neutrophils on a glass cover slip and the two groups of cells processed together. Cell tracker conjugated with phycoerythrin was used to differentiate the venous blood neutrophils from the salivary neutrophils. Neutrophils which were positive for cell tracker (venous blood neutrophils) (fig 4.4.3 D1 & D2) had peripheral membrane location of ezrin, while the salivary neutrophils which were negative for cell tracker (fig 4.4.3 D1 & D2), had cytoplasmic staining of ezrin. To make sure the cell tracker dye which was used to differentiate between the two groups of neutrophils was not influencing the subcellular location of the ezrin, instead of loading the venous blood neutrophils with cell tracker dye, salivary neutrophils were load with cell tracker. The cytoplasmic location of ezrin persisted in salivary neutrophils (fig 4.4.3 C1 & C2), while the venous blood neutrophils retained the plasma membrane location of ezrin (fig 4.4.3 C1 & C2). Using Image J, the cytosol/membrane intensity of ezrin in blood neutrophils and salivary neutrophils were compared (fig 4.4.3, graph 3 & 4). There was a distinct and significant difference in the subcellular distribution of ezrin between these two group of

neutrophils (figure 4.4.3 graph 5&6). This finding provided confirmation that ezrin relocated away from the plasma membrane into the cytosol as the neutrophils extravasated under both experimental as well as physiological condition.  Since the change in ezrin location was persistent and detectable in salivary neutrophils, these findings also give evidence that this change in subcellular location of ezrin associated with extravasation might be due to proteolytic action of calpain or an other mechanism which might cause this relocation of ezrin.
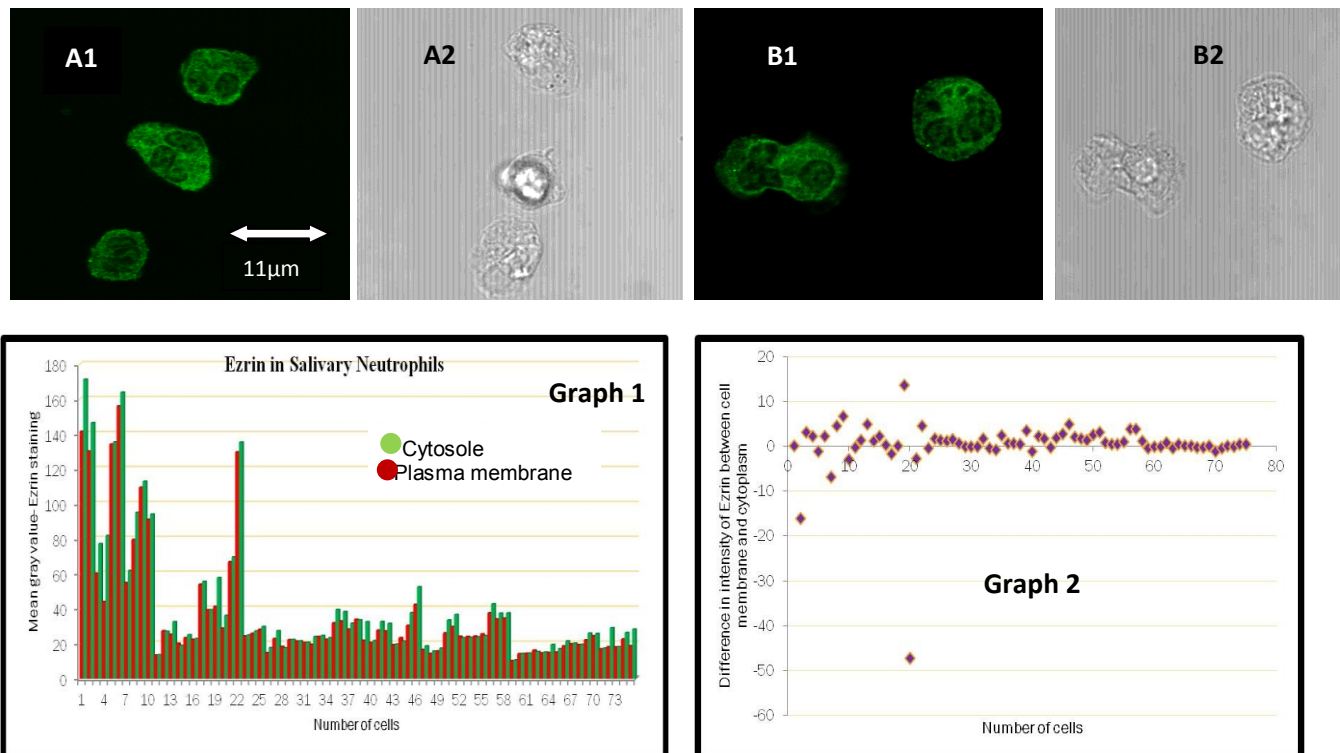
**Figure 4.4.3.:** Subcellular location of ezrin in extravasated neutrophils. 79/87 cells had greater cytoplasmic than membrane staining of ezrin (fig A1 & B1). In the remaining 8 cells, 5 had homogenous staining of ezrin (no difference in the cell membrane staining and cytosol) and 3 cells could not be quantified because the staining was too weak. When the intensity of ezrin was measured between the cell membrane and cytosol, this greater trend towards cytoplasmic ezrin was quantified, but there was no statistical difference in the fluorescence intensity (graph 1&2). Image J was used to measure the intensity of ezrin in salivary neutrophils.



**Blood Neutrophils** negative for cell tracker

**Salivary Neutrophils** positive for cell tracker

**Salivary Neutrophils** Negative for cell tracker

**Blood Neutrophils** Positive for cell tracker
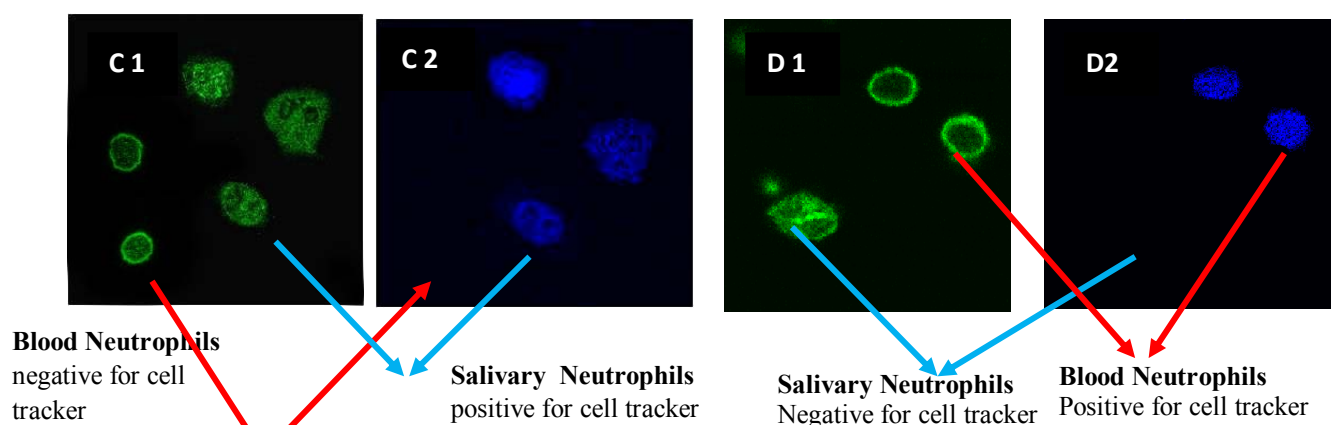
**Figure 4.4.3.** To find evidence that subcellular location of ezrin in salivary neutrophils is not influenced by oral environmental condition. 60/62 blood neutrophils counted had peripheral membrane staining of ezrin (fig C1&C2) and were negative for cell tracker, while 75/83 salivary neutrophils counted had cytoplasmic ezrin, with no detectable staining of ezrin at the cell membrane (fig C1&C2). There was no change in the subcellular location when the oppositepopulation was stained with cell tracker (salivary neutrophils had cytoplasmic position of ezrin and were positive for cell tracker and the blood neutrophils retained its plasma membrane staining of ezrin and were negative for cell tracker) (Fig D1&D2).

Graph 3



Graph 4
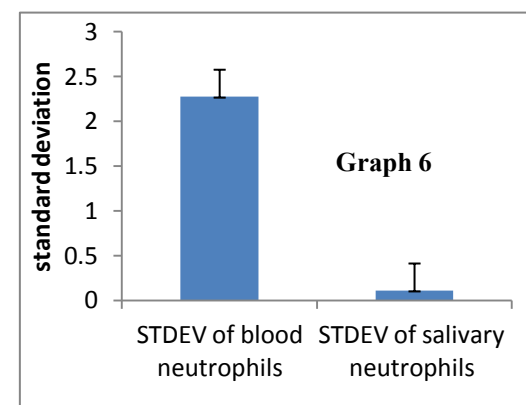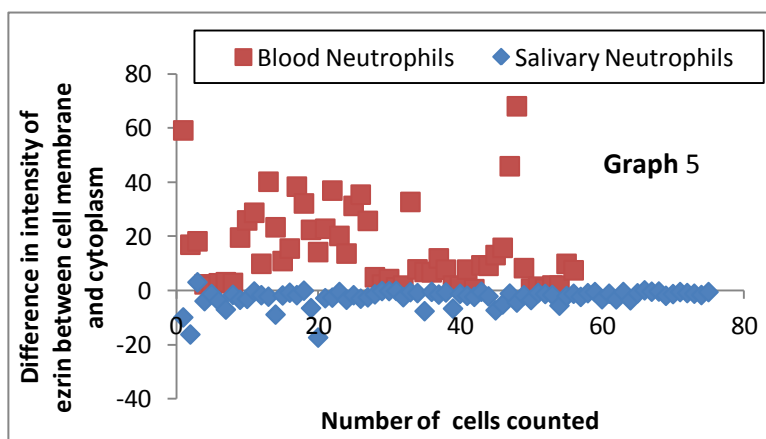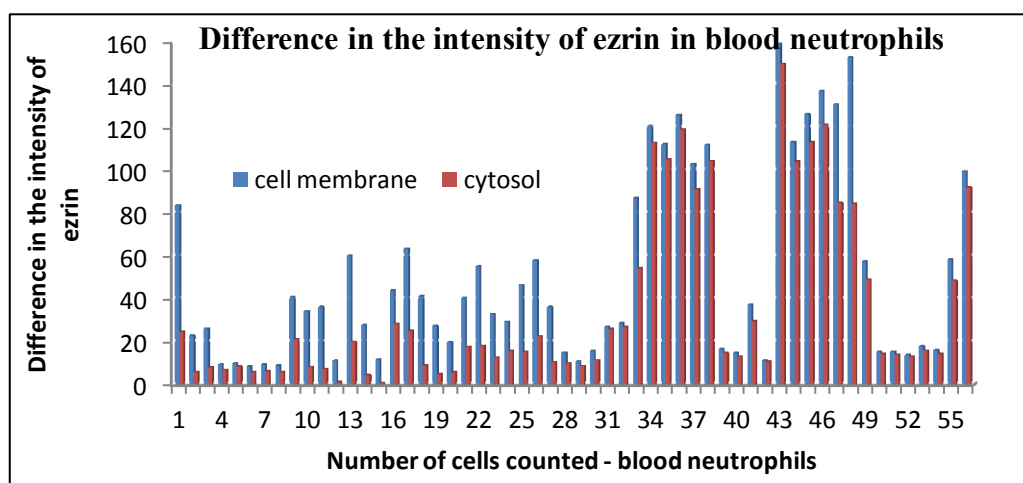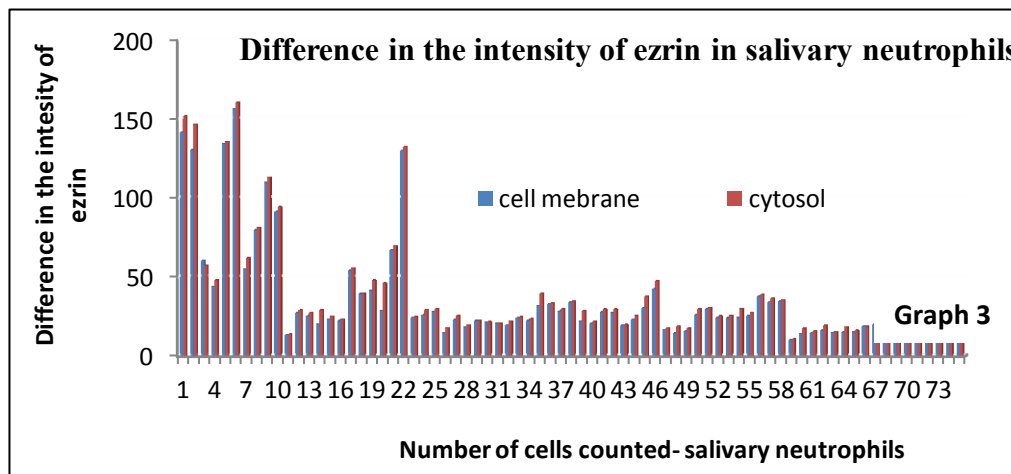


Graph 5



Graph 6

When the difference in the intensity of ezrin was measured using Image J, there was a statistically significant difference in the intensity of ezrin between the blood neutrophils and salivary neutrophils (Graphs 3, 4 & 5).

### 4.4.4  The effect of elevated cytosolic calcium and calpain inhibitor on the subcellular location of ezrin

It is a well know fact that ezrin is a substrate for the calcium-activated proteolytic enzyme, calpain. If the relocation of the subcellular position of ezrin during extravasation and during change in shape of the cell was due to the proteolytic effect of calpain, an elevation in cytosolic level of calcium would be required. In order to study the influence of cytosolic calcium on the subcellular location of ezrin, the blood neutrophils were treated with a calcium elevation cocktail, as discussed in section 4.3.2. This caused approximately 97% of neutrophils to lose ezrin from the plasma membrane (237/245 cells counted) (fig 4.4.4A & B). In contrast, 88% of neutrophils (69/78) treated similarly but with extracellular calcium removed and replaced by EGTA (1mM) had the classical cell membrane staining of ezrin (fig 4.4.4C). This provided evidence for a role of cytosolic calcium as a trigger for the subcellular relocation of ezrin. In order to establish whether a similar response was triggered by physiological triggered cytosolic calcium rise, the receptor agonist FMLP was used. Similar results were obtained when neutrophils were fixed after stimulation with FMLP (1µm). 83% of neutrophils (48/58 cells) counted lost the cell membrane staining for ezrin (fig 4.4.4A). These data showed that calcium had a significant effect on the subcellular location of ezrin.

In order to establish this possible relationship, the effect of a calpain inhibitor, ALLN, was investigated. After treatment with the inhibitor and stimulation with FMLP, 48% of neutrophils (42/87 cells) lost ezrin from the plasma membrane (fig 4.4.4D). This must be compared with 83% of untreated neutrophils and represents approximately 40% inhibition (figure 4.4.4, graph 1)

## Figure 4.4.4A. The effect of FMLP on subcellular location of ezrin
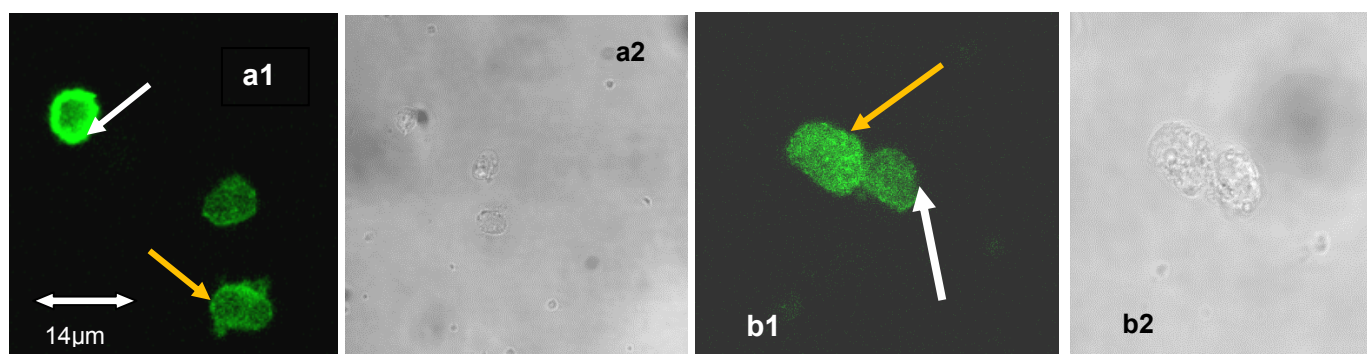


After stimulation of blood neutrophils with *FMLP* (1µM), 48/58 cells examined had no membrane staining for ezrin (figure a1&b1 indicated by **arrow**). Only 10 cells retained their membrane staining of ezrin (fig a1 & b1 indicated by white arrow). Moreover, the cells with peripheral membrane staining of ezrin were smaller in diameter (10µm), while the cells with cytoplasmic location of ezrin were 14µm in diameter. This might be due to polarization of neutrophils under the influence of *FMLP* and this finding suggested that as the neutrophils undergo polarization, ezrin relocates away from the cell membrane into the cytosol.

## Figure 4.4.4B. The effect of elevating cytosolic calcium on subcellular location of ezrin
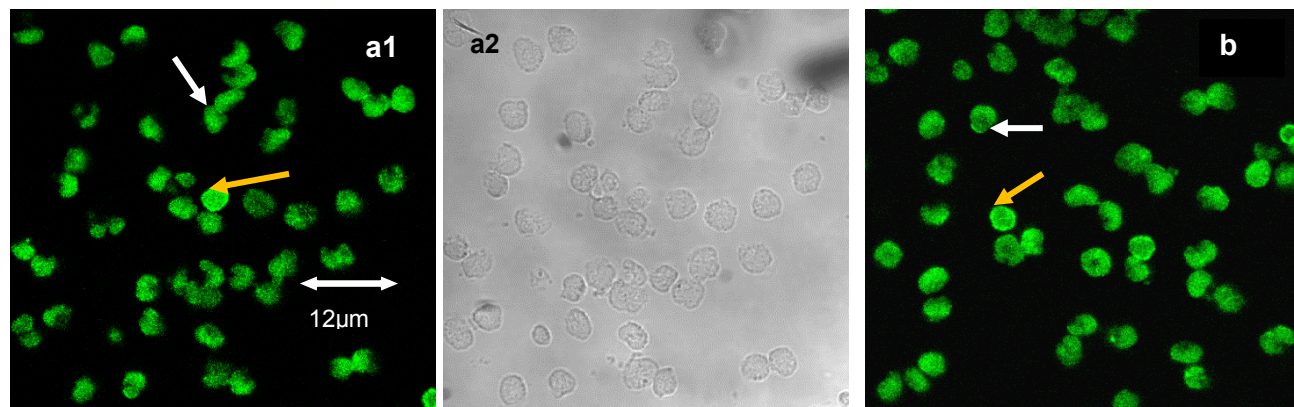


Once the neutrophils were isolated from venous blood, these cells were stimulated with a 'cocktail' of thapsigargin and ionomycin with high extracellular calcium (13mM). 237/245 neutrophils lost the characteristic plasma membrane location of ezrin  (indicated by white arrow in figure a1 & b). The remaining 8 cells retained the peripheral subcellular location of ezrin (indicated by orange arrow figure a1 & b). This gave evidence that relocation of ezrin away from the cell membrane might be triggered by a high level of calcium.

**Figure 4.4.4.C.: The effect of absence of calcium on subcellular location of ezrin.**
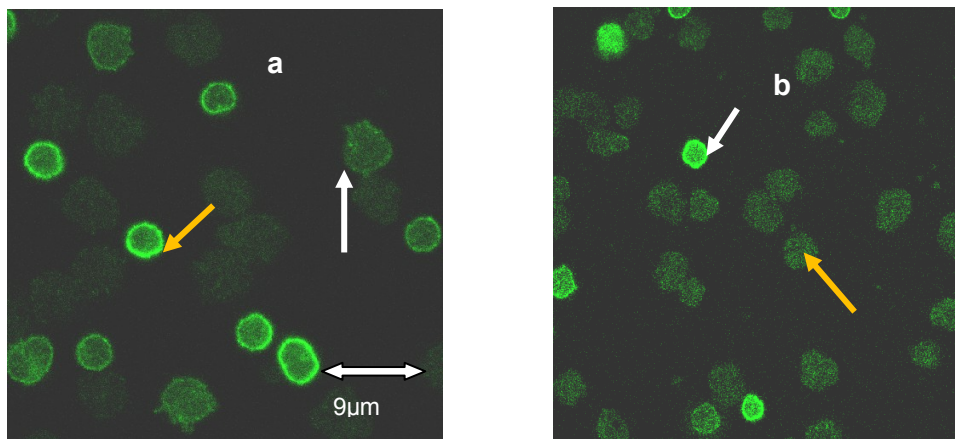


Before fixing the neutrophils isolated from venous blood, these cells were resuspended in 1mM of EGTA which is dissolved in PBS buffer. This setup was left at room temperature for 15 minutes. About 100µl of these neutrophils ($1x10^5$cells/ml) were allowed to adhere to a glass coverslip for 4 minutes, before these cells were probed for ezrin. 69/78 cells retained their plasma membrane location of ezrin and were smaller in size (indicated by orange arrow), when compared to the cells which had cytoplasmic staining of ezrin (9 cells, indicated by white arrow). This gave evidence that absence of calcium in the cells inhibits the relocation of ezrin away from the cell membrane and also inhibits polarization of the cells, which could be the reason for the neutrophils with peripheral membrane staining of ezrin to appear smaller in dimension when compared to the cells with cytosolic position of ezrin.

**Figure 4.4.4.D The effect of calpain inhibitor (ALLN) on subcellular location of ezrin.**
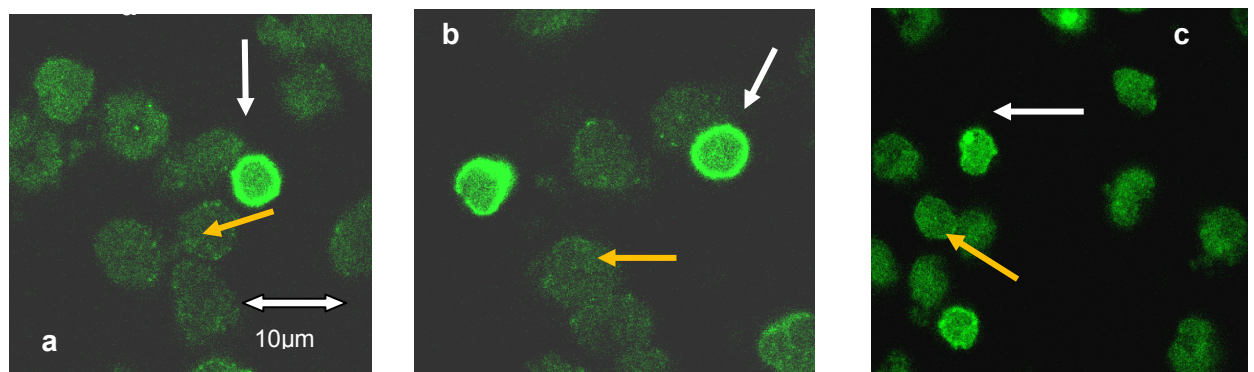


Approximately 48% of calpain inhibited neutrophils lost ezrin from the plasma membrane in response to *FMLP* (42/87 cells) (fig a, b & c indicated by orange **arrow**). The rest of the cells had plasma membrane staining of ezrin (figure a, b & c indicated by white arrow).

**Figure 4.4.4. Graph 1. Change in peripheral membrane position of ezrin under various conditions.**



% cell with membrane ezrin
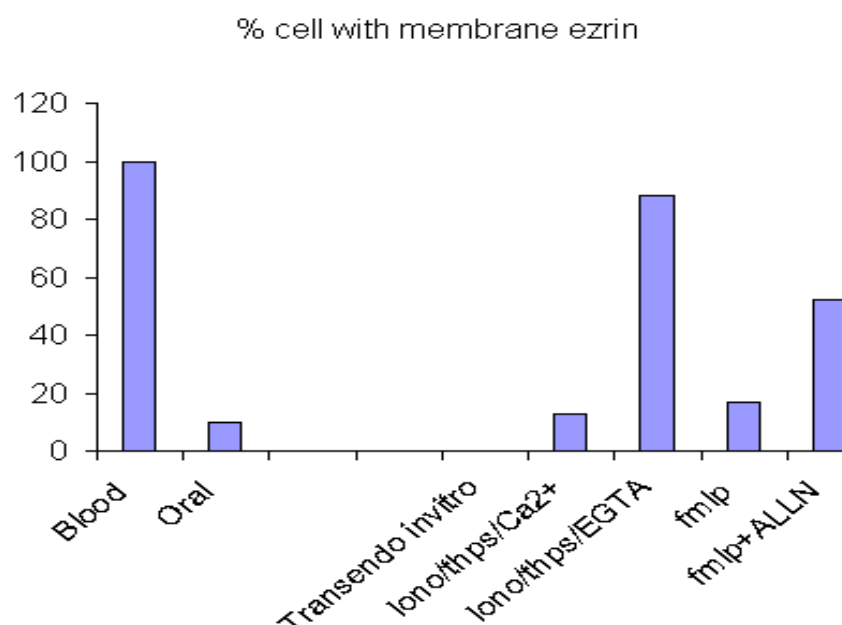
**Figure 4.4.4.(1). Change in peripheral membrane position of ezrin under various conditions.** It is clear from the information given in the above histogram that the loss of characteristic cell membrane staining of ezrin seen in both in experimentally extravasted neutrophils (*in vitro* transendothelial migration), as well as during physiological extravasation (oral neutrophils), is due to an increase in the cytosolic level of calcium and might be due to the proteolytic activation of calpain.

## 4.5   Discussion

Ezrin is one of the ERM family of proteins which may be involved in maintaining cell surface projection like microvilli, by forming a crosslink between the plasma membrane and underlying actin cytoskeleton(Bonilha 2007). Moreover, ezrin is a substrate for the calcium-dependent proteolytic enzyme, calpain.   Ezrin in neutrophils isolated from venous blood generally had a cell membrane location, but was notably absent from areas where there was a change in the curvature or dimension of the plasma membrane

(near the laminopodia, phagocytic cup and phagosomes). This suggested that ezrin might have a role in cell shape. Similarly, neutrophils which had migrated across the endothelium either under experimental conditions or under physiological condition (salivary neutrophils), lost their cell membrane staining of ezrin while the non-migrated neutrophils retained their cell membrane staining of ezrin. This gave a confirmatory finding that ezrin relocates away from the cell membrane into the cytosol as the neutrophils extravasate and when there is dimensional change in the plasma membrane. To establish a possible mechanism involved behind this relocation of ezrin, a role for calcium was investigated. Nearly 97% of cells lost the cell membrane staining of ezrin, when cytosolic calcium was elevated either experimentally or in response to receptor stimulation (83%). This was reduced to 50% by pre-incubation with a calpain inhibitor. This indicates that a change in the sub cellular location of ezrin away from the plasma membrane might be due to the protolytic effect of calpain stimulated by rise in cytosolic calcium level. As the sub-cellular location of ezrin is significantly different between the extravasted and non-migrated cells, ezrin may be used as a biological marker to identify extravasted neutrophils.

# CHAPTER 5

## Proteolysis of ezrin during elevation of cytosolic Ca$^{2+}$

## 5.1 Introduction

In the previous chapter, it was shown that ezrin subcellular distribution was affected by strategies which elevated cytosolic $Ca^{2+}$. In the resting neutrophils, ezrin was located at the cell membrane; whereas after elevation of $Ca^{2+}$ both artificially or as a result of stimulation or extravsation, ezrin was lost from this location and relocated to the cytosol. One possibility was that the relocation of the immunologically recognised ezrin was the result of a $Ca^{2+}$ - activated proteolysis.

Ezrin, also known as cytovillin, belongs to ERM family proteins and as a member of the band 4.1 superfamily, by virtue of the presence of a shared FERM domain at the amino terminus. This protein provide a regulated linkage between the filamentous (F)-actin in the cortex to membrane proteins on the surface of cells.  The ERM groups of proteins are ~75% identical in amino acid sequence. By regulating the linkage between the actin and membrane protein, ezrin may regulates cell shape, phagocytosis and chemotaxis. Moreover, this protein is also involved in membrane-protein localization, membrane transport and signal transduction (Bretshcher 2002).

### 5.1.1  Regulation of ezrin

As discussed in section 1.8.3 ezrin is recruited to the plasma membrane via its $NH_2$-terminal domain (300 residues), which contains both protein and phosphatidylinositol 4,5-bisphosphate (PIP2) binding sites (Algrain et.al.1993; Niggli et al.1995). It binds to F-actin through the last 34 amino acid of their COOH-terminal domain (Turunen et al.1994). In the cytoplasm, ezrin maintained in an inactive conformation through an intra-molecular interaction between their $NH_2$ -terminal ERM association domain (N-ERMAD) and the last 100 residues of the COOH-terminal ERM association domain (C-ERMAD). This interaction masks the membrane and F-actin binding sites (Gary and Bretscher 1995; Magendantz et al.1995). Activation of ezrin, therefore, requires unmasking of the protein binding site which in turn enables ezrin to establish a link between actin and membrane

protein. The activation of ERM proteins, resulting in the unmasking of their functional binding sites, occurs through conformational changes triggered by events including the binding to PIP2 and the phosphorylation of a conserved threonine in the actin binding site of the C-ERMAD (T567 in ezrin). From the data presented in chapter 4, it is clear that neutrophils isolated from the venous blood had peripheral membrane ezrin, indicating that ezrin exist in "active" form in human neutrophils and that when the neutrophils expand their plasma membrane, this active membrane binding is lost. This might indicate that ezrin was proteolytically cleaved by a $Ca^{2+}$-dependent protease such as calpain. Ezrin is a known substrate of Calpain (Shcherbina et al. 1999). Proteolytic cleavage of ezrin by calpain has the capacity to disrupt membrane-cytoskelton linkage (Ya et al.1993).

## 5.2 Aims

The aim of this chapter was to seek biochemical evidence that ezrin proteolysis had occurred during neutrophil activation and elevation of cytosolic $Ca^{2+}$. It was therefore necessary to do the following:-

1. Determine the molecular weight of ezrin in neutrophils.

2. Detect the proteolytic products of ezrin in neutrophils in which cytosolic $Ca^{2+}$ has been elevated.

3. Detect the proteolytic products of ezrin in neutrophils which had undergone a morphological change.

## 5.3 Material and Methods

### 5.3.1 Materials

**a) Primary ezrin antibody**

Ezrin (3C12), from Santa Cruz Biotechnology, was the primary ezrin antibody used in Western blotting, to detect the molecular weight of ezrin in neutrophils and cell lines.

This antibody is a mouse monoclonal antibody raised against amino acids 362-585 of human ezrin and was used at the dilution of 1:500 in 3% and 10% of milk TBS. Once the proteins were transferred onto the nitrocellulose membrane, the membrane was incubated in 3% milk, which had 100µl of Tween 20 and 1% TBS buffer in presence of 1:500 dilution of primary ezrin antibody at 37°C for 1hour on a rotator wheel.

### b) Secondary ezrin antibody

The secondary antibody was a goat anti-mouse IgG-horseradish peroxidise conjugate (Santa Cruz Biotechnology), used at 1:1000 dilution in 3% milk.

## 5.3.2  Methods

### a)  Cell lysate preparation and Novex® NuPAGE® SDS-PAGE Gel System

3-8% precast NuPAGE Tris-acetate gel from Invitrogen was used to separate the protein according to the molecular weight. HiMark™ Pre-Stained High Molecular Weight Protein Standards (Invitrogen) was used as protein standard against which the proteins from the cell lysate were separated. HL60 cells, RAW cells,  3T3 cells,  PLB cells and PZHPV7 cells were used as positive control cell lines, to test the specificity and sensitivity of ezrin antibody (mouse monoclonal $IgG_1$ from Santa Cruz Biotechnology). The cells were counted using cell counting chamber in cell counter (Cellometer®cell counting chamber SD100; Cellometer™ Auto T4 from PeQ Lab Biotechniologie GmbH) before lysing with 50mM of HEPES, 150mM NaCl, 10% glycerol, 1% Triton X100, 1.5mM $MgCl_2$, 5mM EGTA, 5mM EDTA, 1mM $Na_3VO_4$, 1.5mM NaF, 0.1% SDS and 1:1000 dilution of protease inhibitor cocktail (Sigma Aldrich) at 4°C for 1 hour.  The amount of lysis buffer used depended on the size of the pellet or number of cell counted, for instance to lysis cells like HL60, RAW cells and neutrophils from venous blood, 1ml of lysis buffer was used. 500µl of lysis buffer was used to lyse neutrophils isolated from saliva but the

protease inhibitor cocktail was always used as 1:1000 dilutions.  The cell lysate were centrifuging at 14,000rpm for 5 minutes and the pellet was discarded. The amount of protein in each cell lysate was quantified using the BSA assay. Each cell lysate was then boiled at $90^{\circ}$Cfor 10-15 minutes along with NuPAGE$^{®}$ LDS Sample Buffer *(4X)* and NuPAGE$^{®}$ Reducing Agent *(10X)*. A mini 1.0mm thick, 15 well triacetate gels (NuPAGE$^{®}$pre cast 3-8% tris acetate gel) was used. To each well, 20µl of cell lysate with atleast 5µg/ml of protein was added with 15µl of prestained protein ladder. The NuPAGE$^{®}$ SDS-PAGE gel system was set at 55mA, 120mV, for 1hour, in XCell SureLock™ Mini-Cell tank system, the inner chamber of the tank was filled with 200ml of NuPAGE$^{®}$ Tris-Acetate SDS  running buffer (10X) and 500µl of NuPAGE$^{®}$ antioxidant, the outer chamber of the tank was filled with 300ml of NuPAGE$^{®}$ Tris-Acetate SDS  running buffer(10X).

## b) Immunoblotting

The protein was transferred to nitrocellulose membrane (Hydrobond-ECL; Amersham Biosciences) at constant 220mA at 30V for 1 hour, using XCell SureLock™ Mini-Cell tank system. The efficiency of protein transferred was evaluated using ponceau S staining. Then, the membrane was blocked (3% milk) with monoclonal mouse anti-ezrin antibody at dilution of 1:500 in 3%milk/0.5% Tween-20 for one hour. The membrane was washed and incubated overnight at $4^{\circ}$C with goat anti-mouse antibody, conjugated with horseradish peroxide at dilution of 1:1000, then washed and exposed to chemiluminescent protein detection using Supersignal™ West Dura system (Pierce Biotechnology Inc., Rockford, USA), The chemiluminescent signal was detected using a UVITech Imager (UVITech Inc., Cambridge, UK), which contains both an illuminator and a camera linked to a computer which then captures and stores the image. Each membrane was subjected to varying exposure times until the protein bands were sufficiently visible.  These images were then captured and further analysed with the UVIband software package (UVITEC, Cambridge, UK), which allowed for protein band

quantification. In order to confirm reliability of the results, each western blot was carried out three times. Each sample was blotted along with a prestained high molecular weight marker supplied by Invitrogen. Image J was used to measure the RF value, the detailed procedure involved in obtaining the RF value is explained in section 2.5.2.9.

## c) Estimating the molecular weight of ezrin in neutrophils

Neutrophils isolated form venous blood were counted using the cell counting chamber (Cellometer®cell counting chamber SD100) in an automatic cell counter (Cellometer™ Auto T4 from PeQ Lab Biotechniologie GmbH). $1 \times 10^6$ of neutrophils were lysed using 1000μl of lysis buffer and 1:1000 dilution of protease inhibitor cocktail for 1hour at $4^{°}$c. At every 15 minute interval, the cell lysate were vortex. Then, the cell lysates were boiled at $90^{°}$C for 10 minutes, and centrifuged at 14,000 rpm for 5minutes, the cell debris was removed and the protein in the supernatant was quantified using the BSA protein assay. A similar method was followed to isolated protein from the HL60, RAW cells, PLB cells, 3T3 cells and HPZHPV7 and protein obtained from these cell line were diluted using the lysis buffer to equality to the amount of protein isolated from the neutrophils. 15-20μl of cell lysate was added into each well and the technique described in section 5.3.2a & b was followed. A similar technique was followed to identify ezrin in neutrophils isolated from saliva.

## d) Ca$^{2+}$ elevating experiments

Ionophore increases intracellular calcium by transporting $Ca^{2+}$ across the plasma membrane. Thapsigargin increases intracellular $Ca^{2+}$ by inhibiting the CaATPase on the endoplasmic reticulum, which leads to depletion of $Ca^{2+}$ from the intracellular stores and causes the $Ca^{2+}$ channels to open in the plasma membrane causing $Ca^{2+}$ influx. FMLP cause a physiological $Ca^{2+}$ signal in neutrophils. FMLP binds to the formyl peptide receptor (FPR), a G protein coupled receptor (Selvatici et al.2006) which initiates the release of $Ca^{2+}$ from intracellular stores and the opening of $Ca^{2+}$ channels

in the plasma membrane. The neutrophils were treated both in presence of $Ca^{2+}$ and in absence of added $Ca^{2+}$ and in presence of EGTA (1mM). A $Ca^{2+}$ elevating "cocktail" was used to increase $Ca^{2+}$ and inhibit its uptake into intracellular organelles (19M ionophore, 19M thapsigargin and 26mM $CaCl_2$ ). $Ca^{2+}$ elevation was also achieved non-chemically using probe sonication, which permeablised the membrane and so allowed $Ca^{2+}$ entry. Sonication was used for 5-10 seconds before treatment with cell lysis buffer and protease inhibitors. The protein from these samples was separated using the technique discussed in section 5.3.2a & b.

## 5.4    Results

### 5.4.1   Prediction of ezrin fragments of calpain proteolysis

Using CaMPDB (Calpain Modulatory Proteolysis Database) and multiple kernel learning programme designed by DuVerle *et al* (2011), one can predict potential calpain cleavages site in ezrin. Standard peptide cutter programmes which use simple algorithms fail to accurately predict substrate cleavage by calpain. However, this programme, which is a recent extension to the classic support vector machines framework, employs machine-learned algorithms and has greatly improved predictive ablility. This approach showed significant specificity difference across calpain sub-types, despite previous assumptions to the contrary. Prediction accuracy was futher successfully validated using, an unbiased test set, mutated sequences of calpastatin (endogenous inhibitor of calpain) modified to no longer block calpain's proteolytic action. In depth information regarding how these program work can be found (DuVerle et al. 2009) and accessed at http//calpain.org. In order to predict the possible calpain cleavage sites of ezrin, the sequence of ezrin obtained using UniProtKB/Swiss-Prot data base was loaded in the CaMPDB, Calpain Modulatory Proteolysis Database and multiple kernel learning Programme in FASTA-style format. Three possible cleavage site of calpain in ezrin obtained using this database are given in the table below.

**Table 5.4.1**

**a) P15311 (EZRI_HUMAN)  UniProtKB/Swiss-Prot**

| Protein names | **Ezrin** |
|---|---|
| *Recommended name:* | Cytovillin |
| *Alternative name(s):* | Villin-2 |
| | p81 |

| Gene names | Name: | **EZR** |
|---|---|---|
| | Synonyms: | VIL2 |

| Organism | **Homo sapiens (Human)** |
|---|---|
| Taxonomic identifier | 9606 [NCBI] |
| Sequence length | 586 amino acid |
| Post translatory modicatuin | Phosphorylated by tyrosine-protein kinases. Phosphorylation by ROCK2 suppresses the head-to-tail association of the N-terminal and C-terminal halves resulting in an opened conformation which is capable of actin and membrane-binding |
| Sequence | MPKPINVRVTTMDAELEFAIQPNTTGKQLFDQVVKTIGLREVWYFGL HYVDNKGFPTWLKLDKKVSAQEVRNPLQFKFRAKFYPEDVAEELIQ DITQKLFFLQVKEGILSDEIYCPPETAVLLGSYAVQAKFGDYNKEVHK SGYLSSERLIPQRVMDQHKLTRDQWEDRIQVWHAEHRGMLKDNAM LEYLKIAQDLEMYGINYFEIKNKKGTDLWLGVDALGLNIYEKDDKLTP KIGFPWSEIRNISFNDKKFVIKPIDKKAPDFVFYAPRLRINKRILQLCM GNHELYMRRRKPDTIEVQQMKAQAREEKHQKQLERQQLETEKKRR ETVEREKEQMMREKEELMLRLQDYEEKTKKAERELSEQIQRALQLE EERKRAQEEAERLEADRMAALRAKEELERQAVDQIKSQEQLAAELA EYTAKIALLEEARRRKEDEVEEWQHRAKEAQDDLVKTKEELHLVMT APPPPPPPVYEPVSYHVQESLQDEGAEPTGYSAELSSEGIRDDRNE EKRITEAEKNERVQRQLLTLSSELSQARDENKRTHNDIIHNENMRQG RDKYKTLRQIRQGNTKQRIDEFEAL |

**b) The possible cleavage site of ezrin by calpain**

10 Best scores:

1. Pos. **71** - Score: 0.16
2. Pos. **487** - Score: 0.14
3. Pos. **572** - Score: 0.13
4. Pos. **504** - Score: 0.12
5. Pos. **319** - Score: 0.12
6. Pos. **324** - Score: 0.12
7. Pos. **171** - Score: 0.11
8. Pos. **467** - Score: 0.11
9. Pos. **348** - Score: 0.11
10. Pos. **493** - Score: 0.11
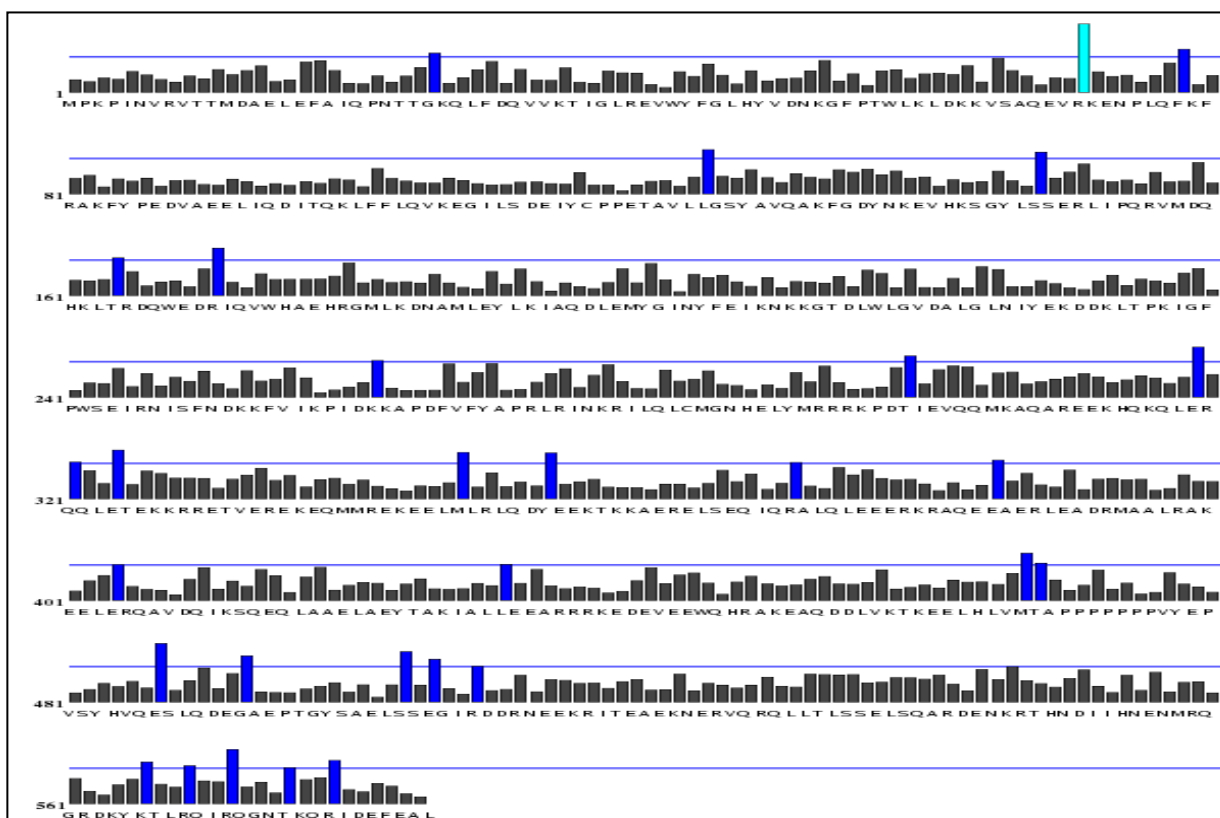
**c) The most probable proteolytic products of ezrin amino acid sequence**

| Fragment 1<br><br>MWt 8237.545 Da | MPKPINVRVTTMDAELEFAIQPNTTGKQLFDQVVKTIGLREVWYFGLHYV DNKGFPTWLKLDKKVSAQEVR |
|---|---|
| Fragment 2<br><br>MWt 61193.159 Da | KENPLQFKFRAKFYPEDVAEELIQDITQKLFFLQVKEGILSDEIYCPPETAV LLGSYAVQAKFGDYNKEVHKSGYLSSERLIPQRVMDQHKLTRDQWEDRI QVWHAEHRGMLKDNAMLEYLKIAQDLEMYGINYFEIKNKKGTDLWLGVD ALGLNIYEKDDKLTPKIGFPWSEIRNISFNDKKFVIKPIDKKAPDFVFYAPRL RINKRILQLCMGNHELYMRRRKPDTIEVQQMKAQAREEKHQKQLERQQL ETEKKRRETVEREKEQMMREKEELMLRLQDYEEKTKKAERELSEQIQRA LQLEEERKRAQEEAERLEADRMAALRAKEELERQAVDQIKSQEQLAAELA EYTAKIALLEEARRRKEDEVEEWQHRAKEAQDDLVKTKEELHLVMTAPPP PPPPVYEPVSYHVQESLQDEGAEPTGYSAELSSEGIRDDRNEEKRITEAE KNERVQRQLLTLSSELSQARDENKRTHNDIIHNENMRQGRDKYKTLRQIR QGNTKQRIDEFEAL |
| Fragment 3<br><br>MWt 49596.558 Da | KENPLQFKFRAKFYPEDVAEELIQDITQKLFFLQVKEGILSDEIYCPPETAV LLGSYAVQAKFGDYNKEVHKSGYLSSERLIPQRVMDQHKLTRDQWEDRI QVWHAEHRGMLKDNAMLEYLKIAQDLEMYGINYFEIKNKKGTDLWLGVD ALGLNIYEKDDKLTPKIGFPWSEIRNISFNDKKFVIKPIDKKAPDFVFYAPRL RINKRILQLCMGNHELYMRRRKPDTIEVQQMKAQAREEKHQKQLERQQL ETEKKRRETVEREKEQMMREKEELMLRLQDYEEKTKKAERELSEQIQRA LQLEEERKRAQEEAERLEADRMAALRAKEELERQAVDQIKSQEQLAAELA EYTAKIALLEEARRRKEDEVEEWQHRAKEAQDDLVKTKEELHLVMTAPPP PPPPVYEPVSYHVQE |

### 5.4.2  Molecular weight of ezrin in neutrophils

Neutrophils isolated from venous blood were counted using cell counting chamber (Cellometer®cell counting chamber SD100) in a cell counter (Cellometer™ Auto T4 from PeQ Lab Biotechniologie GmbH). $9 \times 10^7$ cells/ml were lysed in presence of lysis buffer and 1:1000 dilution of protease inhibitor. A similar procedure was carried out to prepare the cell lysate for various cell line (HL60, RAW cells and PLB cells). Once the cell lysate were prepared, the amount of protein present in each sample were quantified using BSA assay (Graph 5.4.2a & Table 5.4.2b), The amount of protein in each cell lysate was equalized using cell lysis buffer in order to make sure that the difference in the intensity of ezrin protein band between each cell lysate is not due to the amount of protein in each sample used. The sample were run in denatured form by adding NuPAGE® LDS Sample Buffer (4X) and NuPAGE® Reducing Agent (10X) and boiling the sample at 90ºC for 10 minutes. The protein from the samples were separated and transferred into nitrocellulose membrane, as discussed in the section 5.3.2a & b. The apparent molecular weight of ezrin in all cell samples was determined using Image J programme. First, the capture membrane image was inverted in order to quantify the band intensity, using image J. The distance travelled by the standard protein in the pre-stained protein ladder (HiMark™ prestained protein standard) was calculated first and the RF value and the log of the protein standard were plotted. Similar steps were followed to calculate the RF value of protein band observed in each sample. Using the formula generated from the protein standard, the molecular weights of each protein band in the entire cell lysate sample were determined (Table 5.4.2d and Graph 5.4.2e). This gave an estimated molecular weight of ezrin in "immune cell lines" HL60, PLB and RAW cells and in "non-immunological cell lines" 3T3, HECV and prostate cancer cell lines of 80 KDa, similar to that reported for other cells, However, in primary neutrophils, the ezrin band was 72kDa  (Figure 5.4.2.c). While ezrin often runs near 80Kda and is known as p81, its amino acid calculated weight is actually 69kDa.

Figure 5.4.2a. Protein quantification -BSA assay

## Protein Quantification



$y = 1113.9x - 121.52$
$R^2 = 0.9779$

Graph 5.4.2.a shows the protein quantification obtained by using BSA assay. The formula obtained from the assay was used to calculate the amount of protein present in each sample (Table 5.4.2.b). In order to make sure the amount of protein present in each sample (equalised to the amount of protein present in neutrophils sample), cell lysis buffer was used and the samples were run along with sample buffer and reducing agent provided by Invitrogen

Table 5.4.2b. Calculation used to quantify the (ezrin) protein in each samples

| Sample | Optical density 1 | Optical density 2 | Average | Conc (µg/ml) | Conc (µg/µl) |
|---|---|---|---|---|---|
| Lysis buffer | 0.08 | 0.07 | 0.07 | 422.63 | Xxx |
| Neutrophils | 0.15 | 0.15 | 0.15 | 6157.70 | 6.15 |
| PLB | 0.30 | 0.26 | 0.28 | 6323.11 | 6.32 |
| HL60 | 0.31 | 0.37 | 0.34 | 7092.26 | 7.09 |
| RAW | 0.51 | 0.46 | 0.49 | 7229.83 | 7.22 |
| 3T3 | 0.30 | 0.26 | 0.28 | 6425.21 | 6.42 |
| HECV | 0.51 | 0.47 | 0.49 | 7329.25 | 7.32 |
| PZHPV7 | 0.32 | 0.38 | 0.35 | 7087.27 | 7.08 |
| P2CTV2 | 0.35 | 0.42 | 0.38 | 6333.11 | 6.33 |

Figure 5.4.2.c:
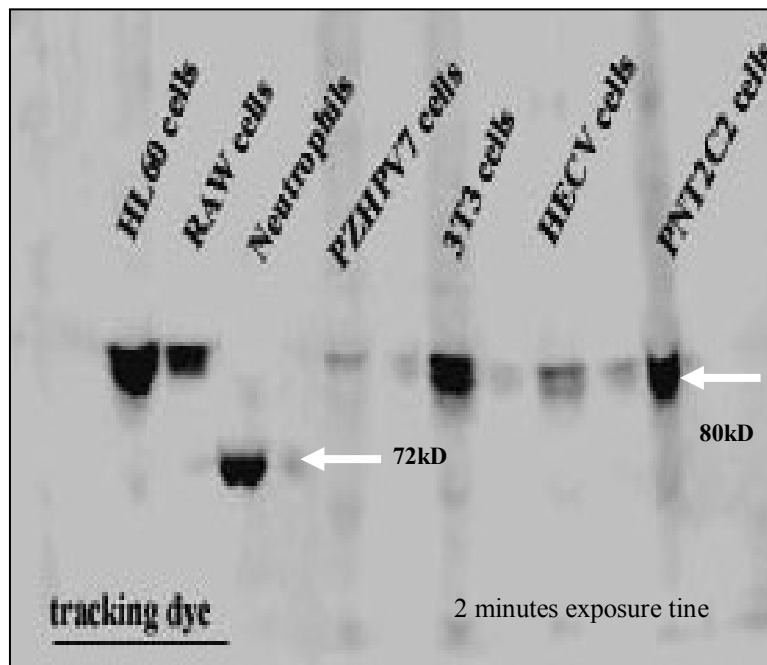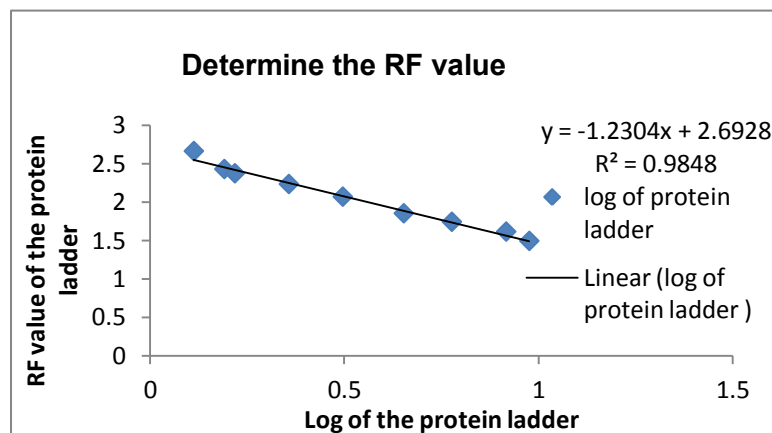


Figure 5.4.2c. Determining the molecular weight of ezrin in neutrophils:

3-8% Tris-acetate gel was used to separate the protein from the cell lysates and the proteins were transferred on to nitrocellulose membrane. Monoclonal mouse anti-ezrin was used to detect the ezrin protein band; chemiluminescence technique was used to exposed the protein band. Despite repeating the experiment three times with neutrophils isolated from different donors, the evident difference in the position of ezrin in neutrophils and the cell-line lysates was consistent (indicated by arrows). Using Image J, the RF value and the molecular weight of ezrin was determined (Table 5.4.2.d and Graph 5.4.2.e), ezrin measured around 72kDa in neutrophils while in other cell lines it was 80kDa. The gel shown is representative of at least three repeats.

Graph. 5.4.2.e



Table 5.4.2.d

| Samples | Distance travel by 1st band (mm) | RF value 1st band | Log value 1st | Antilog 1st band (mol wt in kDa) |
|---|---|---|---|---|
| HL60 | 215 | 0.64 | 1.90 | 80 |
| PLB | 216 | 0.64 | 1.89 | 79.33 |
| Neutrophils | 227.14 | 0.67 | 1.85 | 71.90 |
| RAW | 211.02 | 0.63 | 1.90 | 80.54 |
| 3T3 | 212.51 | 0.64 | 1.90 | 79.52 |
| HECV | 215.01 | 0.64 | 1.90 | 80.00 |
| PNT2C2 | 216.01 | 0.64 | 1.89 | 79.32 |
| PZHPV7 | 214.07 | 0.63 | 1.90 | 80.64 |

Table 5.4.2.d and Graph 5.4.2e. The RF value of the protein ladder. Using this the molecular weight of ezrin in the cell lysate and neutrophils were determined.

## 5.4.3 Proteolytic products of ezrin in neutrophils

Bands of "ezrin" with lower molecular weight (approx 55kDa) were often noticed in preparations of neutrophils. Interestingly, in HL60 cells, despite the full length ezrin running at 81kDa, a second band also had a 55kDa molecular weight (Fig 5.4.3a). Although 55kDa was not predicted to be one of the most likely proteolytic fragments (see section 5.3.1), it may have resulted from proteolysis during inadvertent cell activation. Deliberate cell activation was therefore explored using FMLP and Triton X-100.

**Figure 5.4.3a. 3-8% tris acetate gel probed for detecting ezrin protein**
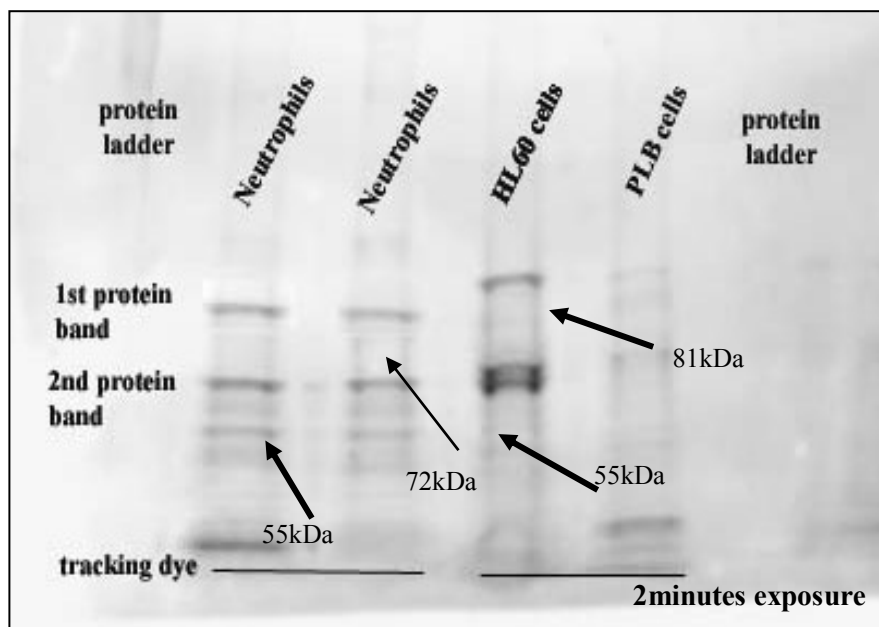


### a. Deliberate cell activation using FMLP and Trition X-100

Stimulation of neutrophils with FMLP (1µM, 1 hour, room temperature) also produced two immunoreactive "ezrin" bands, with RF values corresponding to the molecular weights of 69kDa (the full length amino acid sequence weight) and 51 kDa the potential fragment observed earlier (figure 5.4.3b). Permeabilising the neutrophils with Triton X-100 (1%, 1 hour at room temperature) also produced a band with an RF value corresponding with 51KDa. Interestingly, no 72KDa band was detectable, but instead there was a band at 69KDa (the

molecular weight of the amino acids) (fig 5.4.3c). It is possible that the apparent higher molecular weight of ezrin was the result of post-translatory modification and especially glycosylation. As TritonX-100 releases the contents from neutrophil granules, which include glycosylases, it is possible that the shift down to 69KDa was the result of deglycosylation. (fig5.4.3b, graph 5.4.3c & table 5.4.3.d).

**Figure 5.4.3b 3-8% Tris acetate gel probe for detecting proteolytic products of ezrin**



c) **Determine the RF value**

$y = -1.341x + 2.7936$
$R^2 = 0.9862$
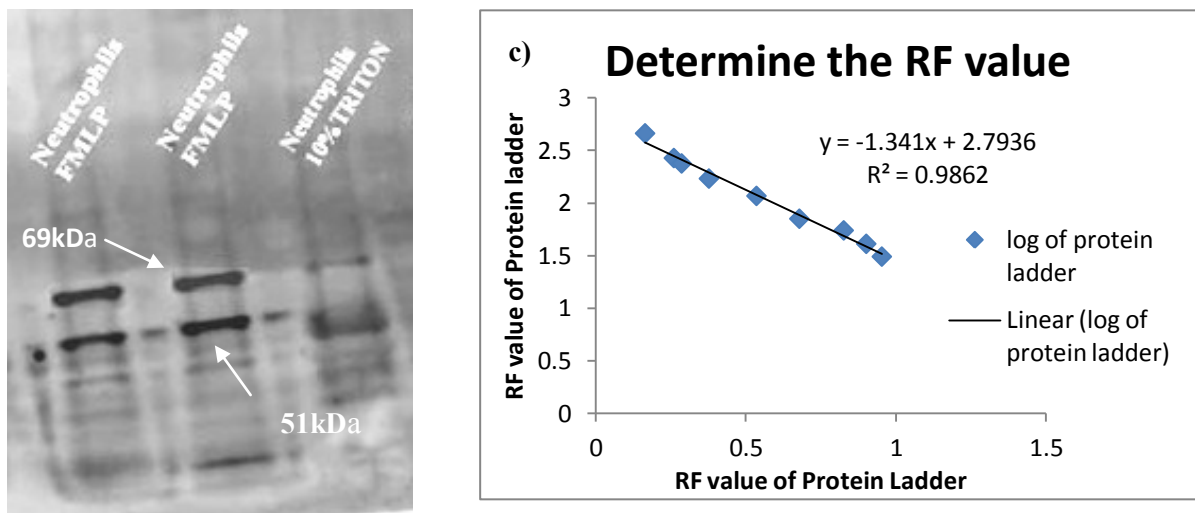
| d) Sample | Distance travel by 1st band (mm) | RF value -1st band | log value- 1st band | Estimated mol wt (kDa)-1st band | Distance travel by 2nd band (mm) | RF value- 2nd band | log value- 2nd band | Estimated mol wt(kDa) |
|---|---|---|---|---|---|---|---|---|
| Neutrophils-FMLP | 279.41 | 0.71 | 1.83 | **68.92** | 314.87 | 0.80 | 1.71 | **51.98** |
| Neutrophils-Triton-x100 | 279.03 | 0.71 | 1.83 | **68.96** | 315.23 | 0.80 | 1.70 | **51.14** |
| Neutrophils-FMLP | 280.01 | 0.71 | 1.82 | **68.43** | 314.27 | 0.80 | 1.71 | **51.48** |

Figure 5.4.3b. The neutrophils isolated from venous blood were lysed in presence of 1μM of *FMLP* and Triton x-100%, separately and the protein were separated in 3-8% tris acetate gel and transferred onto the nitrous cellulose membrane. Two protein bands with molecular weight of 69kDa and 51kDa were observed. Inspite of repeating this experimental twice, the protein bands were consistent. These two protein band observed might be the proteolytic products of ezrin. The graph c and table d show the way the molecular weight of the protein band were estimated.

## 5.4.4 Effect of Ca²⁺ and calpain dependency of ezrin proteolysis

When the membrane was permeabilised by sonication in the presence of extracellular $Ca^{2+}$, there was a dramatic change in the molecular weight of the ezrin. The 69/72kDa form of ezrin (full length) was lost and a new band at 49kDa appeared (fig 5.4.4a). A calpain cleavage product at 49kDa may correspond to fragment 3 (see table 5.4.1) a predicted calpain cleavage product (MWt= 49596.55). In the absence of extracellular $Ca^{2+}$ (ie media containing no added $Ca^{2+}$ and EGTA, 1mM), the 49Kda fragment was reduced and the full length ezrin returned (Fig5.4.4b). Similarly, incubated with ALLN (50µM), a calpain inhibitor (detail about this inhibitor are given in section 4.3.4) for 15 minutes before probe sonication, protected the 69kDa (full length) and reduced the 49kDa band. It was interesting that an additional band at 49kDa were still detected under these conditions, as was the 51kDa band. The 51KDa band may therefore be a calpain/$Ca^{2+}$ independent product. However, proteolysis of ezrin to generate a 49kDa fragment was shown to be both $Ca^{2+}$ and calpain dependent.

**Figure 5.4.4a**
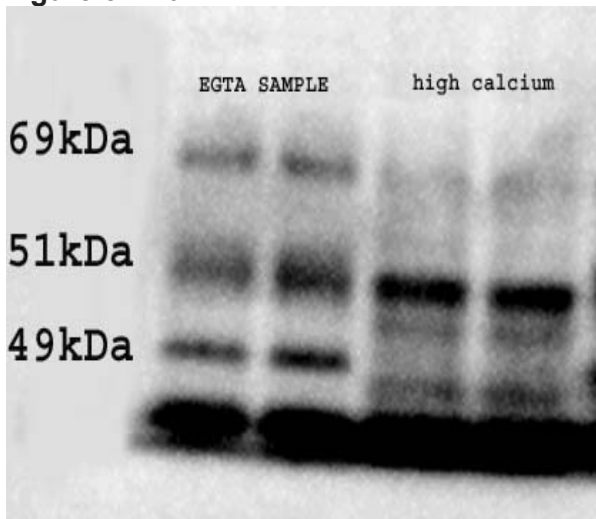
**Figure 5.4.4b**
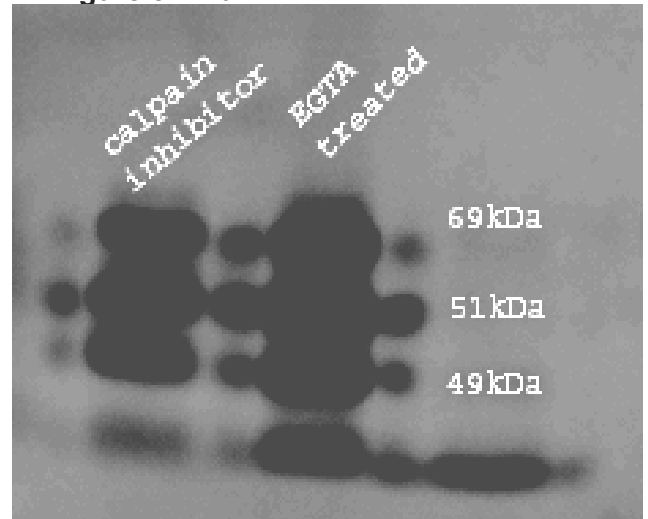


**Figure 5.4.4a and 5.4.4b.** The possible proteolytic products of ezrin. Neutrophils isolated from venous blood was homogenized in presence of cocktail mixture of high calcium (thapsigargin, ionomycine and calcium chloride), 1mM of EGTA and 50µM of calpalin inhibitor (ALLN) before lysing them by adding lysis buffer and in presence of protein inhibitor. Cells prepared in presence of high level of calcium and only one protein band with molecular weight of 51kDa while the sample prepared in absence of calcium (EGTA) and prepared in presence of calpain inhibitor had protein bands with molecular weight of 69kDa band and 49kDa, in addition to 51kDa. The results obtained were consistent.

**Log of protein ladder**

$y = -1.4267x + 2.886$
$R^2 = 0.9999$

◆ log of protein ladder

—— Linear (log of protein ladder)
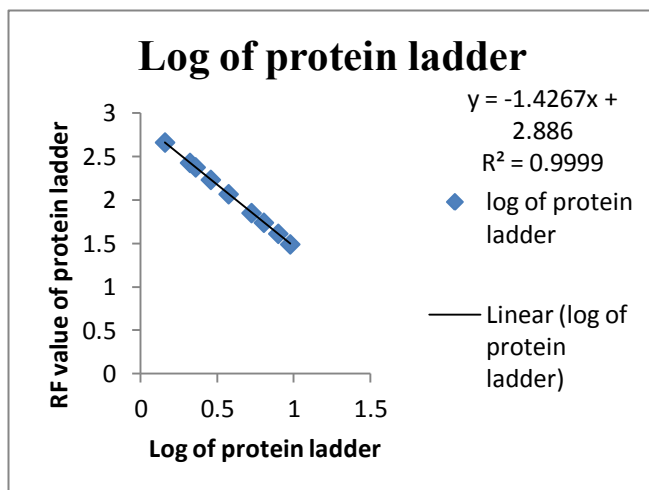
**The graph b and table c** shows the method used to determine the molecular weight of the protein band observed when probed for ezrin .

| Samples | Distance traveld (mm) | RF value | Log value | Estimated molecular weight (kDa) |
|---|---|---|---|---|
| **Sonicated- EGTA** | | | | |
| 1st band | 327.64 | 0.73 | 1.84 | **69.23** |
| 2nd band | 368.63 | 0.82 | 1.70 | **51.22** |
| 3rd band | 372.71 | 0.83 | 1.69 | **49.71** |
| **Sonicated - cocktail high Ca2+** | | | | |
| 1st band | *** | *** | *** | **\*\*\*** |
| 2nd band | 367.03 | 0.82 | 1.71 | **51.83** |
| 3rd band | *** | *** | *** | **\*\*\*** |
| **Sonicated-calpain inhibitor** | | | | |
| 1st band | 328.03 | 0.73 | 1.83 | **69.03** |
| 2nd band | 367.01 | 0.82 | 1.71 | **51.83** |
| 3rd band | 371.07 | 0.82 | 1.70 | **50.68** |

**Full lenghth ezrin-69kDa(sonicated)**

Graph 5.4.4.i



**partially cleaved ezrin-51kDa**
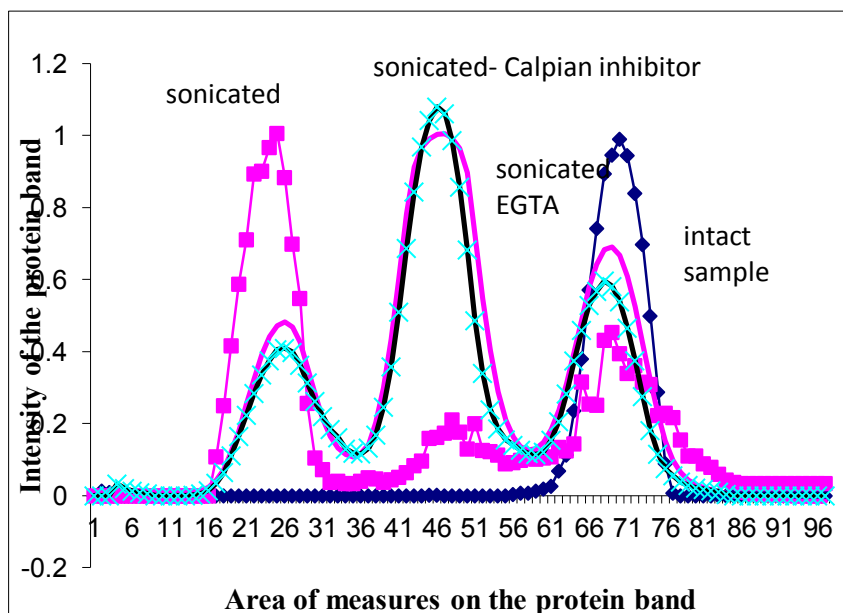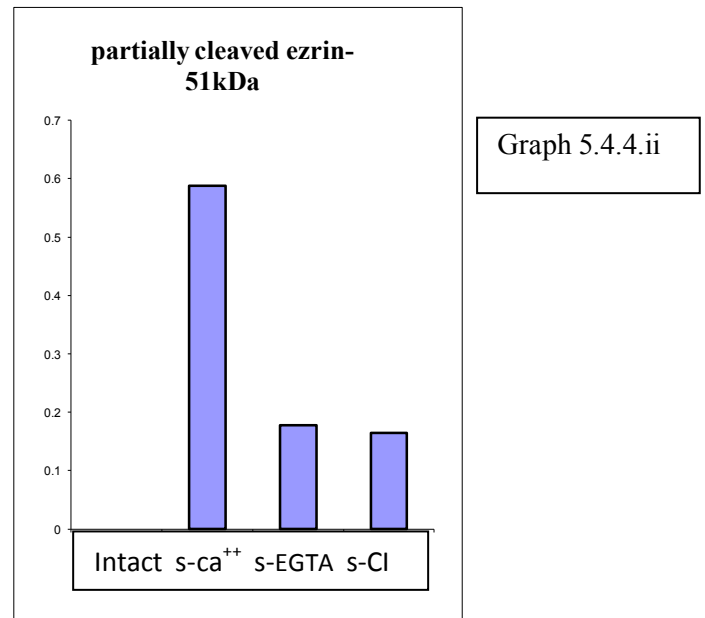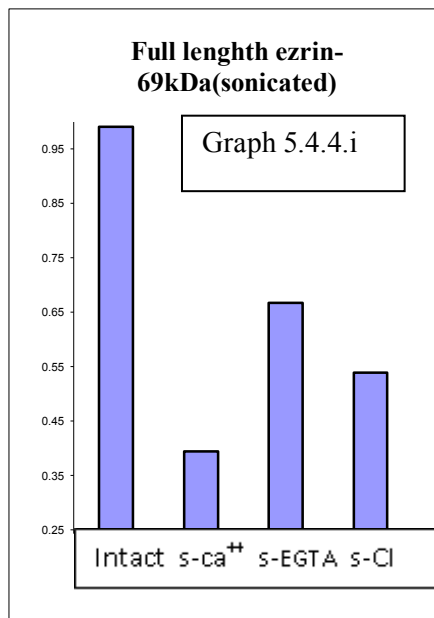
Graph 5.4.4.ii



Graph 5.4.4.iii

**Graph 5.4.4.i, ii, & iii.** Using image J the intensity of possible proteolytic product of ezrin (69kDa, 51kDa & 49KDa) was measured. It is clear from the graph that the fully cleaved ezrin (49kDa) and full length ezrin (69kDa) are unique to neutrophils prepared in presence of calpain and absence of calcium (EGTA) while the partially cleaved ezrin product (51kDa) were not affected by presence of calcium or calpain inhibitor. Intact (non sonicated samples), S-Ca$^{++}$ (samples prepared in cocktail mixture of high calcium and sonicated), S-EGTA (samples prepared in presence of EGTA and sonicated), S-CI (samples preapared in presences of calpain inhibitor and sonicated).

### 5.4.5  Proteolysis of ezrin in migrated neutrophils

In order to find whether similar proteolytic product of ezrin are detectable in extravasated neutrophils, both neutrophils which had crossed an endothelial barrier experimentally *(in vitro)* and physiologically (oral extravasated neutrophils) were investigated.  When probed for ezrin, as before, non-migrated neutrophils had two separate protein bands with molecular weight of 72kDa and 55kDa, while neutrophils which had crossed the endothelial monolayer *in vitro* had lost the 72kDa protein band and had only one protein band detectable with molecular weight of 55kDa (fig 5.4.5a). This gives strong evidence that ezrin had undergone extensive proteolysis as the neutrophils extravasted.  The absence of the full length ezrin was a striking finding and larger than could be produced pharmacologically.

Oral neutrophils which has extravasted under physiological condition, were also examined. Although the number of cell recovered from the oral cavity was low , when probed for ezrin, again no full length ezrin was detectable in extravasted neutrophils and only the protein fragment at  55kDa was observed  (fig 5.4.5b).

**Figure 5.4.5a. Estimating the molecular weight of ezrin in extravasated neutrophils-** *ex vivo*

**1)**



55 kDa

72 kDa

Tracking Dye

12 minutes exposer time

**2)** **Determine the RF value**



y = -1.5603x + 2.9795
R² = 0.992

log of hwm

Linear (log of hwm)
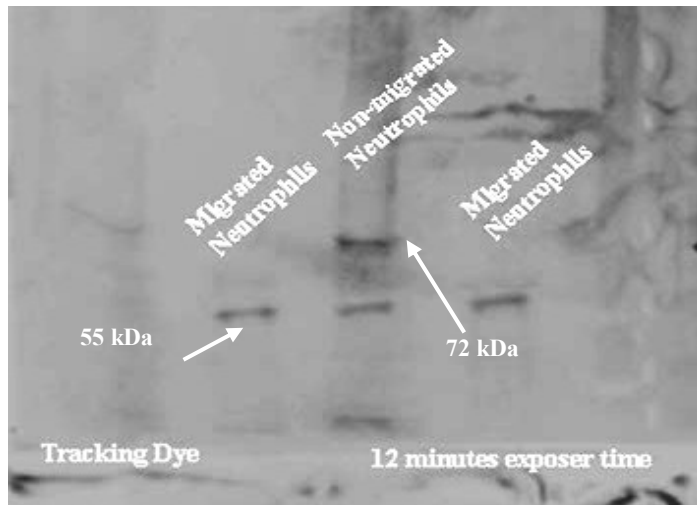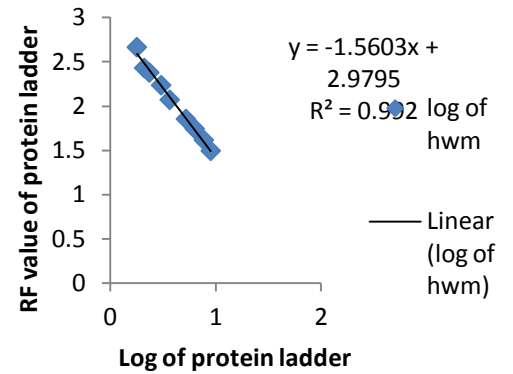
**3)**

| Sample | Distance travel (mm) | RF value | Log value | Estimated mol wt (kDa) |
|---|---|---|---|---|
| **Non-migrated Neutrophils** 1st protein band | 307 | 0.718 | 1.85 | **72.06** |
| 2nd protein band | 338.01 | 0.79 | 1.74 | **55.04** |
| **Migrated Neutrophils** 1st band | *** | *** | *** | ****** |
| 2nd band | 334.01 | 0.79 | 1.74 | **55.16** |

Neutrophils isolated from the venous blood were allowed to cross a monolayer of endothelial cells (HECV cells), grown on a sterile insert by applying a concentration gradient set by 1μM of *FMLP*. The migrated neutrophils were collected in suspension ($1 \times 10^5$ cells/ml) and protein extracted from these cells were separated and transferred in to a nitrocellulose membrane and run along with the non-migrated neutrophils ($1 \times 10^5$ cells/ml). This experiment was repeated twice. Graph2 and table 3 shows the way the molecular weight of protein band were estimated.

**Figure 5.4.5.b. Estimating the molecular weight of ezrin in extravasated neutrophils-**

*in vivo* **salivary neutrophils.** **1)**
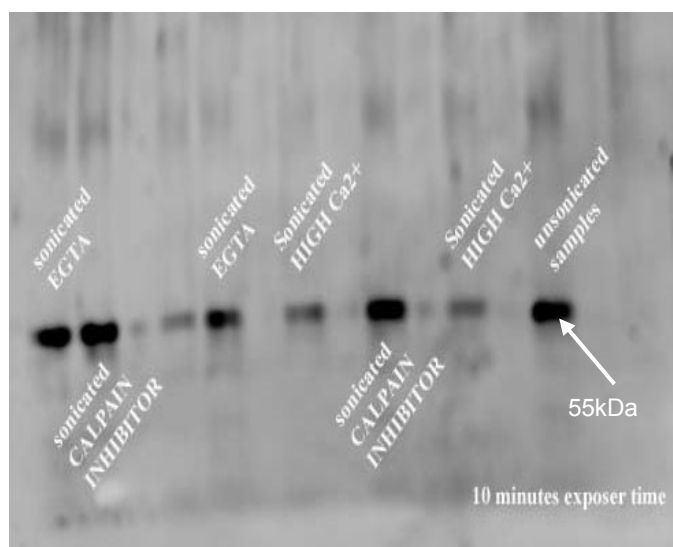
**2)**
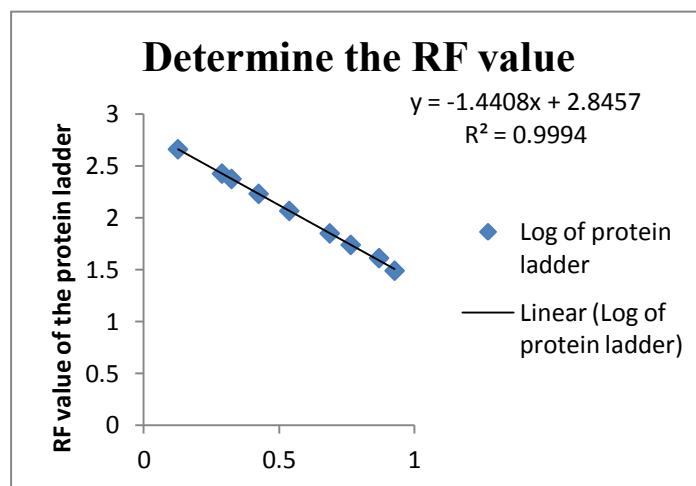


| Samples | Distance travel (mm) | Rf value | Log value | Estimated mol wt (kDa) |
|---|---|---|---|---|
| Sonicated-EGTA | 331.01 | 0.76 | 1.73 | **54.90** |
| Sonicated-HIGH Ca2+ | 330.04 | 0.76 | 1.74 | **55.31** |
| Unsonicated | 329.07 | 0.76 | 1.74 | **55.72** |
| Sonicated-calpain inhibitor | 332.09 | 0.76 | 1.73 | **54.86** |

**Figure 5.4.4b** (1) The protein extracted from neutrophils ($1x10^5$cells/ml) isolated from saliva and sonicated in thepresence of 1mM of EGTA, calpain inhibitor(ALLN), cocktail mixture of thaspigargin, ionomycin and $CaCl_2$ (sonication was used as an external stimuli) and few neutrophils were isolated with no external stimuli (unsonicated). The proteins were separated using 3-8% tris-acetate gel and they were transferred onto a nitrocellulose membrane. When probed for ezrin, irrespective of the conditions under which the neutrophils were isolated, a protein band of 55kDa was observed consistently, this gave evidence that one of the proteolytic products has a molecular weight of 55kDa and this process is irreversible. Graph 2 and the Table 3 shows the way the molecular weight of the protein bands was estimated. To make ensure the reproducible nature of the experiment, this experiment was repeated three times with cells isolated from different individuals. The result obtained were consistent and the protein band was detected each time at 55kDa.

## 5.4.6 Identification of ezrin fragments

Although the loss of full length ezrin was a striking finding, and suggestive of extensive proteolysis under milder conditions, two fragments were commonly observed, one at 55kDa and the other at 49kDa. In order to investigate whether these were genuinely ezrin fragments, peptide fingerprinting was attempted. Mass spectrum analysis of the initiate uncleved fragment at 72kDa was always contaminated with myeloperoxidase (MPO, MWt 83kDa), the major protein in neutrophils accounting for nearly 10% of all its protein. This made it difficult to assign particular small peptides in the other bands to those belonging to ezrin. However, several peptides were generated which did not belong to MPO and could be used to confirm that the 49kDa fragment was from ezrin (fig 5.4.6). It was concluded that the 49kDa band was genuinely of ezin orgin.

**Figure 5.4.6a**. **3-8% gel from which plugs were picked for mass spectrometry analysis.**
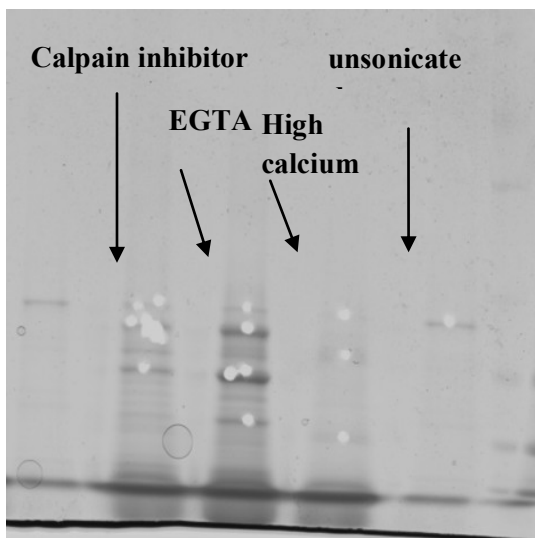


**Figure 5.4.6a** The 3-8% tris acetate gel from which spots were picked and trypsin digestion was carried out, the samples picked were taken for mass spectrum analysis

**Table 5.4.6b.** Sequences detected by agreement between predicted trypsin fragment and weight of fragment generated

| Sequence | Trypsin digested fragment | Fragment size detected (Da) |
|---|---|---|
| EELMLR | 790.4127 | 790.41345 |
| VMDQHK | 757.3661 | 757.38007 |
| FGDYNK | 743.3359 | 743.37567 |
| SGYLSSER | 898.4265 | 898.47327 |
| LFFLQVK | 894.5447 | 894.43652 |
| QQLETEK | 875.4621 | 875.45618 |
| DQWEDR | 848.3533 | 848.46552 |
| NISFNDK | 837.4101 | 837.43054 |
| AQEEAER | 832.3795 | 832.43097 |
| ALQLEEER | 987.5105 | 987.49408 |
| LQDYEEK | 924.4309 | 924.47821 |
| EAQDDLVK | 917.4574 | 917.45172 |
| | 1720.8331 | Not Found |
| | 1651.8173 | Not Found |
| | 1493.6914 | Not Found |
| | 1316.6878 | Not Found |
| APDFVFYAPR | 1182.5942 | 1182.58716 |
| IQVWHAEHR | 1175.6068 | 1175.54846 |

**5.4.6c. Frequences detected shown on the predicted 49kDa fragment (sonicated in high Ca$^{2+}$).**

KENPLQFKFRAKFYPEDVAEELIQDITQK<mark>LFFLQVK</mark>EGILSDEIYCPPETAVLLGSYAVQAK<mark>F</mark>
<mark>GDYNK</mark>EVHK<mark>SGYLSSER</mark>LIPQR<mark>VMDQHK</mark>LTR<mark>DQWEDRIQVWHAEHR</mark>GMLKDNAMLEYLKI
AQDLEMYGINYFEIKNKKGTDLWLGVDALGLNIYEKDDKLTPKIGFPWSEIR<mark>NISFNDK</mark>KFVI
KPIDKK<mark>APDFVFYAPR</mark>LRINKRILQLCMGNHELYMRRRKPDTIEVQQMKAQAREEKHQKQL
ER<mark>QQLETEK</mark>KRRETVEREKEQMMREK<mark>EELMLRLQDYEEK</mark>TKKAERELSEQIQR<mark>ALQLEEE</mark>
<mark>R</mark>KR<mark>AQEEAER</mark>LEADRMAALRAKEELERQAVDQIKSQEQLAAELAEYTAKIALLEEARRRKE
DEVEEWQHRAK<mark>EAQDDLVK</mark>TKEELHLVMTAPPPPPPPVYEPVSYHVQE

## 5.5  Discussion

The data in this chapter shows that ezrin in neutrophils is susceptible to proteolytic cleavage by high Ca$^{2+}$ in a manner which is dependent on calpain activity. These artificial ways of activating cytosolic calpain were less effective than physiologically activating neutrophil to cross endothelial monolayers. Under these conditions, virtual no full length ezrin was detectable (72kDa).  This was dramatic finding which points strongly to a link between ezrin cleavage and the process of neutrophil transendothelial migration. Ezrin was detectable in neutrophils as a protein with a molecular weight of 69-72kDa.  69kDa is the weight of the entire amino acid sequence of ezrin. On stimulating these cells in presence of physiological stimuli (FMLP) or experimental procedures, this band is reduced and bands at 49kDa and 51kDa were observed. In order to find evidence whether these two protein band are the proteolytic produces of ezrin, isolating the neutrophils in a solution with altered calcium level (EGTA and calpain inhibitor), produced three protein bands with molecular weight of 69kDa, 51kDa and 49kDa, which were not observed in neutrophils isolated in presence of high calcium level. This gave evidence that the three protein bands might be

the proteolytic products of ezrin and were sensitivity to the presence of calcium and calpain. To find evidence of such proteolysis in extravasted neutrophils, probing the neutrophils from saliva for ezrin, a protein band of molecular weight of 55kDa was noted moreover even by altering the level of calcium in these neutrophil samples, 55kDa remains the same and no other additional bands were observed. This gave evidence that proteolysis of ezrin might be a irreversible reaction under physiological conditon. However, on probing the migrated neutrophils under experimental condition (tranendothelial migration assay), the non-migrated neutrophils had two ezrin protein band with molecular weight of 72kDa and 55kDa, while the migrated neutrophils had only one ezrin protein band (55kDa). This gave further evidence that ezrin undergoes proteolysis in presence of calcium and calpain and produce two proteolytic products and this proteolysis process is irreverisble in nature under physiological conditon.

The cleavage of ezrin may explain the release of ezrin from the plasma membrane reported earlier in chapter 4.

# CHAPTER 6

## Dynamic change in ezrin imaged during cell activation

## 6.1   Introduction

In the previous chapters, it was shown that ezrin relocates away from the cell membrane into the cytosol as the neutrophils changed shape and after transendothelial migration, both under physiological and experimental condition. This was shown to also occur during changes in the cytosolic level of calcium. This may result from a proteolytic effect of the calcium-activated enzyme, calpain. In order to further study the relocation process dynamically, a neutrophil-similar cell model was used. RAW cells were transfected with GFP-tagged constructs of ezrin (pEGFP-N1 vector and pHJ421), so that its subcellular location could be followed. RAW cells were selected as these cells had similar functional qualities to neutrophils, but were capable of expressing transfected protein, unlike neutrophils.

### 6.1.1   GFP tagged ezrin plasmid

#### 6.1.1.1     pHJ421

In order to achieve a useful cell model, a plasmid containing ezrin-GFP was required. pHJ421 is the plasmid for ezrin with insert size of 1758  tagged with GFP at the C-terminal of ezrin. It is tranducted into a mammalian expression vector backbone (pEGFP-N1) without insert size of 4700. Its cloning sites are 5'.EcoRI and at the SalI. The sequencing primer is GTGCACAAGTCTGGGTAC, the entire plasmid sequence is given below. The plasmid is resistance to kanamycin and the growth strain is DH5α, which produce high copies of plasmid. The selectable marker for this plasmid is neomycin. This plasmid was created and used by Stephen Shaw and has been used by Hao et al. (2010). To determine the possible mechanism involved in activation of ezrin in lymphocytes.

_____
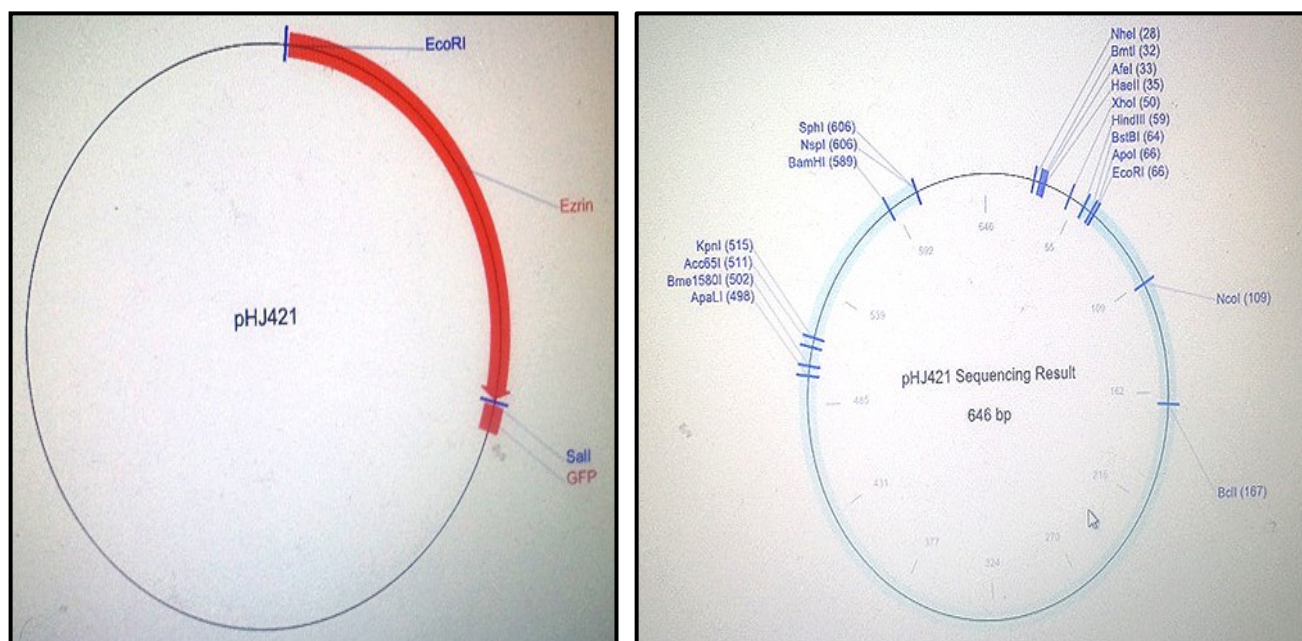
Figure 6.1.1a. Schematic diagram of ezrin plasmid pHJ421. This diagram also shows the sites where the ezrin sequence, GFP and *E.coli* vector were included. This information was obtained from Addgene, USA. Figure 6.1.1b. schematic diagram showing the restriction digestion enzyme band. These enzymes were used to cut the ezrin plasmid. This picture and the information was obtained from website of Addgene, USA (www.addgene.org/)

## Commonly Used Primers

| | |
|---|---|
| CMV Forward | CGCAAATGGGCGGTAGGCGTG (Invitrogen)<br>Human CMV immediate early promoter, forward primer |
| LKO.1 5' | GACTATCATATGCTTACCGT (Weinberg Lab)<br>Human U6 promoter, forward primer |
| LucNrev | CCTTATGCAGTTGCTCTCC<br>5' end of luciferase, reverse primer |
| M13 Reverse | CAGGAAACAGCTATGAC<br>In lacZ gene |
| MSCV | CCCTTGAACCTCCTCGTTCGACC (BD Biosciences)<br>Murine stem cell virus, forward primer |
| pBABE 5' | CTTTATCCAGCCCTCAC (Weinberg Lab)<br>Psi packaging signal, 5' of MCS in pBABE vectors, forward primer |
| pGEX 5' | GGGCTGGCAAGCCACGTTTGGTG<br>3' end of glutathione-S-transferase, forward primer |
| SP6 | ATTTAGGTGACACTATAG<br>SP6 promoter, forward primer |
| T3 | GCAATTAACCCTCACTAAAGG<br>T3 promoter, forward primer |
| T7 | TAATACGACTCACTATAGGG<br>T7 promoter, forward primer |

_____

Chapter 6

```
LOCUS      pHJ421 Sequencing Result     646 bp

DEFINITION  pHJ421 Sequencing Result
 ORGANISM  other sequences; artificial sequences; vectors.
 FEATURES          Location/Qualifiers
 source       1..646
          /organism="pHJ421 Sequencing Result"
          /mol_type="other DNA"
   CDS        complement(57..605)
          /label="ORF frame 3"
/translation="MPHLDPVLPLVPGKFVLVHHSLRDQPLRAEVPRLVHFFVVVPKL
GLHSVGPQEHGSLRGAVDLIAKDSFLHLEEEKFLGDVLDELLSHIFRVELGPELELEGILLPDLLGRHLLIQLQPG
RKSFIIHIVEAKVPHFPEADSLYHLIKKLFSSCIWLDCKL QLCIHGGNSDIDWFRHFREFEA*"


1    GAGCTGGTTT AGTGAACCGT CAGATCCGCT AGCGCTACCG GACTCAGATC 50
51   TCGAGCTCAA GCTTCGAATT CCCGAAAATG CCGAAACCAA TCAATGTCCG 100
101 AGTTACCACC ATGGATGCAG AGCTGGAGTT TGCAATCCAG CCAAATACAA 150
151 CTGGAAAACA GCTTTTTGAT CAGGTGGTAA AGACTATCGG CCTCCGGGAA 200
201 GTGTGGTACT TTGGCCTCCA CTATGTGGAT AATAAAGGAT TTCCTACCTG 250
251 GCTGAAGCTG GATAAGAAGG TGTCTGCCCA GGAGGTCAGG AAGGAGAATC 300
301 CCCTCCAGTT CAAGTTCCGG GCCAAGTTCT ACCCTGAAGA TGTGGCTGAG 350
351 GAGCTCATCC AGGACATCAC CCAGAAACTT TTCTTCCTCC AAGTGAAGGA 400
401 AGGAATCCTT AGCGATGAGA TCTACTGCCC CCCTGAGACT GCCGTGCTCT 450
451 TGGGGTCCTA CGCTGTGCAG GCCAAGTTTG GGGACTACAA CAAAGAAGTG 500
501 CACAAGTCTG GGTACCTCAG CTCTGAGCGG CTGATCCCTC AAAGAGTGAT 550
551 GGACCAGCAC AAACTTACCA GGGACCAGTG GGAGGACCGG ATCCAGGTGT 600
601 GGCATGCGGA ACACCGTGGG ATGCTCAAAG ATAATGCTAT GTTGGA      646
```

## 6.1.1.2 ₚEGFP-N1 vector

pEGFP-N1 encodes a red-shifted variant of wild-type GFP, which has been optimized for
brighter fluorescence and higher expression in mammalian cells. Excitation maximum =
488nm; emission maximum=507nm.). pEGFP-N1 encodes the GFPmut1 variant which
contains the double-amino-acid substitution of Phe-64 to Leu and Ser-65 to Thr. The
coding sequence of the EGFP gene contains more than 190 silent base changes which
correspond to human codon-usage preferences. Sequences flanking EGFP have been
converted to a Kozak consensus translation initiation site to further increase the

translation efficiency in eukaryotic cells. The MCS in pEGFP-N1 is between the immediate early promoter of CMV (PCMV IE) and the EGFP coding sequences. Genes cloned into the MCS will be expressed as fusions to the N-terminus of EGFP, if they are in the same reading frame, as EGFP and there are no intervening stop codons. SV40 polyadenylation signals downstream of the EGFP gene direct proper processing of the 3' end of the EGFP mRNA. The vector backbone also contains an SV40 origin for replication in mammalian cells expressing the SV40 T antigen. A neomycin-resistance cassette (Neor), consisting of the SV40 early promoter, the neomycin/kanamycin resistance gene of Tn5 and polyadenylation signals from the Herpes simplex virus thymidine kinase (HSV TK) gene, allows stably transfected eukaryotic cells to be selected using G418. A bacterial promoter upstream of this cassette expresses kanamycin resistance in *E. coli*. The pEGFP-N1 backbone also provides a pUC origin of replication for propagation in *E. coli* and an f1 origin for single-stranded DNA production. This vector was used by Hao et al. (2010), in order to define the mechanisms controlling the disassembly of ezrin/radixin/moesin (ERM) proteins in lymphocytes.
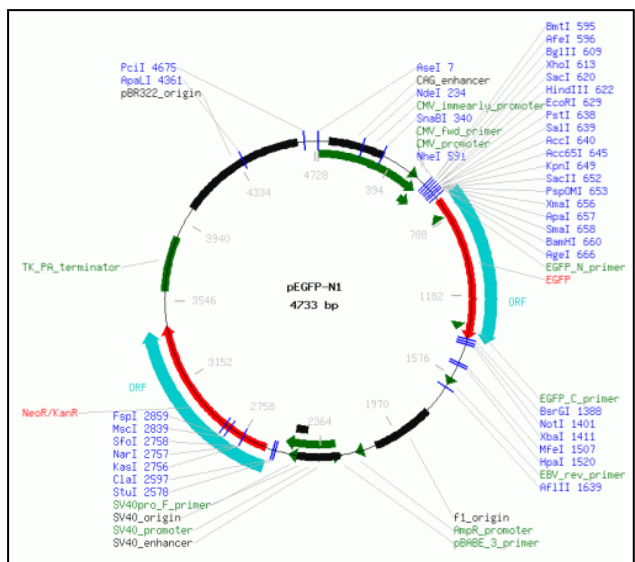


**Figure 6.1. Restriction map and multiple cloning site (MCS) of pEGFP-N1 vector.**
The figure shows the various restriction sites which are unique for this plasmid. All restriction sites shown are unique. The Not I site follows the EGFP stop codon. The Xba I site (*) is methylated in the DNA provided by BD. These details are obtained by Biosciences Clontech. This plasmid for was stable transfected with CMV as its promoter. The plasmid size is 4700bp, CMV-F and EGFP-N as sequencing primer (5'd[CGTCGCCGTCCAGCTCGACCAG]3'. The plasmid can be quantified using kanamycin and neomycin to avoid any bacterial contamination. Further information about this plasmid can be obtained from BD Biosciences Clontech Protocol # PT3027-5 GenBank Accession #U55762 (addgene) Catalog #6085-1. This plasmid was amplified in *E.coli* .

```
591      601      611          621          631          641          651          661
 .        .        .            .            .            .            .            .
G CTA GCG CTA CCG GAC TCA GAT CTC GAG CTC AAG CTT CGA ATT CTG CAG TCG ACG GTA CCG
                          .                        EGFP
                         671
CGG GCC CGG GAT CCA CCG GTC GCC ACC ATG GTG
```

## 6.2 Aims

The aim of the work in this chapter is to establish a model by which the dynamic of ezrin translocation can be studied and specifically to:-

1. Investigated the effect of elevation of cytosolic calcium on the subcellular location of ezrin.

2. To evaluate the change in the subcellular location of ezrin during change in focal dimension of plasma membrane.

## 6.3  Materials and Methods

### 6.3.1 Materials

**1) Confocal microscopy**

Confocal imaging of cells was taken using a Leica SP2 confocal microscope, using a x64 oil immersion objective. Fura red calcium indicator and green fluorescent proteins were excited using the 488nm laser. Emission was detected at the appropriate wavelength for the fluorophore being imaged. Where more than one fluorophore was being imaged in the same sample sequential imaging techniques were employed. Sequential imaging allows for simultaneous imaging at two different wavelengths, whilst minimising interference and 'crosstalk' between the two images by recording the image for the different wavelengths sequentially between frames.

**2) Fura Red**

Fura Red™AM (Invitrogen F3020 ) is a visible light—excitable fura-2 analog that offers unique possibilities for ratiometric measurement of $Ca^{2+}$ in single cells by microphotometry, imaging or flow cytometry when used with single excitation, green-fluorescent calcium indicators. The acetoxymethyl (AM) ester form is useful for non-invasive intracellular loading.

---

The below figure (fig 6.3.1.2) shows the absorption and fluorescence emission spectra for fura red.
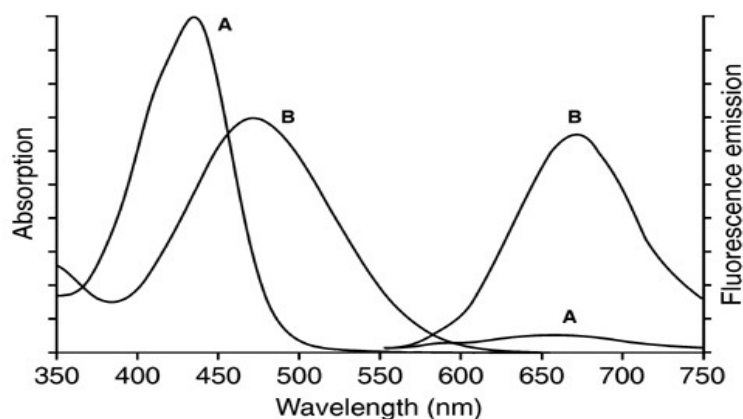


Figure 6.3.1.2. Fluorescence spectrum for Fura Red. Absorption and fluorescence emission (excited at 488nm) spectra of $Ca^{2+}$-saturated (A) and $Ca^{2+}$-free (B) Fura Red™ in pH 7.2 buffer.

Fura Red™ was loaded into the cells in an AM form using the same method described in section 2.5.4.3 for Fura2 (fig 2.5.4.3). Fura red is a non-ratiometric calcium indicator, which is excited at the same wavelength in both the calcium free and calcium bound forms. Calcium free fura red is excited by 488nm light and emits light at 650nm. Calcium bound fura red is excited at 488nm light and emits light at 650nm but at a lower intensity.(fig 2.6.1.2), Changes in cytosolic calcium concentration can be detected by the decrease in fluorescence intensity of the indicator. The calcium concentration in the cell at any given time can be calculated from the fluorescence intensity if the indicator using the following equation:

$$[Ca2+]i = Kd \times (Fmax \div F) - 1$$

Where, Fmax is the maximum fluorescence intensity of the indicator and F is the fluorescence of the indicator at any given point, relative to the minimum value of zero.

## 3) Nucleofector™ technology

A nucleofector™ from Lonza Walkersville Inc, USA, was used to transfect the GFP-tagged ezrin plasmid into the RAW cells. Nucleofector™ Technology is a highly efficient non-viral

_____

method for transfection. It is based on two components: Nucleofector™ Device that delivers unique electrical parameters which delivers the genetic material straight to the nucleus of primary cells; and  Cell Line Nucleofector™ Kits, that contain cell-type-specific Nucleofector™ Solutions (VVCA-1003 Cell Line Nucleofector® Kit V (100 RCT), which enables the  highest transfection efficiencies with lowest mortality. The electrical parameters of the Nucleofector™ are different from any other commercially available electroporation device. Each electrical setting is displayed as a distinct program which has been adapted to the requirements of a particular cell type. As the electrical settings are pre-programmed into the Nucleofector™, optimization of the electrical parameters by the user is not necessary. The programme used to transfect RAW cell was program D-023. The description about the device is given below (fig6.3.1.3).

| Cat. | AAD-1001 |
|---|---|
| Weight | 2.6 kg |
| Dimensions | 30 x 23 x 11 cm |
| Power Supply | 110 VAC +10%/-20% or 230 VAC +10%/-20% 50-60 Hz |
| Power Consumption | 20 VA/fuse 0.4 A |
| Protection | IP 22 |

Figure 6.3.1.3.  Nucleofector™ Device. Technical information and picture of the Nucleofector™ Device (Lonza Walkerville Inc, USA) used for transfection of RAW cells.

## 4) Harvesting RAW cell lines

The detailed steps followed in harvesting the RAW cells were explained in section 2.3.6 and the materials used to harvest RAW cell were listed in section  2.1.2.  A cell scrapper was used to detach the RAW cells from the tissue culture flask.

## 5) PLC inhibitor (U73122)

U73122 is an aminosteroid that is reported to act as a specific inhibitor of phospholipase C. It inhibits the hydrolysis of PPI to $IP_3$, which in turn leads to a decrease in cytosolic free

calcium. It also inhibits the coupling of G protein-phospholipase C activation, while remaining unaffected by production of cAMP. This inhibitor is also used to establish the link between phospholipase C activation and cellular $Ca^{2+}$ signalling.

## 6.3.2 Methods

### 6.3.2.1 Purification of plasmid DNA

As the plasmid pHJ421 has already seeded with in *E-coli*, in order to increase the amount of plasmid. The product was seeded in 5ml of LB medium with 50µg/µl of kanamycin. This set up was incubated at 37ºC in a shaker (200RPM) for 4-5hours. Later, 200ml of LB and 200µl of kanamycine was added in order avoid any contamination. This flask was incubated at 37ºC in a shaker (200RPM). Once the flask was confluent, the ezrin plasmid was retrived using Machery-Nagel Nucleobond R Extra Maxi kit.

### 6.3.2.2 Purification and retrieving the plasmid

Ezrin plasmid was purified using Machery-Nagel NucleobondR Maxi kit (Abgene, UK), the methods as listed by the manufacturer were followed. In brief, the bacterial cells from the LB medium were pelleted by centrifugation at 4500- 6000RPM for 15 minutes at 4ºC, to this pellet 12ml of resuspension buffer and RNAse (provided by the manufacture) was added and the pellet was resuspended gently to avoid any lump formation. In order to break the phospholipid bilayer, the protein on the surface of the membrane was denatured by adding lysis buffer (supplied along with the Maxi kit) and incubating the mix at room temperature for 5minutes. Plasmid DNA was separated from other nucleic acids and proteins through anion exchange. The solution was applied to an anion exchange column made from anion exchange resin which consisted of hydrophilic, porous silica beads with a methyl-aminoethanol (MAE) group. This functional group has an overall positive charge which means that under acidic conditions, the negatively charged phosphate backbone of

_____

the DNA binds to the resin. Large double stranded chromosomal DNA was denatured by the addition of an acidic solution to neutralise the column. In its single stranded form, chromosomal DNA will be washed from the column at a lower pH than the double stranded plasmid DNA. Increasing concentrations of salt buffer were added to the column to wash off any protein, RNA and chromosomal DNA. The more interactions that molecule can make with the resin the higher salt concentration is required to wash it off. Small nucleic acids and single stranded DNA make fewer interactions than the double stranded plasmid DNA and so are washed off at a lower pH. A high salt concentration elution buffer was then applied to the column finally to wash off the plasmid DNA. The plasmid DNA is then recovered from the supernatant by ethanol precipitation. This precipitate was then re-suspended in a buffer of double distilled water. Plasmid were digested with a mix of multicore buffer (Promega), 1µl of ECORI, 1µl of XBAL and 15 µl of double distilled water. 1µl of ezrin plasmid was added to this mixture and incubated at 37$^{\circ}$C for 1hour. In order to check plasmid integrity and cut plasmid, the plasmid was run on a 0.8% agarose gel at 100 volts for approx 45 minutes. Plasmids were quantified (0.035µg/µl) using a spectrophotometer to analyse absorbance at 260nm. Where plasmid concentration was too low, plasmids were precipitated using sodium acetate precipitation were 10% of the sample volume of 3M sodium acetate (pH 5.2) was added to the plasmid along, with double the sample volume ice cold 100% ethanol. Sample was vortexed and centrifuged for 15 minutes at maximum speed at 4$^{o}$C. The supernatant was removed carefully without disturbing the pellet and resuspended in double distilled water and the plasmid was stored at 4$^{o}$C until used.

### 6.3.2.3 Preparation of RAW cells for transfection

As RAW cells were naturally adherent, a cell scrapper was used to remove all the cells from one of the T-25 tissue culture flask, before transfecting these cells with GFP

tagged ezrin, the cells were counted using a Cellometer cell counting instruments. $1 \times 10^6$ RAW cells/ml were centrifuged at 750rpm for 10minutes and to this pellet 100µl Nucleofector® Solution and 10µl of purified ezrin plasmid was added and the entire mixture of solution was transferred into a cuvette (supplied with Cell Line Nucleofector® Kit V). The cuvette was placed in the Nucleofector® device and program D-023 was selected (Nucleofector® Solution and programme with the highest efficiency and lowest mortality). Once the trasfection was completed, 500µl of fresh warm DMEM medium was added immediately to the cuvette and with a sterile plastic pipettes (Cell Line Nucleofector® Kit V), the transfected cells were added into a sterile glass-bottomed petridish which has pre-incubated at 37°C with 2ml of fresh DMEM medium. The transfected cells were then incubated at 37°C for 4-6 hours, after which the entire medium was replaced with 1000µl of fresh DMEM medium, containing 1mM of Fura Red™. After incubation at 37°C for 45 minutes, excess Fura Red™ was removed by washing with DMEM medium and the transfected cells were kept on a heating staged (37°C)  and viewed under a confocal microscope. The exitation wavelength used for the pHJ421 and Fura Red™ are explained in section 6.3.1.


## 6.3.2.4  Altering the calcium level

Ionophore increases intracellular calcium by creating artificial calcium channels in the plasma membrane which allows calcium to enter the cell. Thapsigargin increases intracellular calcium by inhibiting the CaATPase on the sarcoplasmic and endoplasmic reticulum. This increases intracellular calcium by stopping the cell from pumping calcium from the cytoplasm into the intracellular calcium stores. Depletion of calcium from the intracellular stores then causes the plasma membrane calcium channels to open, causing further calcium influx. A cocktail mixture of ionophore, thapsigargin and calcium chloride was used to study the effect of calcium on the subcellular location of ezrin. Cells were then

treated with 19µM ionophore, 19µM thapsigargin and 26mM CaCl$_2$ was added 50:50 to their medium bathing the cells, so that the final concentration of CaCl$_2$ in the medium was 13mM to further increase the intracellular calcium. Fura Red™ was used to quantify the change in intracellular calcium levels.

### 6.3.2.5 Opsonization of zymosan particles with mouse serum

1mg of zymosan powder was mixed in 50µl of krebs buffer and to this, 50µl of mouse serum was added and the setup was left in the incubator at 37°C for 30 minutes to enable opsonisation to take place. Excess serum was removed by repeatedly centrifuging the sample at 2000rpm for 10 minutes and resuspending in krebs buffer until the supernatant was clear (approximately 3 spins). The final pellet was resuspended in 500µl of krebs buffer and kept at -20°C until further use.

## 6.4   Results

### 6.4.1   Change in cytosolic calcium levels in RAW cells

Before evaluating the effect of Ca$^{2+}$ on the subcellular position of ezrin, the Ca$^{2+}$ signal in RAW cells was determined to make sure that these cells can produce Ca$^{2+}$ signals with the stimulating cocktail (ionomycine and thapsigargin). RAW cells which were cultured in T-25 tissue culture flasks were detached using a sterile cell scrapper and the number of RAW cells counted by Cellometer. 1x10$^6$cell/ml were added into a glass-bottomed sterile petri dish in 2ml of pre-incubated (37°C, 5% CO$_2$) DMEM medium. This set was left in the incubator for 4-6 hours at 37ºC, before adding the calcium indicator (Fura Red™), the dead and non-adherent RAW cells were removed by washing the petri dish with sterile DMEM medium. 1µM of Fura Red was added and the petridish was incubated at 37°C for 45minutes. Using a confocal microscope, a field of well adhered

RAW cells was selected; the DMEM medium from the petri dish was removed and replaced by 1ml of fresh DMEM medium. Whilst recording, the cocktail mixture of ionophore, thapsigargin and $CaCl_2$ was added to the cells and the change in fluorescence intensity of Fura Red was used to evaluate the calcium signalling in RAW cells. The entire experiment was carried out by confocal microscopy (Fura Red excited using 488nm laser). The fig 6.4.1a shows the recorded calcium signal in RAW cells measured using Fura Red. To test the reproducibility of this calcium signal in these cells, this experimental set up was repeated three times and calcium signals were measured with Fura Red and  also with Fluo 4 (fig 6.4.1b).The calcium signal was observed and recorded consistently.

_____

**Figure 6.4.1.a. Measurement of calcium signal in RAW cells using Fura Red as indicator.**
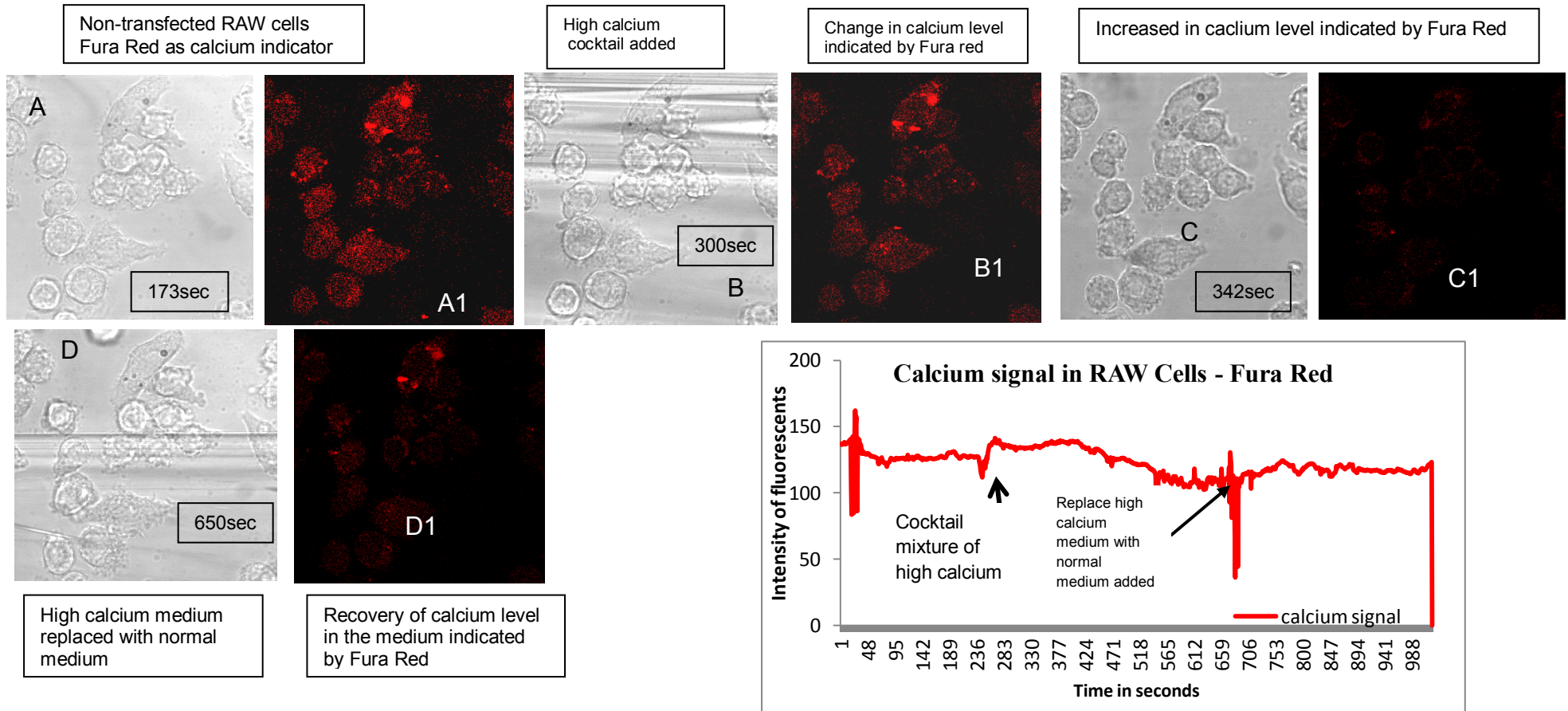


The above sequential images show the change in calcium level following calcium altering stimulation. RAW cells were grown on a glass bottomed petri dish and incubated for 45minutes with 1µM Fura Red at 37°C (fig A & A1). Addition of a cocktail mixture of 19µM ionophore, 19µM thapsigargin and finally 13mM $CaCl_2$ to these cells (time frame of 300sec, figure B & B1) resulted in a gradual increase in calcium level, indicated by decrease in the fluorescent intensity of Fura Red (time frame 342sec- 645sec, fig C & C1), when the high cocktail medium was replaced by normal medium, a slow recovery of calcium was noted as shown in fig D1. The associated graph quantifies the recorded change in fura red intensity in RAW cells. Out of 11 cells counted, 8 cells showed calcium signal which was indicated by change in fluorescence of Fura Red. This experiment indicated that the RAW cells were capable of exhibiting calcium signals as other similar phagocytic cells, like neutrophils. This gave sufficient evidence that the RAW cell model could be used as a substitute to study the change in subcellular position of ezrin during change in dimension of plasma membrane in neutrophils.

_____

Chapter 6

## Figure6.4.1b. Measurement of calcium signal in RAW cells using -Fluo 4 as indicator

Non-transfected RAW Cells
Fluo4 as calcium indicator

High calcium
cocktail added

Change in calcium level
indicated by Fluo 4

Increased in calcium level indicated by Fluo 4



A  77sec

A1

263sec  B

B1

301sec  C

C1

D  410sec

D1

High calcium medium replaced with normal medium

Recovery of calcium level in the medium indicated by Fluo4

### Calcium signal in RAW cell

Cocktail mixture of high calcium added

Replaced high calcium media with normal media

Intensity of fluorescence (fluo4)

Time (seconds)

The above sequential images shows the change in calcium level following stimulation. RAW cells were grown on a petridish and incubated for 45minutes with 1μM of Fluo4 at 37$^{\circ}$C (figA & A1). When a cocktail mixture of 19μM ionophore, 19μM thapsigargin and finally 13mM $CaCl_2$ was added to these cells (time frame of 263sec, fig B & B1), a gradual increase in calcium level was noted as indicated by increase in the fluorescent intensity of Fluo4 (time frame 301sec- 4025sec, fig C&C1). When the high cocktail medium was replaced by normal medium, a slow recovery of calcium was noted as shown in fig D1 (time frame 410sec). The associated graph quantified the change in fluo 4 intensity in RAW cells. Out of 7 cells counted, all cells showed calcium signal which was indicated by change in fluorescence of Fluo4. This experiment indicated that the RAW cells were capable of exhibiting calcium signals as other similar phagocytic cells like neutrophils. This gave sufficient evidence that a RAW cell model can be used as a substitute to study the change in subcellular position of ezrin during change in dimension of plasma membrane in neutrophils

_____

## 6.4.2 Mobility of ezrin-GFP in RAW cells

In order for ezrin-GFP to provide a useful indicator of dynamic changes in ezrin within cells, it was first important to examine its mobility within RAW cells. Obviously, if ezrin-GFP were covalent bound or immobilised in some way, it would not be possible to see dynamic changes. Local fluorescence recovery after photobleaching (FRAP) experiments were therefore performed.

Cells with peripheral staining of ezrin and well adhered to the glass petri dish were selected and laser photobleaching of one region of plasma membrane was performed (fig 6.4.2a). By approximately 65 sec, ezrin-GFP in the bleached area had been restored to levels in the non-bleached zones. However, it was found that localised photobleaching had an effect on the whole cell fluorescent signal, an effect known as FLAP (fluorescence loss after photobleaching). This indicates that molecules were free to move from within the bleaching zone (at the plasma membrane) to the cytosol. Thus, it seemed likely that recovery of fluorescence at the plasma membrane after bleaching was the result of molecular movement from the cytosol to the plasma membrane. In order to test this, ezrin fluorescence was quantified in different zones within cells during the post-bleach recovery period. It was found that the ezrin in the membrane of the non-bleached zones also declined (fig 6.4.2a). This finding indicated that ezrin at the plasma membrane was in equilibrium with the cytosolic ezrin and moved relatively freely to restore fluorescent ezrin at the bleached membrane. The association of ezrin with the plasma membrane was therefore not static, but was dynamic.

_____

**Figure 6.4.2a. Effect of photobleaching on membrane position of ezrin.**



b1 time 001 seconds
b2 time 011 seconds
b3 time 017 seconds
b4 time 018 seconds
b5 time 022 seconds
b6 time 025 seconds
b7 time 049 seconds
a1
a2
a3
a4
a5
a6
a7
b8 time 059 seconds
a8
b9 time 072 seconds
a9
b10 time 090seconds
a10
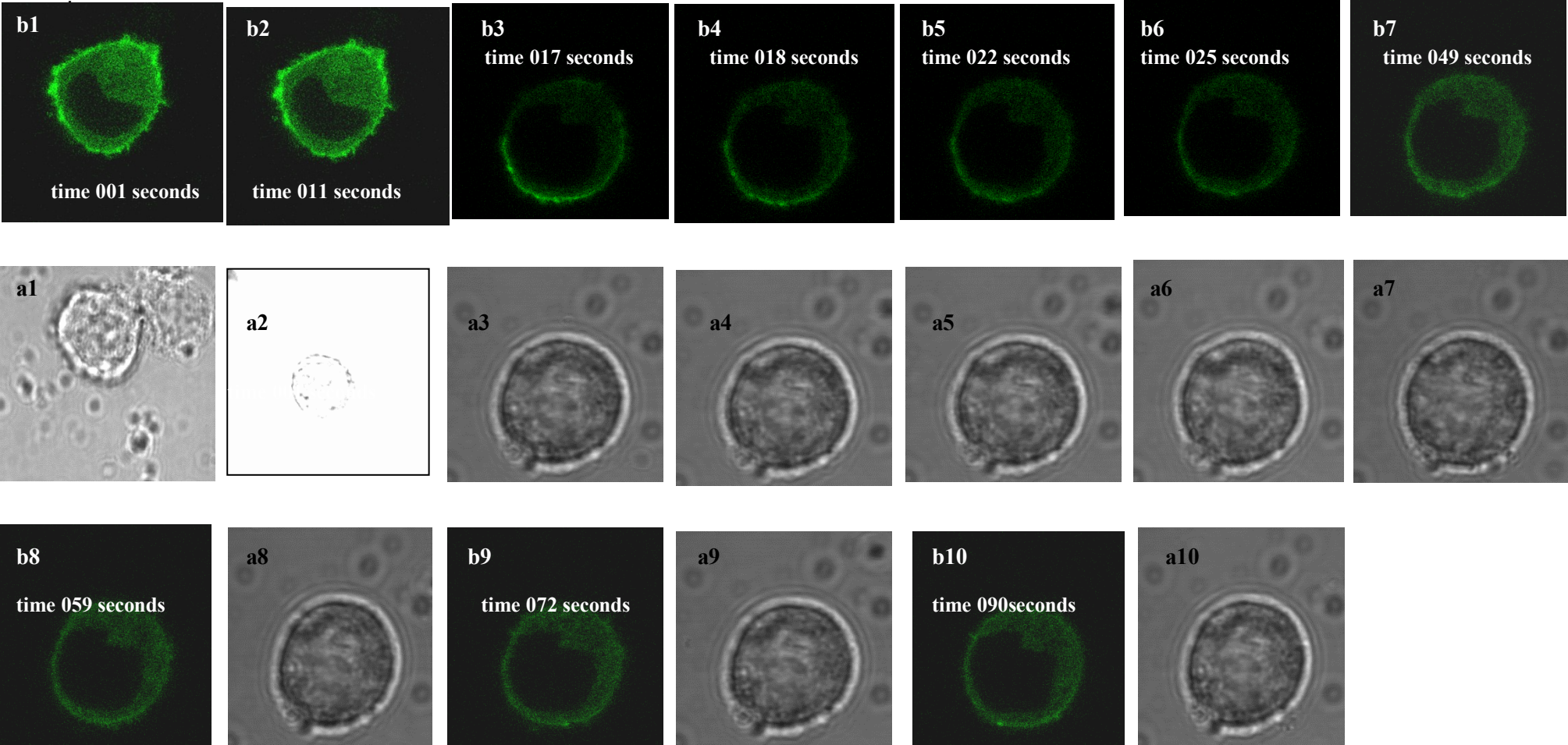
RAW cells transfected with GFP-tagged ezrin plasmid were allowed to adhere on a sterile petri dish; and cells with peripheral staining of ezrin were selected. After removing dead and unadhered cells by washing and replacing the tissue culture medium, one part of the cells was exposed to high intensity laser power for less than 1 sec(time 011 sec), which was sufficient to bleach the entire fluorescence on the exposed part of the cells. The outcome of this bleaching effect was recorded in real time. This brief period of photobleaching caused the disassociation of ezrin from the cell membrane of unbleached area of the cell which moved towards the bleached area of the cells (time 025-072sec); and this change was associated with increase in the cytosolic staining of ezrin. The process of recovery from the bleaching took approximately 62sec..

**Figure 6.4.2b. Measuring the effect of photobleaching on the subcellular position of ezrin**
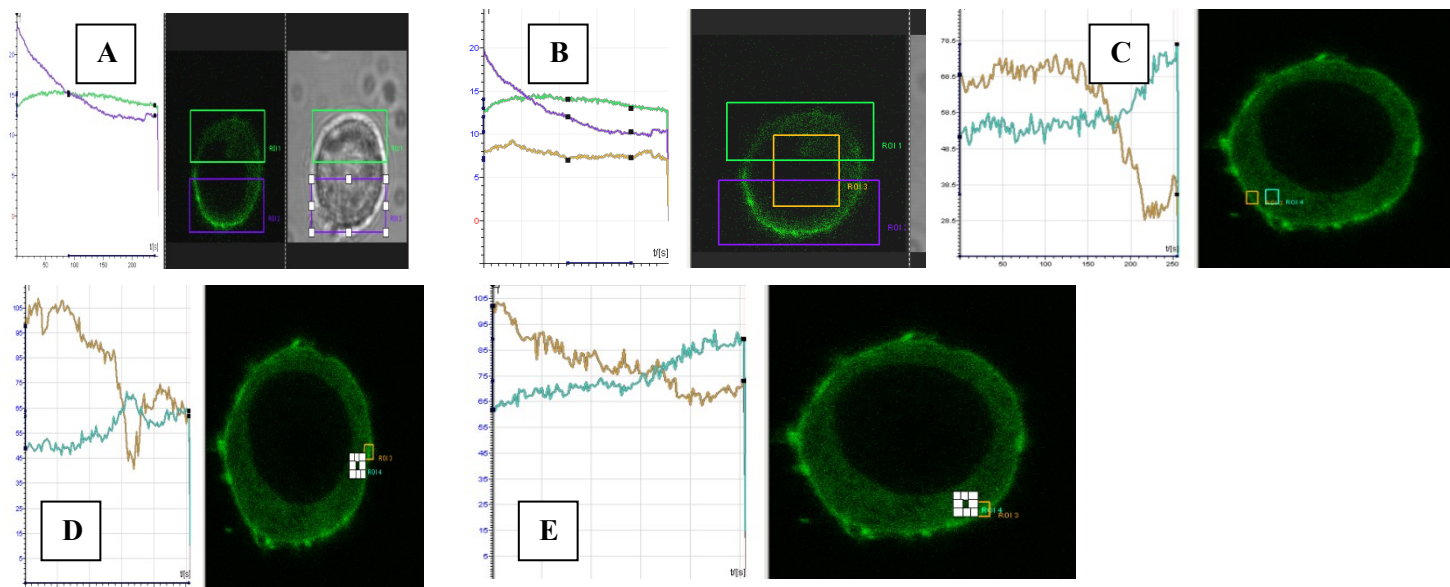


In order to measure the effect of photobleaching on the subcellular position of ezrin, Leica lite software was used to quantify the difference in the intensity of fluorescence of ezrin between the bleached and unbleached area (in both plasma membrane and cytosol A, B) The entire process of bleach recovery was measured, revealing the intensity of ezrin around the plasma membrane of the cells unbleached area gradually decreased (purple box/line) which was associated with increases in the ezrin intensity in the cytosol of the cells (green & orange, graph A and B). This finding was confirmed when the fluorscence intensity of ezrin present on the cell membrane (orange) and cytosol (blue) was compared in three different areas on the same cell during recovery phase (graph C ,D & E). This showed that as the cell recovers from the bleaching effect, there was gradual decrease in the fluorescence of ezrin on the plasma membrane associated with increase in the cytosolic staining of ezrin, this indicates that translocation of ezrin is dynamic in nature

_____

## 6.4.3 Changes in cytosolic Ca$^{2+}$ lead to changes in subcellular location of ezrin

In order to evaluate the effect of a change in the calcium concentration over the subcellular location of ezrin, RAW cells which were cultured in a T25 tissue culture flask (as discussed in section 6.3.2.3) were detached using cell scraper. 1x10$^{6}$ cells/ml of RAW cells were resuspended in transfection reagent, added into a cuvette and were transfected with GFP-tagged ezrin plasmid, as described in section 6.3.2.3 and transferred to glass bottom petri dishes. After an incubation period of 4-6hours, the DMEM medium was replaced with 1ml of fresh medium and to this medium 1µM of Fura Red was added and left in the incubator for 45minutes at 37°C. The cells which were now loaded with Fura Red and stuck to the bottom of the petri dish were mounted on a heating stage which had been set at 37°C. The remaining experimental setup was carried out using confocal microscopy and the change in cytosolic calcium level, as well as associated change in subcellular location of ezrin were recorded in real time. Before adding a 'cocktail' mixture of high calcium, all the dead and detached cells were removed by washing and replacing medium with 1ml of fresh tissue culture medium. The efficiency of transfection was noted, in nearly 60% of transfected RAW cells, the ezrin was present along the plasma membrane. Only those cells which had peripheral membrane staining of ezrin and which were loaded with Fura Red were selected for this experiment. To these cells, a 'cocktail' mixture of ionophore, thapsigargin and CaCl$_2$ was added to increase the intracellular calcium. As the cytosolic calcium level increased in these cells (indicated by decrease in the fluorescent intensity of Fura Red), there was a loss of peripheral membrane ezrin and an increase in cytosolic ezrin (fig 6.4.3a). Ezrin relocated away from the plasma membrane into the cytosol and inspite of replacing the high calcium medium with normal medium to restore cytosolic Ca$^{2+}$, this relocation of ezrin was not reversible. Since the photobleaching experiments showed that ezrin rapidly re-equilibrated to the membrane, this showed that the membrane 'binding sites' for ezrin were absent or blocked by truncated (non-fluorescent) ezrin in this area. This indicated that the change in

subcellular position of ezrin was irreversibly associated with increase in cytosolic level of calcium. Similar results were observed when the cells were treated with ionophore, thapsigargin and $CaCl_2$ separately. The subcellular shift in position of ezrin was slower than the cells treated with cocktail mixture of above mentioned reagents. These finding indicates that subcellular shift in position of ezrin was associated with increase in cytosolic calcium level (500nM to 1200nM). ImageJ software programme was used to measure and compare the difference in fluorescent intensity of ezrin between the cell membrane and cytosol as the calcium level increased within the cells. Fig6.4.3a shows the recorded sequential image showing the calcium signal and associated changes in position of ezrin and the associated graph shows the change in fluorescent intensity between the cell membrane and the cytosol as the calcium level increased (Leica confocal software was used to capture images, fig 6.4.3b).

_____

Chapter 6

**Figure 6.4.3a.Change in subcellular position of ezrin with increase in cytosolic level of calcium.**
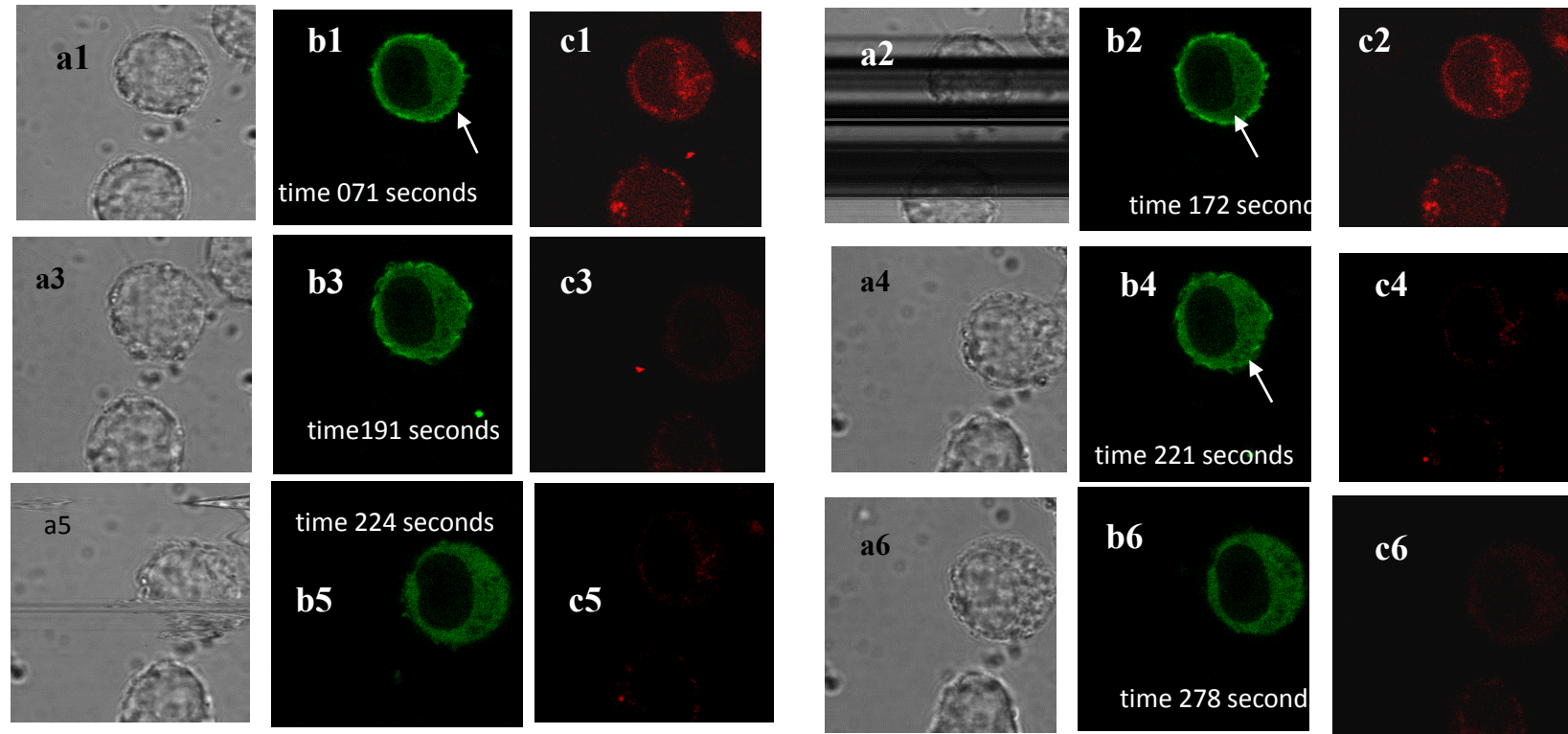


RAW cells were harvested from tissue culture flasks and $1x10^6$cell/ml were transfected with GFP-tagged Ezrin plasmid, and left in the incubator in a sterile petridish for 4-6 hours. After removing the dead and unattached cells by washing with fresh tissue culture medium, 1μM of Fura Red indicator was added to these cells and incubated at 37°C for 45minutes. The petridish with the transfected cells were mounted over a heating stage which was maintained at a temperature of 37°C under the confocal microscope. RAW cells with plasma membrane staining of ezrin and loaded with Fura Red were selected (a1, b1 & c1 time 071sec). To these cells, a 'cocktail' mixture of ionophore, thapsigargin and finally 26mM $CaCl_2$ was added 50:50 to their existing medium so that the final concentration of the $CaCl_2$ in the medium was 13mM (figure a2, b2, c2, time 172 sec).

_____

As the cytosolic calcium level increased, as indicated by decrease in the fluorescence of Fura Red (a3, b3, c3), the plasma membrane staining of ezrin was progressively lost (time 191sec to 221sec) which was associated with increase in cytosolic staining of ezrin (a4, b4, c4). Despite replacing high calcium medium with normal medium (a5,b5,c5, time 224 sec) with ordinary tissue culture medium, the subcellular change in position of ezrin away from the plasma membrane into the cytosol was irreversible (a6,b6,c6,time 278sec). This gave evidence that the change in subcellular position of ezrin was associated with increase in cytosolic level of calcium.

**Figure 6.4.3b. Measuring calcium levels associated with change in subcellular position of ezin**
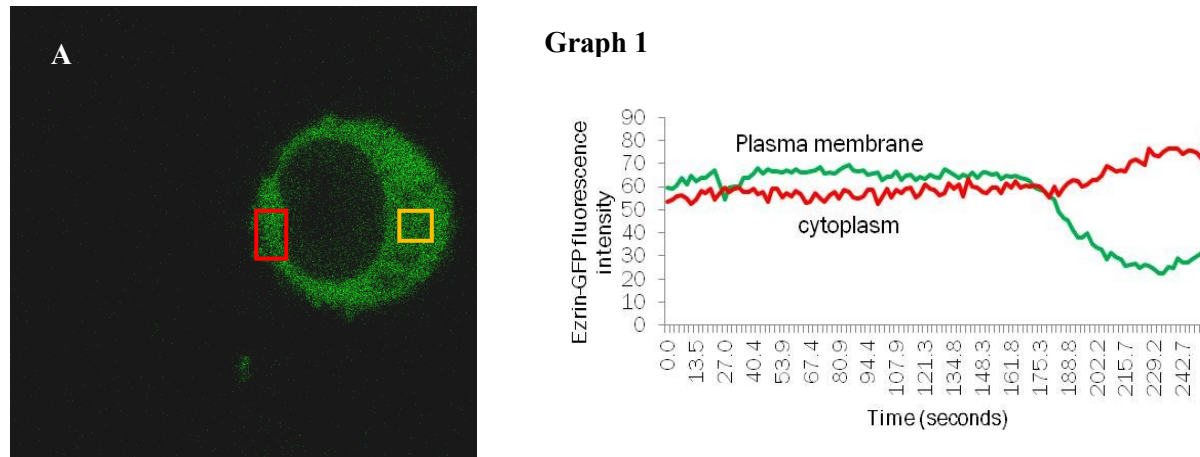


Two areas of interest on the RAW cells were marked using Leica lite software (fig A) and the difference and the change in the fluorescence of ezrin in both the plasma membrane and the cytosol was calculated over time (graph1). The cytosolic calcium concentration was quantified over time and related to this relocation of ezrin (graph 2).As the cytosolic calcium level inside the cells increased, the fluorescence of ezrin in the plasma membrane decreased (graph1) and this was associated with a corresponding increased in the fluorescence of ezrin in the cytosol (graph 1).

Chapter 6

## 6.4.4  Local expansion of the plasma membrane and relocation of ezrin

As it has established that change in calcium level causes a change in subcellular location of ezrin away from the cell membrane into the cytosol, to determine whether similar changes occur when there is local change in dimension of plasma membrane, phagocytosis was induced in transfected RAW cells. The RAW cells which were cultured in T25 tissue culture flask were detached using cell scrapper (section 6.3.2.3) and $1\times10^6$cells/ml were transfected with GFP-tagged ezrin plasmid, as described in section 6.3.2.3. Zymosan particles which were oposonized with mouse serum was used for this experiment (section 6.3.2.5). 10µl of the stock opsonized zymosan were suspended in 1ml of tissue culture medium. Before mounting these cells on heated stage (maintained at temperature of 37°C), the dead and unattached RAW cells were removed by washing and replacing the tissue culture media with 1ml of fresh normal medium and to these cells, 1µM of Fura Red calcium indicator was added and incubated at 37°C for 45minutes.  100µl of opsonized zymosan particles was added to these cells and allowed to settle down. Using a micropipette controlled by a micromanipulator (Eppendorf Injectman), one single zymosan particle was picked and positioned next to a transfected RAW cell which had peripheral staining of ezrin and the entire phagocytosis sequence was recorded at real time by confocal microscopy (fig 6.4.4a). As the pseudopodia formed, the peripheral staining of ezrin was lost along the phagocytic cup. When formed, the phagosome consequently was devoid of membrane ezrin. Image J was used to quantify the change in intensity of Fura Red (calcium concentration) and change in intensity fluorescence of ezrin around the developing phagosome. This revealed that the loss of membrane location of ezrin at the pseudopodia/phagosome was associated with an increase in calcium level (graph 6.4.4b). Fig6.4.4a shows the phagocytosis sequence recorded in transfected RAW cells.

Figure 6.4.4.a. Effect of change in plasma membrane dimension (phagocytosis) over the subcellular position of ezrin.



1x10$^6$cells/ml RAW cells were transfected with GFP-tagged ezrin plasmid and were incubated in a sterile petridish at 37$^\circ$C for 4-6hours. After washing away dead and unattached cells, to the remaining cells 1µM of Fura Red was added and incubated at 37°C further for 45minutes. The petri dishes were then mounted over a heated stage (temperature maintained at 37°C) and viewed by confocal microsocopy. RAW cells with peripheral membrane staining of ezrin and positive for Fura Red were selected, and using a micropipette (fig a1, arrow), a zymosan particle opsonized with mouse serum was selected and placed near the cell. The entire process of phagocytosis was recorded in real time. As the pseudopodia (fig b2) was stretched towards the opsonized zymasan particle, the peripheral ezrin was lost at this site and it was lost around the developing phagocytic cup (fig b3-6) aswell as around the phagosome (fig b8), while rest of the membrane (which are not involved in phagosome formation retained its peripheral membrane staining of ezrin. This shift in the position of ezrin was in association with an increase in the cytosolic calcium level, indicated by decrease in fluorescence intensity of Fura Red (c1-11). This indicated that a change in the plasma membrane dimension stimulates the relocation of ezrin away from the cell membrane into the cytosol. Images a1-a11 are the bright field.

Enlagred picture of 6.3.4a-b3

Enlagred picture of 6.3.4a-b5

Enlagred picture of 6.3.4a-b10

The above three picture are the enlarged figs 6.3.4a – b3, b5 and b10, to show the change in the subcellular position of ezrin in area of cell membrane (indicated by arrow) involved in phagocytosis in ezrin-GFP tagged trasfected RAW cells.

Figure 6.4.4.b. Measuring the change in membrane ezrin with change in the cytosolic level of calcium



RAW cells with GFP -taggeed ezrin plasmid

Plasma membrane

Phagocytic cup

Change in calcium level

Change in membrane distribution

Fura Red loaded Raw cells
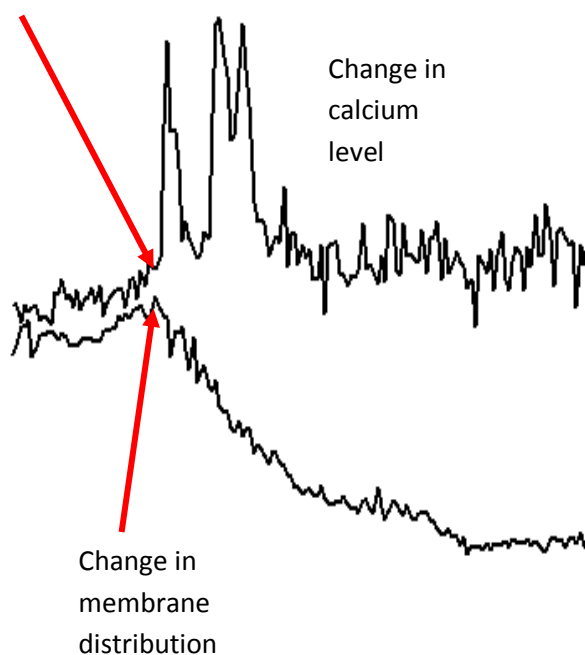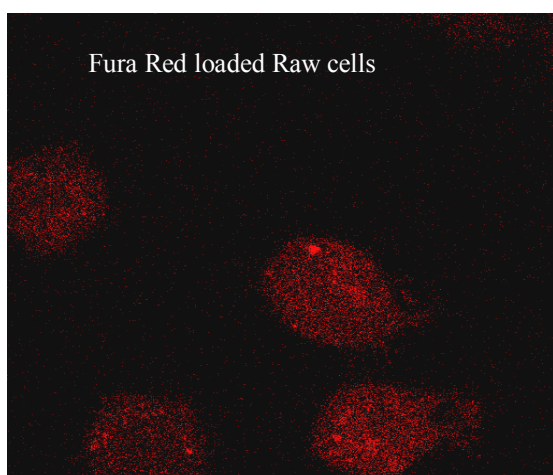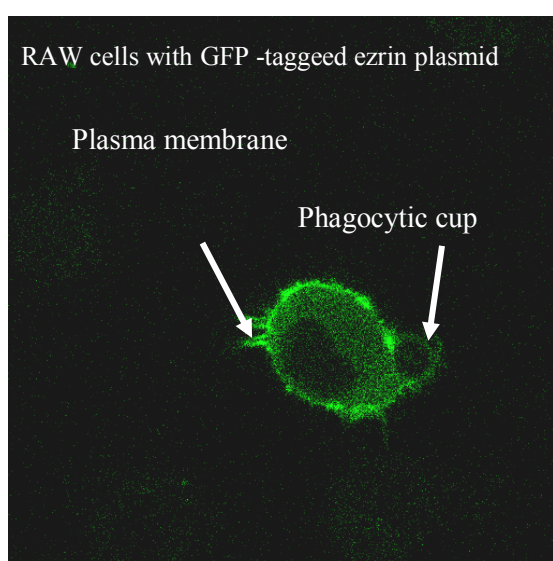
The change in fluorescence of ezrin around the plasma membrane involved in phagocytic cup formation was compared with the change in level of calcium level (Leica Lite software and Image J software programme). The above graph demonstrates that the loss of peripheral membrane position of ezrin was associated with the timing of the calcium increase (associated with formation of phagocytic cup).

### 6.4.5 Mechanism of the relocation of ezrin

The data here shows that ezrin moves away from the cell membrane into the cytosol with an elevation of cytosolic $Ca^{2+}$. Since ezrin binding to the plasma membrane involves PIP2 (see section 1.6.7), and PIP2 is reduced by PLC, the possibility existed that $Ca^{2+}$ elevation which activates PLC, may reduce PIP2 levels sufficiently to release ezrin. This possibility was investigated by testing the effect of a PLC inhibitor (U73122). The characteristics of this inhibitor are described in section 6.3.1.5. RAW cells with peripheral GFP-ezrin were selected and treated with U73122 (Sigma Aldrich) for 15minutes before addition of the $Ca^{2+}$ elevating cocktail (section 6.3.2.4). Despite the presence of the PLC inhibitor, ezrin moved away from the plasma membrane into the cytosol, as the cytosolic level of calcium increased (indicated by a decrease in fluorescent intensity of Fura Red). This showed that relocation of ezrin involved a mechanism which does not require activation of PLC (fig 6.4.5a). In order to determine whether the proteolytic action of calpain over ezrin might cause the change in its subcellular position, RAW cells transfected with GFP-tagged ezrin which have loaded with Fura Red™ were treated with calpain inhibitor (ALLN at room temperature for 15 minutes) before addition of the $Ca^{2+}$ elevating cocktail . Again, ezrin moved away from the plasma membrane into the cytosol. This results were consistent (5/5 experiments) indicating that proteolysis of ezrin might not involve activation of calpain or that the inhibitor used was inefficient or unable to block the activation of calpain activation at the $Ca^{2+}$ influx sites.

_____

Chapter 6

# Figure 6.4.5a. Effect of calpain inhibitor (ALLN) on the subcellular location of ezrin:



Cocktail mixture of high calcium added **(t 50sec)**
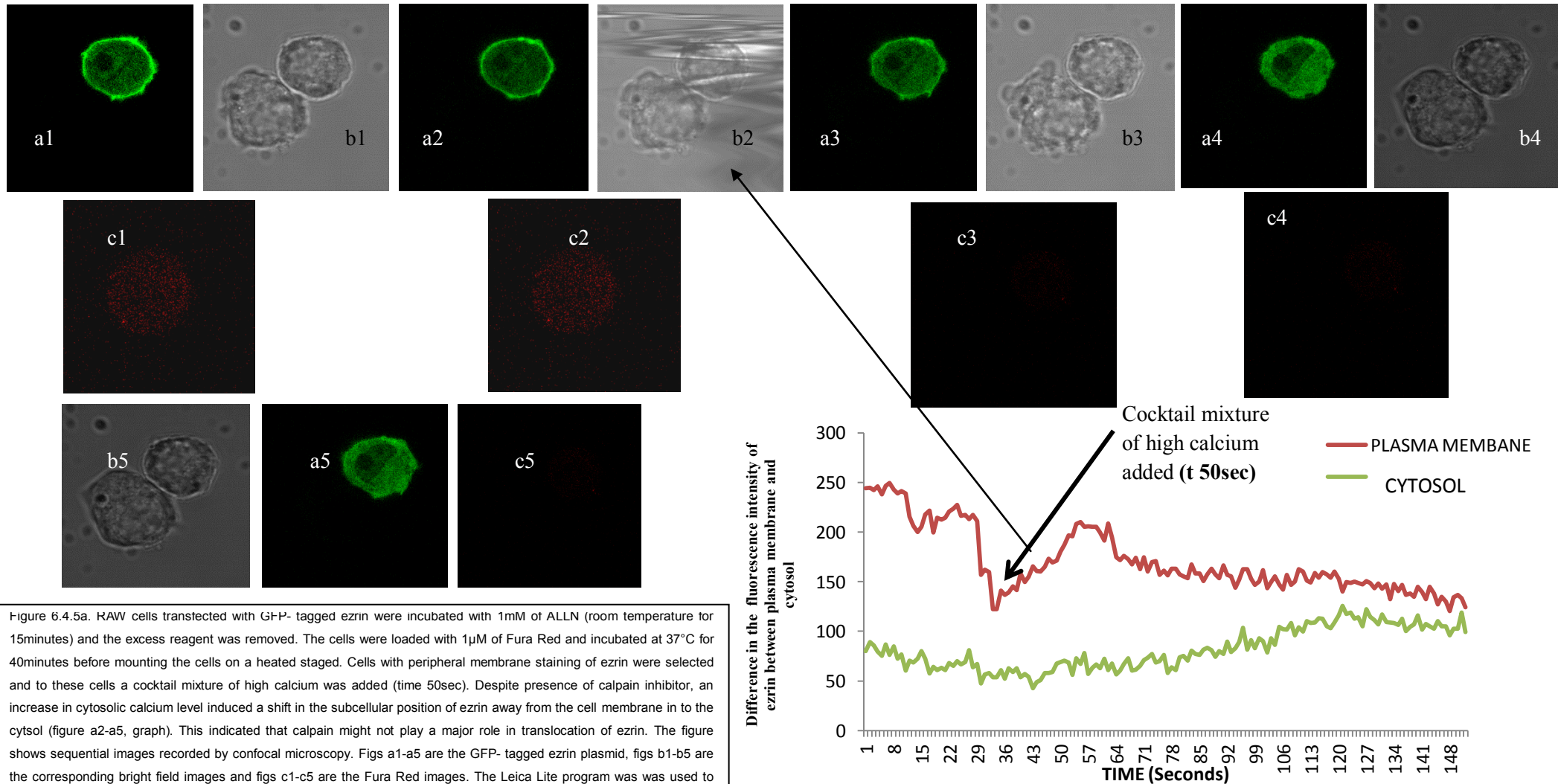
Figure 6.4.5a. RAW cells transfected with GFP- tagged ezrin were incubated with 1mM of ALLN (room temperature for 15minutes) and the excess reagent was removed. The cells were loaded with 1μM of Fura Red and incubated at 37°C for 40minutes before mounting the cells on a heated staged. Cells with peripheral membrane staining of ezrin were selected and to these cells a cocktail mixture of high calcium was added (time 50sec). Despite presence of calpain inhibitor, an increase in cytosolic calcium level induced a shift in the subcellular position of ezrin away from the cell membrane in to the cytsol (figure a2-a5, graph). This indicated that calpain might not play a major role in translocation of ezrin. The figure shows sequential images recorded by confocal microscopy. Figs a1-a5 are the GFP- tagged ezrin plasmid, figs b1-b5 are the corresponding bright field images and figs c1-c5 are the Fura Red images. The Leica Lite program was was used to measure the difference in fluorescent intensity between the cell membrane and cytosol throughout the experiment (graph).

**Figure 6.4.5b: Effect of PLC inhibitor (U73122) on the subcellular location of ezrin.**
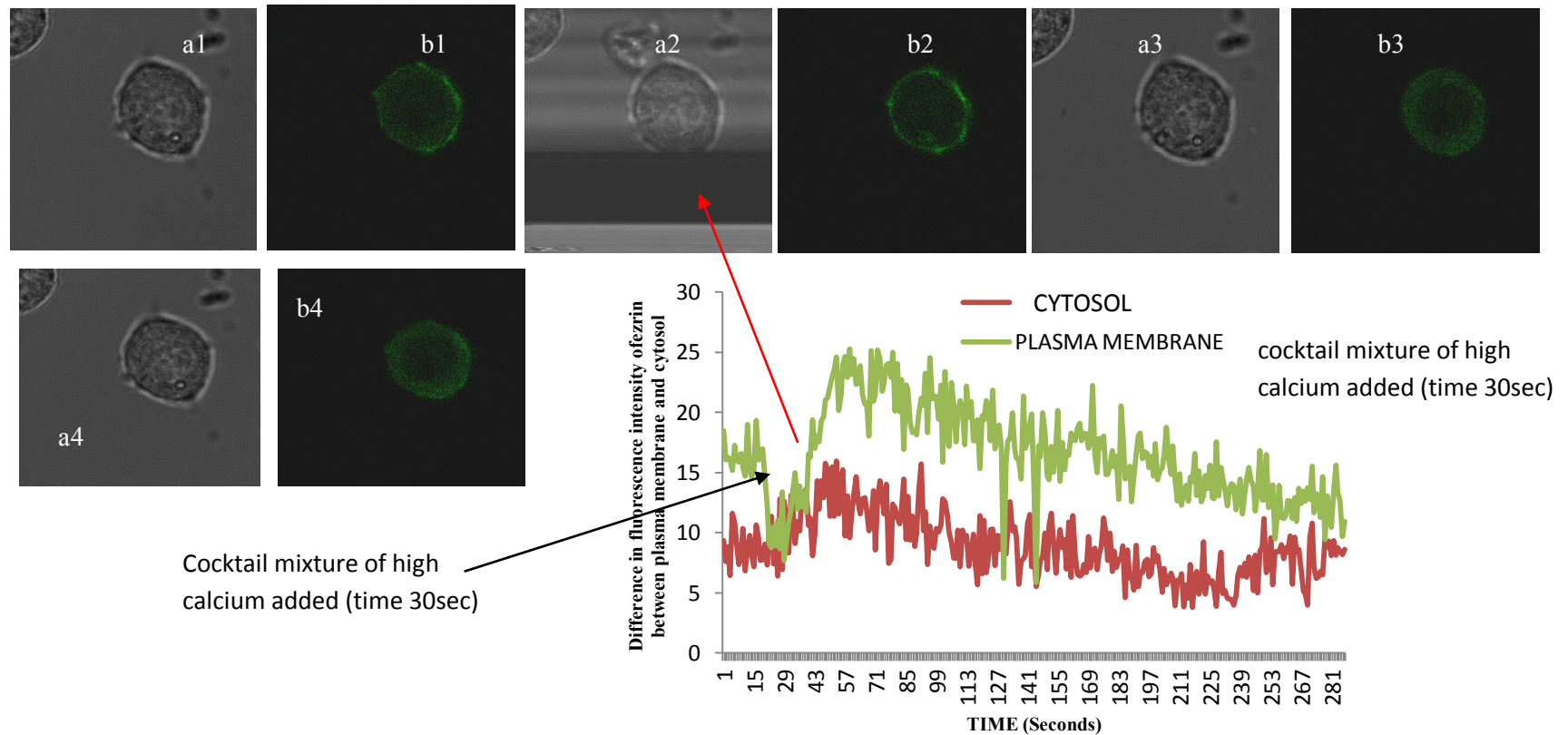


1x10$^6$ RAW cells/ml were transfected with GFP -tagged ezrin. After incubating at 37°C for 4-6hours, the dead and unattached cells were removed by replacing with fresh ordinary tissue culture medium, then to these cells 1mM of U73122 was added and left at room temperature for 15minutes, before the excess of reagent was removed. Before mounting the cells on the heating staged of the confocal microscope, cells were loaded with 1μM Fura Red and incubated at 37°C for 40minutes. Cells with peripheral membrane staining of ezrin were selected and to these cells a cocktail mixture of high calcium was added (time 30sec), Despite the presence of PLC inhibitor, an increase in the cytosolic calcium level induced a shift in the subcellular position of ezrin away from the cell membrane in to the cytosol (figs b2-b4, graph). This indicates that calpain might not play a major role in translocation of ezrin. figs a1-a4 are the GFP- tagged ezrin plasmid, figs b1-b4 are the corresponding bright field images, both captured by confocal microsopy.

## 6.5  Discussion

From the previous chapters using fixed cells, it has been established that ezrin moves away from the cell membrane into cytosol when the cell changes its shape or when the cell is active. In order to establish the mechanism behind this change in subcellular position of ezrin, RAW cells which had been transfected with GFP-tagged ezrin were used. These transfected cells had fluorescent ezrin located along the cell membrane (similar to neutrophils). When the calcium level inside the cell increased, the ezrin moved away from the cell membrane into the cytosol. What was noted moreover, this change in position was in discrete portions, ie this shift in position of ezrin from the cell membrane was not uniform. This might show that only in those area of cell membrane where there is unfolding of wrinkles, there was shift in position of ezrin. This shift in position of ezrin is an irreversible process (replacement of high calcium medium with original medium). When phagocytosis was induced in transfected RAW cells, peripheral staining of ezrin was lost only at the cell membrane which was in contact with the zymosan, pseudopodia, phagocytic cup, as well as along the phagosome also. This gave a clue that relocation of ezrin is associated with change in dimension of plasma membrane. This finding was further confirmed when photobleaching was performed in one region of plasma membrane, ezrin from the remaining portion of plasma membrane moved not only into the cytosol, but also moved to fill the bleached region in the cell membrane. This indicates that relocation of ezrin is a dynamic process and is unidirectional. But when these transfected RAW cells were treated with a cocktail mixture of high calcium in presence of PLC inhibitor, as well as in the presence of a calpain inhibitor, still the relocation of ezrin was not inhibited. This observation might indicate that movement of ezrin away from cell membrane into cytosol might not depend on PLC pathways nor activation of calpain in phagocytic cells; or this might be due to use of less efficient inhibitors which might not block completely the activation of PLC or calpain.

# CHAPTER 7

**Subcellular location of ezrin in**

**pathologically extravasated neutrophils**

## 7.1 Introduction

From the previous chapter, evidence has been provided that relocation of ezrin away from the plasma membrane into cytosol occurs in neutrophils which have extravasated both under experimental conditions (transendothelial migration *in vitro*) and under physiological conditions (*in vivo* in the mouth, ie salivary neutrophils). Moreover, evidence has been provided that this change in subcellular position of ezrin is triggered by raised cytosolic Ca$^{2+}$ and accompanies the apparent expansion of the plasma membrane (eg during phagocytosis in transfected RAW cells). Neutrophils taken from clinically inflamed gums and synovial fluids (osteoarthritis knee joint) were therefore studied in order to establish whether a similar event occurs during extravastion of neutrophils into pathologically inflamed regions. Such a change in subcellular location of ezrin would identify neutrophils which had extravasted from blood and thus, act as a marker of extravasation rate.

### 7.1.1 Gingivitis

Gingivitis is an inflammatory condition of the soft tissues surrounding the gingiva and is a direct immune response to the dental microbial plaque building in and on the teeth. It is characterized clinically by gingival redness, oedema, bleeding, changes in contour, loss of tissue adaptation to the teeth and increased flow of gingival crevicular fluid (GCF) (KInane D 2001). The development of gingivitis requires the presence of plaque bacteria, which are thought to induce pathological changes in the tissues by both direct and indirect means. These bacteria are capable of synthesizing products like collagenase, hyaluronidase, protease, chondroitin sulfatase or endotoxin that cause damage to epithelial and connective tissue cells, as well as to intercellular constituents, such as collagen, ground substance and glycocalyx (cell coat). This result in widening of the spaces between the junctional epithelium (which lines the gingival space) which permits injurious agents derived from bacteria or

bacteria themselves, to gain access to the connective tissue. These microbial products activate both innate and acquired immunity which may lead to complete removal of the microorganisms and the resolution of gingivitis. If not, it may lead to periodontits. Page and Schoreder (2003) developed a system to categorize the clinical and histopathological observations by subdivision of gingivitis into 4 stages (appendix 1). The initial lesion appears as an acute inflammatory response with characteristic infiltration by neutrophils. Vascular changes, epithelial cell changes and collagen degradation are also apparent. These initial changes are probably due to chemotactic attraction of neutrophils by bacterial constituents and direct vasodilatory effects of bacterial products, as well as activation of host systems, such as the complement and kinin systems and arachidonic acid pathways. If the etiology causing gingivitis (dental plaque) is not removed or if the host immune system is inefficient in clearing the microbes, periodontitis may result (Keisari Y et.al.1997).

## 7.1.2  Gingival crevicular fluid (GCF).

The presence of gingival crevicular fluid (GCF) has been known since the nineteenth century, but the pioneering works of Waerhayg and Brill (1959) and Krasse (1982) elucidated its composition and possible role in oral defence mechanisms more than half a century ago. However, there is still controversy over whether GCF is inflammatory exudate or transudate. According to Alfano and Pashely (1974), GCF in gingival health is a tissue fluid like transudate that enters the gingival crevice through the basement membrane and the relatively wide intercellular spaces of the variable thickness junctional epithelium and sulcular epithelium. As the gingival inflammation sets in, due to increase in permeability of the extensive capillary network that directly underlies the junctional and sulcular epithelium, the GCF turns into an inflammatory exudates. This results in both an increase in the flow of GCF and a change in its composition to that of plasma-like inflammatory exudate, rich in immunoglobulin and inflammatory cells. In humans, about 2-3ml of GCF flows in the mouth

daily. The clinical significance of  increases not only in inflammatory processes, but also in physiological situation like circadian periodicity (increase from 6am to 10pm and a decrease afterwards), pregnancy, ovulation and hormonal contraceptives all increase gingival fluid production. Furthermore, mechanical stimulation like chewing and gingival brushing will increase GCF flow. Smoking and periodontal therapy also increases the flow. The main function of gingival fluid is as a host defence, initially through the flushing action in the vulnerable gingival crevice and which keep it free from microorganisms, their products and other noxious substances. Secondly, gingival fluid helps in differentiation of junctional epithelium by providing nutrition (healthy conditions) and also by exposing them to various bacterial and immunological components during pathological condition. Moreover, the GCF are characterized both by enzymatic and by non-enzymatic components as well as cellular and non-cellular components (listed in appendix 2), which play a vital role in host defence. Many compounds found in GCF can be host-derived or produced by the bacteria in the gingival crevice, but their sources can be hard to elucidate. Much research efforts have attempted to use GCF components to detect or diagnose active disease to predict patents at risk for periodontal disease.

### 7.1.3  Origin of gingival neutrophils

Fresh saliva contains three easily recognized cellular elements, namely bacteria, epithelial cells and leukocytes. Prior to the 1960s, the origin of these leukocytes and the mechanism of their entry into the oral cavity were unknown. Stephens and Jones (2007) observed that erratic populations of inflammatory cells were found in oral fluids, while numbers of these cells circulating in the peripheral blood remained fairly constant. It was also demonstrated that the number of leukocytes found in the saliva decreased as patients lost teeth, resulting in very few white blood cells being found in the saliva of edentulous patients, compared to those of dentate individuals. Leukocytes have also been detected in both clinically healthy

and diseased tissue of experimental animals and humans. In 1960, Sharry and Krasse determined that 47% of all cells obtained from the gingival sulcus were leukocytes, while these cells represented less than 2% of cells isolated from various other extra-oral and intra-oral sites. This led to the theory that the major route of entry into the oral cavity for these cells was via the gingival sulcus, which was later confirmed by numerous subsequent studies (appendix III). The neutrophil was the predominant inflammatory cell type isolated from the GCF (reviewed by Van Dyke. 1985, and Van Dyke et .al.1985). These cells exit the inflamed vessels of the microcirculation and migrate along a gradient of chemoattractant through the connective tissues and junctional epithelium, to form a barrier between the subgingival microbial plaque and the gingival tissue. The neutrophils in the oral cavity can be divided into two major groups: (1) gingival or crevicular PMNs (GPMNs), which are found in the gingival crevice, before migrating into the oral cavity (Sharry and Krasse,1960) and (2) salivary PMNs (SPMNs 82%), which are found in saliva and originate mainly in gingival crevices (GPMN 47%) (Schiott and Lue1970). GPMNs have been comprehensively investigated, and their role in periodontal health and disease is well-established (Miller et.al.1984; Genco and Slots.1984; Cohen et.al.1985; Fine and Mandel.1986). In histological sections of clinically healthy or slightly inflamed gingival, these cells are found in the intercellular spaces of the junctional epithelium and occasionally along the tooth surface in close proximity to aggregates of plaque. These inflammatory cells appear most numerous at the base of the sulcus and decrease in number towards the entrance of the sulcus. The persistent emigration of these cells from the peripheral blood circulation and their localization in the region of the gingival sulcus are believed to be initiated by chemotactic factors   generated by the bacteria found in the local plaque mass and in saliva.

In health, neutrophils are found to reside in the superficial layer of the epithelium and at the sulcus base while the mononuclear cells are located predominately in the basal and

supra-basilar positions of the junctional epithelium. The proportion of the neutrophils to mononuclear cells has been shown to be independent of the degree of inflammation, but the absolute numbers of all these cells increase with the severity of the inflammatory process. During the development of gingivitis, the number of leukocytes migrating to the sulcus increases and under inflamed conditions, 60% or more of the junctional epithelium space can be occupied by neutrophils. It has been demonstrated that while there was a 2.1 fold increase of neutrophils during a 21 day period of experimental gingivitis, the GCF flow increased almost 5.5 fold during the same period. In addition, leukocytic infiltration was seen throughout the junctional epithelium and neutrophils were always found in the sulcus, even in clinically healthy situations where the flow of GCF was relatively low. This would lead to the conclusion that inflammatory cell transmigration through the junctional epithelium and the flow of GCF were two distinct phenomena although they occur concomitantly. In addition, migration of inflammatory cells from the gingival connective tissue, through the junctional epithelium and into the sulcus is an active and continuous process, directed along gradients of chemoattractants. In the sulcus, the concentration of neutrophils can far exceed the concentration of these cells in the peripheral blood. Once in the sulcus, neutrophils begin to create a leukocyte wall, forming aggregates of inflammatory cells along the margins of the advancing plaque front. At this point, neutrophils may attempt to phagocytose and eliminate pathogens or may elaborate and secrete an armoury of enzymes to destroy these microorganisms without internalizing them.

### 7.1.4  Osteoarthritis

Osteoarthritis (OA), also known as degenerative arthritis or degenerative joint disease or osteoarthrosis, is a group of mechanical abnormalities involving degradation of joints

(Sandell and Aigner 2001), including articular cartilage and subchondral bone. Symptoms may include joint pain, tenderness, stiffness, locking and sometimes an effusion. A variety of causes hereditary, developmental, metabolic and mechanical, may initiate processes leading to loss of cartilage. When bone surfaces become less well protected by cartilage, bone may be exposed and damaged. As a result of decreased movement, secondary to pain, regional muscles may atrophy, and ligaments may become more lax (Conaghan 2008). Treatment generally involves a combination of exercise, lifestyle modification and analgesics. If pain becomes debilitating, joint replacement surgery may be used to improve the quality of life. OA is the most common form of arthritis. Osteoarthritis can be classified into either primary, which is a chronic degradative disorder caused by changes associated with inflammatory changes in joint capsule; or the other type of OA is secondary, which is due to known or unknown identifiable underlying causes like diabetes, inflammatory diseases, injury, obesity, etc. Even though this inflammatory condition is not mediated by neutrophils, the neutrophils which are collected in the synovial fluid have extravasted from blood vessels, so they form a good source of extravasted neutrophils.

## 7.2  Aims

The aims of this chapter were to establish whether changes in the subcellular location of ezrin could be identified in neutrophils which had extravasated pathologically, either into the gingival crevicular fluid or synovial fluid.  The particular goals were:-

1.  To determine the subcellular position of ezrin in neutrophils collected in gingival crevicular fluid.

2.  To determine the subcellular position of ezrin in neutrophils collected in the synovial fluid of patients with oesteoarthritis of the knee.

3. To determine whether ezrin can be used as a biological marker to identify extravasated neutrophils.

## 7.3 Methods and Materials

### 7.3.1 Collection of GCF

GCF was collected using a fine glass capillary, with inner dimension of 2 mm and 4 cm in length (from Sigma- Aldrich UK), 10µl of heparin (CP Pharmaceuticals Ltd, Wrexham, UK), sterile eppendorff tubes, cytospin, glass slides, primary ezrin antibody and secondary antibody were discussed in sections 2.3.1.& 2.3.2. All materials used for immunocytochemistry to study the position of Ezrin in these neutrophils were discussed in section 2.4.4.The collection of GCF samples was ethically approved (Study title: Gingival crevicular fluid as a source of extravasated human neutrophils for the study of neutrophil behaviour and molecular signalling Project ID: 11/DEN/5063, REC number:11/,WN0152).

### 7.3.2 Collection of synovial fluid from Osteoarthritis patients

The Osteoarthritis samples used in this study were from the synovial joint of knee from patients who were undergoing knee replacement surgery. The samples and the study were ethically approved (Study Title: Arthritis Research UK Biomechanics and Bioengineering Centre-Multi Project Ethical Submission, REC reference number: 10/MRE09/28, Protocol: 2.)

### 7.3.3 Isolation of neutrophils from GCF

Capillary tube collection, otherwise known as micropipette technique, was used to collect GCF. After obtaining consent from the patients, an overall assessment of gingival and periodontal condition of the patients was done using BPI index (appendix IV). Only those subjects who had PI scores of 1 to 2; and clinical signs of early gingivitis and early periodontitis were selected.

GCF was collected only from the maxillary front teeth (to avoid contamination from saliva) and from only those teeth which showed clinical signs of gingivitis (bleeding on probing). As an internal control sample, GCF was also collected from teeth which were clinically healthy gingiva (same subject). First the tooth from which GCF to be collected was isolated using cotton roles and dried using cotton. The capillary tube was inserted into the entrance of the gingival crevice (fig7.4.1) for an interval of 2minutes and GCF was collected for 10-15 minutes from the selected tooth. GCF was collected from two different surfaces of the selected tooth. The GCF flow from the crevice migrates into the tube by capillary action. At the end of 2 minutes, the capillary tubes were immediately emptied into an eppendoff which had 1µl of heparin (250 IU/ml) dissolved in 50µl of Krebs buffer. Heparin is used inorder to prevent blood clot formation. All the GCF collected for 10-15minutes were pooled into a sterile new eppendorff and the cellular content of GCF was fixed using 4% formaldehyde for 15 minutes before forcing the cellular content on to a glass slide using cytospin (2500rpm for 5minutes). Following this, the samples were processed for immunocytochemical staining (described in section 2.5.6.1). A similar method was used to process samples collected from health gingiva (internal control).
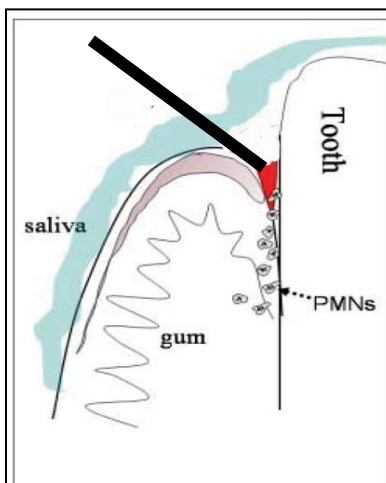


A
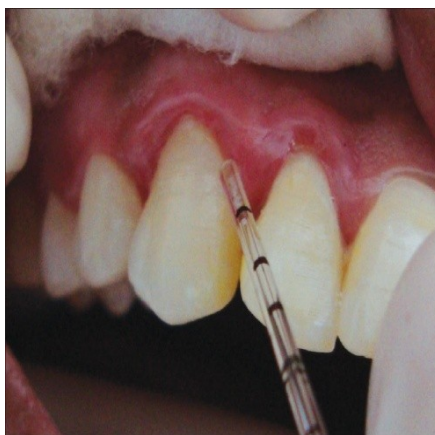
B

Figure 7.3.3A. Method of collecting GCF. Schematic diagram shows the way of collecting GCF from gingival.The micropipette was placed inside the gingival crevices to collect GCF from both gingivitis area as well as healthy gums.

Figure B. Clinical picture of GCF collection. Photo showing the collection of GCF using micropipeette technique, GCF flows inside the pipette by capillary action.

### 7.3.4 Isolation of neutrophils from synovial fluid

Synovial fluids received from patients undergoing knee replacement surgery for osteoarthritis of the knee in Cardiff & Vale hospitals in Wales, were collected and used for this study. Those samples which had obvious blood contamination were discarded. As the synovial fluid received were too viscous, the samples were diluted with 15ml of Krebs buffer and the cellular content was pelleted out by centrifuging at 2000rpm for 10minutes; and the pellet was resuspended in 500µl of Krebs buffer. The cells in the sample were fixed in suspension by adding 4%formaldehye, later these cells were forced onto a glass slip using a cytospin (2000 rpm for 5minutes). These cells were then processed for immunocytochemistry (section 2.5.6.1).

## 7.4   Results

### 7.4.1   Subcellular location of ezrin in neutrophiils isolated from GCF

Neutrophils isolated from GCF, as described in section 7.4.1, were stained with ezrin antibody (section 2.5.6.1). 7 GCF samples were collected from clinically inflamed gingival. As an internal control, GCF was also collected from teeth with clinically healthy gingiva in the same patients. Neutrophils from inflamed gingiva included both cells with peripheral ezrin (19 cells in total, maximum of 4/5 cells per sample, fig 7.4.1a) as well as cytoplasmic ezrin (17 cells in total, maximum of 5-6 cells per sample, fig 7.4.1a). In contrast, neutrophils from GCF isolated from internal control sites (healthy gingiva) only cytoplasmic ezrin was noted (25 cells in total, figure 7.4.1b & c). This observation indicated that some neutrophils present in the area of gingivitis must have extravated through the endothelial lining (indicated by the cytosolic location of ezrin), but others (with

peripheral ezrin) had not crossed the endothelial lining, possible arriving in the fluid as a result of micro-bleeding (a histological feature of early gingivitis). On the other hand, all neutrophils in health had crossed both the endothelial lining, as indicated by the cytosolic location of ezrin.
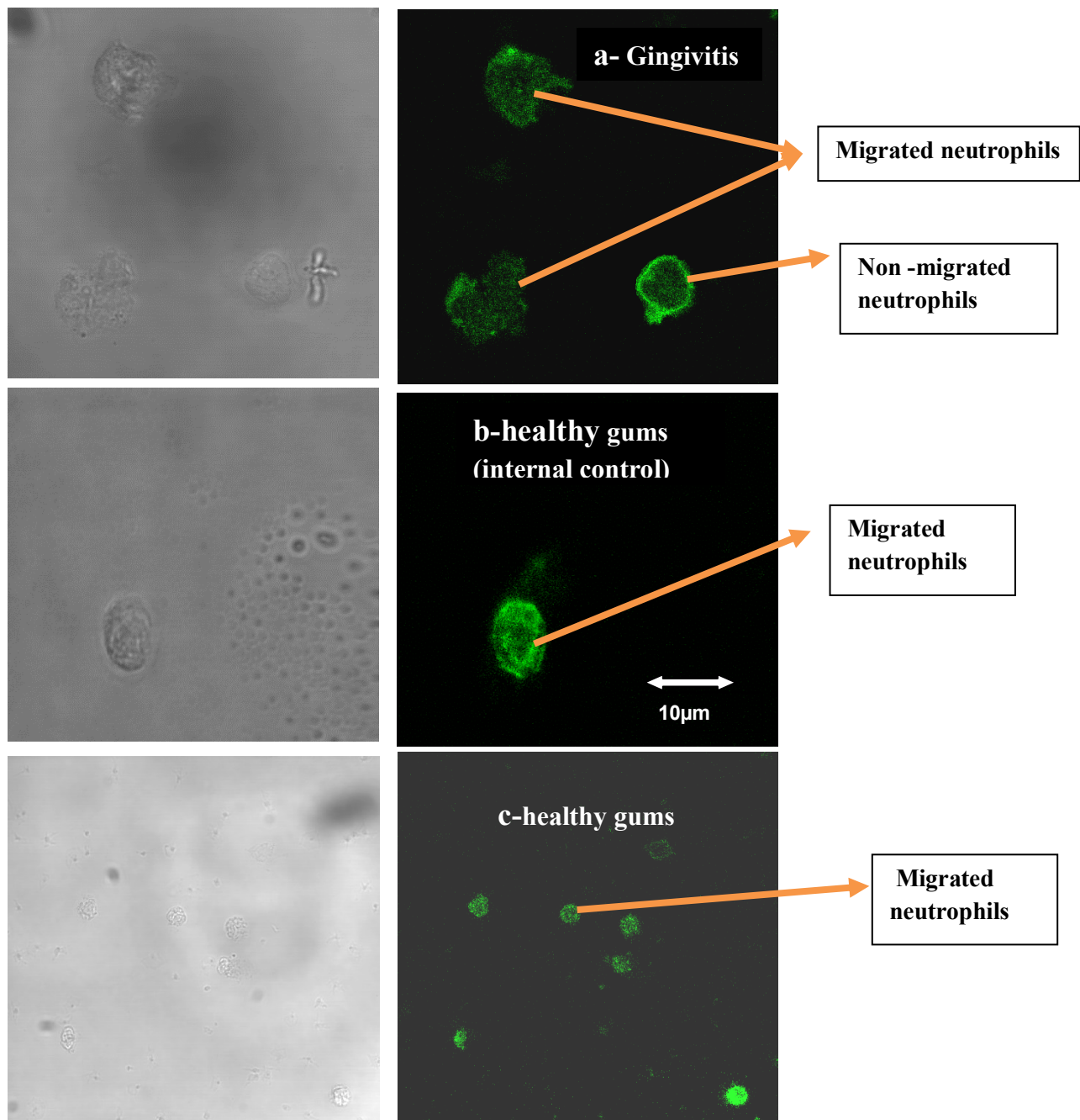
**Figure 7.4.1. Subcellular position of ezrin in neutrophils isolated from GCF**: The above two pictures (a&b) are representative images of cells from the same patient who had clinical signs of gingivitis.The neutrophils were isolated from GCF collected from (a) a tooth with inflamed gingiva (labial surface of maxillary incisor,FDI 11) and (b)from a tooth with healthy gums in the same patient (labial surface of maxillary left canine FDI 23). Neutrophils from the inflamed site (a) showed both peripheral plasma membrane staining of ezrin (non-migrated neutrophils), as well as cytoplasmic staining of ezrin (migrated neutrophils). On the other hand, neutrophils collected from the control site (healthy gums, b) had predominantly cytoplasmic staining of ezrin. In this participant, the total number of cells counted (healthy gingival-internal control) were 5/5 cells had cytoplasmic staining of ezrin (fig b). GCF collected from individual with healthy gum (fig c), neally all cells had cytoplasmic staining of ezrin. In this participant, out of 7 cells counted, 6 cells had cytoplasmic staining of ezrin while the remaining 1 cell had plasma membrane staining of ezrin. Similar results were observed when neutrophils were isolated from all the subjects with healthy gums (fig c).

## 7.4.2  Subcellular location of ezrin in neutrophils isolated from synovial fluid of osteoarthritis patients

Neutrophis were isolated from synovial fluid of knee from 5 osteoarthritis patients. Out of 27 cells counted in all the osteoarthritis samples, 18 cells had cytoplasmic staining of ezrin while the remaining 9 cells had peripheral staining of ezrin. This observation again indicated that two different pattern of ezrin indicated two different group of neutrophils [migrated neutrophils - cytoplasmic staining of ezrin (fig 7.4.2a), non-migrated neutrophils - plasma membrane staining of ezrin (fig 7.4.2b&c)]. This finding again indicates that change in subcellular position of ezrin occurs when the neutrophils extravates into the pathological site and dynamic change in position of ezrin may be used to identify extravasated group of neutrophils.   Though OA is not an inflammatory reaction caused primarily by neutrophils, neutrophils are often the predominant cellular components which infiltrate the synovial fluid. These samples represent one source of extravasted neutrophils, which was reason why they were used in this study. From the results observed from neutrophils isolated from both GCF and OA, it can be said that the characteristic cell membrane staining of ezrin is lost when the neutrophils extravasated. This proves that ezrin acts as a'biological memory' left behind by extravasted neutrophils and thus, can be used as a marker to identify extravasted neutrophils.

**Figure 7.4.2.** Subcellular position of ezrin in neutrophils isolated from synovial fluid of OA patients. The below three ezrin antibody staining images are of neutrophils isolated from the synovial fluid collected from three different patient who underwentknee replacement surgery for osteoarthritis. Neutrophils both with plasma membrane staining of ezrin, as well as cytoplasmic staining of ezrin, was observed. The neutrophils which had cell membrane staining of ezrin represent non-migrated neutrophils and those neutrophils which had cytosolic staining of ezrin indicated migrated neutrophils.
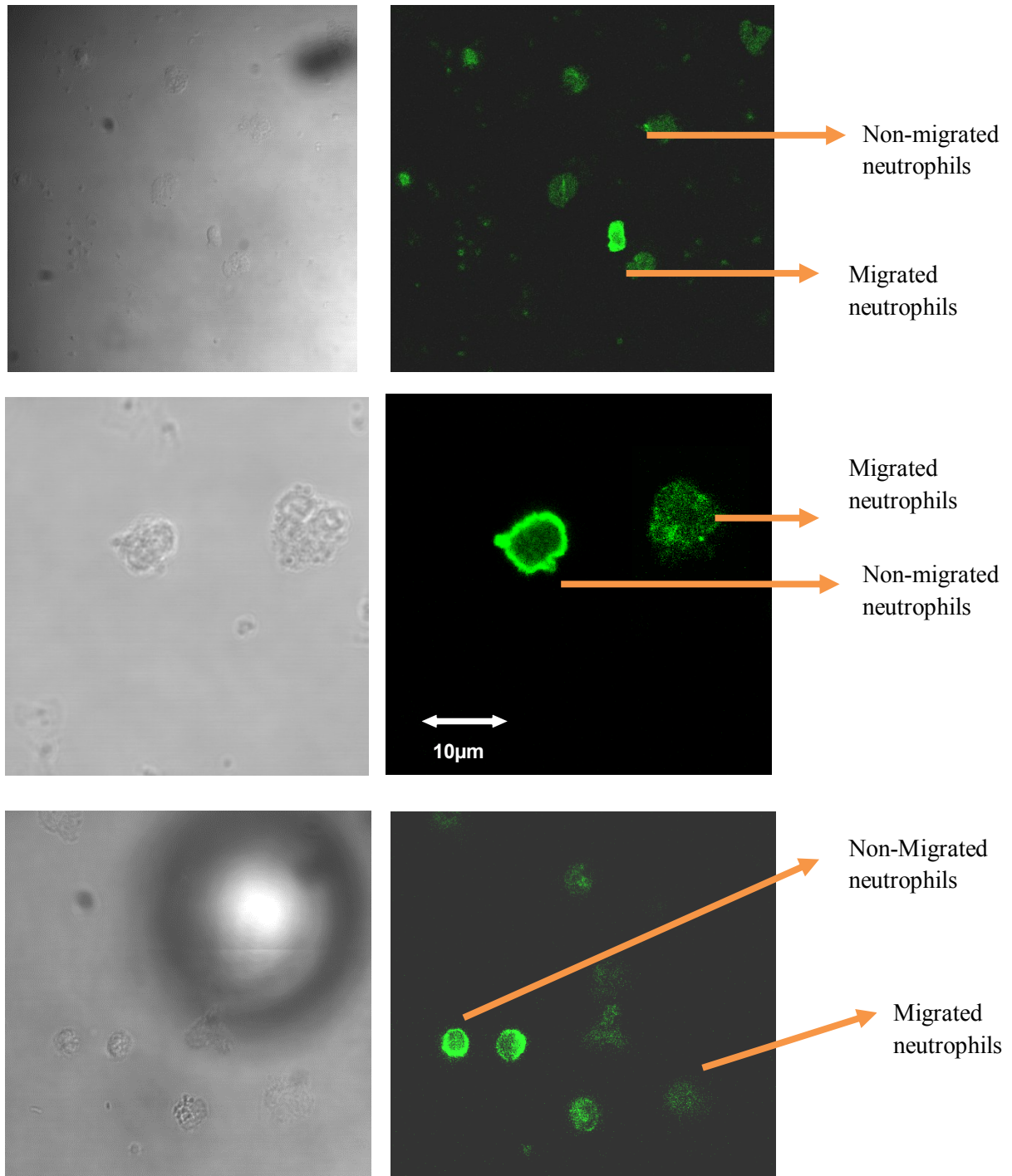
## 7.5    Discussion

It has been established from the previous chapter that ezrin relocated away from the cell membrane into the cytosol when the neutrophils crossed an endothelial monolayer either under experimental conditions or under physiological conditions. Moreover, it has been shown that this change in subcellular position of ezrin occurs when there is a change in dimension of the plasma membrane and this change in position of ezrin is a dynamic process (see chapter 6). In order to provide evidence that ezrin can be used as a biological marker to identify extravasated neutrophils, neutrophils isolated from two different pathologically inflamed sites - gingiva (gingivitis, GCF) and knee (osteoarthritis, synovial fluid) were studied. In both conditions, neutrophils with plasma membrane ezrin, as well as cytoplasmic ezrin, were observed. On the other hand, neutrophils with only cytoplasmic ezrin were observed in neutrophils from healthy gingival, as well teeth with healthy gums, in patients with early stage of gingivits (internal control). These findings confirm that ezrin can be used as a biological marker to identify the extravasated group of neutrophils. However, the number of neutrophils and samples obtained in this study was not sufficient to undertake ezrin protein isolation (for western blotting). Moreover, the number of neutrophils found in both the conditions was few and make statistical analysis difficult. However, the results observed were convincing and suggested that ezrin location may act as a "biological memory" within extravasated neutrophils.

# CHAPTER 8

# DISCUSSION

## 8.1 Summary of results presented in this thesis

Before discussing the implications of the results in this thesis, I will briefly summarise the main findings.

### 8.1.1 Subcellular location of talin and kindlin in neutrophils

The peripheral plasma membrane location of talin observed in neutrophils isolated from blood was lost after they had extravasated across an endothelial cell layer, either under *in vitro* conditions and *in vivo*, under physiological conditions (salivary neutrophils). Surprisingly, antibodies to the head group of talin were unable to detect talin in neutrophils but could in other cells.

Kindlin-3, which is structurally similar to the head group of talin also, could not be detected in neutrophils. It is possible that the head group of talin (and kindlin3) was associated with integrins in such a way that the head group of talin was either hidden deep within integrin or it was otherwise sterically hindering the binding of antibody.

### 8.1.2 Subcellular location of ezrin in neutrophils

Ezrin in blood neutrophils was located at the cell membrane but when stimulated with FMLP or cytosolic $Ca^{2+}$ was elevated artificially, the ezrin at the membrane was lost. The loss of plasma membrane ezrin was also observed in neutrophils which have extravasted both under physiological (salivary neutrophils) and under experimental conditions (*in vitro* transendotheial migration). The cell membrane location of ezrin was also locally lost in areas of pseudopodia, formed during phagocytosis. This was consistent with a role for proteolytic cleavage of the bridges between the cell membrane and ezrin during activation. It was suggested that proteolysis might be by activation of calpain by elevated $Ca^{2+}$ during cell stimulation.

---

### 8.1.3 Proteolytic products of ezrin

Ezrin extracted from neutrophils had a molecular weight of 72kDa, (or 69kDa if totally de-glycosylated). However, after the cells were permeablised in the presence of $Ca^{2+}$, bands at 55kDa and 49kDa were formed. A similar fragmentation of ezrin was detected in neutrophils which had crossed endothelial barriers. This suggested that the loss of ezrin from the plasma membrane was a consequence of a proteolytic step.

### 8.1.4 Mechanism of proteolysis of ezrin

RAW cells expressing ezrin-GFP showed a clear peripheral location for ezrin. This was lost when cytosolic $Ca^{2+}$ was elevated. This change is an irreversible process and was dependent on the dynamic nature of ezrin association-dissociation (shown by photo bleaching). The relocation of ezrin into the cytosol was also observed in those areas of cell membrane undergoing active expansion with localised loss of peripheral ezrin at forming pseudopoodia, phagocytic cups and around formed phagosomes.

### 8.1.5 Ezrin location as biological maker of extravasated neutrophils

The majority of neutrophils isolated from healthy gingival fluid had cytoplasmic, rather than peripheral, ezrin. It was probable that this was result of transendothelial migration, suggesting that normally cells must cross the endothelial barrier to reach the gingival space. In contrast, nearly all the neutrophils isolated from pathologically inflamed gingival crevicular fluid of inflamed gingiva or synovial fluid of osteoarthritis knee had cell membrane associated ezrin. The cells which retained a membrane location of ezrin may therefore have arrived at the inflamed site by another route (eg via microbleeding from blood vessels). The subcellular position of ezrin thus

_____

gives some indication of the previous history of the neutrophil, and may be a useful biological marker to distinguish the routes by which neutrophils arrive at inflamed sites.

## 8.2 Further research

These findings could be exploited in several ways. For example, in determining dental prognosis and in understanding the basic cell biology of neutrophils.

### 8.2.1 Prognosis of patients with periodontal pathologies

Many studies has been done to show that prognosis of periodontal disease is retarded by amount of neutrophils entering the sulcus. If the number of neutrophils entering the sulcus through micro-bleeding is identified (using subcellular ezrin relocation) as a marker, they could be treated accordingly. Further clinical research would be required to test this. However, it will be possible to collect gingival fluid from patients to establish whether the ezrin status predict the prognosis of the periodontal diseases.

### 8.2.2 Knock-out house model

Knock-out mouse model, either ezrin-null or with aberrant ezrin resistant to calpain, could be designed to evaluate the characteristics of neutrophils which lack ezrin or lack the abilty to release ezrin from there plasma membranes. It is predicted that these defects would have a significant influence on the functional properties of neutrophils.

_____

## 8.3   Conclusion

Neutrophils are the first cells to infiltrate into inflammatory site by crossing the endothelial lining. They do so by interacting with various cell membrane receptors present on the endothelium, as well as on the neutrophils, which are regulated by various membrane linker protein like ezrin. From the results obtained from this study, ezrin undergoes proteolytic cleavage in the presence of elevated cytosolic $Ca^{2+}$ which might leads to unfolding of wrinkles present on the neutrophil surface, enabling cell shape changes which involve expansion of the plasma membrane including phagocytosis and extravastion. Because proteolysis is irreversible, the location of ezrin within neutrophils may act as a biological molecular "memory" left behind in extravasted neutrophils. This memory may be important as the extravasated cells would be more ready to undergo phagocytosis (as observed during priming). It also has an important implication, as the subcellular location of ezrin could serve as a molecular marker for identifying extravasted neutrophils in inflamed sites under various conditions.

_____

# REFERENCES

Ahuja,S.K. and Murphy,P.M. 1996. Human Interleukin-8 Receptor. Journal of Biological Chemistry 271(34), pp. 20545-20550.

Alcaide,P. et al. 2008. p120-Catenin regulates leukocyte transmigration through an effect on VE-cadherin phosphorylation. Blood 112(7), pp. 2770-2779.

Alcaide,P., Auerbach, S. and Luscinskas, F. W. 2009. Neutrophil Recruitment under Shear Flow: It's All about Endothelial Cell Rings and Gaps. Microcirculation 16. pp. 43-57.

Allingham, M. J. et al. 2007. ICAM-1-Mediated, Src- and Pyk2-Dependent Vascular Endothelial Cadherin Tyrosine Phosphorylation Is Required for Leukocyte Transendothelial Migration. The Journal of Immunology 179(6), pp. 4053-4064
.

Alon, R. and Ley, K. 2008. Cells on the run: shear-regulated integrin activation in leukocyte rolling and arrest on endothelial cells. Current Opinion in Cell Biology 20(5), pp. 525-532.

Alon, R. et al. 1996. Interactions through L-selectin between leukocytes and adherent leukocytes nucleate rolling adhesions on selectins and VCAM-1 in shear flow. Journal of Cell Biolology 135, pp. 849-865.

Anderson, D.C. and Springer, T.A. 1987. Leukocyte Adhesion Deficiency: An Inherited Defect in the Mac-1, LFA-1, and p150,p 95 Glycoproteins. Annual Review of Medicine 38(1), pp. 175-194.

Anderson, D. C. et. al. 1984. Abnormalities of polymorphonuclear leukocyte function associated with a heritable deficiency of high molecular weight surface glycoproteins (GP138): Common relationship to diminished cell adherence. Journal Clinical Investigation 74, pp. 536-551.

Anthis, N. J. et. al. 2009. The structure of an integrin/talin complex reveals the basis of inside-out signal transduction. Journal of EMBO 28(22), pp. 3623-3632.

Arias-Salgado, E.G. et. al. 2003. Src kinase activation by direct interaction with the integrin β cytoplasmic domain. Proceedings of the National Academy of Sciences 100(23), pp. 13298-13302.

Ashkenazi, M. and Dennison, D. K. 1989. A New Method for Isolation of Salivary Neutrophils and Determination of Their Functional Activity. Journal of Dental Research 68(8), pp. 1256-1261.

Astrid, F. N; Cagna ,G et. Al. VE-PTP maintains the endothelial barrier via plakoglobin and becomes dissociated from VE-cadherin by leukocytes and by VEGF. 2008 . Journal of Experimental  Medicine. 205: 2929-2945.

Babi, L.F.S., Moser, B., Soler, M.T.P., Moser, R., Loetscher, P., Villiger, B., Blaser, K. and Hauser, C. 1996. The interleukin-8 receptor B and CXC chemokines can mediate transendothelial migration of human skin homing T cells. European Journal of Immunology 26, pp. 2056-2061.

Bargatze, R. F. et al. 1994. Neutrophils roll on adherent neutrophils bound to cytokine-induced endothelial cells via L-selectin on the rolling cells. Journal of  Experimental  Medicine. 180, pp. 1785-1792.

Barreiro, O. and Sánchez-Madrid, F. 2009. Molecular basis of leukocyte endothelium interactions during the inflammatory response. Journal of Leucocyte Biology 62(5), pp. 552-562.

Barreiro, O. et al. 2002. Dynamic interaction of VCAM-1 and ICAM-1 with moesin and ezrin in a novel endothelial docking structure for adherent leukocytes. The Journal of Cell Biology 157(7), pp. 1233-1245.

Barreiro, O. et al. 2008. Endothelial adhesion receptors are recruited to adherent leukocytes by inclusion in preformed tetraspanin nanoplatforms. The Journal of Cell Biology 183(3), pp. 527-542.

Barreiro, O., De La Fuente, H., Mittelbrunn, M. and Sánchez-Madrid, F. 2007. Functional insights on the polarized redistribution of leukocyte integrins and their ligands during leukocyte migration and immune interactions. Immunological Reviews 218, pp. 147-164.

---

Beckerle, M.C. 1990. The adhesion plaque protein, talin, is phosphorylated *in vivo* in chicken embryo fibroblasts exposed to a tumor-promoting phorbol ester. Cell Regulation 1(2), pp. 227-236.

Beckerle, M. C. et al. 1989. Activation-dependent redistribution of the adhesion plaque protein, talin, in intact human platelets. The Journal of Cell Biology 109(6), pp. 3333-3346.

Belliveau, M.J. et al. 1995. Schwannomin: new insights into this member of the band 4.1 superfamily. Biochemistry and Cell Biology 73(9-10), pp. 733-737.

Berman, M. E. and Muller, W. A. 1995. Ligation of platelet/endothelial cel adhesion molecule 1 (PECAM-1/CD31) on monocytes and neutrophils increases binding capacity of leukocyte CR3 (CD11b/CD18). J Immunol 154, pp. 299-307.

Berton, G. 1999a. Degranulation. Current opinion in Hematology 6  p. 703.

Berton, G. 1999b. Tyrosine kinases in neutrophils. Current Opinion In Hematology 6, pp. 51-58.

Bessis, M. 1973. Living Blood Cells and their Ultrastructure. Berlin: Springer.

Bienvenu, K. and Granger,D.N. 1993. Molecular determinants of shear rate-dependent leukocyte adhesion in postcapillary venules. American Journal of Physiology - Heart and Circulatory Physiology 264(5), pp.1504-1508.

Bing-Hao Luo, C.V.C., and Timothy A. Springer. 2007. Journal of Cell Biology, 143(2), pp.370-379.

Blixt A,J.P., Braide M, Bagge U. 1985. Microscopic studies on the influence of erythrocyte concentration on the post-junctional radial distribution of leukocytes at small venular junctions. International Journal of  Microcirculation in Clinical Experiment. 4(2), pp. 141-156.

Blouin, E. et al. 1999. Redox regulation of b2-integrin CD11b/CD18 activation. Europena Journal of Immunology 29, pp. 3419-3431.

Bonilha , L. 2007. Focus on Molecules: Ezrin. Experimental Eye Research, 84. 613- 614.

Borowsky, M.L. and Hynes, R.O. 1998. Layilin, A Novel Talin-binding Transmembrane Protein Homologous with C-type Lectins, is Localized in Membrane Ruffles. The Journal of Cell Biology 143(2), pp. 429-442.

---

Borregaard, N. et al. 1996. Granules and secretory vesicles of the human neutrophil. International Journal of Pediatric Hematology/Oncology 3(5), pp. 307-319.

Bouaouina, M. et al. 2008. The N-terminal Domains of Talin Cooperate with the Phosphotyrosine Binding-like Domain to Activate β1 and β3 Integrins. Journal of Biological Chemistry 283(10), pp. 6118-6125.

Brenner, B. et al. 1996. L-selectin activates the Ras pathway via the tyrosine kinase p56lck. Protocol in National Academic Science USA 93, pp. 15376-15381.

Bretscher A., Fehon R.G 2002. ERM proteins and merlin: integrators at the cell cortex. 586e599. Nature Review of Molecular Cell Biology, 3, 586-599.

Bretscher, A. et al. 1997. Ezrin A protein requiring conformational activation to link microfilaments to the plasma membrane in the assembly of cell surface structures. Journal of Cell Science 110(24), pp. 3011-3018.

Brockhaus, M. et al.1990. Identification of two types of tumor necrosis factor receptors on human cell lines by monoclonal antibodies. Protocol in National Academic Science USA 87, pp. 3127-3131.

Burridge, K. and Connell, L. 1983. A new protein of adhesion plaques and ruffling membranes. The Journal of Cell Biology 97(2), pp. 359-367.

Burwen, S.J.and Satir, B. H. 1977. Plasma membrane folds on the mast cell surface and their relationship to secretory activity. The Journal of Cell Biology 74(3), pp. 690-697.

Butcher, E.C. 1991. Leukocyte-endothelial cell recognition: Three (or more) steps to specificity and diversity. Cell 67(6), pp. 1033-1036.

Byzova TV, G.C., Pampori N, Thomas KA, Bett A, Shattil SJ, Plow EF. 2000. A mechanism for modulation of cellular responses to VEGF: activation of the integrins. Molecular Cell 6, pp. 851-860.

Calderwood, D.A. 2004. Integrin activation. Journal of Cell Science 117(5), pp. 657-666.

Calderwood, D.A. et al. 1999. The Talin Head Domain Binds to Integrin β Subunit Cytoplasmic Tails and Regulates Integrin Activation. Journal of Biological Chemistry 274(40), pp. 28071-28074.

Calderwood, D.A. et al. 1999. The Talin Head Domain Binds to Integrin β Subunit Cytoplasmic Tails and Regulates Integrin Activation. Journal of Biological Chemistry 274(40), pp. 28071-28074.

Calderwood, D.A. et al. 2002. The Phosphotyrosine Binding-like Domain of Talin Activates Integrins. Journal of Biological Chemistry 277(24), pp. 21749-21758.

Campbell, I. D. and Ginsberg, M. H. 2004. The talin-tail interaction places integrin activation on FERM ground. Trends in Biochemical Sciences 29(8), pp. 429-435.

Capodici, C. et al. 1998. Phosphatidylinositol 3-kinase mediates chemoattractant-stimulated, CD11b/CD18-dependent cell-cell adhesion of human neutrophils: Evidence for an ERK-independent pathway. J Immunol 160, pp. 1901-1909.

Carman,C.V. 2009. Mechanisms for transcellular diapedesis: probing and pathfinding by `invadosome-like protrusions'. Journal of Cell Science 122(17), pp. 3025-3035.

Carman, C. V. and Springer, T. A. 2004. A transmigratory cup in leukocyte diapedesis both through individual vascular endothelial cells and between them. The Journal of Cell Biology 167(2), pp. 377-388.

Carman, C. V. and Springer, T. A. 2008. Trans-cellular migration: cell-cell contacts get intimate. Current Opinion in Cell Biology 20(5), pp. 533-540.

Carman, C. V. et al. 2007. Transcellular Diapedesis Is Initiated by Invasive Podosomes. Immunity 26(6), pp. 784-797.

Charles N. Serhan, P. A. W., Derek W. Gilroy ed. 2010. fundamentals of inflammation. Cambridge University Press.

Cheretakis, C. et al. 2005. A noninvasive oral rinse assay to monitor engraftment, neutrophil tissue delivery and susceptibility to infection following HSCT in pediatric patients. Bone Marrow Transplant 36(3), pp. 227-232.

Corada, M. et al. 2005. Junctional adhesion molecule-A-deficient polymorphonuclear cells show reduced diapedesis in peritonitis and heart ischemia-reperfusion injury. Proceedings of the National Academy of Sciences of the United States of America 102(30), pp. 10634-10639.

Courts, F.J. et al. 1977. Detection of Functional Complement Components in Gingival Crevicular Fluid from Humans with Periodontal Disease. Journal of Dental Research 56(3), pp. 327-331.

Cowan, K.J. et al. 2000. Identification of Shc as the Primary Protein Binding to the Tyrosine-phosphorylated β3 Subunit of αIIbβ3 during Outside-in Integrin Platelet Signaling. Journal of Biological Chemistry 275(46), pp. 36423-36429.

Critchley, D. R. and Gingras, A. R. 2008. Talin at a glance. Journal of Cell Science 121(9), pp. 1345-1347.

Croall, D. E. and Demartino, G. N. 1991. Calcium-activated neutral protease (calpain) system: Structure, function, and regulation. Physiological Reviews 71(3), pp. 813-847.

Dangerfield, J. et al. 2002. PECAM-1 (CD31) Homophilic Interaction Up-Regulates α6β1 on Transmigrated Neutrophils *In vivo* and Plays a Functional Role in the Ability of α6 Integrins to Mediate Leukocyte Migration through the Perivascular Basement Membrane. The Journal of Experimental Medicine 196(9), pp. 1201-1212.

Datta, A. et al. 2002. Phosphorylation of β3 Integrin Controls Ligand Binding Strength. Journal of Biological Chemistry 277(6), pp. 3943-3949.

Davies E.V., Hallett M.B. 1996. Near membrane $Ca^{2+}$ changes resulting from store release in neutrophils: detection by FFP-18. Cell Calcium.19. pp.355–362. .

Davies, E. V. and Hallett, M. B. 1998. High Micromolar Ca2+beneath the Plasma Membrane in Stimulated Neutrophils. Biochemical and Biophysical Research Communications 248(3), pp. 679-683.

Del Maschio, A. et al. 1996. Polymorphonuclear leukocyte adhesion triggers the disorganization of endothelial cell-to-cell adherens junctions. J Cell Biol 135, pp. 497-510.

DePasquale, J. A. and Izzard, C. S. 1991. Accumulation of talin in nodes at the edge of the lamellipodium and separate incorporation into adhesion plaques at focal contacts in fibroblasts. The Journal of Cell Biology 113(6), pp. 1351-1359.

DEWITT, S. & HALLETT, M. 2007. Leukocyte membrane "expansion": a central mechanism for leukocyte extravasation Journal of Leukocyte Biology, 81, 1160-1164.

DEWITT, S. & HALLETT, M. B. 2002 Cytosolic free Ca2+ changes and calpain activation are required for β integrin–accelerated phagocytosis by human neutrophils The Journal of Cell Biology, 159, 181-189.

Dewitt, S. and Hallett, M. 2007. Leukocyte membrane "expansion": a central mechanism for leukocyte extravasation. Journal of Leukocyte Biology 81(5), pp. 1160-1164.

Dewitt, S. and Hallett, M. B. 2002. Cytosolic free Ca2+ changes and calpain activation are required for β integrin–accelerated phagocytosis by human neutrophils. The Journal of Cell Biology 159(1), pp. 181-189.

Di Paolo, G. et al. 2002. Recruitment and regulation of phosphatidylinositol phosphate kinase type 1[gamma] by the FERM domain of talin. Nature 420(6911), pp. 85-89.

Domadia, P. N. et al. 2010. Functional and structural characterization of the talin F0F1 domain. Biochemical and Biophysical Research Communications 391(1), pp. 159-165.

Downey GP, W. G., Henson PM, Hyde DM. 1993 Neutrophil sequestration and migration in localized pulmonary inflammation. Capillary localization and migration across the interalveolar septum. Am Rev Respir Dis 1, pp. 168-176.

Doyle, N. A. et al. 1997. Neutrophil margination, sequestration, and emigration in the lungs of L-selectin-deficient mice. J Clin Invest 99, pp. 526-533.

Eerri, L. E. P, Jose .Seely, Andrew J. E.; Chaudhury, Prosanto ; Christou, Nicolas V. . 2002,. Soluble L-selectin attenuates tumor necrosis factor-[alpha]-mediated leukocyte adherence and vascular permeability: A protective role for elevated soluble L-selectin in sepsis LABORATORY INVESTIGATIONS 30(8), pp. 1842-1847.

Eiserich, J. P. et al. 2002. Myeloperoxidase, a Leukocyte-Derived Vascular NO Oxidase. Science 296, pp. 2391-2394.

Evans, E. et al. 1993. Synchrony of cell spreading and contraction force as phagocytes engulf large pathogens. The Journal of Cell Biology 122(6), pp. 1295-1300.

Evans, R. et al. 2009. Integrins in immunity. Journal of Cell Science 122(2), pp. 215-225.

Feng D, N. J., Pyne K, et al. 1998. Neutrophils emigrate from venules by a transendothelial cell pathway in response to FMLP. Journal of experimental medicine 187, pp. 903-915.

Fernandez HN, H. P., Otani A, Hugli TE. 1978. Chemotactic response to human C3a and C5a anaphylatoxins: Evaluation of C3a and C5a leukotaxis in vitro and under stimulated *in vivo* conditions. Journal of Immunology 120, pp. 109-115.

Firrell, J. C. and Lipowsky, H. H. 1989. Leukocyte margination and deformation in mesenteric venules of rat. American Journal of Physiology - Heart and Circulatory Physiology 256(6), pp. H1667-H1674.

Fischer, A. et al. 1983. Bone-marrow transplantation for inborn error of phagocytic cells associated with defective adherence, chemotaxis, and oxidative response during opsonised particle phagocytosis. Lancet 2, pp. 473-476.

Folkesson, H. G. et al. 1995. Acid aspiration-induced lung injury in rabbits is mediated by interleukin-8-dependent mechanisms. J Clin Invest 96, pp. 107-116.

Ford-Hutchinson AW, B. M., Doig MV, Shipley ME, Smith MJ. . 1980. Leukotriene B, a potent chemokinetic and aggregating substance released from polymorphonuclear leukocytes. Nature 286, pp. 264-265.

Foxman, E. F. et al. 1999. Integrating conflicting chemotactic signals: The role of memory in leukocyte navigation. J Cell Biol 147, pp. 577-588.

Franco, S. et al. 2004. Isoform specific function of calpain 2 in regulating membrane protrusion. Experimental Cell Research 299(1), pp. 179-187.

Franco, S. J. and Huttenlocher, A. 2005. Regulating cell migration: calpains make the cut. Journal of Cell Science 118(17), pp. 3829-3838.

Fuortes, M. et al. 1999. Role of the tyrosine kinase pyk2 in the integrin-dependent activation of human neutrophils by TNF. J Clin Invest 104, pp. 327-335.

Gallin, JI, Goldstein (1988), I M; Inflammation: Basic Principles and Clinical Correlates. 1st Edition.

García-Alvarez, B. et al. 2003. Structural Determinants of Integrin Recognition by Talin. Molecular Cell 11(1), pp. 49-58.

García-Alvarez, B. et al. 2003. Structural determinants of integrin recognition by talin. Molecular Cell 11(1), pp. 49-58.

_____

Gil-Parrado, S. et al. 2003. Subcellular Localization and *in vivo*Subunit Interactions of Ubiquitous μ-Calpain. Journal of Biological Chemistry 278(18), pp. 16336-16346.

Gingras, A. R. et al. 2005. Mapping and Consensus Sequence Identification for Multiple Vinculin Binding Sites within the Talin Rod. Journal of Biological Chemistry 280(44), pp. 37217-37224.

Gingras, A. R. et al. 2008. The structure of the C-terminal actin-binding domain of talin. EMBO J 27(2), pp. 458-469.

Goll, D. E. et al. 2003. The Calpain System. Physiological Reviews 83(3), pp. 731-801.

Goult, B. T. et al. 2009. The Structure of an Interdomain Complex That Regulates Talin Activity. Journal of Biological Chemistry 284(22), pp. 15097-15106.

Granger, D. N. and Kubes, P. 1994. The microcirculation and inflammation: modulation of leukocyte-endothelial cell adhesion. Journal of Leukocyte Biology 55(5), pp. 662-675.

Hallett, M. B. and Dewitt, S. 2007. Ironing out the wrinkles of neutrophil phagocytosis. Trends in Cell Biology 17(5), pp. 209-214.

Hallett, M. B. et al. 1990. Oxidase activation in individual neutrophils is dependent on the onset and magnitude of the Ca2+ signal. Cell Calcium 11(10), pp. 655-663.

Hallett, M. B. et al. 2008. Chemotaxis and the cell surface-area problem. Nat Rev Mol Cell Biol 9(8), pp. 662-662.

Hallett, M. B., Von ruhland, C. J. & Dewitt, S. (2008) Chemotaxis and the cell surface-area problem. Nat Rev Mol Cell Biol, 9, 662-662.

Hallmann R, H. N., Selg M, et al. 2005. Expression and function of laminins in the embryonic and mature vasculature. physiological Reviews 85, pp. 979-1000.

Hamada, K. et al. 2000. Structural basis of the membrane-targeting and unmasking mechanisms of the radixin FERM domain. EMBO J 19(17), pp. 4449-4462.

Hamill, O. P. and Martinac, B. 2001. Molecular Basis of Mechanotransduction in Living Cells. Physiological Reviews 81(2), pp. 685-740.

Hammond, M. E. et al. 1995. IL-8 induces neutrophil chemotaxis predominantly via type I IL-8 receptors. The Journal of Immunology 155(3), pp. 1428-1433.

Hayashi, M. et al. 1999. The Behavior of Calpain-Generated N- and C-Terminal Fragments of Talin in Integrin-Mediated Signaling Pathways. Archives of Biochemistry and Biophysics 371(2), pp. 133-141.

Herant, M. et al. 2003. The Mechanics of Neutrophils: Synthetic Modeling of Three Experiments. Biophysical Journal 84(5), pp. 3389-3413.

Herant, M. et al. 2005. Mechanics of neutrophil phagocytosis: behavior of the cortical tension. Journal of Cell Science 118(9), pp. 1789-1797.

Herant, M. et al. 2006. Mechanics of neutrophil phagocytosis: experiments and quantitative models. Journal of Cell Science 119(9), pp. 1903-1913.

Hidalgo, A. et al. 2007. Complete Identification of E-Selectin Ligands on Neutrophils Reveals Distinct Functions of PSGL-1, ESL-1, and CD44. Immunity 26(4), pp. 477-489.

Hillson, E. J., Dewitt, S., Hallett, M. B. . 2006. IP3-induced cell spreading of human neutrophils requires Ca2+ influx. Molecular Biology of Cell 17((Supplement. L45)).

Hirschi, K. K. and D'Amore, P. A. 1996. Pericytes in the microvasculature. Cardiovascular Research 32(4), pp. 687-698.

Hixenbaugh, E. A. et al. 1997. Stimulated neutrophils induce myosin light chain phosphorylation and isometric tension in endothelial cells. American Journal of Physiology - Heart and Circulatory Physiology 273(2), pp. 981-988.

Huber AR, K. S., Todd RF 3rd, Weiss SJ. 1991. Regulation of transendothelial neutrophil migration by endogenous interleukin-8. Science 254(5028), pp. 99-102.

Hughes, P. E. and Pfaff, M. 1998. Integrin affinity modulation. Trends in Cell Biology 8(9), pp. 359-364.

Humphries, J. D. et al. 2007. Vinculin controls focal adhesion formation by direct interactions with talin and actin. The Journal of Cell Biology 179(5), pp. 1043-1057.

Imhof, B. A. and Aurrand-Lions, M. 2004. Adhesion mechanisms regulating the migration of monocytes. Nature Review In Immunology 4(6), pp. 432-444.

Inomata, M. et al. 1989. Properties of erythrocyte membrane binding and autolytic activation of calcium-activated neutral protease. Journal of Biological Chemistry 264(31), pp. 18838-18843.

Isenberg, G. et al. 2002. Membrane fusion induced by the major lipid-binding domain of the cytoskeletal protein talin. Biochemical and Biophysical Research Communications 295(3), pp. 636-643.

Ivetic, A. 2004. Ezrin/radixin/moesin proteins and Rho GTPase signalling in leucocytes. Immunology 112(2), pp. 165-176.

Ivetic, A. et al. 2002. The Cytoplasmic Tail of L-selectin Interacts with Members of the Ezrin-Radixin-Moesin (ERM) Family of Proteins. Journal of Biological Chemistry 277(3), pp. 2321-2329.

Jaconi, M. E. et al. 1991. Multiple elevations of cytosolic-free Ca2+ in human neutrophils: initiation by adherence receptors of the integrin family. The Journal of Cell Biology 112(6), pp. 1249-1257.

Jones, S. L. et al. 1998. Two signaling mechanisms for activation of [agr]M[bgr]2 avidity in polymorphonuclear neutrophils. Journal of Biology and Chemisty, 273, pp. 10556-10566.

Kanwar, S. et al. 1997. The Association between α4-Integrin, P-Selectin, and E-Selectin in an Allergic Model of Inflammation. The Journal of Experimental Medicine 185(6), pp. 1077-1088.

Kawasaki, H. and Kawashima, S. 1996. Regulation of the calpain-calpastatin system by membranes (Review). Molecular Membrane Biology 13(4), pp. 217-224.

Kay, R. R. et al. 2008. Changing directions in the study of chemotaxis. Nature Review in Molecular Cell Biology 9(6), pp. 455-463.

Keisari Y, et al. 1997. Phagocyte-bacteria interactions.Advances In Dental Reserch.11(1 ). pp. 43-49.

Kinane D.F. 2001. Causation and pathogenesis of periodontal disease. Periodontology 2000, Vol. 25, pp. 8–20.

Kitayama,J. et al. 1997. Contrasting responses to multiple chemotactic stimuli in transendothelial migration. Heterologous desensitization in neutrophils and augmentation of migration in eosinophils. Journal of Immunology 158, pp. 2340-2349.

Kolanus, W.et al. 1996. Integrin LFA-1 binding to ICAM-1 induced by Cytohesin-1, a cytoplasmic regulatory molecule. Cell 86, pp. 233-242.

Krump, E. et al. 1997. Chemotactic peptide N-formyl-met-leu-phe activation of p38 mitogen-activated protein kinase (MAPK) and MAPK-activated protein kinase-2 in human neutrophils. J Biol Chem 272, pp. 937-944.

Kruskal, B. A. et al. 1986. Spreading of human neutrophils is immediately preceded by a large increase in cytoplasmic free calcium. Proceedings of the National Academy of Sciences 83(9), pp. 2919-2923.

Kuijpers, T. W., and Roos, Dirk . 2001. Neutrophils [Online]. Chichester: eLS. John Wiley & Sons Ltd. Journal of lecuocyte Biology, 179(7), pp.103-110

Laemmli, U. K. 1970. Cleavage of Structural Proteins during the Assembly of the Head of Bacteriophage T4. Nature 227(5259), pp. 680-685.

Larjava, H. et al. 2008. Kindlins: essential regulators of integrin signalling and cell-matrix adhesion. EMBO Rep 9(12), pp. 1203-1208.

Lamster I.B. 1992. Host Mediators in Gingival Crevicular Fluid: Implications for the Pathogenesis of Periodontal Disease. Critical Reviews in Oral Biology and Medicine, 3:31-60.

Lawrence, M. B. and Springer, T. A. 1993. Neutrophils roll on E-selectin. Journal of Immunology 151, pp. 6338-6347.

Lawson, M. A. and Maxfield, F. R. 1995. Ca2+- and calcineurin-dependent recycling of an integrin to the front of migrating neutrophils. Nature 377(6544), pp. 75-79.

Leitinger, B. et al. 2000. The regulation of integrin function by Ca2+. Biochimica et Biophysica Acta (BBA) - Molecular Cell Research 1498(2-3), pp. 91-98.

Ley, K. et al. 1995. Sequential contribution of L- and P-selectin to leukocyte rolling *in vivo*. J Exp Med 181, pp. 669-675.

Ley, K. et al. 2007. Getting to the site of inflammation: the leukocyte adhesion cascade updated. Nature Reviews Immunology 7(9), pp. 678-689.

Li, X. et al. 1998. Regulation of L-selectin-mediated rolling through receptor dimerization. Journal of Experimenal Medicine 188, pp. 1385-1390.

Ling, K. et al. 2002. Type I[gamma] phosphatidylinositol phosphate kinase targets and regulates focal adhesions. Nature 420(6911), pp. 89-93.

Ling, K. et al. 2003. Tyrosine phosphorylation of type Iγ phosphatidylinositol phosphate kinase by Src regulates an integrin–talin switch. The Journal of Cell Biology 163(6), pp. 1339-1349.

Liu S, C. D., Ginsberg MH. . 2000. Integrin cytoplasmic domain-binding proteins. Journal of Cell Science 113, pp. 3563-3571.

Louvet–vallée (2000 ) ERM proteins: From cellular architecture to cell signaling. Biology of the Cell 92 305-316.

Lowell, C.A. and Berton, G. 1999. Integrin signal transduction in myeloid leukocytes. J Leukocyte Biol 65, pp. 313-320.

Luo BH, Structural Basis of Integrin Regulation and Signaling. Annual Review of Immunology 25, pp. 619-647.

Luscinskas.F.. 2008. Assays of Transendothelial Migration in vitro

Lyck, R. a. E., B. . 2006. In Vitro Transendothelial Migration Assay, in Leukocyte Trafficking: Molecular Mechanisms, Therapeutic Targets, and Methods. In: B, H.A.a.E. ed. Weinheim: Wiley-VCH Verlag GmbH & Co.

Marks, P. W. and Maxfield, F. R. Local and global changes in cytosolic free calcium in neutrophils during chemotaxis and phagocytosis. Cell Calcium 11(2-3), pp. 181-190.

Martel, V. et al. 2001. Conformation, Localization, and Integrin Binding of Talin Depend on Its Interaction with Phosphoinositides. Journal of Biological Chemistry 276(24), pp. 21217-21227.

Martin-Padura, I. et al. 1998. Junctional Adhesion Molecule, a novel member of the immunoglobulin superfamily that distributes at intercellular junctions and modulates monocyte transmigration. J Cell Biol 142, pp. 117-127.

Matsumoto, T. et al. 1997. Pivotal role of interleukin-8 in the acute respiratory distress syndrome and cerebral reperfusion injury. J Leukoc Biol 62, pp. 581-587.

_____

McEver, R. P. and Cummings, R. D. 1997. Role of PSGL-1 binding to selectins in leukocyte recruitment. J Clin Invest 100, pp. S97-S103.

Medzhitov, R. 2010. Inflammation 2010: New Adventures of an Old Flame. Cell 140(6), pp. 771-776.

Michetti, M. et al. 1997. Calcium-binding properties of human erythrocyte calpain. Biochem. J. 325(3), pp. 721-726.

Middleton, J. et al. 1997. Transcytosis and surface presentation of IL-8 by venular endothelial cells. Cell 91, pp. 385-395.

Millan, J. et al. 2006. Lymphocyte transcellular migration occurs through recruitment of endothelial ICAM-1 to caveola- and F-actin-rich domains. Nature Cell Biology 8(2), pp. 113-123.

Molinari, M. and Carafoli, E. 1997. Calpain: A Cytosolic Proteinase Active at the Membranes. Journal of Membrane Biology 156(1), pp. 1-8.

Monkley, S. J. et al. 2001. Analysis of the Mammalian Talin2 Gene TLN2. Biochemical and Biophysical Research Communications 286(5), pp. 880-885.

Moore, K. L. et al. 1995. P-selectin glycoprotein ligand-1 mediates rolling of human neutrophils on P-selectin. Journal of Cell Biology 128, pp. 661-671.

Moser M, Bauer M, Schmid S, Ruppert R, Schmidt S, Sixt M, Wang HV, Sperandio M, Fässler R Kindlin-3 is required for beta2 integrin-mediated leukocyte adhesion to endothelial cells.. Nature Medcine. 2009 Mar;15(3):300-5

Moser M, Legate KR, Zent R, Fässler R. 2009.The Tail of Integrins, Talin,and Kindlins 2009; Science;324;895-899

Mueller, H. et al. 2010. Tyrosine kinase Btk regulates E-selectin-mediated integrin activation and neutrophil recruitment by controlling phospholipase C (PLC) γ2 and PI3Kγ pathways. Blood 115(15), pp. 3118-3127.

Muller WA. and Luscinskas F W (2008) Assays of Transendothelial Migration in vitro. Methods in enzymology, 443; 155-176

Muller, W. A. et al. 1993. PECAM-1 is required for transendothelial migration of leukocytes. J Exp Med 178, pp. 449-460.

Mulligan MS, J. M., Bolanowski MA, Baganoff MP, Deppeler CL, Meyers DM, Ryan US, Ward PA. 1993. Inhibition of lung inflammatory reactions in rats by an anti-human IL-8 antibody. . ;:. Journal of Immunology 150, pp. 5585-5595.

Mulligan, M. S. et al. 1991. Role of endothelial-leukocyte adhesion molecule 1 (ELAM-1) in neutrophil-mediated lung injury in rats. The Journal of Clinical Investigation 88(4), pp. 1396-1406.

Mulligan, M. S. et al. 1994. Requirements for L-selectin in neutrophil-mediated lung injury in rats. The Journal of Immunology 152(2), pp. 832-840.

Nagel, W. et al. 1998. Phosphoinositide 3-OH Kinase activates the b2 integrin adhesion pathway and induces membrane recruitment of Cytohesin-1. J Biol Chem 273, pp. 14853-14861.

Nakamura, F. et al. 1995. Phosphorylation of Threonine 558 in the Carboxyl-terminal Actin-binding Domain of Moesin by Thrombin Activation of Human Platelets. Journal of Biological Chemistry 270(52), pp. 31377-31385.

Newman, H.N and Addison,I .E.1982. Gingival crevice neutrophil function in periodontosis. Journal of Periodontology 53(9):pp.578-8

Nick, J. A. et al. 1997. Common and distinct intracellular signaling pathways in human neutrophils utilized by platelet activating facror and FMLP. J Clin Invest 99, pp. 975-986.

Nieminen, M. et al. 2006. Vimentin function in lymphocyte adhesion and transcellular migration. Nat Cell Biol 8(2), pp. 156-162.

Niggli, V. and Keller, H. 1997. The phosphatidylinositol 3-kinase inhibitor wortmannin markedly reduces chemotactic peptide-induced locomotion and increases in cytoskeletal actin in human neutrophils. Eur J Pharmacol 335, pp. 43-52.

Niggli, V., Kaufmann, S., Goldmann, W. H., Weber, T. and Isenberg, G. . 1994. Identification of Functional Domains in the Cytoskeletal Protein Talin. European Journal of Biochemistry 224, pp. 951-957.

Nottebaum.A.,C. G., Winderlich. M. 2008. VE-PTP maintains the endothelial barrier via plakoglobin and becomes dissociated from VE-cadherin by leukocytes and by VEGF

Nourshargh, S. et al. 2006. The role of JAM-A and PECAM-1 in modulating leukocyte infiltration in inflamed and ischemic tissues. Journal of Leukocyte Biology 80(4), pp. 714-718.

Nüsse, O. and Lindau, M. 1988. The dynamics of exocytosis in human neutrophils. The Journal of Cell Biology 107(6), pp. 2117-2123.

Ostermann.G, W. K. S. C. 2002. JAM-1 is a ligand of the bold beta2 integrin LFA-1 involved in transendothelial migration of leukocytes. Nature Immunology 3, pp. 151 - 158.

Papayannopoulos, V. et al. 2010. Neutrophil elastase and myeloperoxidase regulate the formation of neutrophil extracellular traps. The Journal of Cell Biology 191(3), pp. 677-691.

Patel, K. D. et al. 1995. Neutrophils use both shared and distinct mechanisms to adhere to selectins under static and flow conditions. Journal of Clinical Investigation 96, pp. 1887-1895.

Pearson, M. A. et al. 2000. Structure of the ERM Protein Moesin Reveals the FERM Domain Fold Masked by an Extended Actin Binding Tail Domain. Cell 101(3), pp. 259-270.

Pellegatta, F. et al. 1998. Functional association of platelet endothelial cell adhesion molecule-1 and phosphoinositide 3-kinase in human neutrophils. Jounal of Biology and Chemical 273, pp. 27768-27771.

Perry, M. A. and Granger, D. N. 1991. Role of CD11/CD18 in shear rate-dependent leukocyte-endothelial cell interactions in cat mesenteric venules. The Journal of Clinical Investigation 87(5), pp. 1798-1804.

Peters, A. M. 1998. The pulmonary granulocyte pool. Clinical Science 94, pp. 7-19.

Pettit, E. J. & Hallett, M. B. (1998) Release of 'caged' cytosolic Ca2+ triggers rapid spreading of human neutrophils adherent via integrin engagement Journal of Cell Science, 111, 2209-2215.

Pettit, E. J. and Hallett, M. B. 1998. Release of 'caged' cytosolic Ca2+ triggers rapid spreading of human neutrophils adherent via integrin engagement. Journal of Cell Science 111(15), pp. 2209-2215.

Petty, H. R. and Todd, R. F. 1996. Integrins as promiscuous signal transduction devices. Immunology Today 17, pp. 209-212.

Phillipson, M. et al. 2006. Intraluminal crawling of neutrophils to emigration sites: a molecularly distinct process from adhesion in the recruitment cascade. Journal of Experimental Medicine 203(12), pp. 2569-2575.

Phillipson, M. et al. 2009. Vav1 Is Essential for Mechanotactic Crawling and Migration of Neutrophils out of the Inflamed Microvasculature. The Journal of Immunology 182(11), pp. 6870-6878.

Pillinger, M. H. and Abramson, S. B. 1995. The neutrophil in rheumatoid arthritis. Rheum Dis Clin North Am 21, pp. 691-714.Premack, B. A. and Schall, T. J. 1996. Chemokine receptors: Gateways to inflammation and infection. Nature Medicine 2, pp. 1174-1178.

Ptasznik, A. et al. 1996. A tyrosine kinase signaling pathway accounts for the majority of phosphatidylinositol 3,4,5-trisphosphate formation in chemoattractant-stimulated human neutrophils. Journal Of Biology And Chemical 271, pp. 25204-25207.

Ratnikov, B. I., Partridge, A. W. and Ginsberg, M. H. 2005. Integrin activation by talin. Journal of Thrombosis and Haemostasis 3, pp. 1783-1790.

Rees, D. J. G. et al. 1990. Sequence and domain structure of talin. Nature 347(6294), pp. 685-689.

Richard O, H. 2002. Integrins: Bidirectional, Allosteric Signaling Machines. Cell 110(6), pp. 673-687.

Rieu, P. and Arnaout, M. A. 1996. The structural basis and regulation of [bgr]2 integrin interactions. Clinical Science 87 pp. 89-42.

Roberts, G. and Critchley, D. 2009. Structural and biophysical properties of the integrin-associated cytoskeletal protein talin. Biophysical Reviews 1(2), pp. 61-69.

Rocha e Silva, M. 1994. A brief survey of the history of inflammation. Inflammation Research 43(3), pp. 86-90.

Rollins, B. J. 1997. Chemokines. Blood 90, pp. 909-928.

Rose, D. M., Alon, R. and Ginsberg, M. H. . 2007. Integrin modulation and signaling in leukocyte adhesion and migration. Immunological Reviews 218, pp. 126-134.

Rosen, S. D. 1993. Cell surface lectins in the immune system. Seminars in Immunology 5(4), pp. 237-247.

Roth, S. J. et al. 1995. C-C chemokines, but not the C-X-C chemokines interleukin-8 and interferon-gamma inducible protein-10, stimulate transendothelial chemotaxis of T lymphocytes. Eurpean Journal of Immunology 25, pp. 3482-3488.

Rowe, R. G. and Weiss, S. J. 2008. Breaching the basement membrane: who, when and how? Trends in Cell Biology 18(11), pp. 560-574.

Sampath, R. et al. 1998. Cytoskeletal Interactions with the Leukocyte Integrin β2 Cytoplasmic Tail. Journal of Biological Chemistry 273(50), pp. 33588-33594.

Saotome I., C. M., Mcclatchey A.I., (2004) Ezrin is essential for epithelial organization and villus morphogenesis in the developing intestine. Developmental Cell Biology, 6, 855 - 864.

Schenkel, A. R. et al. 2004. Locomotion of monocytes on endothelium is a critical step during extravasation. Nature Immunology 5(4), pp. 393-400.

Schiffmann.E , C. B. A., and Wahl. S M. 1975. N-formylmethionyl peptides as chemoattractants for leucocytes. Proceedings of the National Academy of Sciences of the United States of America 72(3), pp. 1059-1062.

Schlessinger, J. and Lemmon, M. A. 2003. SH2 and PTB Domains in Tyrosine Kinase Signaling. Science.(191), pp. re12-.

Schmid-Schönbein, G. W. et al. 1980. The interaction of leukocytes and erythrocytes in capillary and postcapillary vessels. Microvascular Research 19(1), pp. 45-70.

Scott, A. et al. 2004. What is "inflammation"? Are we ready to move beyond Celsus? British Journal of Sports Medicine 38(3), pp. 248-249.

Seely, A. J. E. et al. 2003. Science review: Cell membrane expression (connectivity) regulates neutrophil delivery, function and clearance. Critical Care 7(4), pp. 291-307.

Sekido, N. et al. 1993. Prevention of lung reperfusion injury in rabbits by a monoclonal antibody against interleukin-8. Nature 365, pp. 654-657.

Senetar, M. A. and McCann, R. O. 2005. Gene duplication and functional divergence during evolution of the cytoskeletal linker protein talin. Gene 362, pp. 141-152.

Sengelov, H. et al. 1995. Mobilization of granules and secretory vesicles during *in vivo* exudation of human neutrophils. The Journal of Immunology 154(8), pp. 4157-4165.

Shao, J. Y. and Hochmuth, R. M. 1996. Micropipette suction for measuring piconewton forces of adhesion and tether formation from neutrophil membranes. Biophysical Journal 71(5), pp. 2892-2901.

Shcherbina, A. et al. 1999. Moesin, the major ERM protein of lymphocytes and platelets, differs from ezrin in its insensitivity to calpain. FEBS Letters 443(1), pp. 31-36.

Shcherbina, A. et al. 2001. WASP and N-WASP in human platelets differ in sensitivity to protease calpain. Blood 98(10), pp. 2988-2991.

Sheerin, N. S. et al. 1997. Protection against anti-glomerular basement membrane (GBM)-mediated nephritis in C3- and C4-deficient mice. Clinical Experimental Immunology 110, pp. 403-409.

Sherwood, E. R. and Toliver-Kinsky, T. 2004. Mechanisms of the inflammatory response. Best Practice & Research Clinical Anaesthesiology 18(3), pp. 385-405.

Simon, S. I. et al. 1995. L-selectin (CD62L) cross-linking signals neutrophil adhesive functions via the Mac-1 (CD11b/CD18) beta 2-integrin. Journal Of Immunology 155, pp. 1502-1514.

Skapski H, Lehner T. A crevicular washing method for investigating immune components of crevicular fluid in man. Jounal Of Periodontal Research. 1976 Feb;**11**(1):19–24

Skapski, H. and Lehner, T. (1976), A crevicular washing method for investigating immune components of crevicular fluid in man. Journal of Periodontal Research, 11: 19–24

Sligh, J. E., Jr. et al. 1993. Inflammatory and immune responses are impaired in mice deficient in intercellular adhesion molecule 1. Process Of Nation Acadamic Science U S A 90, pp. 8529-8533.

---

Smart. SJ, 1994b. Pulmonary epithelial cells facilitate TNF-alpha-induced neutrophil chemotaxis. Jounal of Immunology 152, pp.:4087-4094.

Smart.SJ, 1994a. TNF-alpha-induced transendothelial neutrophil migration is IL-8 dependent. American journal of physiology 266, pp. L238-L245.

Somers, W. S. et al. 2000. Insights into the molecular basis of leukocyte tethering and rolling revealed by structures of P-and E-seiectin bound to SLe(X) and PSGL-1. Cell 103(3), pp. 467-479.

Sousa.A. D. and Cheney, R. E. 2005. Myosin-X: a molecular motor at the cell's fingertips. Trends in Cell Biology 15(10), pp. 533-539.

Spertini,O. et al. 1991. Leukocyte adhesion molecule-1 (LAM-1, L-selectin) interacts with an inducible endothelial cell ligand to support leukocyte adhesion. The Journal of Immunology 147(8), pp. 2565-2573.

Springer, T. A. 1994a. Traffic Signals for Lymphocyte Recirculation and Leukocyte Emigration - the Multistep Paradigm. Cell 76(2), pp. 301-314.

Springer, T. A. 1994b. Traffic signals for lymphocyte recirculation and leukocyte emigration: The multistep paradigm. Cell 76, pp. 301-314.

Springer, T. A. 1994c. Traffic signals for lymphocyte recirculation and leukocyte emigration: The multistep paradigm. Cell 76(2), pp. 301-314.

Steeber, D. A. et al. 1997. Ligation of L-selectin through conserved regions within the lectin domain activates signal transduction pathways and integrin function in human, mouse, and rat leukocytes. Journal Of Immunology 159, pp. 952-963.

Steeber, D. A. et al. 1998. Optimal selectin-mediated rolling of leukocytes during inflammation *in vivo* requires intercellular adhesion molecule-1 expression. Process National Academic Science USA 95, pp. 7562-7567.

Stewart, M. and Hogg, N. 1996. Regulation of leukocyte integrin function: Affinity vs. avidity. Journal Of Cell Biochemistry 61, pp. 554-561.

Stewart, M. P. et al. 1998. LFA-1–mediated Adhesion Is Regulated by Cytoskeletal Restraint and by a Ca2+-dependent Protease, Calpain. The Journal of Cell Biology 140(3), pp. 699-707.

_____

Stites. D.P , T. A. I., Parslow.T.G. ed. 2001. Medical Immunology. 9th edition ed. Lange Medical Books/McGraw-Hill Medical Publishing Division.

Strieter RM, K. A., Antony VB, Fick RB Jr, Standiford TJ, Kunkel SL. 1994. The immunopathology of chemotactic cytokines: the role of interleukin-8 and monocyte chemoattractant protein-1. The journal of laboratory and clinical medicine 123(2), pp. 183-197.

Su, W.-H. et al. 2000. Endothelial [Ca2+]i signaling during transmigration of polymorphonuclear leukocytes. Blood 96(12), pp. 3816-3822.

Tadokoro, S. et al. 2003. Talin Binding to Integrin ß Tails: A Final Common Step in Integrin Activation. Science 302(5642), pp. 103-106.

Ting-Beall, H. P. et al. 1993. Volume and osmotic properties of human neutrophils. Blood 81(10), pp. 2774-2780.

Todd, R. and Petty, H. R. 1997. Beta 2 (CD11/CD18) integrins can serve as signaling partners for other leukocyte receptors. Journal Of Laboratory Of Clinical Medicine 129, pp. 492-498.

Tohya, K. and Kimura, M. 1998. Ultrastructural evidence of distinctive behavior of L-selectin and LFA-1 (α<sub>L</sub>β<sub>2</sub> integrin) on lymphocytes adhering to the endothelial surface of high endothelial venules in peripheral lymph nodes. Histochemistry and Cell Biology 110(4), pp. 407-416.

Tu, L. et al. 1999. The cutaneous lymphocyte antigen is an essential component of the L-selectin ligand induced on human vascular endothelial cells. Journal Experimental Medicine 189, pp. 241-252.

Utgaard, J. O. et al. 1998. Rapid secretion of prestored Interleukin 8 from Weibel-Palade bodies of microvascular endothelial cells. Journal Experimental Medicine 188, pp. 1751-1756.

Van Kooyk, Y. et al. 1999. The actin cytoskeleton regulates LFA-1 ligand binding through avidity rather than affinity changes. Journal Of Biology Chemistry 274, pp. 26869-26877.

Vaporciyan, A. A. et al. 1993. Involvement of platelet endothelial cell adhesion molecule-1 in neutrophil recruitment *in vivo*. Science 262, pp. 1580-1582.

Voisin M-B, P. D., Nourshargh S. 2009. Venular basement membranes ubiquitously express matrix protein low expression regions: Characterization in multiple tissues and remodelling during inflammation. American journal of pathology.

Voisin, M.-B. et al. 2009. Monocytes and Neutrophils Exhibit Both Distinct and Common Mechanisms in Penetrating the Vascular Basement Membrane In Vivo. Arteriosclerosis, Thrombosis, and Vascular Biology 29(8), pp. 1193-1199.

Wang, S. et al. 2006. Venular basement membranes contain specific matrix protein low expression regions that act as exit points for emigrating neutrophils. The Journal of Experimental Medicine 203(6), pp. 1519-1532.

Weber, C. et al. 2007. The role of junctional adhesion molecules in vascular inflammation. Nat Reviews of Immunoogyl 7(6), pp. 467-477.

Welch, H. and Maridonneau-Parini, I. 1997. Lyn and Fgr are activated in distinct membrane fractions of human granulocytic cells. Oncogene 15, pp. 2021-2029.

Wheeler, J. S. A. 1993. The neutrophils. IRL Press/Oxford University Press, Oxford.

Wilhelm, D. L. 1973. Mechanisms responsible for increased vascular permeability in acute inflammation. Inflammation Research 3(5), pp. 297-306.

Wilton, J. M. R. and Lehneer, T. 1977. A Functional Comparison of Blood and Gingival Inflammatory

Witko-Sarsat, V. et al. 2000. Neutrophils: Molecules, Functions and Pathophysiological Aspects. Laboratory Investigation 80(5), pp. 617-653.

Wittchen.E. 2009. Endothelial signaling in paracellular and transcellular leukocyte transmigration Frontiers in Bioscience 14, pp. 2522-2545.

Wojcikiewicz.E, K. R. 2009. LFA-1 Binding Destabilizes the JAM-A Homophilic Interaction During Leukocyte Transmigration. Journal of biological physics 96(1), pp. 285-293.

Wolff, B. et al. 1998. Endothelial cell [ldquo]memory[rdquo] of inflammatory stimulation: Human venular endothelial cells store interleukin 8 in Weibel-Palade bodies. Journal Of Experimental Medicine 188, pp. 1757-1762.

_____

Woodfin, A. et al. 2007a. JAM-A mediates neutrophil transmigration in a stimulus-specific manner *in vivo*: evidence for sequential roles for JAM-A and PECAM-1 in neutrophil transmigration. Blood 110(6), pp. 1848-1856.

Woodfin, A. et al. 2007b. PECAM-1: A Multi-Functional Molecule in Inflammation and Vascular Biology. Arteriosclerosis, Thrombosis, and Vascular Biology 27(12), pp. 2514-2523.

Woodfin, A. et al. 2009. Endothelial cell activation leads to neutrophil transmigration as supported by the sequential roles of ICAM-2, JAM-A, and PECAM-1. Blood 113(24), pp. 6246-6257.

Woodfin, A. et al. 2010. Recent developments and complexities in neutrophil transmigration. Current Opinion in Hematology 17(1), pp. 9-17.

Worthen, G. S. et al. 1994. FMLP activates Rac and Raf in human neutrophils: Potential role in activation of MAP kinase. Journal of Clinical Investigation 94, pp. 815-823.

Yago,T. et al. 1999. P-selectin promotes the adhesion of monocytes to VCAM-1 under flow conditions. Journal Of Immunology 163, pp. 367-373.

Yago, T. et al. 2010. E-selectin engages PSGL-1 and CD44 through a common signaling pathway to induce integrin $\alpha L\beta 2$-mediated slow leukocyte rolling. Blood 116(3), pp. 485-494.

Yan, B. et al. 2001. Calpain Cleavage Promotes Talin Binding to the $\beta 3$Integrin Cytoplasmic Domain. Journal of Biological Chemistry 276(30), pp. 28164-28170.

Yang, L. et al. 2005. ICAM-1 regulates neutrophil adhesion and transcellular migration of TNF-$\alpha$-activated vascular endothelium under flow. Blood 106(2), pp. 584-592.

Yokomizo, T. et al. 1997. A G-protein-coupled receptor for leukotriene B4 that mediates chemotaxis. Nature 387, pp. 620-624.

Zarbock, A. et al. 2008. PSGL-1 engagement by E-selectin signals through Src kinase Fgr and ITAM adapters DAP12 and FcR$\gamma$ to induce slow leukocyte rolling. Journal of Experimental Medicine 205(10), pp. 2339-2347.

Zarewych, D. M. et al. 1996. LPS induces CD14 association with complement receptor type 3, which is reversed by neutrophil adhesion. Journal Of Immunology 156, pp. 430-433.

Ziegler, W. H. et al. 2006. The structure and regulation of vinculin. Trends in Cell Biology 16(9), pp. 453-460.

Zimmerman, GA, P. S., McIntyre TM. 1992. Endothelial cell interactions with granulocytes: tethering and signaling molecules. Immunology Today 13(3), pp. 93-100.

# Appendix I. Stages of Gingivitis

| Stage | Time (days) | Blood vessels | Junctional & sulcular epithelium | Predominant immune cells | Collagen | Clinical finding |
|---|---|---|---|---|---|---|
| Initial stage (sub clinical gingivitis) | 2-3 | Vascular dilatation, vasculitis. | Infiltration by PMN. | PMN | Perivascular loss. | Gingival fluid flow. |
| Early lesion. | 4-7 | Vascular proliferation. | Same as stage 1, rete peg formation atrophic areas. | Lymphocytes | Increased loss around infiltrate. | Erythema bleeding on probing. |
| Established lesion. | 14-21 | Same as stage1 pluse blood stasis. | Same as stage 1 but more advanced. | Plasma cells | Continued loss. | Changes in color, size, texture, etc. |
| Advance lesion. | Extension of lesion into alveolar bone, phase of periodontal breakdown. | | | | | |

# Appendix II: Composition of GCF

| Inflammatory /innate components | Cellular components | Humoral componts | soluble |
|---|---|---|---|
| Prostaglandins, leukotrients, IL-1α,IL-1β.IL2,IL6,IL-8, interferons α, colony stimulating factor α, acute-phase proteins, transferring | PMN, leukocytes, monocytes,T cells, B cells | IgG, IgM , IgA | Complement components, prealbumin, albumin, fibrinogen, ceruloplasmin, transferring, haptoglobin, hemopexin, β- lipoprotein, cytokines, chemokines, prostanoids |
| Cellular elements | Epithelial cells,Leuckocytes (95%-97% PMNs,1-2% lymphocytes 2-3%monocytes),Bacteria | | |
| Electrolytes | Calcium,Sodium, Potassium, Fluoride | | |
| Organic compound | Carbohydrate,Lipid, Protein,Complement, Immunoglobulin | | |
| Metablolic and bacterial products | Lactic acid, Hydroxyproline Prostaglandins,Urea, Endotoxins, vytotoxic substance | | |
| Antibacterial factors | Enzymes and enzymes inhibitors, acid phosphatase. alkaline phosphatase,pyrophosphatase,glucoronidase,lysozymes, hyaluronidase, Proteloytic enzymes,Lactic dehydrogenase, collagenase | | |

# Appendix III: Various researches done to determine the features of oral neutrophils

| Researchers | Finding | Year |
|---|---|---|
| Stephens and Jones | Fluctuation in neutrophils count in the saliva and not in blood | 1934 |
| Calonius and Calonius and Berg | Leucocyte count is low in edentulous persons | 1958 |
| Gilerson and Rovelstad | No relationship between caries and neutrophils | 1958 |
| Kolliker | Neutrophils are found in saliva not in the salivary glands and the duc | 1865 |
| Wrught | Confirmed the above finding | 1959 |
| Pfluger | No neutrophils in the salivary gland | 1871 |
| Jassinowski | Cells from the throat are swallowed and hardly likely to enter the anterior part of the mouth. Neutrophils count increase during gingivitis | 1925 |
| Isaacs and Danielian | Leucocytes appear in saliva through the mucous membrane | 1927 |
| Mitsui | Gingival margin as well as the palatine tonsils are the most significant sites of origin of salivary neutrophils | 1949,1952 |
| Sasaki | Gingival sulcus or pocket was the predominant intraoral site of origin of these white blood cells | 1952 |
| Venzin | Neutrophils emerge from blood vessels in the mucous membrane | 1953 |
| Wright | Salivary neutrophils arouse from blood vessels in the oral cavity | 1959 |
| Maclendon and Arnim | Chief sources of the red and white blood cells are the gingival fluid and gingival sulcus | 1959 |
| Calonius and Berg | Neutrophils enter oral cavity | 1958 |

| | | |
|---|---|---|
| | via the blood capillaries in the oral cavity | |
| Orban and Glickman | Neutrophils are found in the connective tissue of all marginal gingiva in both health and inflamed condition | 1948,1953 |
| Lundquist | The sulcular epithelium is rarely intact and this lack of integrity could be the site of transfer of leucocytes from subepithelial tissue of the sulcus | 1940 |
| Bill | Tissue fluids pass through pocket epithelium but not throught other normal oral epithelium and the various means it enter the gingival sulcus | |
| Dewar and Trot | Sulcular epithelium is not keratinized | 1955, 1957 |
| Duran- Reynals and Mccrea | Both sulcular epithelium and connective tissue are highly permeable during injury | 1953 |
| Florey | Active movements probably insinuating snall processes into the junctions between the endothelial cells which is used by neutrophilis to extravasate | 1958 |
| Brill | Salivary neutrophils are those which are transported from the gingival sulcus | 1959 |
| Waerhaug | Anatomy of the sulcus and its transformation into a gingival pocket during the course of periodontitis | early 1950s |
| Brill | physiology of GCF formation and its composition | late 1950s and early 1960s |
| Löe | use of GCF as an indicator of periodontal diseases | |
| Egelberg | analyze GCF ,studies on the dentogingival blood vessels and their permeability as they relate to GCF flow | |
| Schroeder Listgarten | understanding dentogingival structure and physiology | 1970s. |
| Attström | Migration of neutrophils and their function in gingival | 1970 |

_____

| | tissue and GCF | |
|---|---|---|
| Sueda, Bang and Cimasoni | Presence and functions of proteins, especially enzymes in GCF | 1987 |
| | | |
| Ohlsson, Golub and Uitto | Discovered that collagenase and elastase in GCF are derived primarily from human cells, most notably neutrophils, and that their activity is correlated with gingival inflammation and gingival pocket depth | 1992 |

# Appendix IV:  Basic periodontal  Index

**Periodontal Index (PI)**

This Index was developed by Russell A.L. (1956) to assess the prevalence and severity of gingivitis and  destructive periodontal  disease.The  PI  was intended  to  estimate  deeper periodontal disease by measuring the presence or absence of gingival inflammation and its severity, pocket formation and masticatory function. The scale of value for the PI ranges from 0 – 8 with increasing prevalence and severity of disease. The PI is a composite index because it records both the reversible changes due to gingivitis and the more destructive; and presumably irreversible  changes  brought  by  deeper  periodontaldisease.Because  of  this,  it  is  an epidemiological index with a true biological gradient.All the teeth present are examined. Gingival tissue is assessed for gingival inflammation and periodontal involvement.Third molars are not taken into consideration.

**Instruments used**  Mouth mirror and explorer are supplemented by CPITN probe.

**Scoring Criteria**

Russell chose the scoring values (0,1,2,4,6,8) in order to relate the stages of the disease in an epidemiological survey to the clinical conditions observed.

**Calculation of the index**

The PI score per individual is obtained by adding all of the individual scores and dividing by the number  of  teeth  present  or examined.  i.e.  PI  score  per  person  = Sum  of  individual scores/number of teeth. PI score per group = Sum of scores of all individuals/number of individuals.

_____

## Criteria for clinical studies

| SCORE | Criteria | Additional radiographic criteria |
|---|---|---|
| 0 | No overt inflammation, nor loss of function due to destruction of supporting tissue. | Normal appearance. |
| 1 | Mild gingivitis – an overt area of inflammation in free gingival, not circumscribing the tooth. | Normal appearance. |
| 2 | Gingivitis, inflammation completely circumscribing the tooth. No apparent break in the epithelial attachement. | Normal appearance. |
| 4 | Used only when radiographs available. | Early notch like resorbtion of alveolar crest. |
| 6 | Gingivitis with pocket formation. The epithelial attachment has been broken and there is a true pocket. There is no interference in mastication. The tooth is firm and not drifted. | Horizontal bone loss in whole of the alveolar crest, up to half of the length of the tooth root. |
| 8 | Advanced destruction with loss of masticatory function. The tooth may be losse, drifted with dull sound on percussion or may be depressible in its socket. | Advanced bone loss involving >1/2 of tooth root or a definite infrabony pocket with widening of periodontal ligament. There may be root resorption or rarefaction of apex. |

_____